WASCAL
West African Science Service Centre on Climate Change and Adapted Land Use

Federal Ministry of Education and Research

Université de Lomé

FACULTY OF HUMANITIES AND SOCIAL SCIENCES

DEPARTMENT OF GEOGRAPHY

DOCTORAL SCHOOL OF ARTS AND HUMANITIES

WASCAL DOCTORAL RESEARCH PROGRAMME
«Climate Change and Disaster Risk Management»

FUTURE TRENDS IN COASTAL FLOOD RISK UNDER CLIMATE CHANGE SCENARIOS ALONG THE PORT-BOUËT BAY (COTE D'IVOIRE)

UNIQUE DOCTORAL THESIS IN GEOGRAPHY

by:

Kouassi Marcel De Paul KOUAKOU

Under the supervision of:

Kissao GNANDI,

Full Professor, University of Lomé, Togo

And the co-supervision of:

Eric Valère DJAGOUA,
Full Professor, University Félix Houphouët-Boigny of Abidjan, Cote d'Ivoire

Dr. Yvonne WALZ
Institute of Environmental and Human Security, United Nations University, Bonn, Germany

Members of the jury:

President:	GNONGBO Tak Youssif, Full Professor, University of Lomé
Rapporteurs:	ADJOUSSI Passièzoum, Full Professor, University of Lomé
	HAUHOUOT Célestin, Full Professor, University Felix Houphouët-Boigny
Members:	GNANDI Kissao, Full Professor, University of Lomé
	DJAGOUA Éric Valère , Full Professor, University Felix Houphouët-Boigny
	Yvonne WALZ, Doctor, United Nations University, Bonn , Germany

NOVEMBER 2023

FUTURE TRENDS IN COASTAL FLOOD RISK UNDER CLIMATE CHANGE SCENARIOS ALONG THE PORT- BOUËT BAY (COTE D’IVOIRE)

DOCTORAL DISSERTATION

by

Kouassi Marcel De Paul KOUAKOU

This dissertation has been approuved by:

Supervisor:

Kissao GNANDI
Full Professor, University of Lomé, Togo

And Co-Supervisors

Eric Valere DJAGOUA
Full Professor, University Felix Houphouet-Boigny of Abidjan, Cote d‘Ivoire

Dr. Yvonne WALZ
Institute of Environmental and Human Security United Nations University, Bonn, Germany

UNIVERSITY OF LOMÉ
FACULTY OF HUMANITIES AND SOCIAL SCIENCES

WASCAL

November 2023

LIST OF CONTENTS

LIST OF CONTENTS I

DEDICATION II

ACKNOWLEDGEMENTS III

ABSTRACT V

RÉSUMÉ VII

LIST OF ABBREVIATIONS IX

INTRODUCTION 1

CHAPTER 1: UNDERSTANDING THE ELEMENTS OF COASTAL FLOOD RISK 8

CHAPTER 2: STUDY AREA: PHYSICAL, SOCIOECONOMIC AND ENVIRONMENTAL CHARACTERISTICS 30

CHAPTER 3: QUANTIFYING CHANGES IN EXTREME SEA LEVELS (ESLS) 53

CHAPTER 4: COASTAL FLOOD MAPPING AND EXPOSURE ASSESSMENT 79

CHAPTER 5: ASSESSMENT OF COASTAL FLOOD RISK IN A CHANGING CLIMATE 104

RECOMMENDATIONS & CONCLUDING REMARKS 132

REFERENCES 138

LIST OF FIGURES 163

LIST OF TABLES 166

ANNEXES 167

TABLE OF CONTENTS 177

DEDICATION

It is my privilege and honour to dedicate this thesis:

To GOD Almighty,

my Creator and the centre of my life. I am grateful for His infinite wisdom, inspiration, and guidance, which have been the foundation of my strength and success throughout this program.

To my beloved Parents,

who have been a constant source of love, encouragement, and support. Your words of wisdom and prayer have been instrumental in my academic journey. I am forever grateful for your sacrifices, guidance, and endless love.

To my dear Wife and son,

Your unwavering support, patience, and encouragement have has kept me going, even when the journey was tough. I cherish the memories we share, and I am grateful for the warmth and comfort of our little family.

To my brothers and Sisters,

Your unyielding belief in me has been a source of motivation and inspiration, and I am thankful for the joy and laughter we share.

ACKNOWLEDGEMENTS

This is my thesis, marking the end of my PhD journey, which has been both challenging and rewarding. As I reflect on this experience, I realize that every moment of the process, including the successes and setbacks, was valuable. I am immensely grateful for the guidance, help, and support I received from many individuals who played a significant role in this journey.

I express my deepest appreciation to the **West African Climate Change and Adapted Land Use (WASCAL)** program, which provided financial support for my research project through funding from the **German Federal Ministry for Education and Research**.

I would like to express my deepest gratitude to my main supervisor, **Professor Kissao GNANDI** of the University of Lomé (Togo). Thank you, Professor, for giving me the opportunity to pursue this exciting PhD research under your supervision. It is a great honour and pleasure for me, and my heartfelt appreciation for your patience, encouragement, great support, and help, as well as your valuable advice about research.

I am also blessed to have worked under the co-supervision of **Professor Eric Valère DJAGOUA** from the University Félix Houphouët-Boigny of Abidjan (Cote d'Ivoire). Thank you, Professor, for your great guidance and support throughout this journey. I appreciate your tireless roles both in the fieldwork and through writing papers, which helped advance this thesis.

I am very grateful to **Dr. Yvonne WALZ**, my second co-supervisor from the United Nations University in Bonn, Germany, for her kind support, great help, and guidance throughout this process. I have greatly valued and appreciated our productive discussions. Many thanks for your extensive knowledge and valuable comments, which helped me to improve and complete this research.

I extend my special thanks to all committee members who evaluated my thesis and provided constructive comments and suggestions that broadened my perspective from different angles.

I am deeply grateful to **Professor Komi AGBOKA**, Director of WASCAL-Togo, and his staff, for providing me with the necessary resources and support to complete this program. Their dedication to excellence has been a true inspiration.

I appreciate the support, advice, and valuable comments of **Dr. Frederic BONOU** of the University of Abomey (Benin), **Dr. Jacques André TIEMELE** of the University Félix Houphouët-Boigny of Abidjan (Cote d'Ivoire), and **Dr. Mouhamed IDRISSOU**, Scientific Coordinator of WASCAL-Togo, during the publications of my articles.

I thank **Dr. Sofia CAIRES** and **DELTARES** for sponsoring the license of the ORCA software, which facilitated the estimations of extreme sea levels within the framework of this research.

I also extend my thanks to **Mr. Isaac AMOUTCHI**, **Mr. Ferdinand BEBO**, and **Ms. Charlotte TEHIYA** for their help during the field data collection.

I am grateful for the encouragement and shared experiences in research and life that I received from my friends and colleagues, both in Lomé and from my homeland. Their presence has been a source of balance and support throughout my journey.

I would like to extend my gratitude to **Mr. Francis AKA** and **Mr. Michel TANOH** for their respective guidance and prayers that have been a source of strength and inspiration in this endeavour.

Finally, I express my heartfelt appreciation and thanks to my father (**Koffi Louis KOUAKOU),** mothers (**Marguerite YAO and Flaure MOGUESSAN**), brothers and sisters (**Marthe, Marie, Emillienne, Roselyne, Daniel, Wilfred and Rachelle**), in-laws, and relatives for their never-ending care, encouragement, support, and unconditional love. I am grateful for their belief in me and their support in pursuing my ambitions. Foremost, I thank my beloved wife (**Blemin Armande KOUAKOU**), and little boy (**Assena Matthis)** for their love, encouragement, and constant companionship throughout the ups and downs of this journey.

ABSTRACT

The increasing risk of coastal flooding in urban areas, driven by climate change and socioeconomic development, underscores the importance of accurate information for adaptation planning and risk mitigation. Yet, in Port-Bouët Bay, Cote d'Ivoire, there is a notable lack of comprehensive studies on coastal flood risk, despite it being a real and pressing concern. Existing research has predominantly focused on coastal erosion and overlooking key aspects like exposure and vulnerability when addressing coastal flood risk. These gaps hinder access to critical information necessary for effective action. Our research seeks to address these knowledge gaps by examining the spatial and temporal evolution of coastal flood risk over the current century using a systematic methodology. Using numerical and GIS-based modelling, empirical computations, statistical analysis, and index calculations, we derived meaningful insights from diverse data sources. Focusing on the neighbourhoods of Vridi, Petit-Bassam, and Sogefiha, our study was conducted at the neighbourhood scale. By incorporating all aspects of risk analysis—hazard, exposure, and vulnerability, we enabled a comprehensive analysis in these specific locations. Our findings reveal that current coastal flood events are linked to relatively high extreme sea level conditions, projected to escalate with rising sea levels. Consequently, flooding will directly affect more areas, populations, and key assets, with the flood-prone area expected to nearly double by 2100, particularly under the SSP5-8.5 scenario. Sogefiha emerges as the most vulnerable neighbourhood, facing higher susceptibility and potential damage than Vridi and Petit-Bassam. While current coastal flood risk appears relatively low based on risk component indices, future trends vary across neighbourhoods and climate change scenarios. By 2100, Vridi is anticipated to have very low risk, but a shift to high risk is conceivable under the SSP5-8.5 scenario. Conversely, Petit-Bassam is expected to sustain low risk under all scenarios, while Sogefiha may face high to very high-risk levels, particularly under SSP5-8.5. The present study provides decision-makers with tools and insights to understand coastal flood risk evolution in the Port-Bouët Bay. It also provides targeted recommendations for adapting to and mitigating coastal flood risks, as well as promoting sustainable coastal management in Côte d'Ivoire and the broader West African region.

Keywords: Coastal flood risk; sea-level rise; socioeconomic vulnerability; local-scale analysis; climate change adaptation.

RÉSUMÉ

Le risque croissant d'inondations côtières dans les zones urbaines, alimenté par le changement climatique et le développement socio-économique, souligne l'importance d'informations précises pour la planification de l'adaptation et l'atténuation des risques. Pourtant, dans la baie de Port-Bouët, en Côte d'Ivoire, il y a un manque notable d'études exhaustives sur le risque d'inondation côtière, malgré qu'il soit une préoccupation réelle et pressante. La recherche existante s'est principalement concentrée sur l'érosion côtière, en négligeant des aspects clés comme l'exposition et la vulnérabilité lors de la prise en compte du risque d'inondation côtière. Ces lacunes entravent l'accès à des informations critiques nécessaires pour une action efficace. Notre recherche vise à combler ces lacunes en examinant l'évolution spatiale et temporelle du risque d'inondation côtière au cours du siècle actuel en utilisant une méthodologie systématique. En se concentrant sur les quartiers de Vridi, Petit-Bassam et Sogefiha, notre étude a été menée à l'échelle du quartier. Nos résultats révèlent que les événements actuels d'inondations côtières sont liés à des conditions de niveau de la mer extrême relativement élevées, projetées pour augmenter avec la montée du niveau de la mer. En conséquence, les inondations affecteront directement plus de zones, de populations et d'actifs clés, la zone à risque d'inondation devant presque doubler d'ici 2100, en particulier sous le scénario SSP5-8.5. Sogefiha apparaît comme le quartier le plus vulnérable, faisant face à une susceptibilité et des dommages potentiels plus élevés que Vridi et Petit-Bassam. Bien que le risque actuel d'inondation côtière semble relativement faible selon les indices des composantes du risque, les tendances futures varient selon les quartiers et les scénarios de changement climatique. D'ici 2100, on prévoit que Vridi aura un risque très faible, mais un passage à un risque élevé est concevable sous le scénario SSP5-8.5. En revanche, Petit-Bassam devrait maintenir un faible risque dans tous les scénarios, tandis que Sogefiha pourrait être confrontée à des niveaux de risque élevés à très élevés, en particulier sous SSP5-8.5. La présente étude fournit aux décideurs des outils et des perspectives pour comprendre l'évolution du risque d'inondation côtière dans la baie de Port-Bouët. Elle propose également des recommandations ciblées pour l'adaptation et l'atténuation des risques d'inondations côtières, ainsi que la promotion d'une gestion côtière durable en Côte d'Ivoire et dans la région ouest-africaine.

Mots-Clés : risque d'inondation côtière ; hausse du niveau marin ; vulnérabilité socio-économique; analyse à l'échelle locale ; adaptation au changement climatique.

LIST OF ABBREVIATIONS

AR6	6th Assessment Report Of the IPCC
CFR	Coastal Flood Risk
CCFV	Coastal Cities Flood Vulnerability
CFV	Coastal Flood Vulnerability
DRR	Disaster Risk Reduction
DEM	Digital Elevation Model
RMS	Risk Management Spiral
EBTM	Enhanced Bathtub Model
EVA	Extreme Value Analysis
GPD	Generalized Pareto Distribution
GEBCO	General Bathymetric Chart of the Oceans
GEVD	Generalized Extreme Value Distribution
GIS	Geographical Information System
HDM	Hydrodynamic Model
IPCC	International Panel on Climate Change
JPM	Joint Probability Method
LiDAR	Light Detection and Ranging
MOVE	Methods for the improvement of Vulnerability assessment in Europe
NSE	Nash–Sutcliffe efficiency
ORCA	metOcean data tRansformation, Classification and Analysis
POT	Peak-Over-Thresholds
R2%	Wave Runup 2% exceedance elevation
RCI	Risk Component Index
RI	Risk Index
RMSE	Root Mean Square Error
SDG	Sustainable Development Goal
SETS	Social-Ecological-Technological Systems
SLR	Sea-Level Rise
SSP	Share Socioeconomic Pathway
ST	Storm Tide
UNFCCC	United Nations Framework Convention on Climate Change
WACA-Resip	West Africa Coastal Area Resilience Investment Project

"Coastal flooding is a sleeping giant. If the threat of sea level rise is ignored, the projected increases in economic damage caused by coastal flooding are massive."

(Steffen et al., 2014, *Australian Climate Council****)***

INTRODUCTION

The two largest entities that comprise the Earth's surface are the oceans, accounting for 70%, and the lands or continents, which cover 27%. The transition zone between these two entities, known as the coast, is particularly important due to the wide variety of complex environments it encompasses, the numerous opportunities for development it provides, and the significant percentage of the population it attracts. Coastal zones encompass a range of environments, such as bays, estuaries, deltas, lagoons, marshes, dunes, and beaches (Basan et *al*., 1985), which create the ideal conditions for a diverse and extensive range of fauna and flora. These zones, therefore, harbour abundant natural resources that provide various ecosystem services for human wellbeing. Additionally, coastal lands offer favourable conditions for socio-economic activities, concentrating the majority of global industrial, recreational, tourism, and commercial facilities. Direct access to the sea also enables international trade in these areas through ports. In the European Union, the gross domestic product generated in regions adjacent to the shorelines amounts to 40%, while in West Africa, it reaches 56% (EEA, 2013). Consequently, coastal areas have become increasingly attractive to humans, with 40% of the global population residing within 100 km of the coast, equivalent to 2.4 billion people (United Nations, 2017), up from 1.2 billion in 1990 (Small & Nicholls, 2003). These numbers are expected to rise significantly in the coming decades (Maul & Duedall, 2019). However, the population boom, coupled with economic growth and rapid urbanization of coastal zones, creates a significant pressure on coastal lands by increasing the demand for housing and land use (Creel Liz, 2003). As a result, infrastructure and human settlements are expanding closer to the coast, leading to environmental degradation and destruction.

Coastal zones are also characterized by the dynamics of their environments. From a physical perspective, they exhibit a wide variety of morphological forms. These landforms are formed and evolve following diverse oceanic and continental processes such as sediment inputs from the continent (e.g., streams and rivers) and the ocean (due to marine and wind forces) and the actions of marine energetic factors such as waves and currents (Rizzo & Anfuso, 2020). So, the coastal morpho-dynamics is mainly characterized by the strong relationship that exists between forms and processes (Cowell & Thom, 1994). Coastal change can be both spatial (local- and large-scale) and temporal (Short-, medium- and long-) and thus highly complex. As an example, a large-scale and long- change that could be a shift of coastal environments landward or seaward, will be difficult to illustrate. This morpho-dynamism makes coastal zones, particularly susceptible to climate change. Indeed, the massive emissions of greenhouse gases (GHG) into the atmosphere that began with the industrial revolution, lead to the change of global climate systems with various s consequences throughout the world (IPCC, 2021; Hegerl et *al*., 2007). In the coastal domain, one of the direct consequences of climate change is sea level rise that is the increase of the average sea level induced by oceanic expansion and the melting of glaciers and icesheets (Hegerl et *al*., 2007). Recent research warms that global sea level may rise, in average, by a further 0.38 m ± 0.17 to 0.88 m ± 0.24 by the end of the twenty-first century (Fox-Kemper et *al*., 2021; Garner et al., in prep., 2021). Other effects of coastal climate change include the increase of frequency, intensity, and persistence of climate extreme processes (storms, precipitations, etc.). All these climate change effects contribute significantly to speeding up coastal dynamics, resulting in coastal degradation.

From the above, there is clear evidence that coastal areas are under double pressure: On one side, a pressure from the sea with sea level rise and other influences of climate change and on the other side, a pressure from the land as human settlements and infrastructures increases and densify. Living in these regions therefore brings its own set of hazards (GEF LME LEARN, 2020) . Coastal hazards can occur naturally like tsunamis, cyclones/hurricanes, severe storms and storm surges, or through human activities, for example, oil /chemical spills, habitat removal, algae blooms and many others. But one of the main concerns today in most coastal areas is the coastal flooding hazard, as it causes much destruction, including death and loss of property. Coastal flooding is a natural hazard, caused by a combination of high tides, storm surges and wave conditions, and exacerbated by climate change and the human actions of floodplain developments (Vitousek et al., 2017; Vousdoukas et al., 2018). Given the near-permanent and growing threat that represent this hazard, it is of utmost importance for coastal communities (both urban and rural) to adapt and prepare for future events. However, this can only be achieved if the risk is clearly understood beforehand.

Assessing the risk of a hazard like coastal flood is quite a complex topic since the environmental systems in which it occurs are full of interactions and non-linearities (Rougier et *al*., 2011). This complexity quite limits the complete understanding of the risk as well as the ability to accurately predict its evolution in a context of future global environmental changes. Thus, many governmental and local authorities are lacking key information for implementing appropriate risk management strategies. Accordingly, most coastal communities misapprehend the flood risk they are facing, with, many believing wrong that those exposed are only those previously already affected by past events or those located at short distance from the coastline. (Coquet et *al*., 2018; Ruz et *al*., 2020). Hence, research efforts in improving knowledge on coastal flood risk and its evolution is highly demanded for elaborating new (and/ or revising existing) management strategies to effectively and sustainably adapt and mitigate and guarantee the safety of growing coastal populations (Grases et *al*., 2020). This is the context in which this research project comes into play.

Problem Statement

The global assessment of (Vitousek et *al*., 2017) has revealed that under the effects of climate change, the tropical region with short-tailed flood-level distributions, will experience the largest increase in flooding frequency. Explicitly speaking, the 10 to 20 cm of sea-level rise expected no later than 2050 will more than double the frequency of extreme water-level events in this region, impairing the developing economies of equatorial coastal cities. Paradoxally, little is known about the phenomenon along the West African coast, which belongs to the tropics. Very recently, the total potential flooded areas in five countries were estimated to be around 6,650 km^2 by 2100, including 5,260 km^2 is in Mauritania and Senegal combined, 800 km^2 in Côte d'Ivoire, and 590 km^2 in Togo and Benin combined (World Bank, 2020). However, it is key to know for a particular location what is the risk and how it will evolve through time. Therefore, these regional/ national outcomes need to be downscale to a much smaller scale to support local adaptation and mitigation as emphasized by Serafin et al. (2019).

The paucity of coastal flood risk studies in West Africa comes from the fact that they are mostly carried out in association with the phenomenon of coastal erosion which is the gradual retreat of the shoreline (e.g., Alves et *al*., 2020). Although this seems scientifically logical since both phenomena have the same sources and influence each other (Pollard et *al*., 2019), it is worth noting that they do not have the same exposure i.e., elements at risk from flooding are not always at risk from erosion. For urbanised coasts, the risks associated with flooding could be more significant than erosion. Studying both hazards together has let the coastal erosion dominating the debates whereas the risk of coastal flooding is also real and distinct. Coastal erosion is, today, well-known in the region through several publications at both regional and local scales (Addo, 2013; Ankrah et al., 2023; Diaw, 2018; Djagoua et al., 2016; Gomez et al., 2020; Guerrera et al., 2021; Konan, 2012; Konan, 2014; Konan et al., 2016; M. Touré et al., 2018; Ndour et al., 2017; Philibert & Sylvain, 2012; Saimon, N'Doufou, et al., 2019; Yao et al., 2010). Therefore, it is important that a much more in-depth look be cast on the coastal flood issue, in order to evaluate its specific and detailed contribution in the degradation of the coastal environment across the region.

Another issue in assessing coastal flood risk, across West Africa, lies in the full characterization of the risk variables. The very few researches conducted in the region focused on the hazard and its impacts (e.g., World Bank, 2020), despite the growing consensus that the risk associated with threats to human security cannot be reduced by concentrating solely on the hazard (Birkmann et *al*., 2013). In recent literatures, the risk is understood as an interaction between hazard, exposure and vulnerability (Reisinger et al., 2020) with some possible contextual combinations. According to IPCC (2019), hazard refers to the potential occurrence of an event or trend that may result in losses, damages and disruptions of services. Exposure is the presence of individuals, livelihoods, species or ecosystems, environmental functions, services, resources, infrastructure, or assets in places and settings that could be adversely affected. And, vulnerability refers to the predisposition of the exposed elements to be negatively impacted. Thus, the coastal flood risk at a given location will depend not only on the magnitude and intensity of the hazard, but also on the characterization of the exposed elements and the level of vulnerability of individuals and systems. And all these need to be fully considered in the risk assessment.

The above-mentioned research gaps in the West African context left us with limited understanding of the current and future risk to coastal flood risk. This clearly emphasizes the urgent need for conducting more comprehensive studies on coastal flood risk to fill these knowledge gaps. However, attempts to address these gaps should not be based on speculative scenarios or imaginary circumstances. Instead, it is crucial to consider the most realistic scenarios of extreme sea levels to ensure the relevance and readiness of the research outcomes for integration into the development of coastal adaptations and mitigation strategies.

Objectives and Research Questions

The general aim of this research project is to comprehensively assess coastal flood risk in a densely populated urbanized coastal environment, considering current conditions and future scenarios influenced by climate change. To achieve this aim, the following specific research questions will guide the investigation:

(a) ***What is the spatiotemporal variation of extreme sea levels along the coastline of selected study site?***

(b) ***What elements within the study area are exposed to the impacts of present and future coastal flood scenarios?***

(c) ***How can the current coastal flood risk be characterized, and what are the projected trends in the context of climate change?***

Answering these research questions involves the following specific objectives:

(1) ***To quantify the spatiotemporal changes in the local extreme sea levels along the selected study site's coastline, considering factors such as tide, storm surges, coastal waves and sea-level rise.***

(2) ***To identify and evaluate the exposure of key elements within the study area, including populations, buildings and occupations, to the impacts of both current and future coastal flood scenarios.***

(3) ***To characterize the current coastal flood risk within the study site comprehensively, integrating hazard assessments, exposure analysis, and vulnerability assessments, and to project how this risk will evolve in the context of climate change over the course of the century.***

Throughout this study, special attention will be given to ensuring that all the aforementioned research gaps are effectively addressed. So, this study will be conducted at the local level (neighbourhood scale), allowing for a detailed assessment that captures the inherent complexities and nuances specific to the selected study area. This research will consider all aspects of the risk analysis to provide a holistic understanding of coastal flood risk. This inclusive approach will enable a more accurate assessment of the evolving risks and will contribute to the development of effective adaptation and mitigation strategies tailored to the unique challenges of the selected site. Furthermore, we will ensure that the analysis is based on the robust and realistic scenarios of extreme sea levels.

Thesis Structure

Given all these targeted objectives, this thesis is divided into seven (5) chapters excluding this introductory section and the concluding section. The chapters are structured as follows:

Chapter 1: Understanding the elements of coastal flood risk. Background information on the coastal flood phenomenon is provided as well as the element to be accounted in evaluating the risk. The different frameworks existing in the literature are also reviewed.

Chapter 2: Study area: physical, socioeconomic and environmental characteristics. The study area's diverse characteristics are comprehensively described in relation to the central focus of this thesis, which is coastal flood risk.

Chapter 3: Quantifying changes in extreme sea levels (ESLs). It displays the outcomes related to the first objective. The temporal evolution of compound extreme coastal sea elevation is quantified under different climate change scenarios. The analysis is carried out at the neighbourhood scale in order to detect possible spatial variations.

Chapter 4: Coastal flood mapping and exposure assessment. Using a GIS model, inundation layers are defined for different years and climate change scenarios. Following this, the inventory of all assets exposed to inundation is performed and information on the coastal flood exposure are provided. This chapter covers the second objective.

Chapter 5: Assessment of coastal flood risk in a changing climate. Hazard, exposure and vulnerability indices, all obtained from indicator-based assessments are aggregated to get the overall risk indices for every neighbourhood at the current and future time period. Chapter 5 covers the third and last objectives of this thesis.

It is noteworthy that Chapters 3, 4, and 5 will present the working methodology dedicated to achieving each of the stated work objectives they address. Furthermore, the concluding section of this work will include key recommendations for promoting and improving coastal flood risk reduction and adaptation within the local context.

UNDERSTANDING THE ELEMENTS OF COASTAL FLOOD RISK

1.1. Introduction

The risk of coastal flooding is a highly interesting topic that has garnered the attention of governments, organizations, and academic communities (Fang & Shi, 2021), particularly those in the field of disaster risk management. With the onset of climate change, it has become increasingly studied, mostly in regions where it is increasingly posing a genuine threat to both populations and infrastructure (e.g., Hall et al., 2006; Kebede & Nicholls, 2011; Reguero et al., 2015; Steffen et al., 2014). As a result, there exists a substantial body of knowledge on coastal flooding risk that can be leveraged to enhance our understanding of this phenomenon. The purpose of this chapter is to provide the requisite background information necessary for comprehending the subject matter of this doctoral research. It is rooted in a rigorous review of the extant literature. The various sections and subsections provide definitions of relevant terminology, elucidate the processes at work, and furnish an overview of the factors and framework to be taken into account in evaluating and managing coastal flood risk.

1.2. Coastal flooding

1.2.1. Overview

In a broader sense, the coastal flood refers to the flood occurring in coastal zones (Fang & Shi, 2021). However, for the purpose of this study, coastal flood is defined as natural phenomenon where coastal areas become submerged by the nearby sea (D'Arcy et al., 2022). It occurs suddenly when meteorological conditions become extremely severe, causing sea levels to rise significantly. This rise in sea levels can lead to the overtopping or breaching of coastal defences like dunes and dikes, ultimately resulting in the inundation of low-lying areas (see Figure 1-1). As such, coastal flood leaves little, if any, time for warning and preventative evacuation and results in most cases in significant impacts including damage to coastal infrastructure and ecosystems, harm on human health and disruption of people lives (Steffen et al., 2014; World Meteorological Organization, 2013). They have historically been, and currently are, one of the deadliest and most damaging natural hazards in the world (Idier et al., 2020). In 2005, the average coastal flood losses in the world's 136 largest coastal cities have been estimated to be approximately US$6 billion per year (Hallegatte et *al*., 2013). The deadliest coastal flood ever recorded resulted from the Bhola tropical cyclone in November 1970. The casualties from this event were estimated between 300,000 and 500,000 people killed in Bangladesh and neighbouring countries in the Gulf of Bengal (Cerveny et *al*., 2017).

Figure 0-1: Picture showing a coastal flooding occurrence (Location: South Australia; Sources: https://data.environment.sa.gov.au/coast-and-Marinal-Flood-Mapping-Viewer/PublishingImages/pic1.jpg).

Despite the recent advancements in coastal flood defence techniques and improvements in early warning system in many coastal countries, there have been a number of significant marine flood events throughout the world that still have had deadly and damaging consequences. For example, in France, the coastal flooding event caused by the 2010 storm xynthia on the Atlantic coast killed 53 people and over 1.5 billion Euros of damages (Chauveau et *al.*, 2011; Lang et *al*., 2013). The flooding resulting from a storm surge following the typhon Yolanda on November 2013 in the Philippines, killed more than 6 thousand people in the city of Tacloban (Santos et al., 2015). In west Africa, coastal flood impacts are mostly limited to areas around coastlines and events are generally not well documented. However, the cost of the coastal zone degradation in Benin, Cote d'Ivoire, Senegal and Togo as a result of flooding, erosion and pollution was estimated at $3.8 billion in 2017 (World Bank, 2019).

These coastal flood impacts are likely to be acute with the effects of climate and socio-economic changes in the coming decades (Hallegatte et al., 2013; Hinkel et al., 2014; Vitousek et al., 2017). Future climate change could increase the global average coastal flood losses to US$60 -63 billion per year by 2050 (Hallegatte et *al*., 2013). According to (Kirezci et *al*., 2020), even with a significant GHG reductions, an additional 23 million individuals may be at risk by 2050. And if no action is taken, 20% of global GDP could be threatened by 2100.

1.2.2. Drivers

Coastal flooding can be driven by the dynamic interaction of different physical oceanographic processes, which, may vary across coastal regions. Generally, they include tide, storm surge, wave condition, rising sea level due to climate change (D'Arcy et al., 2022). To these must be added the pathways via which flooding occurs i.e., the local coastal morphological features (Pollard et al., 2019). Figure 1-2 provides a visual representation of these contributing factors, which will be further elaborated on in the following sub-sections, providing a general overview of each driver.

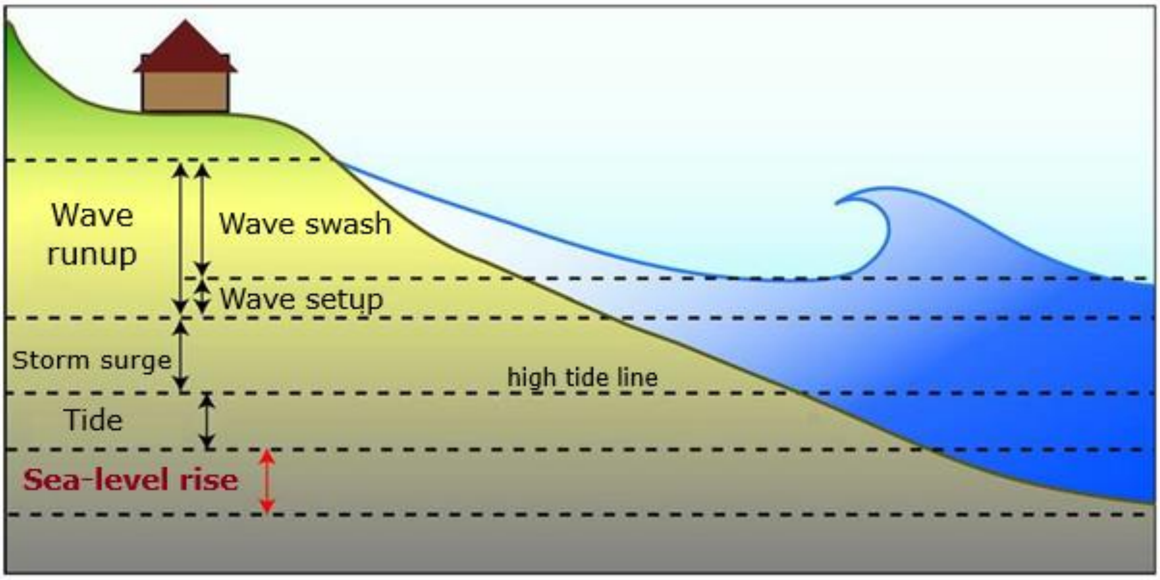

Figure 0-2: The Water-level components that contribute to coastal flooding (Adapted from Vitousek et al., 2017)

1.2.2.1. Tide

Tide is the periodic rise and fall observed in water levels every day due to changes in the attractive forces of the Moon and Sun upon the rotating Earth (Roos, 2014). Tide is considered one of the most reliable occurrences on Earth due to its regular and predictable cycle. In most coastal regions, changes in local water depth are primarily caused by the constant movement of tidal waves in the ocean (Siek, 2011). High tide takes place when the crest or peak of the tide reaches the coast, while low tide occurs when the trough or lowest point of the tide meets the coast. The difference in height between the high and low tide is referred to as the tidal range (TR). The tide also produces a horizontal water movement known as the tidal current. During a period of rising tide, the incoming water, moving towards the land, is referred as flow tide or flood tide. Conversely, after few hours, when the tide is falling, water begins to recede, we refer to the outgoing tide as an ebb tide.

Global tidal patterns are caused by the gravitational pull of both the moon and the sun on the Earth, resulting in the formation of two water bulges that appear on opposite sides of the planet. Due to its closer proximity to the Earth, the moon has the greatest influence on tidal patterns. The sun is 2.16 times less influential than the moon in causing the tide (Hicks, 2006). However, the arrangement of the Earth, Moon, and Sun is a critical factor in determining the variability of tides (figure 1-3). During periods of alignment, known as spring tides, the gravitational forces of both the Moon and Sun are combined, resulting in the highest and lowest tides. These typically occur during full and new moons. On the other hand, during neap tides, which arise during the first and last quarters of the Moon, the Sun and Moon are at right angles to one another, causing the Sun's gravitational pull to partially offset that of the Moon's. This results in lower high tides and higher low tides. Two spring tides and two neap tides can occur during one tidal cycle, which has an average duration of 29.53 days. This means that a spring tide or a neap tide occurs approximately every 14.765 days, which is half the length of the tidal cycle (Hicks, 2006).

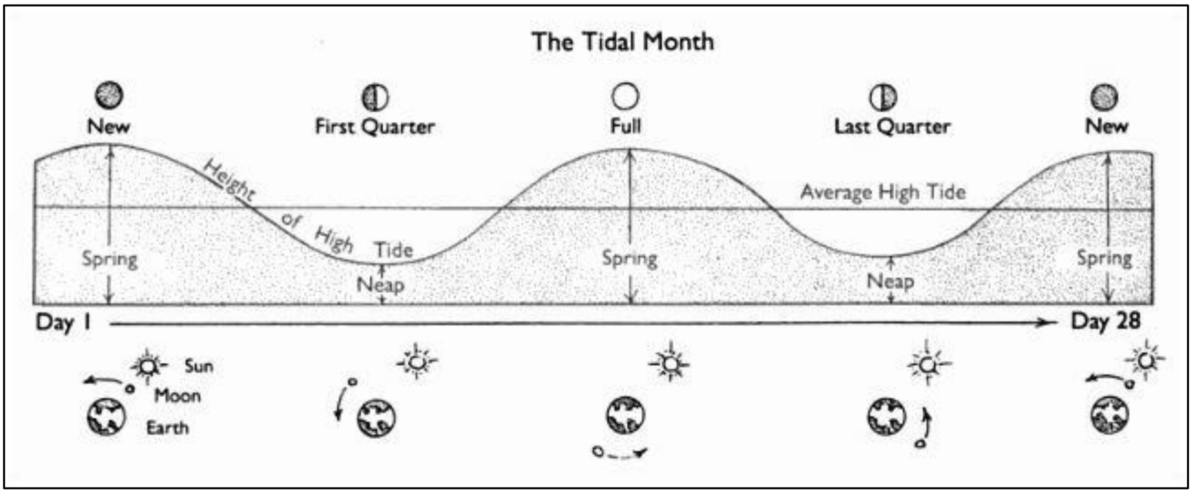

Figure 0-3: Description of Neap and spring tides (Ramsdales, 2023)

Other factors contributing to the global tidal patterns may include (i) the Moon's declination (angle of the Moon's orbit with respect to the Earth's equator) which varies over an 18.6-year cycle from a maximum of ~28° to a minimum of ~18°; (ii) the eccentricity of the Earth's orbit around the sun; (iii) and the eccentricity of Moon's orbit around the Earth (Roos, 2014). At the regional and local level, variations in tidal range may be dramatically affected by underwater bathymetry and the shape of the coastline.

Tides are classified into three types, semidiurnal, diurnal, or mixed, based on their natural period of oscillation in a given body of water. In the semidiurnal tide, there are two high and two low waters each tidal day, with relatively small differences in the respective highs and lows. On the other hand, in the diurnal tide, only a single high and single low water occur each tidal day. In the mixed tide, the diurnal and semidiurnal oscillations are both important factors and the tide is characterized by a large inequality in the high-water heights, low water heights, or in both. Figure 1-4 illustrates these three classes of tide.

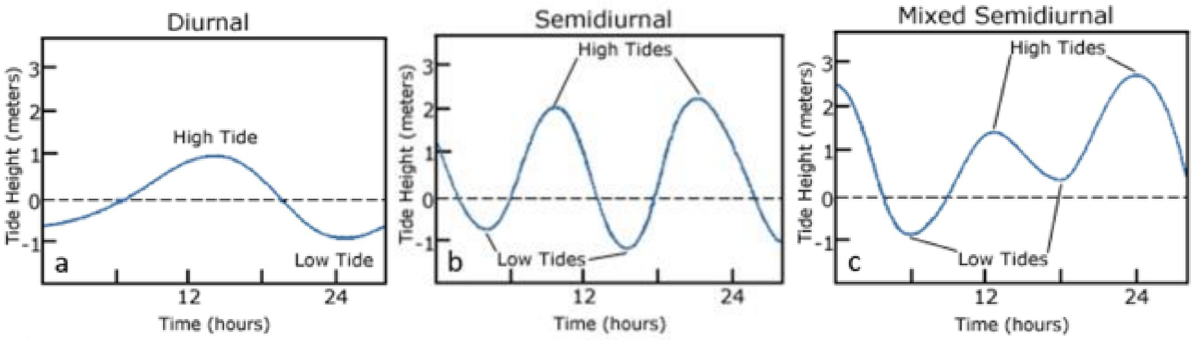

Figure 0-4: Illustration of time series data depicting diurnal [a], semidiurnal [b], and mixed tides from (NOAA, 2023)

The global phenomenon of tides is a constant source of coastal flooding that may mainly occur during high tides. Nevertheless, since high tide may vary across different locations of the world, the impact of tides on the overall water level that results in flooding may depend on the specific tidal attributes of the local area.

1.2.2.2. Storm Surges

Driven by meteorological forces such as strong wind friction and low air pressure, storm surge is a type of long wave motion that is pushed toward the shore (Kohno et al., 2018; Siek, 2011). It oscillates within a range of a few hours to some days depending to the atmospheric weather systems (Flather, 2003). The rise in sea level as a result of storm surge can cause severe flooding in coastal areas (figure 1-5), particularly when the storm tide coincides with the high tides (Mohanty et al., 2023). In some coastal areas, extreme coastal floods can be related to severe storm surge occurrences, such as cyclones, typhoons, or hurricanes that impact the exposed coastline.

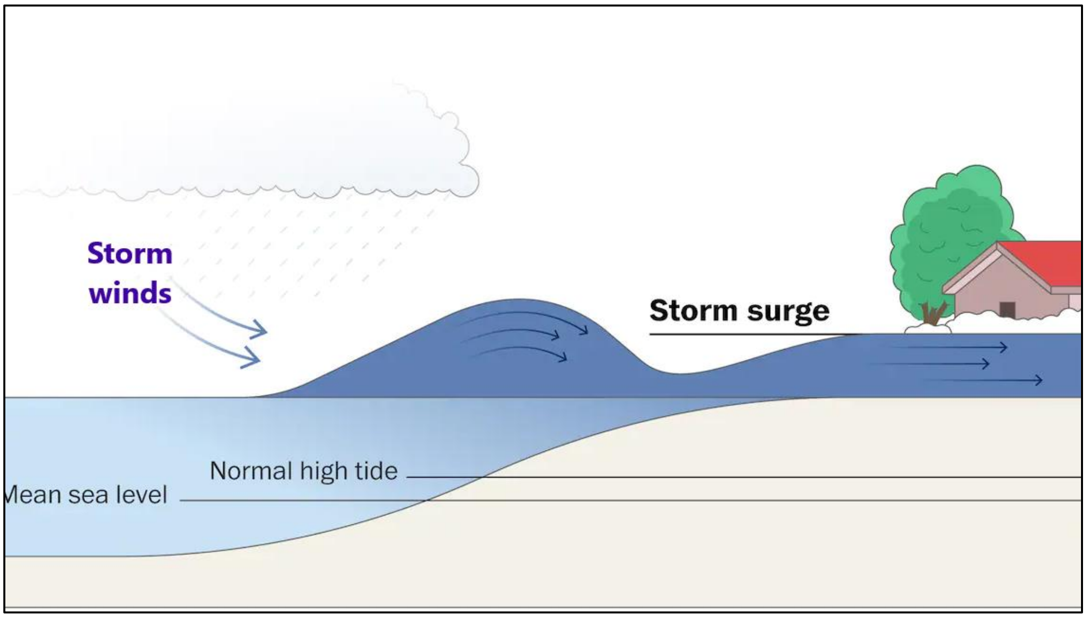

Figure 0-5: Storm surge inundation od the coastal land (modified for Berkowitz & Galocha, 2022)

Unlike tides, storm surges are very unusual (Kohno et al., 2018) as they depend on the meteorological conditions. They are generated on top of the expected tide. Nevertheless, as the surge approaches the coast, it may interact with the regular tide, leading to storm surge amplification or reduction (Velickov, 2004). Storm surge and astronomical tide are generally summed up under the term “storm tide” or “tide surge”. Storm tide may also represent the interaction between the tides and the surges. In practice, the actual interaction is difficult to describe in terms of analytical calculation and some knowledge can be gained from the numerical models (Siek, 2011). Tide-surge interaction on a local scale is very important because it is most apparent in shallow-water areas where large surges may be generated. The nonlinear interaction between the tides and surges may significantly change the return period of extreme storm tide. The storm tide level, also known as still water level (SWL), can be measured locally using tide-gauge equipment. A tide gauge is a device for measuring the change in sea level relative to a baseline or datum which may be the mean sea level (MSL) for instance. From a still water level record, storm surge is derived by simply subtracting the record with the predicted tide based on harmonic analysis (Kohno et al., 2007).

1.2.2.3. Ocean Waves

Ocean waves are formed as a result of the transfer of energy from the blowing wind to the ocean water surface, which is facilitated by the pressure and friction forces that disturb the equilibrium of the ocean surface (Gourlay, 2011; Holthuijsen, 2007; Pecher & Kofoed, 2017). The wave climate at a particular point in the ocean is therefore directly related to the wind fields prevailing in the wave generation area. The duration of a storm and the distance over which the wind blows continuously, known as the fetch, play crucial roles (Pecher & Kofoed, 2017). In principle, Waves in deep ocean start as small ripples and grow in size through consistent wind energy input (figure 1-6). Once energy loss, such as white-capping, counteracts the energy input, the waves become fully developed seas within the fetch, and their growth ceases. Wind speed and fetch determine whether a sea is fully developed or not. Fully developed waves that persist beyond the wind that formed them are known as swell waves, which are more orderly and regular in shape and direction compared to the more chaotic and disordered appearance of seas.

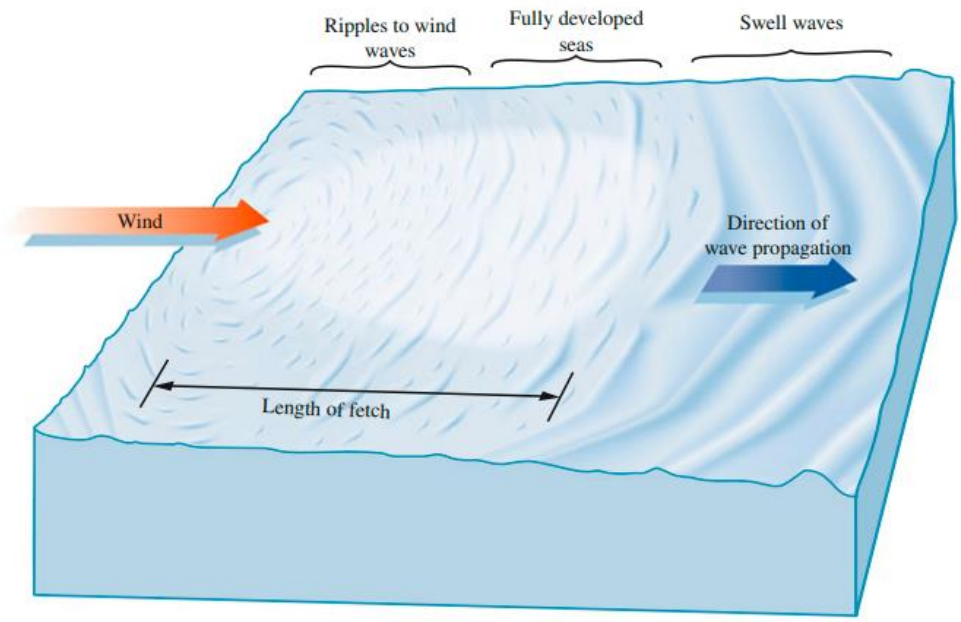

Figure 0-6; Process of ocean waves generation (Pecher & Kofoed, 2017)

In the case of monochromatic linear plane waves in deep water (see figure 1-7), water particles near the surface move in circular paths, making ocean surface waves a combination of longitudinal (back and forth) and transverse (up and down) wave motions (Siek, 2011). The ideal ocean surface wave is characterized by a sinusoidal shape, with identical crests and troughs and a fixed wavelength, moving progressively with water particles following orbital paths to complete one cycle per wave as shown in figure 1-7 (Holthuijsen, 2007). Ocean waves are generally described using parameters such as wave length, height, period and frequency. Wave length is the horizontal distance between adjacent crests or troughs, while wave height is the vertical distance from crest to adjacent trough. The time it takes for consecutive crests to pass a fixed point defines wave period, with wave frequency measuring the number of complete waves occurring per unit time (in hertz or cycles per second). Finally, the speed at which a wave crest moves horizontally across the ocean surface is known as wave celerity or phase speed (m/s).

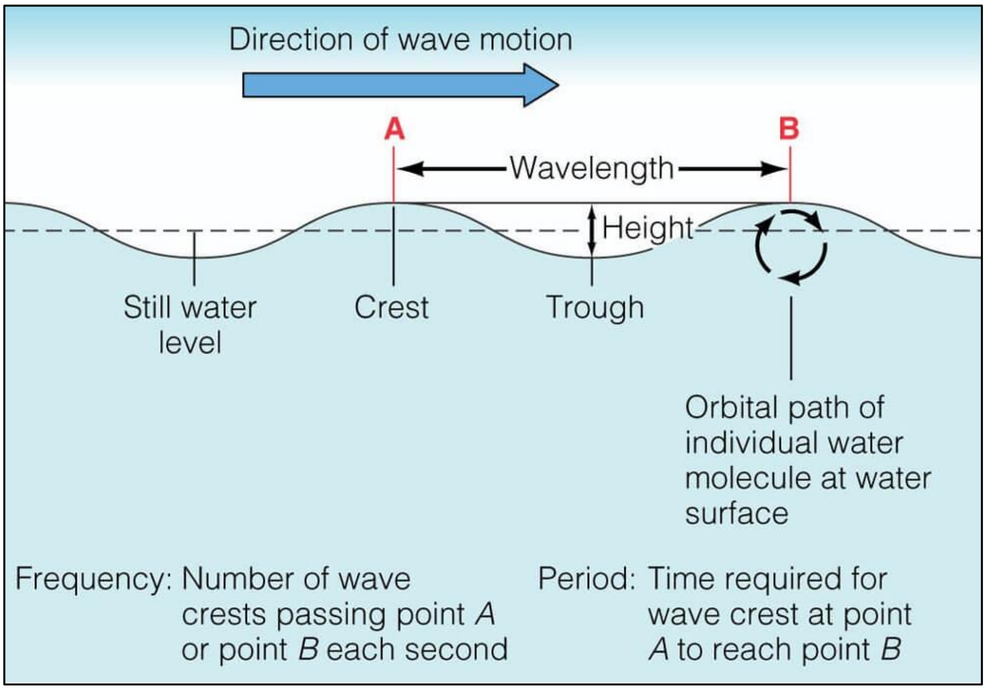

Figure 0-7: Characteristics of the ocean wave (source: Oceans images (educatorpages.com))

Waves propagate along the interface between water and air. This propagation, according to (Siek, 2011) may involve a lot of processes and interactions including wave dissipation, wave frequency-direction interaction, wave's modifications due to boundaries (coastline, islands, icesheet cover), moving boundaries (ship waves), bathymetry (refraction, shoaling, diffraction, breaking, reflection), and baroclinic currents (blocking, refraction by current gradients). When deep sea waves approach the coast, they lose energy and become steeper (Gomes da Silva et al., 2020). The contribution of waves to the total sea level leading to flooding in the coastal domain can be assessed through the wave runup parameter. Wave runup is defined as the set of discrete water-level elevation maxima measured on the foreshore, with respect to the SWL (Stockdon et al., 2006). The wave runup is composed of the wave set-up and the wave swash as shown in figure 1-8. Wave set-up indicates the mean wave height in the surf zone during the waves breaking, while wave swash refers as the amplitude of the time-varying elevation as the waves interact with the beach (Fassardi, 2007; Stockdon et al., 2006).

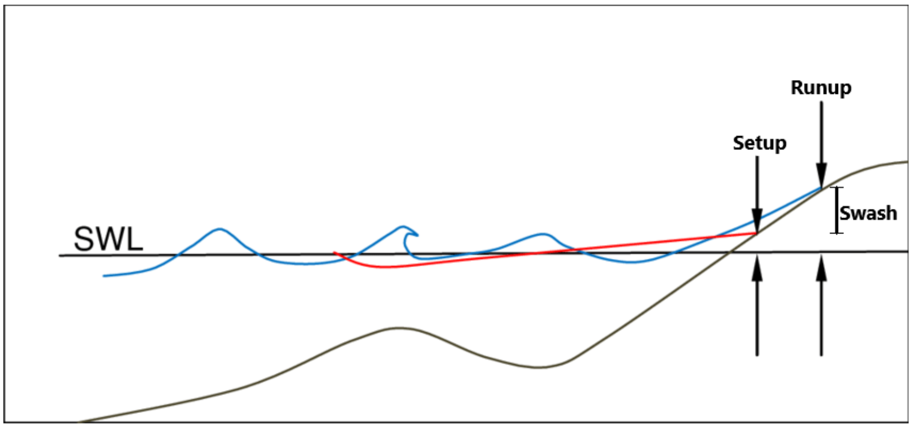

Figure 0-8: Conceptual sketch of wave runup on a beach (blue line) and setup (red shorter line). The difference between wave runup and wave setup is the swash Adapted from Melby et al. (2012).

Wave runup and its components are generally assessed through empirical formulas, physical or numerical models. However, empirical formulas are mostly and frequently used due to their advantage of being simple and easy to apply, allowing for fast and low-cost calculations (Gomes da Silva et al., 2020). They make use of parameters such as beach slope, wave height, and wave length, the latter two of which are taken offshore, specifically at a depth greater than half the wave length (Stockdon et al., 2006). Typically, wave runup is presented in terms of runup statistics such as the maximum runup of the time series (R_{max}) or the runup exceeded by 2% of the waves ($R_{2\%}$).

1.2.2.4. Sea-level Rise

Another significant driver of coastal floods is sea level rise. It refers to the increase in the mean sea level (MSL) induced by the effects of the warming climate. Sea-level rise occurs as a result of thermal expansion and the melting of land-based ice sheets and glaciers (Li et al., 2020) which are the visible effects of the warming climate. Measurements from tide gauges and high-precision altimeter satellites have shown that sea level has been rising since the mid-to-late nineteenth century (Church & White, 2011; Jevrejeva et al., 2008; Nerem et al., 2010). However, the rate of SLR may vary at different spatial and time scales (Woodworth et al., 2019). Large-scale SLR variability are mainly linked to climate change and its global effects. SLR can also vary at smaller scales. For instance, SLR may be different in the coastal and nearby deep ocean areas or in two adjacent coastal areas and. The small scales variability of sea level rise at the coastline are generated by numerous processes including the shallowness of coastal waters, the complexity of coastlines and the seasonal runoff variation from coastal rivers. Due to shallower water depth in the coastal domain, sea-level rise may interact in a certain degree with the other coastal flood drivers i.e., Tide, storm surge and wave, leading to amplification or reduction of the latter drivers. Additionally, the local or regional vertical coastal land motion (uplift and/or subsidence) and groundwater storage may introduce another source of mean sea level variability at a smaller scale (Nicholls et al., 2021). Noteworthy that when the local factors accounted in sea-level rise, it refers as "relative sea-level rise".

Projections of SLR by IPCC, (2021) show accelerated increases by the end of the century as a result of future climate change. According to Clark et al. (2016) and Meehl et al. (2012), Even if efforts are made to limit the warming of the Earth's surface to 2.0° or 1.5°C by the year 2100, it is still expected that there will be global sea level rise for several centuries or even millennia. As the mean sea levels continue to rise, the potential for increased storminess, higher storm surge heights, and larger tidal ranges will increase in certain regions. This could result in more frequent and severe coastal flooding (Taherkhani et al., 2020), which is already known to cause significant socioeconomic damage.

1.2.2.5. Coastal Morphological features

Coastal flood occurrence can also be driven by coastal morphological features such as nearshore bathymetry and coastline and onshore morphologies. These natural pathways modify flooding hazard through their interactions with hydrodynamic conditions (Pollard et al., 2019). They originally act as natural defences against coastal flooding in a certain degree, by attenuating wave energy and reducing the intensity of storm surges (Grases et al., 2020). However, coastal morphologies which are locally-specific may change through time as changes occur in processes responsible for contemporary coastal characteristics (Pollard et al., 2019). These processes involve both hydroclimatic, terrestrial and human factors. Indeed, changes in still water level and wave conditions may sharpen nearshore bathymetry and retreat coastline, altering the natural defences against flooding. Terrestrial factors may include subsidence of the coastal land, which could significantly increase the sea level relative to the land surface. In addition, human activities on dry coastal lands such as constructing on coastal dunes, sand mining, mangroves cutting and land reclamation can also alter or remove the coastal natural defences, making the coast more vulnerable to flooding.

Overall, the complex interplay between natural coastal morphological features, human activities, and hydroclimatic changes may lead to significantly morphological alterations, creating new flood-prone areas or exacerbating the existing ones. Therefore, understanding how temporal changes to coastal morphology will modify flood risk is a substantial for establishing future coastal flood management strategies. Nevertheless, this may be challenging given the lack of datasets characterising historic coastal morphology in many coastal regions.

1.3. The Risk Concept

"Risk" represents the potential for adverse consequences where something of human value (e.g., ecosystem service, people, livelihood and key infrastructure in low-lying coastal area) is at stake and where the outcome of flooding, such as property damage or loss of life, is uncertain (IPCC, 2019). The concept of risk has largely evolved over time, and many attempts have been made to define it in various ways, often reflecting the specific contexts or purposes of different fields of study related to disaster management. Unfortunately, this has led to confusion, with authors and practitioners using the term "risk" interchangeably with other concepts, such as disaster, hazard, and vulnerability. Despite ongoing efforts to clarify these terms, such mistakes continue to be made in the literature. To avoid confusion, first, it is essential to differentiate between "risk" and "disaster." Risk is a measurable probability of adverse consequences from a hazard, based on the exposure and vulnerability of the entity at risk. In contrast, a disaster refers to a serious disruption of the normal functioning of a community or society, caused by hazardous events at any scale (UNDRR, 2020). The consequences of a disaster can be severe, resulting in losses and damages to human health and safety, infrastructure and property, the economy, and the environment. The latest definition of risk is provided by the Intergovernmental Panel on Climate Change (IPCC) Sixth Assessment Report (AR6), which describes it as a dynamic interplay between hazards, exposure, and vulnerability of individuals or systems (Reisinger et al., 2020). This definition will guide the present work.

When considering coastal flooding in the context climate change, the risk is characterized by a dynamic nature (Reisinger et al., 2020), which is attributable to the intricate interactions between natural and human-induced factors rather than being a static phenomenon. Risk is constantly changing and evolving with time. As global temperature rises, climate change and sea-level rise contribute to this dynamism by increasing the likelihood and severity of coastal flooding as increasing extreme high tides, storm surges and wave conditions cause more water to overflow the low-lying areas. In addition to natural factors, human activities such as coastal development, land-use changes, and infrastructure modifications can also contribute to the dynamic nature of coastal flood risk. Furthermore, the perception of coastal flood risk can also be dynamic, influenced by social, economic, and cultural factors. People's attitudes towards coastal flooding can change over time, influenced by past experiences, media coverage, and government policies. Overall, the dynamic nature of coastal flood risk highlights the importance of ongoing monitoring, assessment, and adaptation measures to manage and mitigate the potential impacts of coastal flooding. It also emphasizes the need for a comprehensive and integrated approach that considers the interplay of natural, human, and social factors in determining coastal flood risk.

In the next sections, we discuss the different terminologies used in the coastal flood risk concept in order to avoid confusion or misunderstanding in using terms such as hazard, exposure and vulnerability, which are the mean component of the risk.

1.3.1. Hazard

The term "hazard" typically refers to a physical event or human activity that has the potential to cause harm, whether it be loss of life or injury, damage to property, disruption of social and economic systems, or harm to the environment (IPCC, 2019; UNDRR, 2020). In general, hazards can arise from natural, technological, or mixed processes (Ferreira et al., 2021), and can be single, sequential, or combined in their origin and effects (UNISDR, 2009). Regarding coastal flooding, hazards can result from factors such as high tides, storm surges, or other weather-related events, which are external to the system or elements at risk. However, human activity can modify and exacerbate these hazards, making them internal to the system. For instance, when natural areas like wetlands or coastal vegetation are cleared for human development and/ or beach sands are mined for construction, the natural ability of the landscape to absorb and buffer against flood events is reduced. As a result, flooding hazards are exacerbated, and the potential for damage and loss of life is increased. It is important to distinguish between hazards and the concept of risk, as the former is a key component of the latter. When discussing hazards, it is necessary to specify their basic characteristics, including location, time, intensity, and frequency, as outlined in Table 1-1.

Table 1-1: Description of hazards' characteristics (Modified from Gravley, 2001)

Hazard Characteristics	Definition
Magnitude	It refers to the size or intensity of a hazard. Only those occurrences that exceed some common levels of magnitude are extreme
Frequency	How often an event of a given magnitude may be expected to occur in the long-run average.
Duration	The length of time over which a hazardous event persists, the onset to peak period.
Areal Extent	The space covered by the hazardous event
Speed of Onset	The length of time between the first appearance of an event and its peak
Spatial Dispersion	The pattern of distribution over the space in which its impacts can occur
Temporal Spacing	The sequencing of events, ranging along a continuum random to periodic

1.3.2. Exposure

Flood hazard maps or characteristics generally do not indicate the specific characteristics of the affected buildings or properties. Instead, exposure analysis is conducted to identify the elements at risk of flooding (Kang et al., 2005). Coastal flood exposure refers to the presence of human assets, such as people, infrastructure, housing, and production capacities, in areas that are susceptible to hazards (IPCC, 2019; UNDRR, 2020; Lincke et al., 2022). These assets are therefore at risk of potential losses and damage due to coastal flooding. Assessing exposure involves mapping the location and assets relative to the flood hazard. Exposure analysis is critical in estimating the elements at risk.

Exposure to flooding can have diverse impacts on coastal communities. Such impacts may include economic losses, such as damage to property, infrastructure, and businesses, as well as lost productivity and income. Coastal ecosystems, water quality, and marine habitats may also suffer environmental damage. Additionally, flooding can cause social impacts such as the displacement of communities, loss of cultural heritage, and damage to public health and safety. Understanding these characteristics can help stakeholders develop effective strategies for reducing coastal flood exposure and managing the impacts of coastal flooding.

1.3.3. Vulnerability

Vulnerability is a critical component of risk assessment and management, reflecting on the conditions or processes enabling a person or a community to anticipate, cope with, resist and recover from the impact of a natural or man-made disaster (IPCC, 2019; Rana & Routray, 2018; UNDRR, 2020). The level of vulnerability within a community can be influenced by how well the community is organized to mitigate or amplify potential losses from a hazardous event (Birkmann, 2007; Shepard et al., 2012). Assessing vulnerability is essential for understanding the actual conditions of any exposed element, such as communities, buildings, ecosystems, and critical infrastructure, and for developing effective strategies for reducing vulnerability (Alam et al., 2022). This, in turn, helps decrease the level of overall disaster risk.

Vulnerability is a multifaceted concept that encompasses various critical components and considerations. In the literature, some authors concentrate on the susceptibility of a system to hazard, others emphasize factors such as coping capacity, resilience, and/or recovery. Still, others integrate multiple aspects to provide a more comprehensive understanding of vulnerability. Schneiderbauer & Ehrlich (2004) note that susceptibility most describes pre-event vulnerability, while resilience describes post-event vulnerability. Resilience may be divided into immediate aftermath coping capacity and longer-term recovery (Schneiderbauer & Ehrlich, 2004).

Vulnerability is multidimensional with four main dimensions which are generally related to the physical, environmental, social and economic conditions (UNDRR, 2020). Table 1-2 provided a short description of what each dimension may involve. It is also important to note that several dimension combinations may be possible e.g., socioeconomic, socioecological. The level of vulnerability within a population is a constantly changing characteristic due to changes in physical, environmental, social, and economic conditions (Ford et al., 2018). Nevertheless, the focus of vulnerability research has mainly been on the current state of vulnerability or on or the historical changes in vulnerability, with little attention given to how vulnerability may develop in the future (Fawcett et al., 2017; Li et al., 2023; Magnan et al., 2016). As a result, the study of future vulnerability has been relatively understudied and is mostly described in general terms. One of the primary reasons for this is the lack of projected data, as vulnerability is influenced by a wide range of human behaviours and choices that are challenging to predict (Engle et al., 2014; Nelson et al., 2016).

Table 1-2: The different dimensions of Vulnerability

Dimension	Reference
Physical	Vulnerability of the built environment and infrastructure to damage and destruction
Environmental / ecological	Vulnerability of the natural environment and ecosystem to damage and degradation.
Social	Vulnerability of the communities and populations to harm and disruption
Economic	Vulnerability of the community's economic systems and activities to disruption and loss

Various conceptual frameworks exist to model vulnerability related to a hazard e.g., the MOVE framework (Birkmann et al., 2013), the coastal cities flood vulnerability (CCFV) framework (Balica et al., 2012), the coastal flood vulnerability (CFV) framework (Wu, 2021), the urban social-ecological-technological systems (SETS) flood vulnerability framework (Chang et al., 2021), and many others. These frameworks provide a systematic way to understand and analyse the underlying causes of vulnerability, as well as to identify and prioritize interventions to reduce vulnerability and increase resilience Each framework possesses its unique strengths and weaknesses. While certain frameworks specialize in assessing vulnerability related to specific hazard like coastal flood or urban flood, others adopt a broader perspective for evaluating vulnerability in diverse contexts. Ultimately, vulnerability frameworks serve as valuable tools empowering decision-makers and stakeholders to gain deeper insights into vulnerability and effectively address it, fostering the development of more resilient communities and systems.

Depending on the purpose and scope of the vulnerability assessment, various approaches or techniques may be use. Generally, these approaches adopt a socioecological and location-specific perspective, emphasize the importance of human rights, and pinpoint areas of high risk (Alam et al., 2022). Local-level assessments are commonly employed in these models, as vulnerability can differ significantly even among nearby communities (Pandey et al., 2010; Sowman & Raemaekers, 2018). Such precise evaluations are essential for accurate planning and effective stakeholder engagement. Assessing vulnerability can be accomplished through either quantitative or qualitative methods; however, it may be crucial to use both methods, especially when identifying and measuring risks and vulnerabilities both before and after disasters occur (Birkmann, 2007). A mixed methods approach takes into account the social aspects of individuals, households, or communities, and involves their participation in expressing their perceptions of risks within a particular region (Wisner, 2016). Using mixed method makes it possible leverage the strengths of both methods, leading to the emergence of various forms of vulnerability measurement, which may include a deductive approach (Indicator-based) and an inductive or participatory approach that involves populations own perceptions and resilience (Kuhlicke et al., 2011). This integrated approach to vulnerability assessment is crucial in ensuring that risk reduction projects can be successfully implemented.

1.3.4. Risk Equation

The concept of risk as earlier defined is characterized by the dynamic interactions between the level of hazard, exposure and vulnerability which have individually been discussed above. Therefore, risk strongly depends on these three components, as illustrated in Figure 1-9.

Figure 0-9: The interaction of three factors (vulnerability, exposure, and hazard) that influence risk.

To account for this interaction, several formulations have been developed in the literature. However, the one that has been widely accepted and applied in research on disaster risk management (e.g., Hadipour et al., 2020; Paranunzio et al., 2022) can be expressed as Equation 1-1.

$$Risk = Hazard \times Exposure \times Vulnerability \qquad (Equation\ 1\text{-}1)$$

So, for a given climate change scenarios and time period, the coastal flood risk is obtained by multiplying the corresponding level of hazard, exposure and vulnerability. In general rule, the risk equals 0 if one of the three components of hazard, exposure or vulnerability is null.

However, if one or more of these components is very high, then there can still be a significant risk even if the other components are very low or absent. For instance, in case of high vulnerability, the risk of a negative outcome is still present even if the hazard and exposure levels are very low or absent.

1.4. Risk Management and Adaptation

1.4.1. Risk Management Spiral (RMS)

Risk management involves the practice of examining, formulating, and implementing decisions in the face of disaster risks (Jones & Preston, 2011). It is composed of processes, methods, and frameworks designed to concurrently minimize the impacts of hazards and maximize opportunities. As such, it requires expertise from various scientific disciplines. Disaster or risk management has been acknowledged as a cyclical and multi-stage process (Coppola, 2015; Rana et al., 2021; Sawalha, 2020), characterized by several distinct phases. Ideally, this process begins with conducting a comprehensive risk analysis to understand potential risks (a). Subsequently, mitigation measures are implemented to minimize the potential impacts of future events (b). Finally, an effective response and recovery phase is initiated following a disaster (source) (c). However, given that all the different components of risk management are spatially and temporally variable, the concept can be best understood by envisioning the cycle as an infinite risk management spiral (Aubrecht et al., 2013), which accommodates the dynamic nature of risk management processes.

The disaster or risk management spiral (RMS) is a crucial tool in comprehending the risk management steps and facilitating the effectiveness of risk management. The spiral emphasizes that different phases of disaster management involve interconnected activities (Aubrecht et al., 2013; Dodman et al., 2013), which can be categorized into two main phases: pre-event and post-event phases. Pre-event activities include mitigation and preparedness, while response and recovery are port-event activities. Pre-event activities are conducted as proactive approach while the activities conduct after the disasters are called reactive approach. Below, we describe the four steps involved in the RMS based on information from Coppola (2015) and from Iftekhar and Charlesworth (2014). Figure 1-10 illustrates this modern RMS.

- **Mitigation**, also known as Disaster Risk Reduction (DRR), encompasses both structural and non-structural measures that are implemented with the aim of reducing or eliminating the likelihood and/or consequences of a hazard, thus treating the hazard in a way that has a lesser impact on society.

- **Preparedness** involves a series of activities and measures taken in advance to ensure a swift and effective response to disasters. The primary goal is to provide people who may be affected by a hazard with the necessary tools to increase their chances of survival and reduce the negative impact on their financial and personal well-being. Preparedness measures may include developing practical disaster plans, ensuring the availability of essential resources, and providing comprehensive training to personnel involved in disaster response. Preventive factors may either be applied to preparedness or mitigation.
- **Response**: Response is the provision of assistance or intervention immediately after a disaster to meet the life preservation and basic subsistence needs of those affected. It involves taking action to reduce or eliminate the impact of disasters to prevent further suffering or financial loss. Response measures are directed towards saving lives, protecting property, and dealing with the immediate damage caused by disasters. The success of response depends on good preparedness, and its effectiveness has a considerable bearing on subsequent recovery requirements and activities. Response operations are often difficult to implement, disruptive, and traumatic, and require sound planning, organization, and training.
- **Recovery:** Recovery is the process of restoring or improving the pre-disaster living conditions of a community, while reducing the risk of future disasters. It involves returning victims' lives to a normal state following the impact of disaster consequences. The recovery phase begins after the immediate response has ended and can last for months or years. Recovery includes restoration, reconstruction and development.

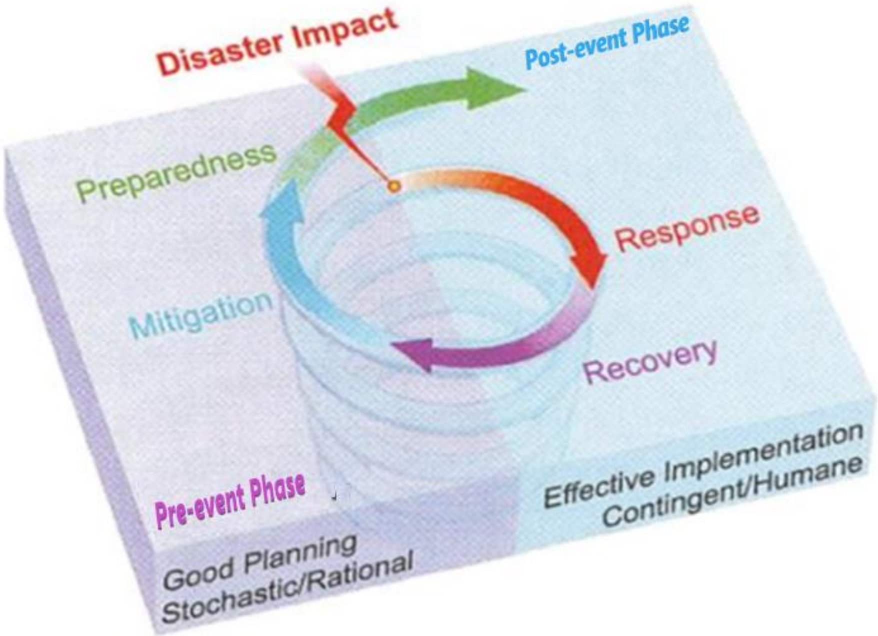

Figure 0-10: The Risk management Spiral (Adapted from Aubrecht et al.(2013))

In the past, there has been a predominant reactive approach to dealing with disastrous events, rather than a proactive one. Unfortunately, lessons learned from past events were not adequately considered, leading to a vicious cycle where subsequent disasters often had similar or even worse effects (Van Westen, 2013). Additionally, the lack of effective communication and coordination further complicates post-event crisis and disaster management (Aubrecht et al., 2013). By incorporating forward-looking activities such as forecasting, prediction, foresight, and strategic planning, and involving multiple stakeholders in participatory risk assessment, greater emphasis can be placed on the pre-event stage (Aubrecht et al., 2013), particularly in terms of preparedness. Envisioning future developments and integrating past findings, as well as current characteristics, can help minimize potential impacts before disasters occur. However, it is important to acknowledge that achieving zero risk is impossible. Despite continuous improvements in risk management, there are always residual risks that keep the spiral of risk management ongoing. This ongoing spiral of risk management underscores the need for continued efforts in keeping good management practises, even in the absence of immediate threats.

1.4.2. Adaptation

In order to address current and upcoming risks, it is essential for nations and communities to devise adaptation solutions. Lately, adaptation measures for climate-related risks have gained more recognition, notably within the United Nations Framework Convention on Climate

Change (UNFCCC), and among disaster and development experts (van Aalst et al., 2008). Adaptation essentially refers to the process of adjusting to changes in the ecological, social, and economic systems in response to actual and anticipated risks, with a similar aim as the risk management spiral, which is to minimize negative impacts and maximize beneficial opportunities (IPCC, 2012). Adaptation actions can take on many forms and are generally contextually customized (Morgan et al., 2019). Adaptation measures may differ across temporal and spatial scales. Short-term adaptation is often viewed as a reactive response, whereas adaptation at larger scales is typically seen as an anticipated outcome through the implementation of policies, projects, and current plans and actions (Jia et al., 2021). The process for effective adaptation, also known as the adaptation cycle is shown in Figure 1-11.

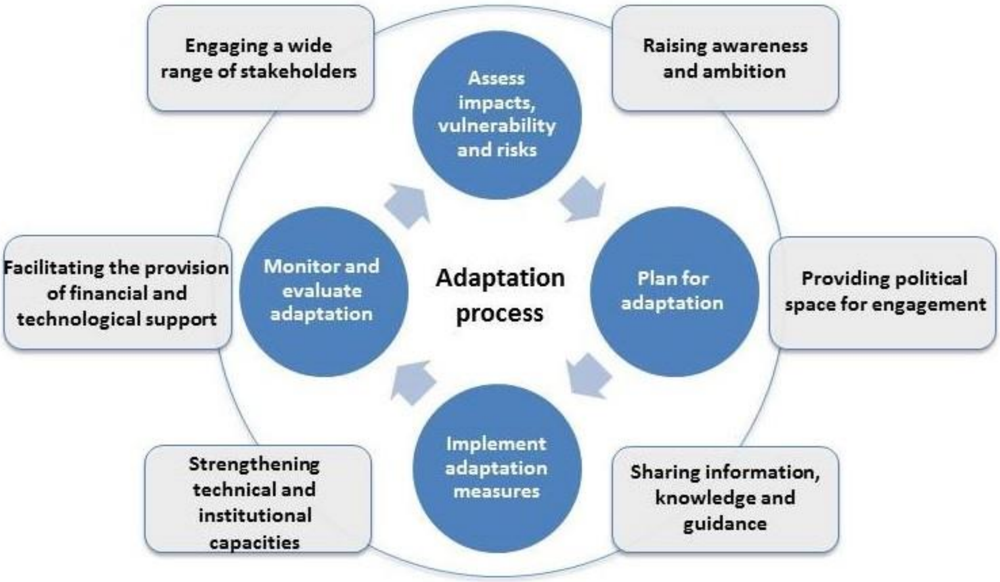

Figure 0-11: The adaptation cycle under the UN climate change regime (UNFCCC, n.d.)

According to UNFCCC (2018), successful adaptation requires:

- The active and sustained engagement of stakeholders, including local communities, national, regional, multilateral, and international organizations, and effective management of knowledge.
- The use of the best available science, traditional knowledge, knowledge of indigenous peoples, and local knowledge systems, with a view to integrating adaptation into socioeconomic and environmental policies and actions
- The use of a country-driven, gender-responsive, participatory, and fully transparent approach, considering vulnerable groups, communities, and ecosystems.

It is important to acknowledge that the ongoing discussions regarding the improvement of the risk management cycle highlight the need for integrated risk management. It has become widely recognised that successful risk reduction cannot be achieved without incorporating climate change adaptation into the disaster management cycle (Birkmann & von Teichman, 2010; Nalau et al., 2016). As a result, there have been several proposed alternatives such as panarchy and resilience frameworks (Berkes & Ross, 2016; Manyena et al., 2019; Pescaroli & Alexander, 2016), which aim to comprehensively address climate-related risks.

1.5. Conclusion

The threat of coastal flooding is a significant concern for coastal communities in the context of global climate change. These floods are caused by a complex interplay of physical (Tide, coastal Morphology), environmental (sea-level rise), and climatic (storm surge, ocean waves) factors that can lead to severe damage to coastal areas. The risk associated with coastal flooding is equally complex, resulting from the interplay of hazard, exposure, and vulnerability. To effectively address this risk, a coordinated effort is necessary to mitigate, prepare for, respond to, and adapt to coastal flooding events. By taking appropriate actions, we can reduce the risk of flooding and create resilient coastal communities for the future.

STUDY AREA: PHYSICAL, SOCIOECONOMIC AND ENVIRONMENTAL CHARACTERISTICS

2.1. Introduction

Coastal flooding poses a significant and complex threat that can cause severe damage to both human communities and the natural environment (Idier et al., 2020; Nicholls et al., 2007; World Bank, 2019). The risk of flooding in a particular coastal area is influenced by a range of natural and anthropogenic factors. Natural factors such as topography, hydrodynamics, and meteorological patterns can greatly affect the likelihood and severity of flooding, while human factors such as urbanization, land use change, and infrastructure development can worsen the risk. A comprehensive understanding of these factors in the local context is crucial for effectively assess the risk to coastal flooding.

This chapter aims to provide a thorough characterization of the study area in relation to the main issue of the research, which is the potential risk of coastal flooding. The chapter emphasizes the exploration and description of the physical, socio-economic, and environmental setups that contribute to the area's susceptibility to flooding. The physical setup includes the geology, geomorphology, sedimentology, drainage, climate and metocean conditions. The socio-economic setup includes population density and economic activity. Finally, the environmental setup refers to describing the urban habitat. To provide an evidence-based analysis, the descriptions and analyses presented in the chapter are based on relevant literatures, maps, and secondary data available for the site.

2.2. Location of the Study

The area chosen for this study is the coastal city of Port-Bouët, a town located southeast of the district of Abidjan. It is a peninsula, stretching for nearly 22 kilometres of coast, between the Atlantic Ocean and the lagoon of Ébrié. More precisely, it is situated between the latitudes 5.245˚N - 5.280˚N and the longitudes 3.955˚W – 4.020˚W and covers a total surface area of 111 km^2 (about 12.3% of the Abidjan urban area). The terrain is relatively flat (low-laying) with depressions in some places, particularly because of its sandy soil (Coulibaly et al., 2004). Port-Bouët is a densely populated area that has a long history of coastal development. It is composed of dozens of neighbourhoods among which seven (7) namely Vridi, Petit-Bassam, Sogefiha, Derriere-Wharf, Adjouffou, Jean-Folly and Gonzagueville, are directly on the edge of the ocean. In the current configuration, Port-Bouet displays a very contrasting urban landscape, which interweaves key infrastructures such as airport, port, military base, industrial zone., formal residential estates with pockets of precarious settlements. According to *UN-Habitat (2012)*, the city can be divided into three (3) main sections (see figure 2-1):

- A western section, west to the Vridi canal (sector of Vridi-Ako), extends over nearly 5 km of coastline. It is occupied by plantations and bush, and houses;
- A central section that located in front of a small marine bay: the Port-Bouët Bay (see figure 2-1). Stretching over 5.5 km, its seafront is occupied by the neighbourhoods of Vridi, Petit-Bassam and Sogefiha. This urban land of Port-Bouët comprises some of the facilities of the Port of Abidjan, the industrial zone, businesses, real estate transactions, pockets of precarious housing and local facilities;
- An eastern section, wider, is occupied by the Airport, the French military camp, and a large concentration of precarious habitats. Natural areas such as bushes and agricultural lands can also be found in this section of the city. A demolition operation carried out in 2014, made it possible to relocate populations and occupations from the seaside of this eastern Port-Bouët to prevent damages from coastal flood and erosion.

The whole city of Port-Bouët is very exposed to coastal flood hazard (IMDC, 2017; Tiemele et *al*., 2020; World Bank, 2019). The city is part of the top 20 world's cities ranked in s of population exposed to coastal flooding by 2070 and exhibiting current exposure (Nicholls et *al*., 2007). It has suffered several coastal flood events in the past among which the most recently documented are those of August 2007, August 2011 and May 2014 (Konan, 2012*;* Konan et *al*., 2016; Sadia, 2014; Tiemele et *al.*, 2020; Yao et *al*., 2018). In term of damages, the event of August 2007 destroyed dozens of houses were destroyed. In August 2011, three consecutive days of ESLs were observed, which caused the destruction of hundreds of dwellings and left more than a thousand families without shelters (Sadia, 2014). The event of August 2011, for example, generated by high waves exceeding 3 meters generated, caused significant physical damages and displaced about thousand families (Sadia, 2014). This event is still present in the memory of residents. The central section of the city, however, appears to be the most vulnerable to coastal flooding in views of the high density of housing and economic activities very close to the sea, but also the morpho-hydrodynamic specificities that prevail in this area (*see chapter 3*). Along this sector, the sandy dunes that normally serve as natural defence to the sea, are almost entirely occupied by infrastructures and dwellings. The many attempts to protect this portion of the coast with blocks of rock ended in failure, because of poor planification. Riverine communities are living in fear of being affected by the coming events of flooding.

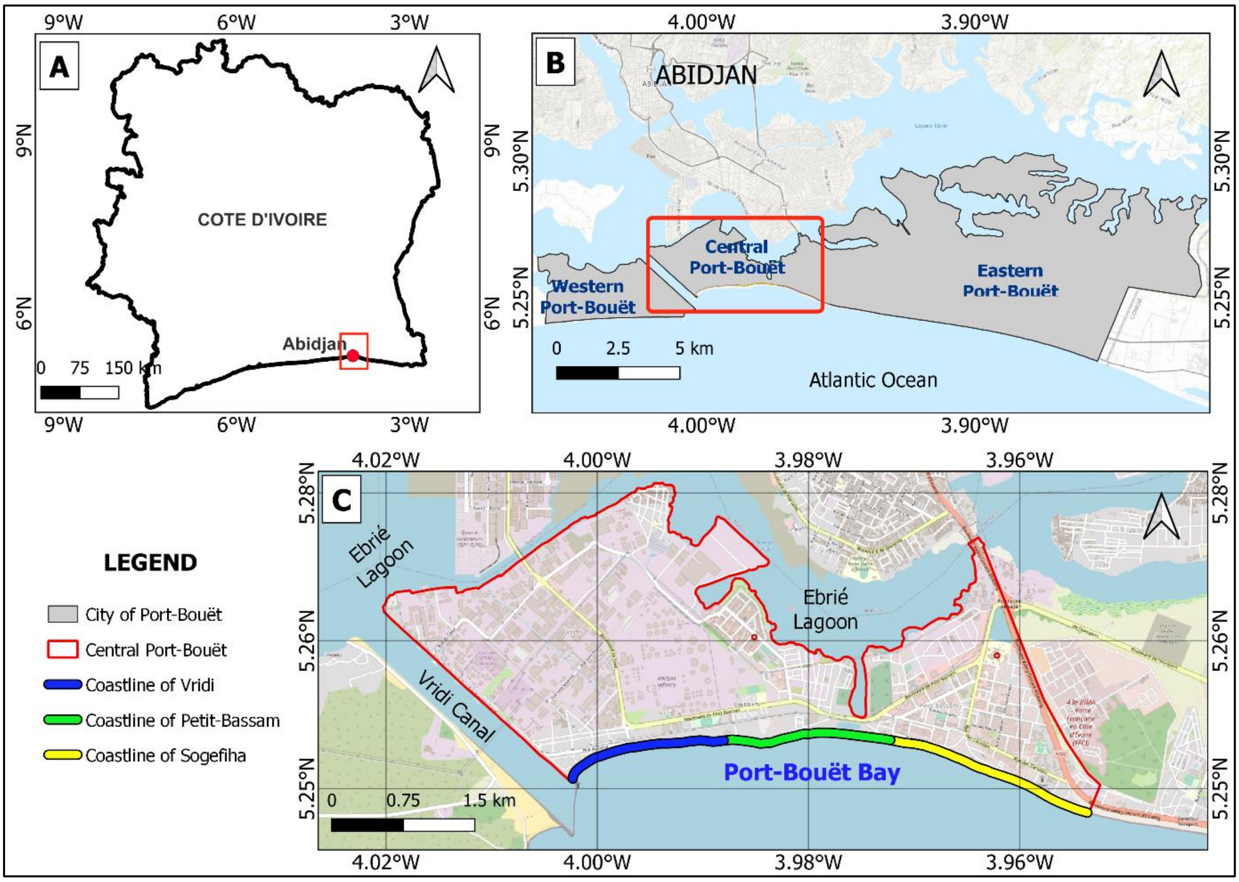

Figure 0-1: Map of the Study Area: (a) Cote d'Ivoire context; (b) the entire city of Port-Bouët; (c) The sector of the Port-Bouët Bay with its coastline subdivided according to the three neighbourhoods situated along: Vridi (in blue), petit-Bassam (in green) and Sogefiha (in yellow). This subdivision is for study purpose and does not follow administrative limits. Background outlines in (b) and (c) are from Esri Topographic and standard OpenStreetMap standard respectively

To summarise, Port-Bouët is a vibrant city with diverse socio-economic stakes in a densely populated geographic area. It has had many past coastal flood incidents and has potential for much serious future events. The central section of the city (the sector of the Port-Bouët Bay), apparently more vulnerable, will capture our attention in answering the research questions elaborated within the framework of this project. This particular area covers about 11.5 km^2 and lies between the Ebrié lagoon and the Atlantic Ocean with a width varying between 0.2 and 5 km.

2.3. Physical Characteristics

2.3.1. Geology

The Port-Bouët Bay belong to the emerged portion (onshore) of the Ivorian sedimentary basin which represents 2.4% of the country's surface area versus 97.6% for the Precambrian bedrock. This onshore sedimentary basin stretches 360 km from Fresco to the Cote d'Ivoire-Ghana border, occupying about 3/5 of the country's coastline. A larger part of the overall sedimentary basin extends at sea and forms the offshore sedimentary basin. Considering both onshore and offshore, the Ivorian sedimentary basin gives a total coverage of 30,000 km^2 while the onshore section alone is a little less than 8,000 km^2 (Koffi, 2017).

The Cote d'Ivoire sedimentary basin developed as a 'mega-pull apart' basin. It is characterized by a wide and deep rhomb-shaped depression. This depression is bordered on its sides by two subparallel overlapping strike-slip faults: the Saint-Paul fracture zone to the west and the Romanche fracture zone to the east. At its ends, the basin is defined by a west–east trending normal fault, also known as the 'lagoon rift' or 'Lagoon fault' (see Figure 2-2). The formation of this basin is associated with the opening of the equatorial Atlantic at the transform Côte d'Ivoire-Ghana Margin, during the lower cretaceous (145MA to 112 Ma) ((Mascle et al., 1997). This geological setting influences the basin's morphology and sedimentary fill, shaping the coastal landscape and susceptibility to flooding.

The "lagoon rift" divides the onshore basin into two parts with different sedimentary fill (see figure 2-3). As described in Wozazek & Krawinkel (2002), the characteristics of these zones are as follows:

- The zone north to the "lagoon rift", about 5000 Km^2, represent an East-West coastal band of 20 to 30 km wide. It is characterized by deposits of about 200 to 300 m thick. This zone meets the sea west of the city of Grand-Lahou where plateaus and coastal plains are observed. Sediment of this zone are tertiary formations (mainly from Mio-Pliocene), deposited in various marginal marine environments.
- The zone south of the "lagoon rift" where the Port-Bouët Bay is situated, is smaller (about 3000km^2) and characterized by very thick deposition (more than 5000 m). This zone mainly consists of turbiditic sediments deposited in an open marine environment during the quaternary period.

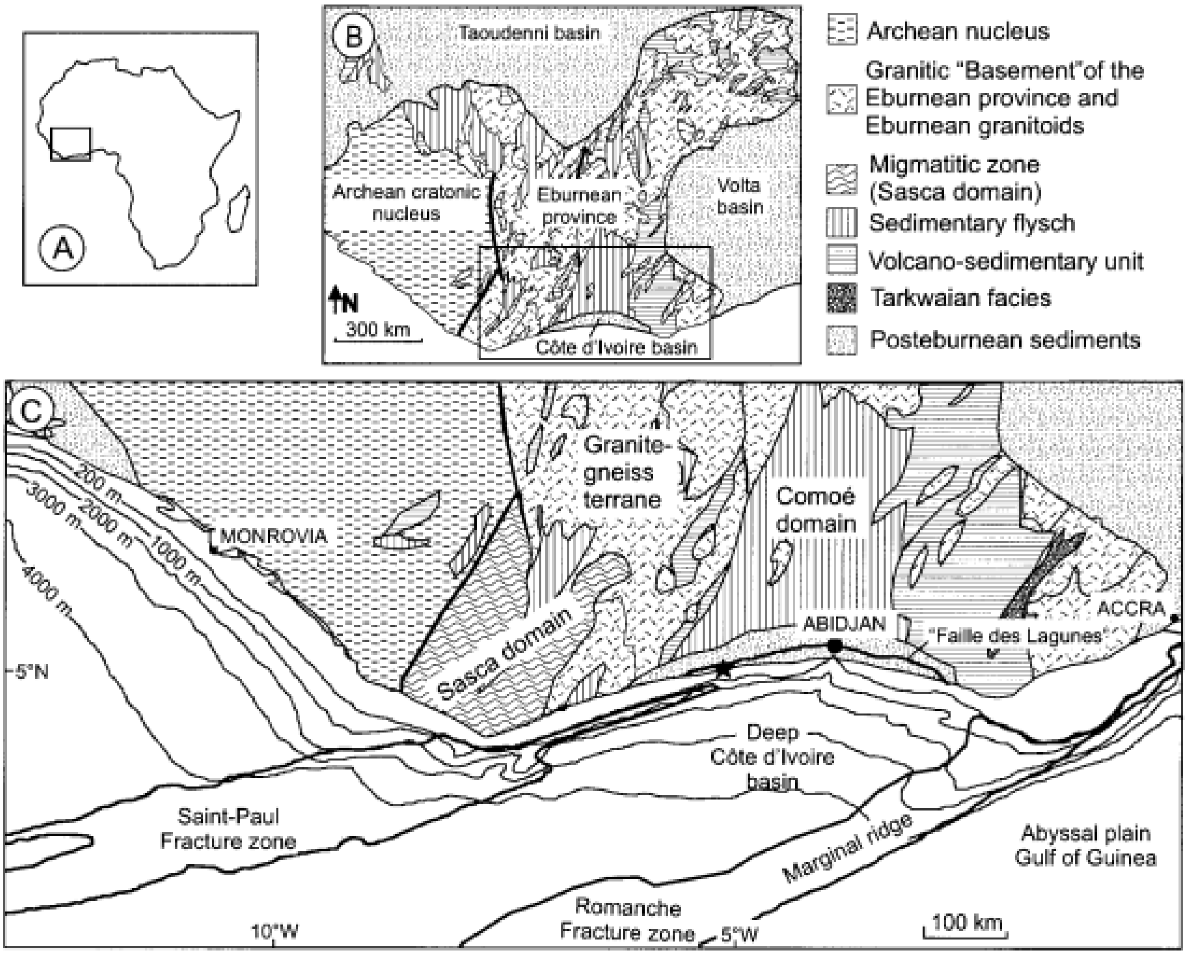

Figure 0-2: Location of the Côte d'Ivoire sedimentary basin: ***A****- the African context;* ***B****- Regional (west-African) geological framework;* ***C****- Geological map of southern Côte d'Ivoire and offshore bathymetry and structural (from Wozazek & Krawinkel(2002).*

As for the offshore basin, it extends along the entire length of the littoral from the shoreline to the deep water. The morphology of the offshore basin is quite regular except in front of the Port-Bouët Bay, where a large submarine canyon known as "Trou sans fond" notches it deeply. This canyon begins at the coast and ends 220 km away, at a depth of 5000 m in the Abyssal plain of the gulf of Guinea (Martin, 1974). The canyon influences sediment transport, coastal erosion, and the dynamics of offshore processes, potentially exacerbating coastal flood risk in the bay area.

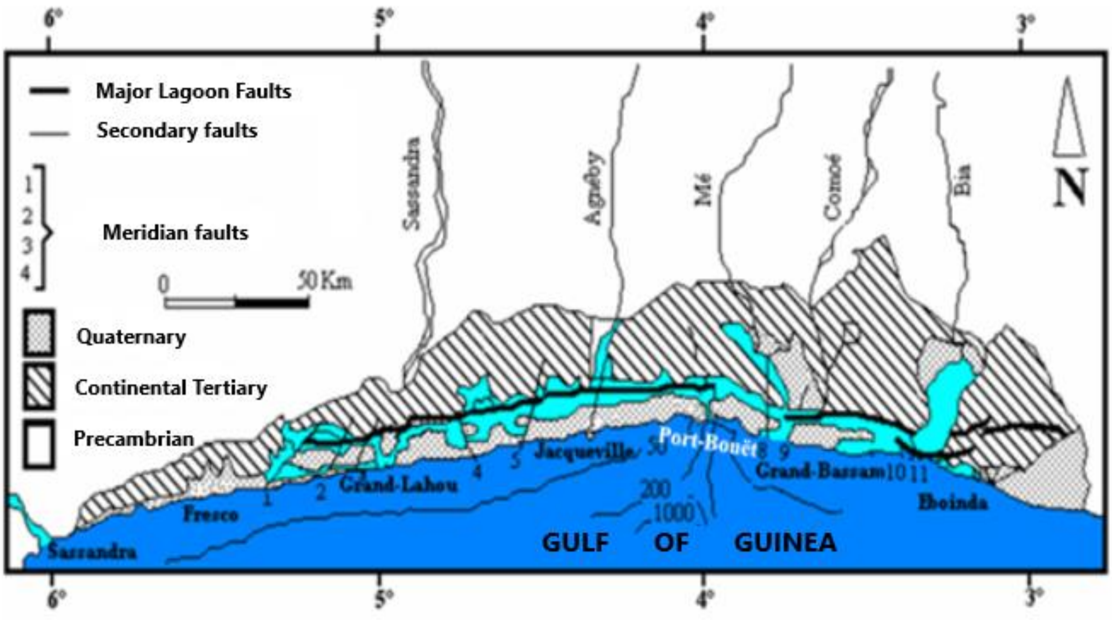

Figure 0-3: Detailed presentation of the Côte d'Ivoire Sedimentary basin, Modified from Yao (2012).

2.3.2. Geomorphology

The Port-Bouët Bay reflects a homogeneous topographic land, characterised by coastal plains. Indeed, the entire study site is below 10 m elevation, topography varies from 0 m to 7.8 m (JICA, 2015) which means that the area is a low elevation coastal zone (LECZ). It can also be viewed from figure 2-4 that the highest points in the area are located near the coast, which means that the land slopes gently decrease northward. This configuration makes the location at risk to coastal flood hazard in a sense that if a breaching of the coastal dunes by rough sea would have to happen, a large part of this area would face flooding. It should also be noted that there are some parts of this land, which are lower than the surrounding water, because they have been reclaimed from the lagoon.

The coast here is the steepest on the Ivorian shoreline. The beach slopes can vary a lot depending on the season, but they usually range from 5% to 10%. The continental shelf is very thin in this area because of the presence of the canyon "Trou Sans Fond". It is made up of different slopes, with 5% to 20% of it being very steep (Koffi, 2017). The 30-m isobath is close to the shore. It is about 200 meters away (see figure 2-5). The proximity to the shoals and the presence of multiple secondary notches connecting the canyon to the shore make this area a very turbulent with a strong bottom roughness (Koffi et *al.*, 1993).

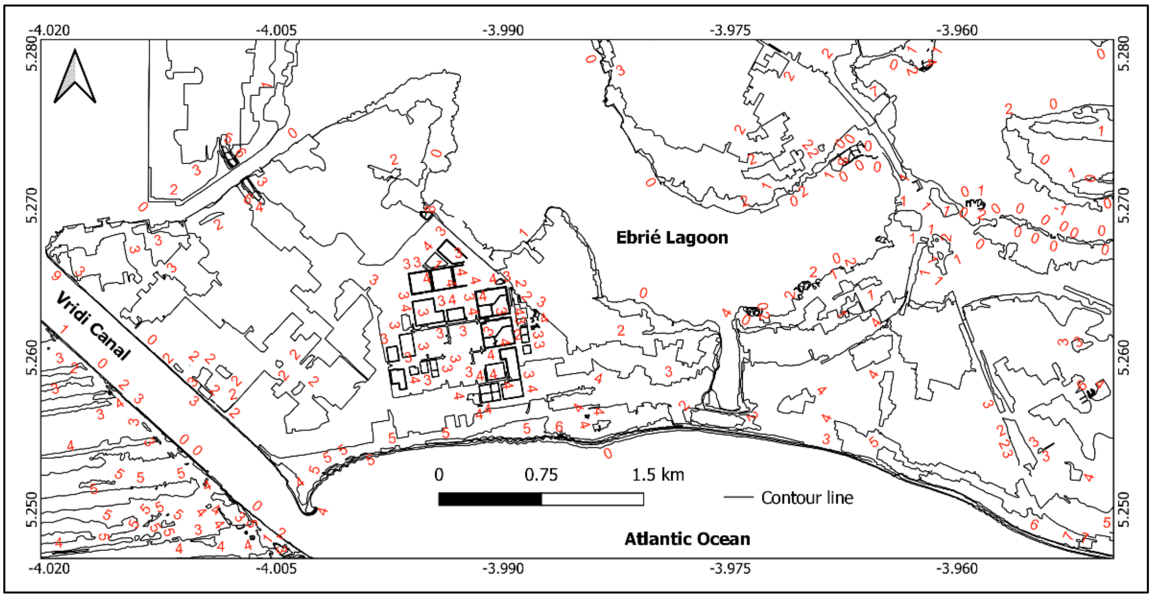

Figure 0-4: Topographic contour lines of the study site (Data source: JICA, 2015)

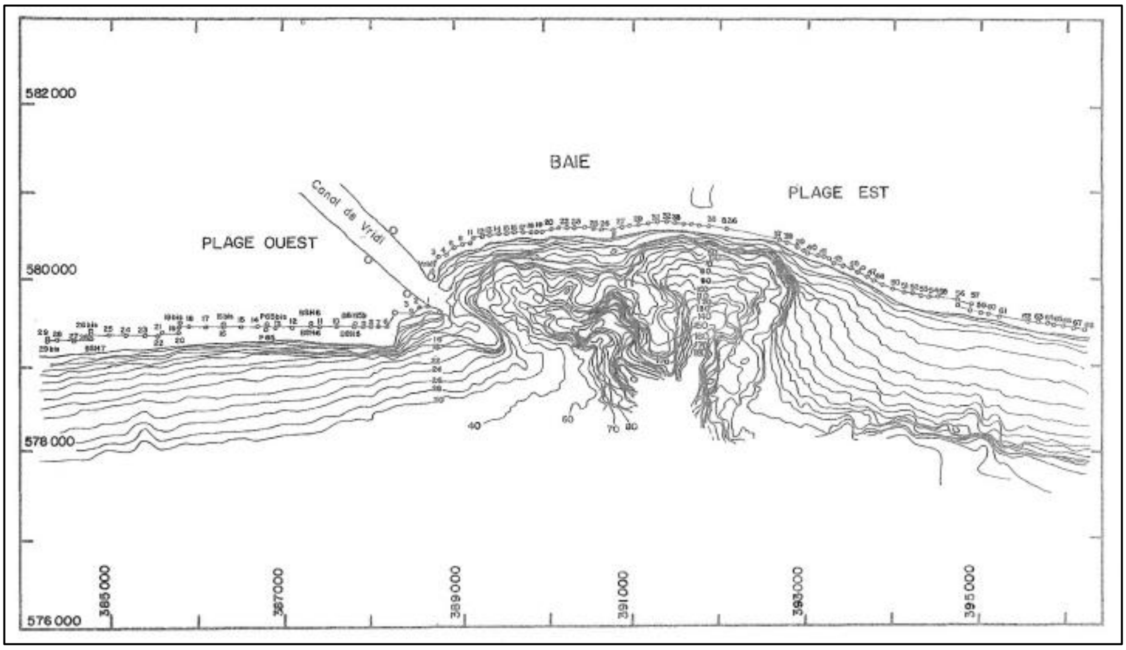

Figure 0-5: Bathymetric map of the Port-Bouët littoral zone (Koffi et al., 1993)

2.3.3. Sedimentology

The soil within the Port-Bouët Bay is composed of quaternary leaked sands. Depending on the season, the depth of the groundwater table may vary from 0 to 6 m (Lamothe & Rognon, 1975). Along the coast, quaternary to recent sands is observed. The coastal dynamic agents generate granulometric variations of surface sediments ranging from coarse sand (0.5 – 1.0 mm) to very coarse sand (1.0 – 2.0 mm). This range of grain size testifies to the reflective character of this portion of the Ivorian coastline. The study of N'guessan et *al*. (2018) revealed a gradual decrease in the sediment grain size from West to East within the study area. It also showed a slight decrease in the grain size from the surface to the depth at all the sampling sites. These variations can be explained by the simple facts that the energy of sediment depositions decreases eastwards and that for each sampling site, there exist different deposition environments. Generally, on reflective coast, there is a positive correlation between the wave energy and grain size, meaning that the more the wave energy is, the coarser the grain size will be and vice versa (Komar, 1998; Prodger et *al*., 2016). This correlation highlights the importance of wave dynamics in shaping coastal sedimentology and vulnerability to flooding. A five-years beach morphology monitoring by Saimon, Konan, et al. (2019) has shown that sediment sizes during low wave energy period (October-April) are coarser than those of the high wave energy period (May-July). This contrast could find explanations through other factors, more probably the intertidal beach face slope which also influence the grain size distribution on the beach (Mcfall, 2019)

The sediment transport within the area follows the main direction of the country's littoral drift i.e., from West to East. The average volume of sands transported per year is estimated to be around 400,000 m^3 (Tastet, 1987), underscoring the magnitude of coastal dynamics in the area. There is a general tendency for erosion in the zone. According to N'guessan et *al*. (2017), the average rate of the shoreline retreat varies between 0.2 and 1.5 m/year. Although the sediment balance is in favour of coastal erosion, it should be noted that for each sector of this coast, there is an alternation between the erosive and accretive phases, which indicates a natural self-balance of beach sedimentation (Saimon, N'Doufou, et *al*., 2019), and that significantly contribute in slowing the speed of the coastline retreat in the area.

2.3.4. Drainage

The Port-Bouët Bay is 87% surrounded by water to the south there is the Atlantic Ocean, to the north the Ebrié lagoon and to the west, the Vridi canal which serves as a junction between these two bodies of water. The lagoon water body to the north of the study site is also a bay (the Biétri Bay), which means that this selected area is sandwiched between two bays: a lagoon bay to the north and an ocean bay to the south. This geographical positioning exposes it to significant coastal flood risk. Water movements around the study site are therefore governed by both the tidal cycle and the hydrology of the rivers that flow into the Ebrié lagoon. Thus, at high tide during the dry seasons (period of low river discharge), significant inflow of marine water is observed in the lagoon, while at low tide during the wet seasons (period of high river discharge), the fresh waters pour considerably into the sea.

Freshwater inflows into the Ebrié lagoon are ensured by three main rivers: the Comoé (to the East of the city of Grand-Bassam), the Mé (Northeast of Bingerville) and the Agneby (to the East of Dabou). The largest freshwater inputs into the lagoon comes from the Comoé river. The average monthly discharges from the Comoé river is estimated to be varying between the maximum of 467.4 m^3/s in wet season (September -October) and a minimum of 1.3 m^3/s in dry season (January - March) (Fekete et *al*., 2002). The annual volume of freshwater brought by the Comoé, Mé and Agneby are 7.1×10^9 m^3, 1.5×10^9 m^3 and 0.9×10^9 m^3 respectively (Durand & Guiral, 1994).

The seasonal variations in both salt- and freshwater inputs strongly influence the physicochemical properties of the lagoon water, which vary in time and space. For example, during the rainy seasons and wet river periods, the salinity of the Biétri bay drops considerably (< 10 $g.l^{-1}$), whereas during the dry river seasons, it exceeds 25 $g.l^{-1}$ due to the predominance of ocean influence (Amani et *al*., 2019; Arfi & Guiral, 1994).

2.3.5. Climate

The climate of the Port-Bouët Bay reflects that which prevails over the whole district of Abidjan. It is basically a sub-tropical, hot and humid climate. The area experiences four seasons including two dry seasons and two rainy seasons. The distinction between the seasons is based on the average monthly rainfall (Abé, 2005). From figure 2-6, we can see that Avril to July brings heavy rains (long rainy season) while shorter rains occur during October and November. The influx of water during these rainy seasons, combined with the potential for high tides, can elevate the risk of flooding along the coast and low-lying areas. Shorter dry season occurs during August to September October and the main dry season occurring from December to Mars. January and June are the month with the lowest and highest average rainfall respectively.

Temperatures in the study area are comprised between a minimum of 22.19˚C and a maximum of 32.29˚C. The highest temperatures are observed in March while the lowest occurs during the month of August. In terms of annual variability, figure 2-6 shows two major trends throughout the year, from March to August, the average temperature decreases gradually from the maximum to the minimum while from August to November it increases from the minimum to the value of 27.51˚C. Such temperature fluctuations throughout the year can influence sea levels and storm intensity, both of which are critical factors in coastal flooding.

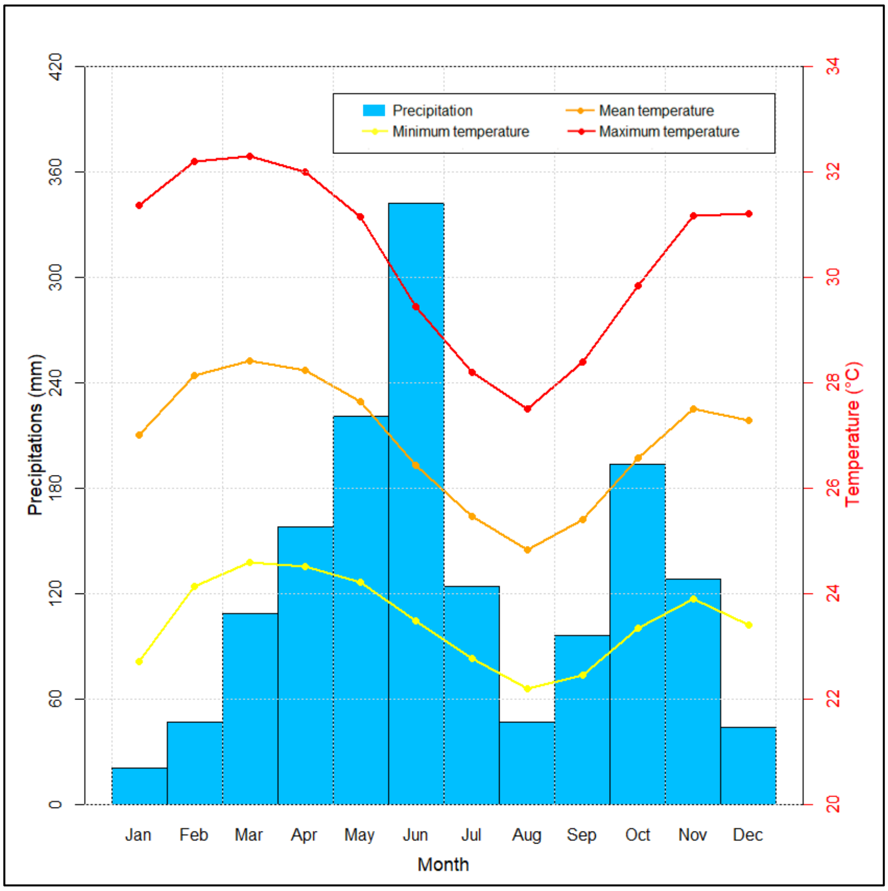

Figure 0-6: Monthly climatology of minimum, Mean & maximum temperature and precipitation from 1991 to 2020 in the Abidjan District (Data source: World Bank Group, 2021)

Regarding the historical evolution of the aforementioned climatic variables, the plottings obtained from datasets collected from the World Bank Group Climate Change Knowledge Portal (World Bank Group, 2021), make it possible to have an idea. In fact, these plottings illustrate the decadal trends of temperature and rainfall for each month through color representation. Historical temperature plottings clearly show a warming trend from 1991 to 2020. Most recent monthly mean temperatures are above the three-decade average trend (see figure 2-7). However, for precitations, it is much more difficult to discern a systematic trend over time. But as we can see from figure 2-8, in recent times (2011-2020), precipitations are increasingly getting higher during the rainy in comparison to those measured during previous decades. This trend suggests a higher likelihood of flooding in low-lying areas, including the coastal region of Port-Bouet Bay.

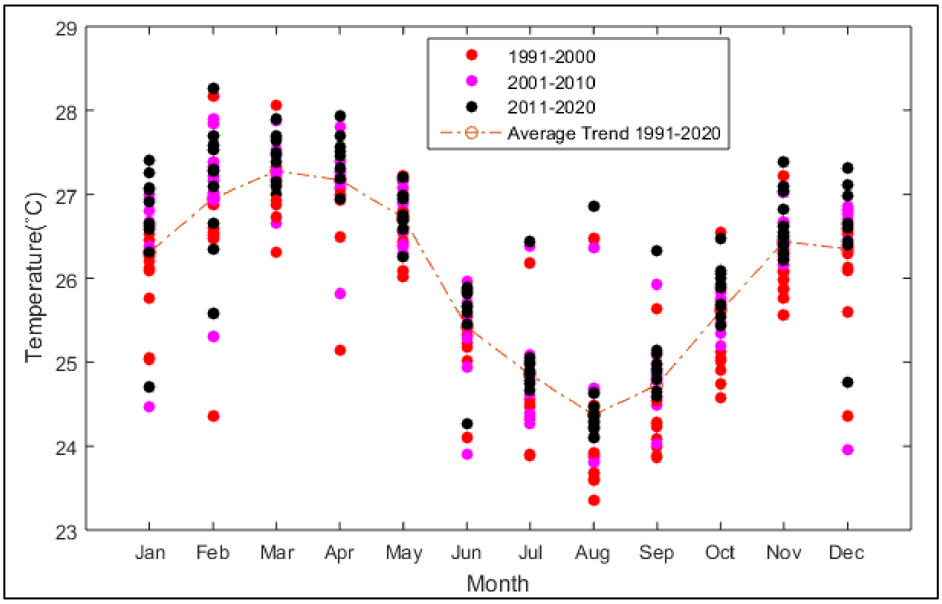

Figure 0-7: Variability and Trends of mean temperature across seasonal cycle from 1991 to 2020 in the Abidjan District (Data source: World Bank Group, 2021)

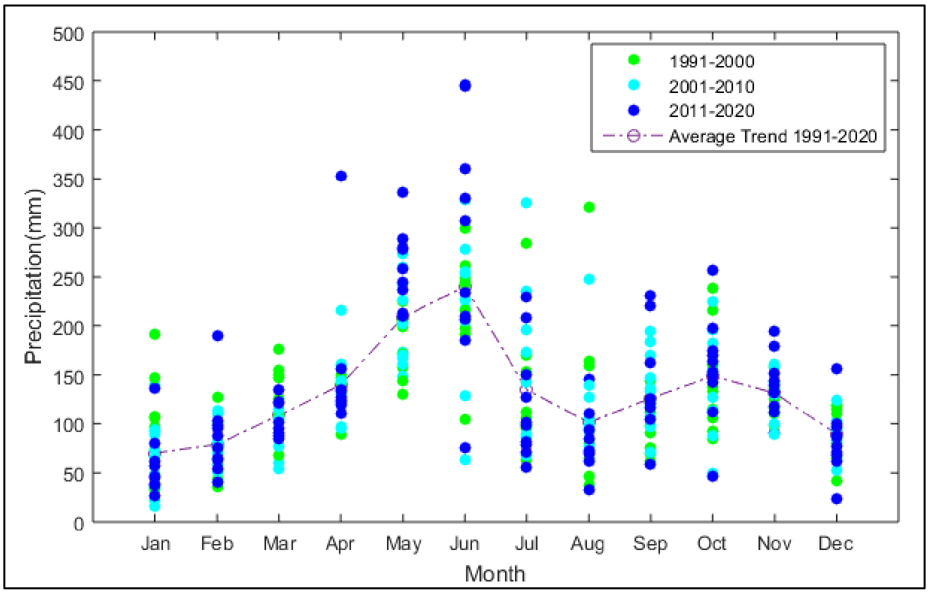

Figure 0-8: Variability and Trends of precipitation across seasonal cycle from 1991 to 2020 in the Abidjan District (Data source: World Bank Group, 2021)

2.3.6. Metocean Conditions

2.3.6.1. Tides and sea level change

In the Port-Bouët Bay like the entire Ivorian coastline, the tide is semi-diurnal with diurnal inequalities, meaning that there are two unequal tidal cycles (two different high tides or two different low tides) approximatively each day. The tidal range recently measured at the port of Abidjan is estimated to be varying between 1.2 m during spring tide and 0.5 m during neap tide

(Samassy, 2019). The coastline of the Port-Bouët Bay is thus microtidal (tidal range < 2 m). The interaction between the astronomical tide, precipitation and rivers discharges creates periodic variations in extreme water levels on both the lagoon and sea sides around the study area. In this regard, Samassy (2019) found that the highest water level on the sea side are observed in March and April. Whereas, in the Vridi canal and the Ebrié lagoon, the highest water level can be seen in October-November. The collection of tide gauge data over a sufficiently long period is very crucial for estimating and projecting the average trends of sea level evolution at this site. Samassy (2019), using tidal data from about 30 years (see figure 2-9), calculated the sea level change for the periods of February-March- Avril (period where precipitation and river discharges have very less effects on tide) and found an average sea level rise of 2.89 mm/year. This rate serves as a warning sign for potential exacerbation of coastal flood risk in the future. For projections of future sea level change in the area, IPCC (2021) provides relevant insights (see chapter 4).

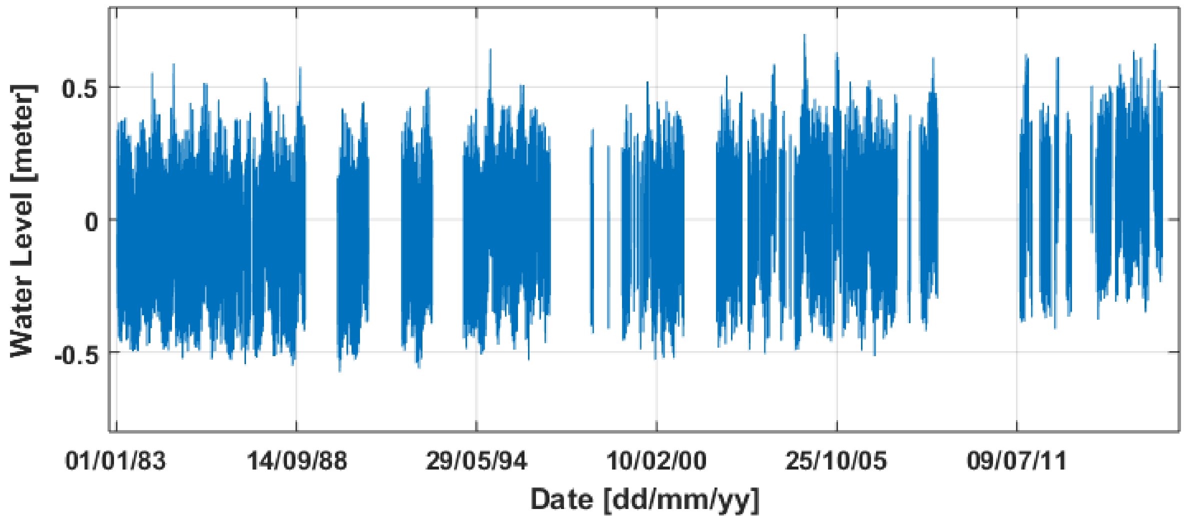

Figure 0-9: Water level measurements from 1983 to 2016at the Quai-Nord station of the Port of Abidjan

2.3.6.2. Wave and wind climate

The wave climate along the Ivoirian coastline is characterized by long-crested waves or swells (Roelvink et *al*., 2013). Off the coast of Port-Bouët, swells are generated in the deep-sea area under strong wind speed and reach the coast predominantly from the South, Southwest (SSW) direction as shown in figure 2-10 (Brière et *al*., 2015; Yao et *al*., 2018). On seabed greater than 20 m, the amplitudes of the swells vary between 0.5 and 2.5 m with period (T) between 7 and 20 s. However, the maximum annual significant wave height (Hs) is estimated as 3.3 m and could reach 4.2 m in a decadal assessment (Quelennec, 1984). These long-crested waves, with varying amplitudes and periods, play a significant role in shaping nearshore conditions and influencing coastal processes. The swell climate presents a seasonal variation. According to Tastet (1985) the heaviest swells ($H_s = 1.8 - \ 2\ m\ and\ T = 10 - 20s$) occur mainly in the months of May and June while the lowest ($H = 0.8 - 1.0m\ and\ T = 7 - 11s$) appear in November and December. The other periods of the years are characterised by moderate swell ($H = 0.8 - 1.8m\ and\ T = 10s$). The mean wave direction at Port-Bouët Bay is approximately 200 degrees, which differs slightly from the surrounding areas, where it is about 186 degrees (refer to figures 2-10 and 2-11). West of the study area, the mean wave direction aligns with that of deep-sea wave direction. However, on the eastern side, near Grand-Bassam, it is estimated to be around 190 degrees (see figure 2-11).

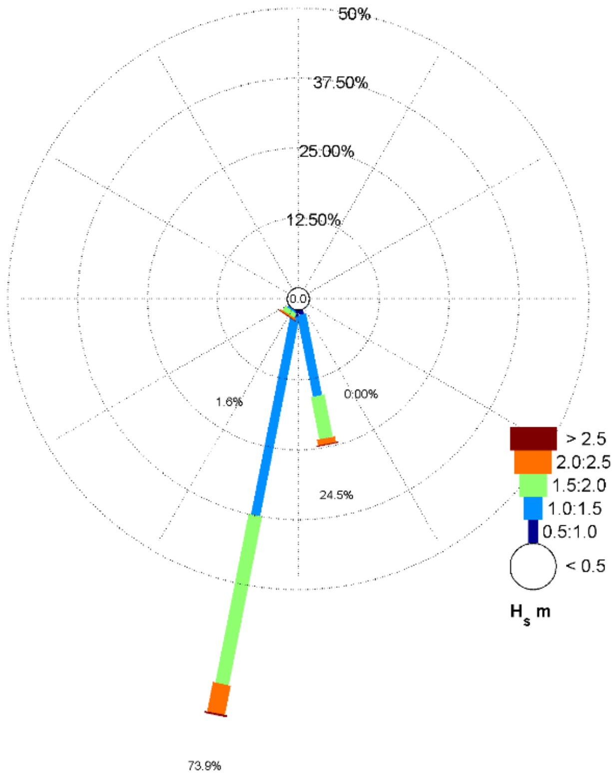

Figure 0-10: Wave rose off the coast of Port-Bouët precisely at the location 4.5 N -3.75 E for the period 1979-2014 (Brière et al., 2015). The average Hs is 1.51m for a main direction of 186 degrees

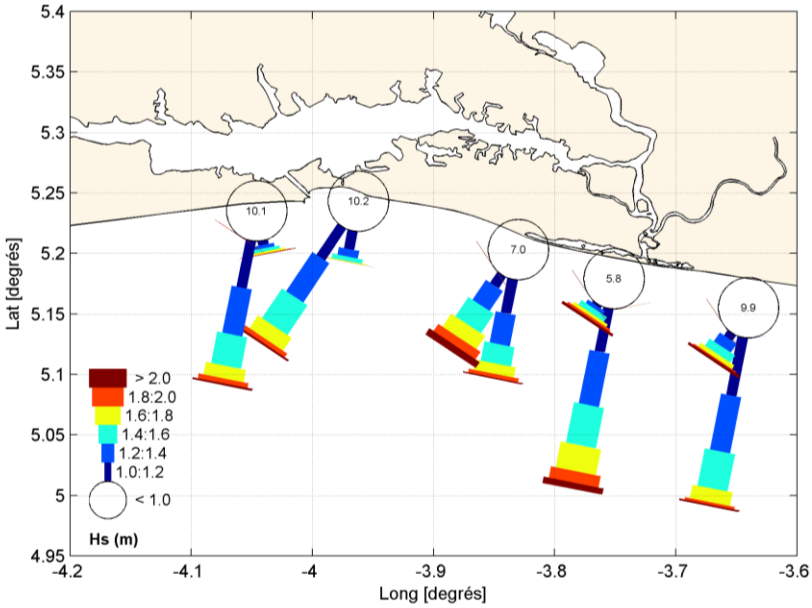

Figure 0-11: Variations in coastal wave direction from Western Port-Bouët to the Eastern side of Grand-Bassam. The wave direction at Port-Bouët Bay appears slightly higher than the surrounding area (Brière et al., 2015).

As swell waves approach the shoreline, the shallower seabed affect the waves and makes them to break i.e., they become steeper as they begin to slow down under the effect of bottom friction. This generally start occurring where water depth is equal to half the deep-water wavelength and contributes to coastal inundation and erosion. So, within the nearshore zone (area between the offshore limit and the shoreline) swell waves are described with the terms "Wave runup", "wave set-up" and "wave swash" that have already been discussed in chapter 1. Very little is known about local coastal wave conditions, probably due to the difficulty of measurements in the nearshore zone (high turbulence). However, the application of recent innovative techniques of data collection like the video imagery could be very beneficial.

It should also be noted that the influence of climate change on the local swell climate is also poorly known. Nevertheless, from the global assessment of (Hemer et *al*., 2013; Mentaschi et *al*., 2017), it appear evident that climate change will make extreme swell to be more frequent and intense with significant implications for coastal flood risk, as more frequent and intense waves can amplify the impacts of storm surges and exacerbate coastal flood and erosion.

The local winds blow from the South-Western directions (Austral Trade winds) with an average velocity of 4.06 m. s^{-1} for a mean direction of 208 degrees (Brière et *al*., 2015). As winds reach inland from the sea, they get weaker (Arfi & Guiral, 1994). Within the study area, the wind strength and direction are seasonal. The strongest trade winds occur in August with an average speed of 5 m.s^{-1} and a main direction of 205 degrees. The lowest winds, with an average velocity of 3.2 m. s^{-1} blowing from 190 degrees, are observed in December (Brière et *al*., 2015). The period from December to February is much dominated by Boreal winds also called “Harmattan”, which is a dry air mass coming from the Northeast direction. In recent time, this type of winds blows only for few days over this coastal area. A direction/ speed wind rose using 1979-2014 data is presented in the figure 2-12. Note that the seasonal variations in wind strength and direction, coinciding with changes in wave climate, could further complicate the assessment of coastal flood risk. This would necessitate comprehensive modelling approaches.

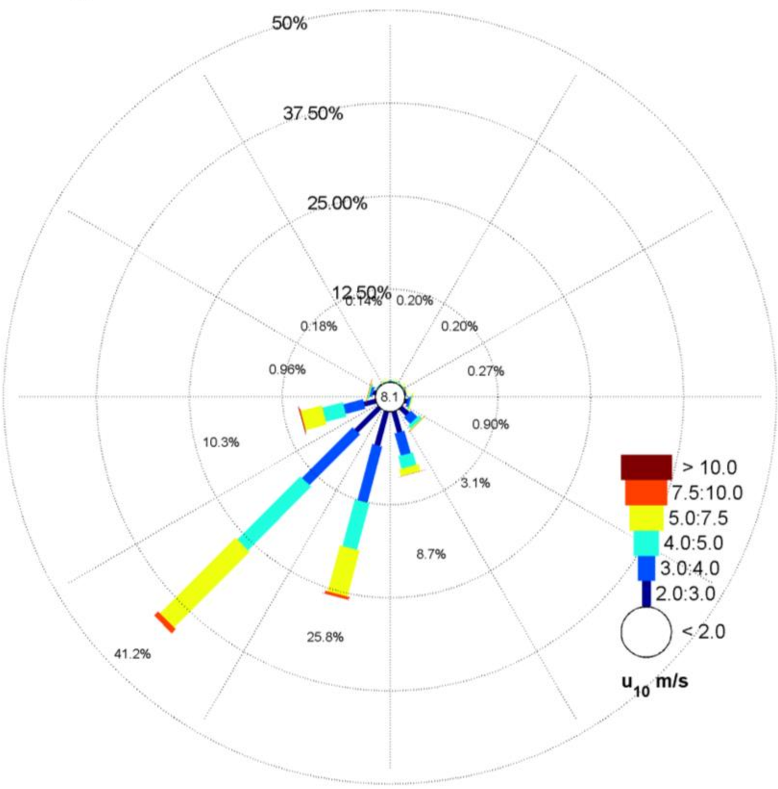

Figure 0-12: Wind Rose at the location 4.5 N; -3.75 E for the period 1979-2014. The average wind speed is 4.06 m. s^{-1} m for a main direction of 208 degrees (Brière et al., 2015).

2.3.6.3. Storm surges Conditions

Storm surges are produced by storm wind forces pushing the ocean water to the shore. They can be very high in some locations of the globe and can cause many damages. Understanding their occurrence and magnitude is essential for assessing coastal flood risk and implementing appropriate mitigation measures. Within our study area, storm surges levels are relatively very low (they generally do not exceed 0.5 m). Their frequencies vary between 3 - 13% depending on the seasons. They mostly occur they occur from October to March and during the heavy rains season (June - July). Samassy (2019) identified the ten majors storm surge events in Abidjan from 1979 to 2015. Among these, the highest storm surge event with an amplitude of

0.46 m was observed on 09 August 1979. And the lowest of the ten was observed on 25 February 1999 with an amplitude of about 0.3 m.

Note that although storm surge and swell are both meteorological in origin, their occurrence do not always coincide. This distinction is critical for accurately modelling and predicting coastal inundation events, as each phenomenon presents unique challenges and impacts on coastal areas.

2.3.6.4. Currents

Current patterns around Port-Bouët are generated in several ways. On the seaside, surface water currents are largely dominated by the so-called "Guinea Current" which moves predominantly from West to East. This surface current carries warm waters towards the coasts at a variable speed (>60 cm/s (Lemasson & Rebert, 1973)), the highest of which is during the warm seasons. At about 40 m depth on the continental shelf, there is a counter-current "the Ivorian under-current" (Lemasson & Rebert, 1968, 1973), oriented towards the west with very low speeds (< 10 cm/s).

In the lagoon, currents patterns may be generated from tides, rivers discharges and by wind action. But the primary type of currents in the lagoon is the tidal current. They are produced by tide water entering and leaving the Ebrié lagoon. However, in some parts of the lagoon where tides have limited effects, the wind can play the major role in the circulation. The measurements taken by (Sogreah, 2000) at water surface in the lagoon showed great variability in both time and space. The maximal current speed may reach 2 m/s in the Vridi canal (Durand & Guiral, 1994), highlighting the potential for rapid water movement, which can exacerbate coastal flooding and erosion in vulnerable areas of the Port-Bouët Bay.

2.4. Socioeconomic Characteristics

2.4.1. Demography

According to the General Census of Population and Housing of 2021 (INS, 2021), the whole city of Port-Bouët has a population of 618,795 inhabitants including 48% of woman and 52% of men. With this population, Port-Bouët is the fourth most populated municipality within the district of Abidjan. There are approximately 146,903 households in the city with an average household size of 4.2 persons per household. The annual population growth rate estimated over the period from 2014 to 2021 is around 5.3%, a rate higher than the national and district averages of 3.48% and 2.79% respectively. This growth rate results from two factors that are specific to the Ivorian national context: (i) strong natural growth and (ii) a largely positive migratory balance (BNETD, 2018). The native populations of Port-Bouët are the Ebriés (also called the Atchans). But the city is characterized by a cosmopolitan population made up of Ivorians and non-Ivorians. In general, the population is subject to the general political and administrative organization consecrated by the state power. Alongside this socio-political organization of modern type, there is a traditional organization based on the ethnic affiliation or the geographical origin of the populations. Generally, the social organization of native people differs from that of allochthonous and allogeneic communities.

Looking at the city's population density, which is of 84 /ha, the population of the selected study area, may be estimated at about 96,600 people. The concentration of populations in this relatively small coastal area increase exposure to flood hazards and can exacerbate the impacts of inundation on infrastructure, livelihoods, and public health.

2.4.2. Economic Activities

Because of its location, the Port-Bouët Bay is an economically strategic zone. There are several important economic infrastructures within the area. These include the industrial zone of Vridi, which is the largest in the country, the southern sector of the port of Abidjan (figure 2-13a), the Ivorian refining company (figure 2-13b), the slaughterhouse (the main deserving all the District of Abidjan), the lighthouse and the international road leading to the country's border with Ghana.

(a) (b)

Figure 0-13: Pictures of the industrial area east of the Vridi canal (a) and the Ivorian refining company (b) located in Vridi, both are located within the study zone

Economic activities occupy a larger part of this land and are distributed into the following sectors of activity (BNETD, 2018; ONU-Habitat, 2011).

- Primary sector: there is little agricultural activity in the region. Nevertheless, there are some few farms and fishing activities. Only 6% of the City's workload is dedicated to this type of activity.
- Secondary sector: this sector provides 20% of employment in the whole Port-Bouët. Occupations include raw material processing industries (coffee, cocoa, Hevea, etc.), oil and gas industries, dairy and beverage industries, construction industries and textile industries.
- Tertiary sector: it creates more jobs than the two previous sectors. The sector employs approximately 74% of the city's workers. Here, the three most productive sub-sectors are wholesale and retail trade (30.3%), social services (9.85%) and transport and telecommunications services (9.47%).

Besides these above-mentioned sectors, several other services can be found within the selected area. They include various banking institutions, petrol service stations. The presence of these important economic infrastructures underscores the economic importance of the area. However, these infrastructures are also vulnerable to coastal flooding, which can disrupt operations, damage facilities, and disrupt supply chains, leading to significant economic losses.

2.5. Environmental Characteristics

Due to its high level of urbanization and the presence of numerous industries as well as the port, the Port-Bouët Bay is subject to many environmental challenges, leading to various types of pollution. These pollutions may concern water bodies, the living environment and air quality (Adingra & Kouassi, 2011)

- *Pollution of water bodies*

The lagoon bay to the north of the study site (Bay of Biétri) is subject to heavy pollution due to the unceasing discharges of wastewater (without or with very little pre-treatment) and solid waste into the lagoon by industries and populations. This pollution is even more accentuated as the Bay of Biétri has a low rate of renewal, partly due to the low supply of fresh and marine water in this part of the Ebrié lagoon. The study of Amani et *al*. (2019) revealed a high content of suspended matters (52 mg/l), which is directly linked to the discharge of wastewaters into the bay. This heavy pollution of the Bay of Biétri, not only poses significant ecological risks but also contributes to coastal erosion. Pollution from wastewater discharge and solid waste deposition can degrade shoreline habitats and accelerate coastal erosion processes. Weakening coastal ecosystems through pollution increases the susceptibility of coastal areas to flooding and inundation, further exacerbating the impacts of extreme weather events.

In the marine domain, environmental problems arise from the invasion by aquatic plant waste and plastic waste, which generally washes up, on the beach (see figure 2-14). This waste is of continental origin. They therefore reach the marine domain by passing through the Vridi channel. However, we note that some of this waste can come from the open sea (deliberate or accidental dumping by ships). To these problems already listed, we can add the accidental spillage of hydrocarbons due to maritime transport and the operations of tankers in the port of Abidjan. In addition, the pollution from chemical pesticides used in plantations within the Abidjan district and that can reach the water bodies through runoff.

Figure 0-14: discharge of plastic and organic wastes by the sea on the beach of the Port-Bouët Bay (Photo credit: K.M.D.P. KOUAKOU on the 2022-02-04)

The impacts of this water bodies pollution can be ecological with losses of shoreline habitats, bottom degradation, fragmentation of plastics and ingestion by marine fauna. Impacts can also be on economic activities that are based on the attractiveness of the sandy beaches:

- *Degradation of the living environment*

The dwellings located alongside the lagoon and the coastline are mostly precarious. The major problem for households of this area is then about sanitation, which is mainly of the autonomous type (disposal of wastes on the ground and by septic tank). According to Coulibaly et *al*. (2004), in precarious households of Port-Bouët, 73-99% of domestic wastewater is dumped on the ground (figure 2-15) against 1-22% in septic tanks. In addition, the difficulty of accessing these precarious settlements makes it difficult to collect solid wastes, which leads residents to throw garbage in lagoons, on the beach or in landfills within the living environment. This situation exposes populations to certain diseases such as malaria, diarrhoea and typhoid fever. In such conditions if a climatic disaster would have to occur, the consequences will not only be of a security and economic nature, but also of a health nature.

Figure 0-15: Picture showing dumping of domestic wastes and wastewater (shown by the red arrow) on the ground (Photo credit: K.M.D.P. KOUAKOU on the 2022-02-05)

- *Air pollution (including noise nuisances) from industries*

Data on air pollution in the study area are limited. However, measurements carried out by Bahino (2018) in the district of Abidjan indicate a relatively good overall air quality. But, in the vicinity of the sources of pollution (Traffic and industry / Dump), measurements can sometimes exceed the quality thresholds for certain pollutants (e.g., NO_2, H_2S and Particulate deposits). Therefore, in the Port-Bouët Bay, the coexistence between dwellings (precarious and residential) with industries of all types exposes populations at times to issues related to air pollution (smoke, dust, odours, etc.). The noises emitted by the factories are also sources of discomfort for the local population.

Facing with all these environmental challenges, local authorities are involved in certain actions aiming at reducing pollution and nuisances. These particularly include the pre-collection and transportation of waste to consolidation stations; the construction and management of a waste composting centre; the maintenance of gutters and public green spaces; the fighting against insalubrity, pollution and nuisances. To these, must be added the spontaneous aids from non-profit organisation and associations in cleaning the beaches and sensitizing the residents.

However, noteworthy that much remains to be done to considerably reduce the pollution rate in this area and enhance the resilience of coastal communities to environmental hazards, including flooding. Integrating environmental considerations into coastal flood risk management strategies, such as green infrastructure development, ecosystem restoration, and community-based adaptation initiatives, can help build resilience and promote sustainable coastal development.

2.6. Coastal Management

Along the Ivorian coastline, critical connections exist among physical, socio-economic, and environmental aspects. The Côte d'Ivoire aims for integrated and sustainable management of its coastal zone to ensure coastline integrity, safety, and combat the negative trend of coastal hazards exacerbated by climate change. To achieve this, strategic plans have been developed:

- The White Paper on the Ivorian Coast (2004) outlines a coastal management strategy focusing on land use issues, pollution, institutional frameworks, and public education. However, it lacks adequate measures for addressing climate change challenges.
- The National Environmental Policy (2011) which serves as a comprehensive reference for environmental matters, proposing approaches for environmental protection, including the coastal environment. Though it does not directly tackle coastal hazards issues, it offers valuable insights.

To translate these policies into action, legislative laws are necessary. The Law concerning the development, protection, and integrated management of the Ivorian coastline, adopted in 2017, aims to sustainably manage coastal areas, establishing principles for resource use. Numerous stakeholders, including government ministries, territorial collectivities, civil society organizations, and the private sector, are involved in coastal zone management. However, challenges such as overlapping responsibilities and inadequate coordination persist.

According to the Local Agenda 21 of the Rio de Janeiro Convention 1992, the Ministry in charge of the Environment is responsible for coastal management (PNGEC, 2015). However, cooperation with other ministries is required, highlighting the need for better coordination. Despite efforts, there is no comprehensive strategy for managing coastal flood risk along the Ivorian coastline.

Nevertheless, specific plans exist, such as the Plan for combating lagoon pollution (POLLUMAR), a draft program for integrated coastal zone management under the National

Environmental Action Plan (NEAP), and a pilot case study of a coastal resilience program in Grand-Lahou as part of the WACA-ResIP (West Africa Coastal Area Resilience Investment Program). These initiatives not only highlight the ongoing commitment to coastal management and resilience-building efforts but also underscore the importance of establishing legal frameworks and ensuring effective coordination and implementation across various governmental bodies and stakeholders.

In the case of the Port-Bouët Bay, the absence of a coastal development master plan, the lack of an integrated coastal zone management program and limited financial resources hinder effective implementation.

2.7. Conclusion

The characterization of the Port-Bouët Bay has allowed to know that it is situated is on the Ivorian sedimentary basin which is made up of quaternary sands and endowed with a relatively low topography. The area also has a sub-equatorial climate composed of four seasons and with temperatures not exceeding 32.5˚C. The metocean context is dominated by swells. As for the microtidal tide, it greatly influences the lagoon dynamics. Nevertheless, the temporal evolution of certain climatic parameters in the area, in particular the precipitation, temperature, storm surges and swells, more or less show the effects of climate change.

The analysis of the socio-economic context has shown that the study site is an area of very high economic importance, being characterized by a cosmopolitan population and hosting almost all sectors of economic activity. However, the Port-Bouët Bay is confronted with pollution issues with more or less significant impacts on population health and development of the area. These would exacerbate the impacts of flooding events along this particular coastal area. The implementation of integrated coastal zone management, which could help address the issues more effectively, is hindered by several limitations.

QUANTIFYING CHANGES IN EXTREME SEA LEVELS (ESLS)

Most contents of this chapter have been published in the article:

Kouakou, M., Bonou, F., Gnandi, K., Djagoua, E., Idrissou, M., & Abunkudugu, A. (2023). Determination of Current and Future Extreme Sea Levels at the Local Scale in Port-Bouët Bay (Côte d'Ivoire). *Journal of Marine Science and Engineering*, *11*(4), 756. https://doi.org/10.3390/jmse11040756

3.1. Introduction

Climate change induced by the global rising temperatures generates two majors consequences on the coastal environment (Howard & Palmer, 2019). They include the mean sea level rise (Milne et *al*, 2009; Church et al 2013) and the strengthening of meteorological storms (Marcos et *al.*, 2019). Both processes significantly contributed to increasing the frequency and the intensity of extreme sea level (ESL) occurrences over the last decades in many parts of the globe (Vousdoukas et *al*., 2017; Weisse et *al*., 2014; Wong et *al*., 2022). Extreme sea level indicates the episodic high elevation of the coastal sea during storms. As such, it results from the compounding effects of the different ocean dynamic factors which are storm tide (astronomical tide + storm surge), ocean wave and regional relative sea-level rise (Walsh et al., 2012; Kirezci et *al.*, 2020; Watson, 2022). In general, when at least one among these contributing factors is at an uncommonly high level, the resulting total coastal water level can exceed a certain threshold (Percival 2016), leading to devastating impacts, especially along the densely urbanized coastal areas.

Extreme sea level events are historically rare, but highly variable in both time and space. In other words, ESLs differ from place to place and two consecutive events in a given place may not probably have the same characteristics. Already, a couple of global studies have already investigated on the issue of ESL changes. For example, Vousdoukas et *al*. (2017) and Almar et *al.* (2021) found that changes in future ESLs will be noticeable even with limited variations in mean sea level. Tebaldi et *al*., (2021), showed that the present-day once-a-century ESL will probably become an annual event by 2100 in many locations on the planet. For Frederikse et *al.* (2020), changes in ESLs are likely to come sooner than the end of the century. Nevertheless, Serafin et *al.* (2019) recommends smaller scale studies to enable site-specific adaptation and planning to tackle the possible impacts.

Coastal floodings are almost consistently associated with ESLs (Butler et *al.*, 2007). So, more frequent and intense ESLs would probably mean an increase in the number and the severity of coastal flood events. Knowledge on ESL changes, then, would constitute a crucial basis for assessing coastal flood risk trend for any given coastal zone. However, as ESLs are made up from different variables, their determination requires not only information on the magnitude of individual ESL's component but also an understanding of the probability of their joint occurrence. Though this may appear simple in theory, there may be some practical challenges related to the data unavailability (especially in a data scared country like Cote d'Ivoire) and/or the complexity of combination of methods which may limit the determination of ESLs and therefore the comprehension of coastal flood risk. In such condition, appropriate techniques and tools to overcome the challenges must be applied all along the process of determining extremes. This is what we will try to consider in this part of the work which has the objective of quantifying the changes in ESL under climate change at the different neighbourhoods along the Port-Bouët Bay. The aim here is to develop robust ESL scenarios that can help in coastal flood risk assessment for sustainable and effective coastal management and future planning. The chapter is structured as follows: firstly, the data and methodology to estimate individual ESL's components as well as their combination is presented; secondly, the spatial and temporal distribution of ESL elevations is analysed for the selected study area; finally, discussion and perspectives are made regarding the outcomes of the analysis.

3.2. Data and Methodology

3.2.1. Approach overview

In this study, we define extreme sea level (ESL) as the sum of storm tide (ST), the wave runup ($R_{2\%}$) and sea-level rise (SLR) as shown in Equation 3-1 with all estimation based on the local MSL datum.

$$ESL = ST + R_{2\%} + SLR \qquad \textit{(Equation 3-1)}$$

At any given time, these three components can be combined to calculate the extreme elevation(s) that the sea may reach. However, due to their different time-scale variations, accurate evaluations of contributions from parameters such as storm tide and wave runup can be made better for the present time. Therefore, assuming that the present SLR is negligible, we define the present-day and the future ESLs as expressed in equation 3-2 and 3-3, respectively.

$$ESL_{present-day} = ST + R_{2\%} \qquad \textit{(Equation 3-2)}$$

$$ESL_{future} = ESL_{present-day} + SLR \qquad \textit{(Equation 3-3)}$$

Solving these equations is equivalent to determining each element that composes them. However, the process is not straightforward because extreme sea level (ESL) events are rare and can only be accurately understood by observing sea level over a long period of time (Roberts et *al.*, 2020). In other words, the calculation of ESL requires historical sea level data that is both long and of high quality. For accurate ESL calculations, historical sea level data should ideally be measured at a reference point (datum), sampled at hourly intervals, and free of any data gaps. Meeting these criteria is generally challenging, particularly for developing coastal countries that may lack the necessary resources and equipment. To overcome the lack of quality data, techniques have been developed to calculate extremes from shorter records (Thompson et *al.* 2009). Other techniques involve reconstructing historical sea level time series to increase the necessary data length and/or to fill any gaps. The latter techniques have the advantage of enabling efficient extreme analysis and thus provide accurate estimates. In this study, we opted to reconstruct sea level records over the past 40 years for both storm tide and wave runup using various modelling methods. Figure 3-1 provides an overview of the methodological approach. Below, we provide detailed explanations of the modelling process, statistical methods, and data used.

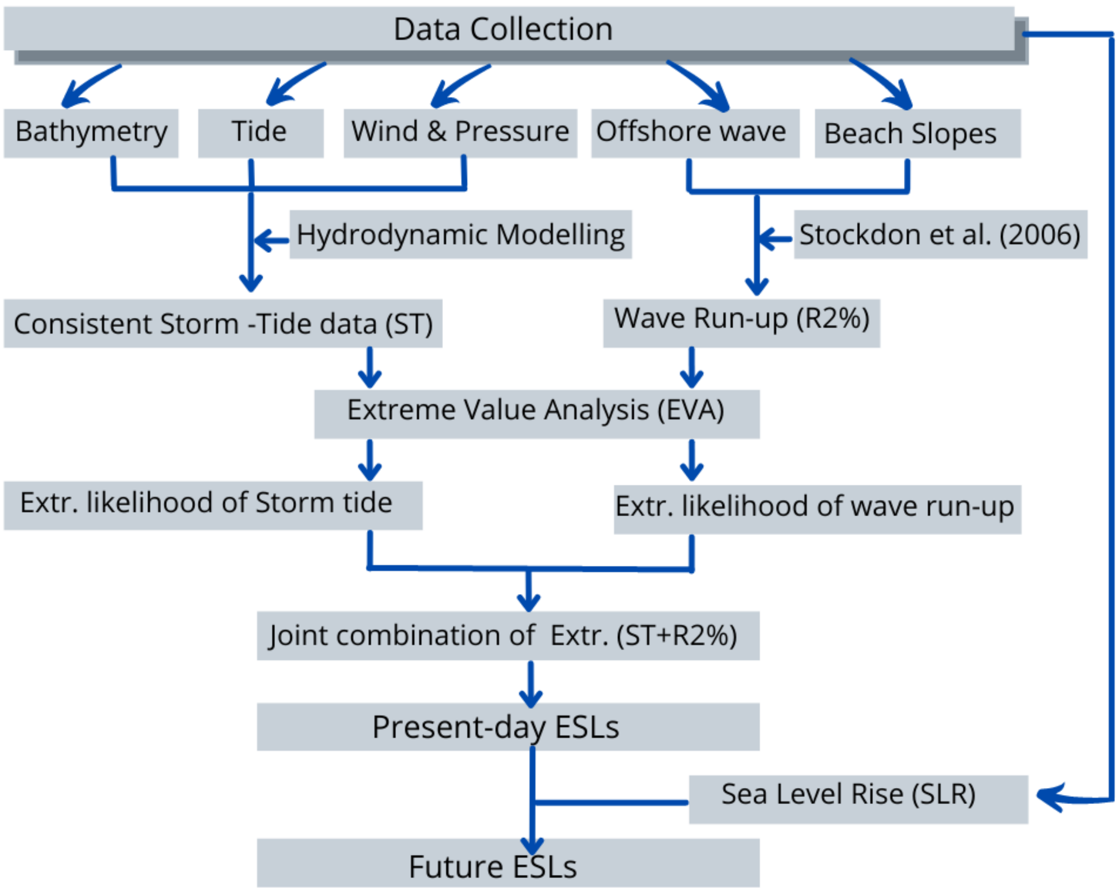

Figure 0-1: Methodological Approach. "Extr." stands for Extreme; "ST" for Storm Tide and the acronym "ESLs" denotes Extreme Sea Levels

3.2.2. Data

To perform this study, some data were necessary. They fall into two categories. On one side, the metocean data, which include offshore wave, wind, atmospheric pressure, tide gauge data and sea level rise projections. On the other side, the morphological data that include beach profiles and bathymetry data.

For the Port-Bouët Bay, water level data are available through the tide gauge stations of the Port of Abidjan. We collected the 33 years (from 1983 to 2016) of available measurements at the former tidal station "Quai-Nord" located on latitude 5° 18.230'N and longitude 4° 1.570'W. This hourly dataset was mostly digitized from archived records and has undergone extensive quality check as part of the study of Samassy (2019), and has been made available for use in this study. Even though, the collected dataset has acceptable overall length, it is limited to the port domain and contain several gaps ranging from a minimum of a single hour to a maximum of 2.6 years of consecutive missing values. The total gaps represent about 46% of the overall length, making the dataset failing to meet the quality requirements for a direct use in an extreme value analysis. Alternatively, it was used as a base dataset for storm-tide modeling.

Offshore wave, wind and atmospheric pressure data were all obtained from the ERA5 global reanalysis database (Hersbach et *al.*, 2018). In Côte d'Ivoire, there is a huge lack of in-situ ocean climate data. In such situation, the ERA5 reanalysis data, with their acceptable performance in several regions of the globe (Bruno et *al.*, 2020; Foli et *al.*, 2021), constitute a good alternative for providing an overview of the offshore condition and overcoming the lack of in situ measurement. For the analysis, we extracted 40-years (1981 – 2020) of historical hourly data for each of pre-cited process. The wave data include the significant height, period and direction of the wave. The collected wind data are the zonal and meridional components of the surface wind field.

The information on sea-level-rise for Port-Bouët was obtained from the 6th IPCC AR6 Sea-Level Projection Tool (Fox-Kemper et *al.*, 2021; Garner et *al.*, in prep., 2021), which provides estimates of future sea-level changes relative to a baseline of 1995–2014 at the regional level. In their latest sea level projections, the IPCC recommends the use of the Shared Socioeconomic Pathways (SSPs) scenarios, which encompass a wider range of greenhouse gas and CO_2 emissions than previous scenarios (Arias et *al.*, 2021). The core set of five SSP scenarios is designed from combinations of processes for which projections can be made with medium confidence, while two additional low-confidence scenarios account for deeply uncertain processes, resulting in seven SSP scenarios. For this study, we focus on three medium-confidence scenarios, namely SSP1-2.6, SSP2-4.5, and SSP5-8.5, which correspond to low, intermediate, and very high greenhouse gas and CO_2 emissions, respectively. Figure 3-2 illustrates the SLR projections for these three SSP scenarios at the coordinate point (4°0.000′N; 4°0.000′W) off the coast of Port-Bouët

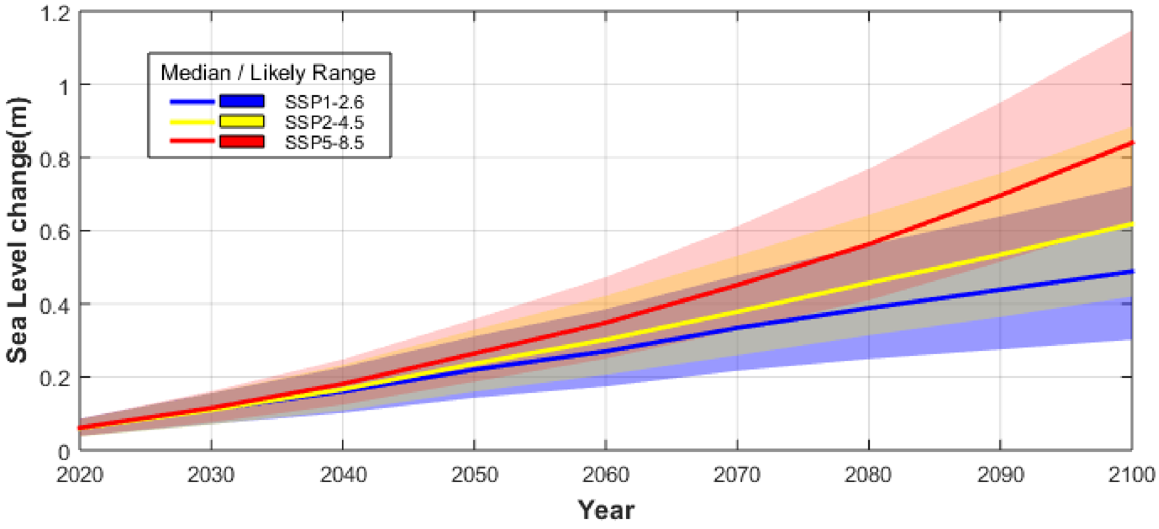

Figure 0-2: Sea level rise projections for SSP1-2.6, SSP2-4.5 and SSP5-8.5 scenarios at the coordinate point (4° 0.000'N; 4° 0.000'W) off the coast of Port-Bouët. Plain lines show the 50th percentile ranges (median range) and the shaded areas indicate the 17th – 83rd percentiles ranges (interpreted by projections' authors as the likely ranges). Data Source: NASA Sea Level Projection Tool.

The morphological data used in this study included bathymetry and beach profiles, which were collected from a variety of secondary sources. Bathymetry data for the areas of interest and surrounding regions were obtained from multiple sources, including the General Bathymetric Chart of the Oceans (GEBCO) at 15 arc-second intervals (GEBCO Company Group, 2021), a lagoon bathymetry survey by Shore Monitoring and research (2014), and a 2019 bathymetric survey conducted by the port of Abidjan. Historical beach profiles from previous studies of Konan (2012), Saimon (2017), Koffi (2017) and Touré et *al.* (2018), covering the period from 2007 to 2016, were also used to provide information on beach slope variations across the study area. It should be noted that although other morphological factors, such as vertical land movements, could significantly influence ESLs in certain regions (Ballu et al., 2011; Wöppelmann & Marcos, 2016), this study did not take these factors into account directly. This was mainly because of the limited information available on past uplift or subsidence in the study area. However, projections for future land motion have been accounted for in sea-level rise projections, with an estimated subsidence of about 5 mm by 2100 and were considered as such in this assessment.

3.2.3. Methods

3.2.3.1. Storm tide modelling

Hydrodynamic modelling of storm tide allows spatial extrapolation of water level from the tide-gauge locations (generally sheltered areas) to other surrounding areas, e.g., the open coasts. It also helps in filling small to large gaps in the water level records. In this work, storm tide simulations were undertaken using the D-Flow Flexible Mesh software developed by Deltares. This tool solves the depth-averaged shallow water equations. Detailed information on the model formulation can be found in in Deltares (2015a). The model domain includes the marine environment and the entire Ebrié lagoon system, both being connected through the Vridi canal (see figure 3-3). This was necessary to account for the interactions between the sea and the lagoon system, which could somehow influence water levels in the area of interest. The computational grid was updated from the one of Brière et *al*. (2015). It is an unstructured grid made up of curvilinear and triangular meshes. The mesh resolution gradually increases as we move towards the study area and the port domain where the tidal station is located. Orthogonality and smoothness are two important grid properties for model accuracy. They respectively denote perpendicularity between flow links and net links and the ratio of neighbouring grid cell dimensions. The grid is in good agreement with the orthogonality and smoothness thresholds defined in the modelling guidelines Deltares (2015b) and therefore satisfies the grid quality requirements. The depth schematization of the computational grids has been carried out by interpolating the different sets of bathymetric data described earlier.

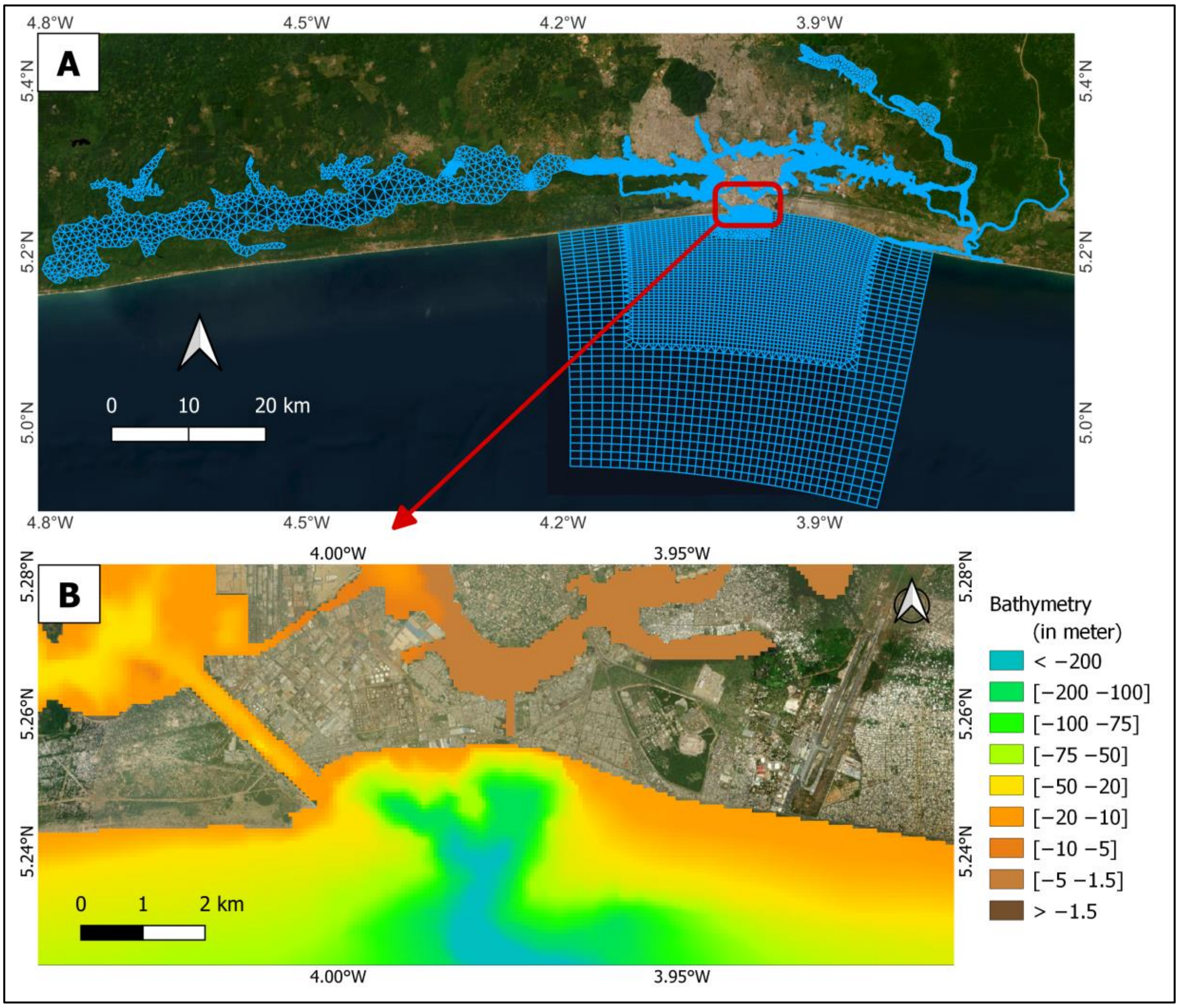

Figure 0-3: Model domain: (a) shows the computational grid built to set up the hydrodynamic model and (b) displays the Bathymetry of the Port-Bouët Bay and its surrounding areas.

The model was forced with tidal and meteorological forcing conditions. The tidal forcing at offshores boundaries as water levels were generated using ten astronomical constituents (M2, S2, N2, K2, K1, O1, P1, Q1 and M4) obtained from the DTU10 global ocean tide model (Cheng & Andersen, 2009). The meteorological forcing, composed of hourly data of near-surface wind and atmospheric pressure, were uniformly inputted over the model domain. The model calibration and validation were performed through comparisons against the water level measurements collected at the tidal station "Quai Nord" of the Port of Abidjan. The calibration process involved parameter changes to achieve the best possible match between the model and observation. For the present study, model calibration mainly focused on the uniform bottom roughness parameter represented by manning's coefficient (*n*). As suggested by Brière et *al*. (2015), a range between *n* = 0.015 s/m1/3 and *n* = 0.030 s/m1/3 was first preselected. This range actually reflects the complexity of the area, characterized by a deep sea and shallow lagoon connected together by a relatively narrow channel (the Vridi canal). Then a series of sensitivity runs were carried out to find the best uniform roughness value. Calibration results showed that the best possible agreement between modelled and observed storm tides is attained when the Manning coefficient (*n*) is equal to 0.029 s/m1/3.

The validation plot is presented in figure 3-4, in which the modelled and observed storm tide levels at the tide-gauge station are compared for the period of 10 December 2014 to 2 January 2015. A critical look at figure 3-4 shows that both the modelled and observed storm tides are in phase, but there is a minimal difference between the amplitudes. However, the calculated model performance through the Nash–Sutcliffe efficiency (NSE) coefficient (Nash & Sutcliffe, 1970) was estimated as 0.79, which is between $0.75 \leq NSE \leq 1.00$. This indicates a "very good" model performance in simulating the storm-tide conditions for the study areas. Following this validation process, the storm-tide model was computed from 1981 to 2020 (plus an additional one-month "December 1980" for spin-up time) at the different locations within the research area. For each of the selected neighbourhood, two to three observation points were set in the model, and their outputs were averaged to get the corresponding storm-tide time series that will be used in the extreme value analysis.

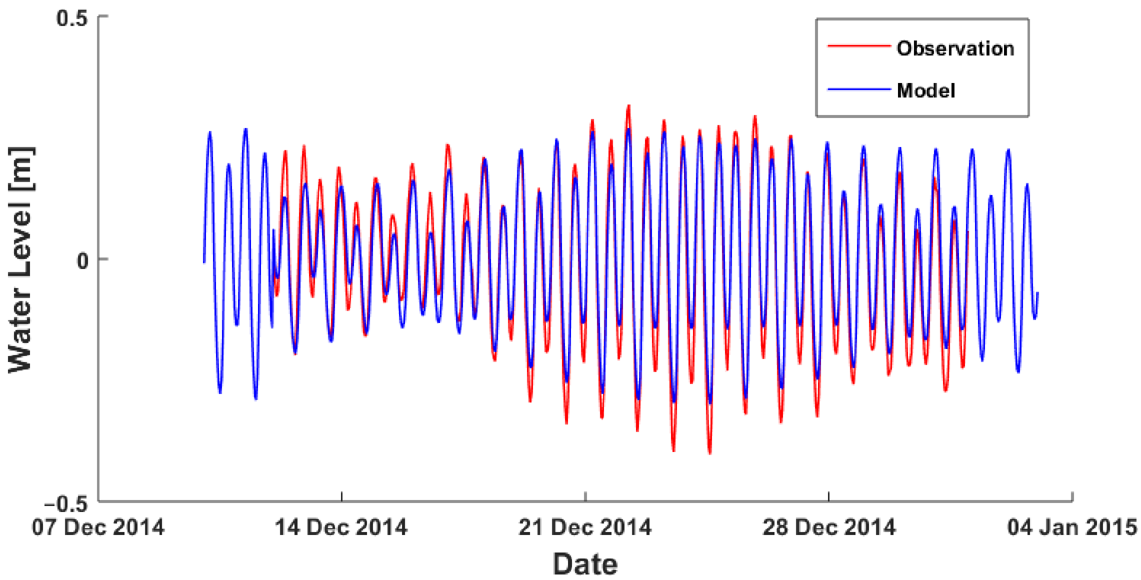

Figure 0-4: Comparison between modelled and observed water level (storm tide) for the period of December 10, 2014 to January 2, 2015 at the tide gauge station "Quai-Nord" of the Port of Abidjan

3.2.3.2. Wave runup calculation

Several different models exist to determine the wave runup, each with its derivation methodology and intended use (FEMA, 2018; Melby et *al*., 2012; Shand et al., 2011). For this calculation, the empirical model of Stockdon et *al*. (2006) will be used. It was developed using field measurements collected from several sandy beach conditions (Serafin et al., 2017; Z. Xu et al., 2017). We therefore expect this model to be appropriate for the sandy coast of Port-Bouët. The model's formulation is presented as Equation 3-4, in which $R_{2\%}$ representing runup 2% exceedance elevation, is parameterized as a function of deep-water significant wave height (H_0), wave length (L_0), and the foreshore beach slope (β_f).

$$R_{2\%} = 1.1\left(0.35\, tan\, \beta_f\, (H_0 L_0)^{0.5} + 0.5\left[H_0 L_0 (0.563\, tan\beta_f^2 + 0.0004)\right]^{0.5}\right)$$

(Equation 3-4)

The wavelength (L_0) is calculated using wave period via the relationship in Equation 3-5.

$$L_0 = \frac{gT_0^2}{2\pi}$$ *(Equation 3-5)*

The beach slope parameter β_f in this study is defined according to Ruggiero et *al*. (2004) and Stockdon et *al*. (2006), as the linear average slope over the beach face which is the region of observed runup $\pm 2\sigma$, where σ is the standard deviation of the existing water-level record. β_f was derived from historical beach profiles surveyed in several points across the study area. Slopes were first calculated for individual profiles, then averaged for each survey points. The representative beach slopes of each neighborhood (see Table 3-1) were obtained by averaging the slopes of surveyed points along each neighborhood.

Table 3-1: representative representation beach slopes (βf) calculated from historical beach profiles

Location	**Vridi**	**Petit-Bassam**	**Sogefiha**
Representative βf	0.134	0.159	0.139

Equation 3-4 was used to reconstruct historical wave runup time series of the same length as the extracted offshore wave climate, i.e., 40 years of hourly wave runup data. However, the validation of these estimations is crucial before their use in the various analyses. Checking the validity of runup estimates in a wave data scare location like in this study area is not easy work. Here, the calculated wave runup was simply compared to the observed runup elevation derived from satellite imagery. The runup boundaries can be seen on satellite images as the demarcation lines between the wet and dry beaches (Figure 3-5). Wet beaches generally appear darker in color than dry beaches on satellite images.

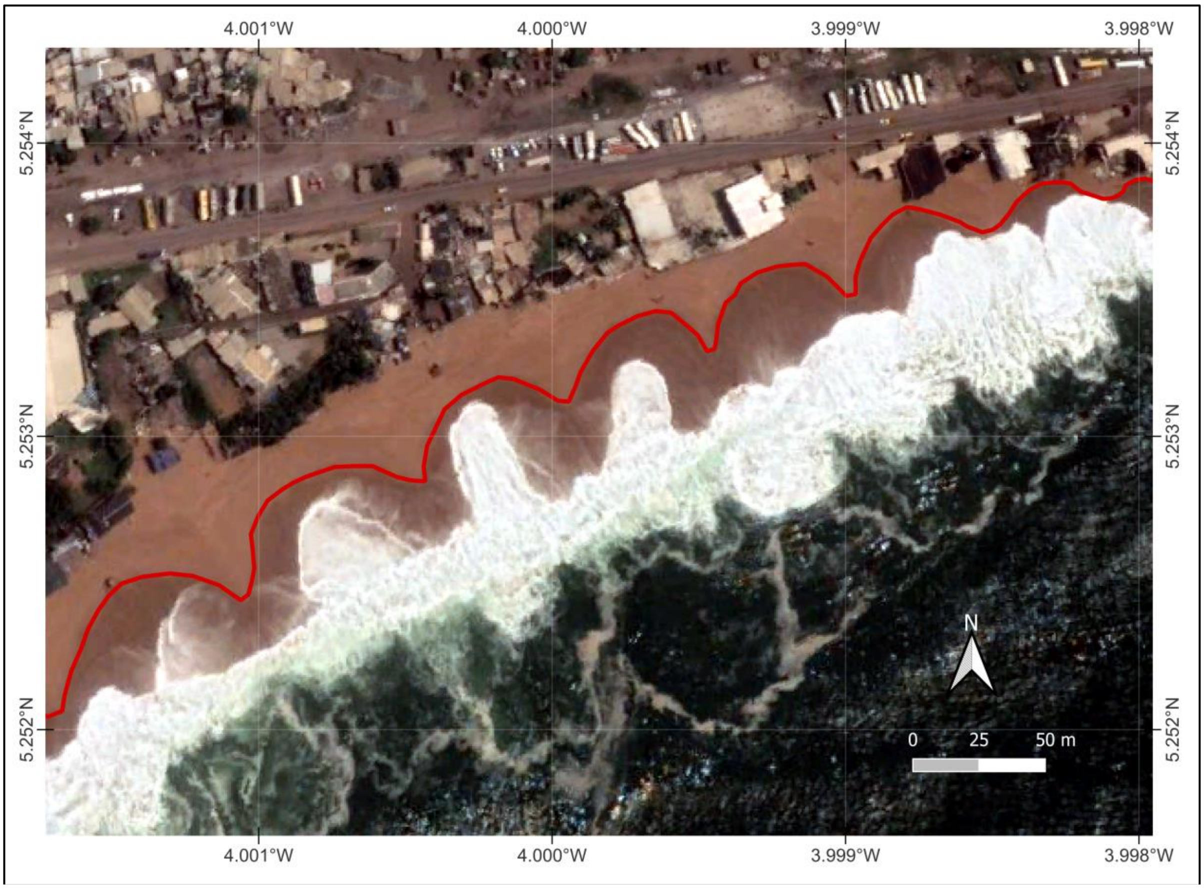

Figure 0-5: Map showing boundary line of runup (in red) on a satellite image (from Google Earth) acquired on August 1st, 2019 in Vridi

The demarcation lines have been digitized in order to extract their average altitude from the available topographical data. This obtained average altitude actually constitutes the observed total sea level. So, the prevailing storm tide value was removed from it to get the observed wave runup that was then compared to the calculated wave runup for the date of acquisition of the satellite image. Two statistical parameters namely root mean square error (RMSE) and scatter index (SI), were used to assess the performance of the applied empirical model at each neighborhood (Table 3-2). They both evaluate the goodness of fit between observation and model. Low values (closer to zero (0)) of the RMSE and SI denotes a better model performance. From Table 3-2, it can be seen that all the RMSE and SI values are all less than 0.5, indicating an acceptable performance and therefore the validity of the wave runup estimates.

Table 3-2: Statistical error parameters obtained from comparison between observed and calculated sea levels.

Location	**Vridi**	**Petit-Bassam**	**Sogefiha**
RMSE	0.376	0.479	0.279
Scatter Index (SI)	0.231	0.201	0.182

3.2.3.3. Extreme Value Analysis (EVA)

Extreme Value Analysis (EVA) is generally used to determine the magnitude (height) and the return period of large and unusual events e.g., extreme storm-tide and wave. Here, the return period' describes the likelihood of occurrence and more particularly the average recurrence interval of extreme events. It actually indicates the duration of time (in years) corresponding to the chance that an extreme event of a given magnitude will be reached or exceeded once in any one year.

The EVA theory is typically based on extrapolation of past sea level records. Two main statistical methods emerge from the literature when it comes to carrying out an EVA. They are the annual block maxima (BM) and the peaks-over-threshold (POT) methods, which are, applied using respectively the generalized extreme value distribution (GEVD) and the generalized pareto distribution (GPD) models (Pan et al., 2022). However, each of these methods has a specific data requirement i.e., the choice of which method to use depends on the characteristics of the available data (e.g., sampling frequency, erroneous/missing values and length). In general, the methods that make use of more of the available data are more accurate than those that use less data, which are in contrast easier to apply (Coles, 2001). For this case, looking at the 40-years of reconstructed hourly sea level, we find efficient to apply the generalized pareto distribution fitted to the peaks-over-threshold (GPD-POT) method. Equation 3-6, where σ and ξ are respectively the scale and shape parameters of the distribution and u is the reference threshold, gives the GPD function.

$$F_u(y) = 1 - (1 + \xi \frac{y}{\sigma})^{-1/\xi} \qquad (Equation\ 3\text{-}6)$$

The GPD-POT method is designed to calculate the likelihood of exceeding a pre-defined threshold (u). In this approach, it is assumed that the sea levels above the threshold in the time-series have a Poisson distribution and are independent and identically distributed from the GPD (Caires, 2011; Cañellas et *al*., 2007; Roscoe et *al*., 2010). The method involves the following steps:

- Defining a high threshold;
- Extracting the exceedances time-series i.e., selection of all values above the defined threshold;
- Definition of clusters of exceedances based on the maximum storm duration (in hours). This separates the meteorological conditions that create extremes. Here we took 72

hours for the wave parameter and 25 hours for storm tide as respectively recommended by Hawkes (2005) and Watson (2022).

- Declustering: this step consists of selecting the peak value within each cluster. It ensures the independency of excesses over the defined threshold, justifying the use of GPD model.
- Finally, the calculation of return level: values that is exceeded in any given year.

The determination of a return level Z_m associated with an *m*-year return period using the GPD-POT method is given by equation 3-7 in which λ_u is the rate of the Poisson process.

$$Z_m = \begin{cases} u + \frac{\sigma}{\xi}\{(\lambda_u m)^{-\xi} - 1, & \text{for } \xi \neq 0 \\ u + \sigma \ln(\lambda_u m)\,, & \text{for } \xi = 0 \end{cases} \qquad \text{(\textit{Equation 3-7})}$$

For this work, the whole process of EVA including the threshold selection was carried out using the software ORCA (*metOcean data tRansformation, Classification and Analysis*), developed by Deltares (Caires & Bos, 2009). This MATLAB-based tool is composed of four main modules, with each of the modules covering a specific aspect of the metocean data analysis. To perform the analysis, two of these modules were particularly useful: the "data validation" module to inspect and structure the datasets and the "extreme conditions" module to apply the GPD-POT method on the data.

3.2.3.4. Joint Probability Analysis (JPM)

Joint probability refers to the chance of two or more separate processes occurring together that their combination may lead to a critical event (Hawkes, 2005; Petroliagkis et *al*., 2016). This simply means that the probability of an ESL event is related to the combined probability of occurrence of all the components involved in that event, e.g., extreme storm tide and wave runup in the case of present-day ESL. However, a m-year return period of storm tide will not always occur at the same time as a m-year return period of wave runup, and if they do, so the resulting event would certainly be different from an ESL of the m-year return period. This is because, very often, ESL components depend on each other to a degree. The dependency between components indicates the way they should be combined to get the total ESL event. The JPM then utilizes the statistical dependence (χ) between storm tide and wave conditions to calculate the likelihood of compound ESL through the relationship given equation in 3-8 (Petroliagkis et al., 2016), in which T stands for the return period and χ values being between 0 and 1.

$$T_{ESL_{present-day}} = \sqrt{T_{ST} \times T_{R2\%} / \chi^2} \quad \textit{(Equation 3-8)}$$

However, the determination of the dependency factor (χ) can be an exhausting process, which needs special statistical tools in some cases. For simplicity in this work, we assumed independence between the storm tide and wave runup (i.e., $\chi = 0$), then their joint return period would be the product of individual return period as given by equation 3-9.

$$T_{ESL_{present-day}} = T_{ST} \times T_{R2\%} \quad \textit{(Equation 3-9)}$$

Using Equation 3-9, the joint return period of various storm tide and wave runup combinations were calculated. For the resultant joint return level, the individual return levels were summed $(\mathrm{ST} + \mathrm{R}_{2\%})$.

3.2.4. ESL's scenarios design

As the present work objective is to determine the present and future ESLs and knowing that ESL is governed by different dynamic factors, it is necessary to define scenarios that depict each case that can be faced. Scenarios are also very important for further exposure and risk assessment. ESL scenarios within the framework of this study are established as follows:

- For the present-day ESLs, six scenarios are defined based on the probability of occurrence of extreme events. These correspond to the best-fit return values for each of the 1, 5, 10, 25, 50- and 100-year return periods.
- For future ESLs, scenarios are designed by combining the present-day ESLs scenarios with the SLR scenarios. Therefore, the present-day ESL return levels are combined with three medium confidence SLR scenarios (precisely SSP1-2.6, SSP2-4.5 and SSP5-8.5) for the years 2030, 2050 and 2100. This combination follows equation 3-3 as defined in the approach overview section.

3.3. Results

3.3.1. Extreme Storm tide and Wave Runup

Applying the GPD-POT method to the modelled time series of storm tide and wave runup helps produce extreme return levels for different return periods. Figure 3-6 and 3-7 show the return value plots from the order of 1 to 100-years return period for each of the selected neighborhoods.

Figure 3-6 displays the return periods and values of an extreme storm tide. The analysis of these results indicates that storm tide hardly varies from one neighborhood to the other. The 1-year to 100-year return levels at Petit-Bassam and Sogefiha are similar, while those of Vridi differs from the two others by only 2 cm. For each location, as the return periods increase, the best-fit lines converge to the asymptotic values of 0.695 m (Vridi) and 0.716 m (Petit-Bassam and Sogefiha). The differences between the 1-year and the 100-year return levels are, therefore, all very small (1 cm). These slight variations in the extreme storm tide magnitudes could be explained firstly by the proximity of the selected neighborhoods and secondly by the fact that the meteorological variable in the storm tide (i.e., storm surge) does not have a significant influence on the total storm tide level. The storm surge contributes about 15% while the tide component is approximately 85%, making extreme storm tide events occur during high spring tide. This is particularly understandable given that the study area is recognized as a storm-free (Almar et al., 2019) and micro-tidal environment (Robin et al., 2004; B. Touré et al., 2012b).

Figure 3-7 presents the EVA results for the wave runup component. It shows that, unlike the storm tide, wave runup variations between locations are well noticeable. The return values of extreme wave runup obtained for Petit-Bassam are 35 to 70 cm higher than those of Vridi and Sogefiha. The difference between the two later neighborhoods is estimated to be around 9–10 cm. The absolute differences between the 1-year and 100-year return levels at each location are 0.97 m for Vridi and Sogefiha, and 1.11 m for Petit-Bassam. These variations in the extreme wave runup conditions are mainly due to the heterogeneity of beach morphological features observed on this coast (M. Touré et al., 2018)

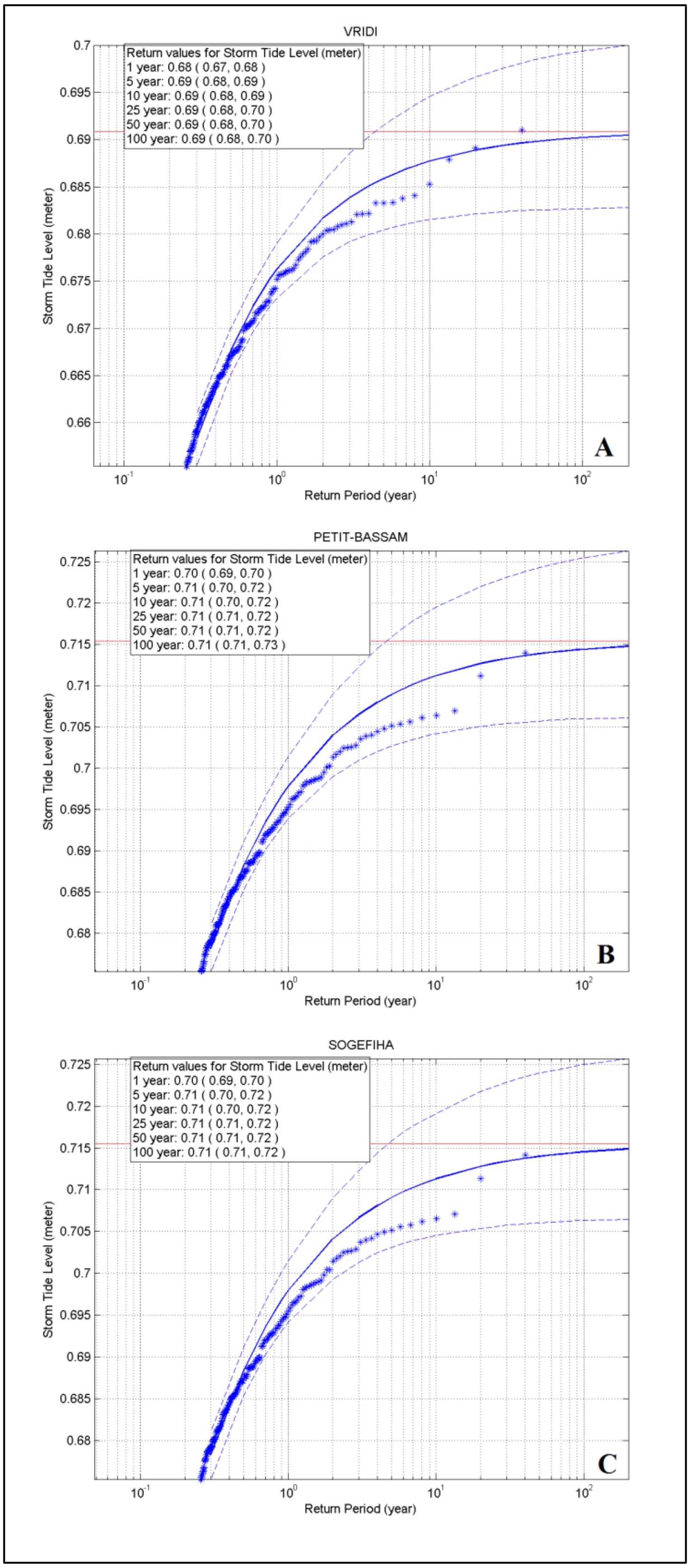

Figure 0-6: Return value plots of the GPD-POT model fitted to Storm Tide data and the associated 95% confidence intervals at Vridi (A), Petit-Bassam (B) and Sogefiha (C). The blue asterisks represent the storm tide levels over the calculated thresholds (extreme values); the plain blue lines are the best-fit distribution to the extreme values; the dashed blue lines show the 95% confidence limits of the fit; and the red horizontal lines are the asymptote lines to the best-fit curves.

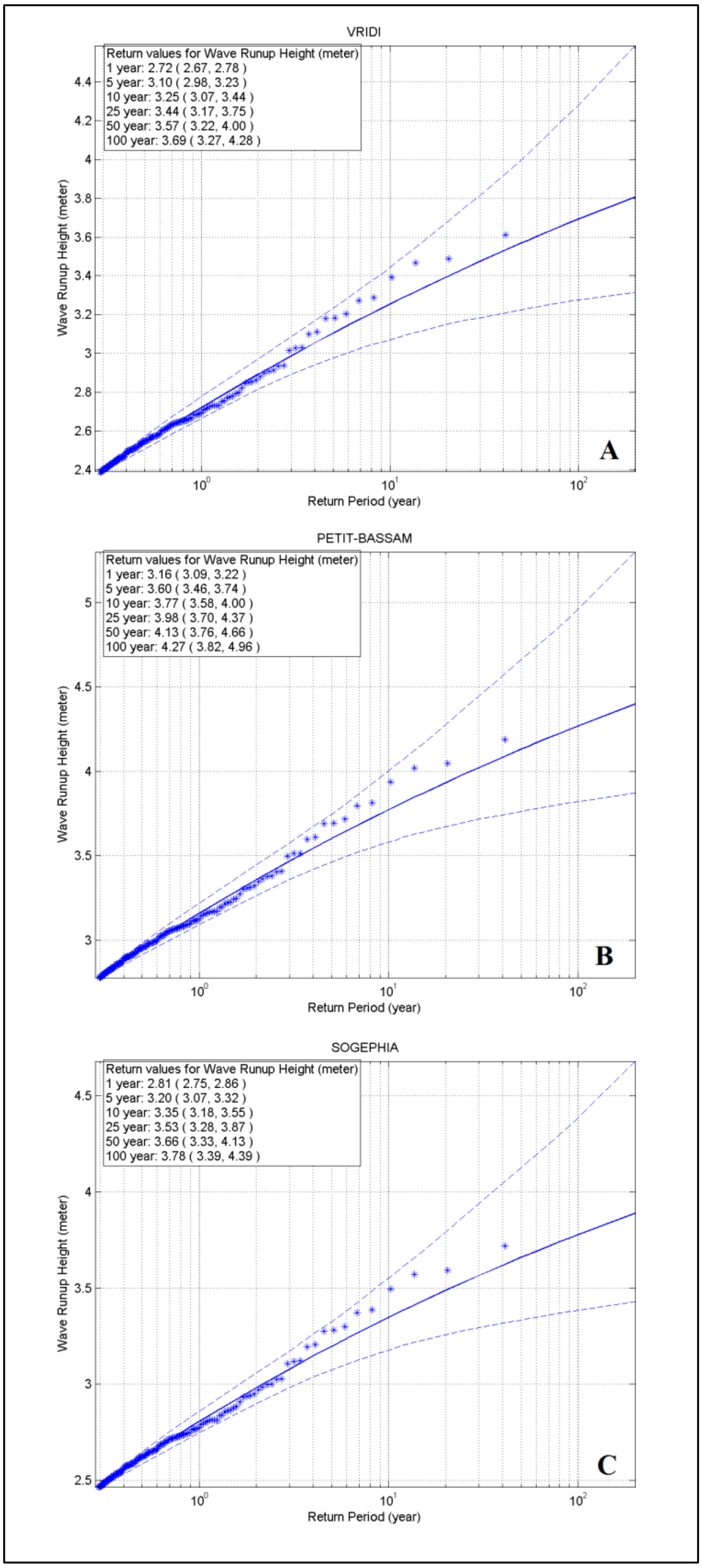

Figure 0-7: Return value plot of the GPD-POT model fitted to Wave Runup data and associated 95% confidence intervals at Vridi (A), Petit-Bassam (B) and Sogefiha (C). The blue asterisks represent the wave runup levels over the calculated thresholds (extreme values); the plain blue lines are the best-fit distribution to the extreme values; the dashed blue lines show the 95% confidence limits of the fit.

From both figure 3-6 and 3-7, it is clear that the wave runup contributes more to the total ESL as compared to the storm tide levels. For example, at Vridi, the 100-year return level of wave runup is estimated as 3.69m against 0.69m for the storm tide (figure 3-6a and 3-7a). Additionally, it can be seen that over the past 40-years, storm tide was quite stable in term of temporal variability, whereas extreme wave runup underwent both seasonal and inter-annual variations.

The maximum runup heights occurred during the meteorological event of September 3rd and 4th, 2016. At this particular event, the calculated runup gave 3.61m, 4.19m and 3.72m respectively for Vridi, Petit-Bassam and Sogefiha. About 37 occurrences of extreme wave runup ≥ 1-year return level were identified within the Port-Bouët Bay from 1981 to 2020. Among these; six were ≥ 10-year and three were ≥ 25-year return level. The seasonal distribution of these extreme wave events (figure 3-8) shows that extreme runup ≥ 1-year return levels occur from April to November and are mostly frequent during the month of August. During the assessment, no extreme wave runup ≥ 1-year return level was observed in January and December.

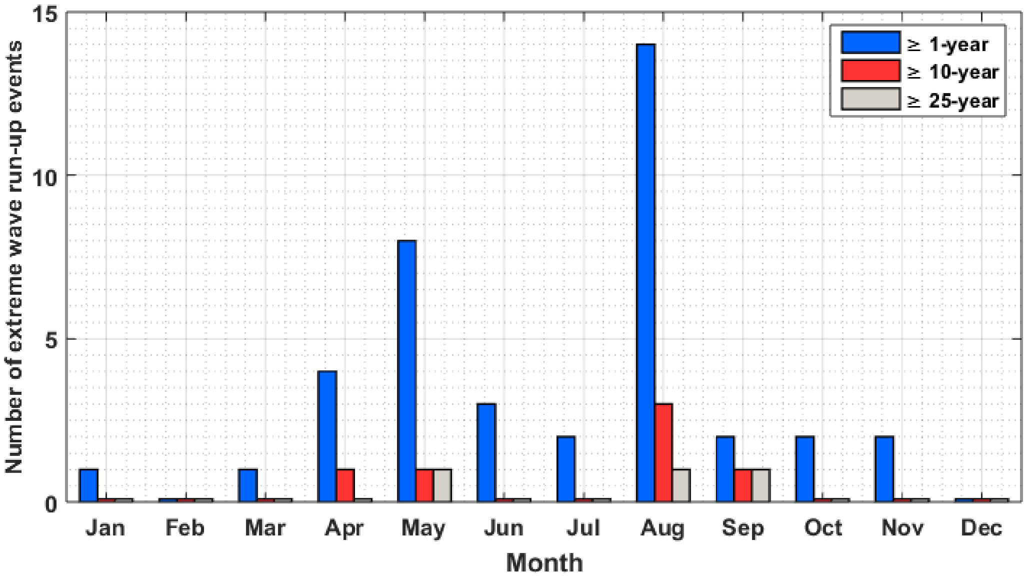

Figure 0-8: Seasonal distribution of occurrences of extreme wave runup higher than 1-year, 10-year and 25-year return levels over the period 1981-2020

In terms of the inter-annual distribution of extreme wave runup occurrences, it has been that there has been an intensification of extreme wave conditions in Port-Bouët Bay. Both the magnitude and the number of wave runup occurrences have increased in these recent decades. As an illustration of this, Figure 3-9 displays the clustering of peaks exceeding the 1-year and 10-year return levels in the neighborhood of Sogefiha. The 1-year and 10-year return levels correspond to 2.81 m and 3.35 m, respectively, as shown in Figure 3-7b. It can be observed in Figure 3-9 that approximately 75% of the extreme runup events ≥ 1-year return level and 83% of those ≥ 10-year return levels occurred during the past two decades.

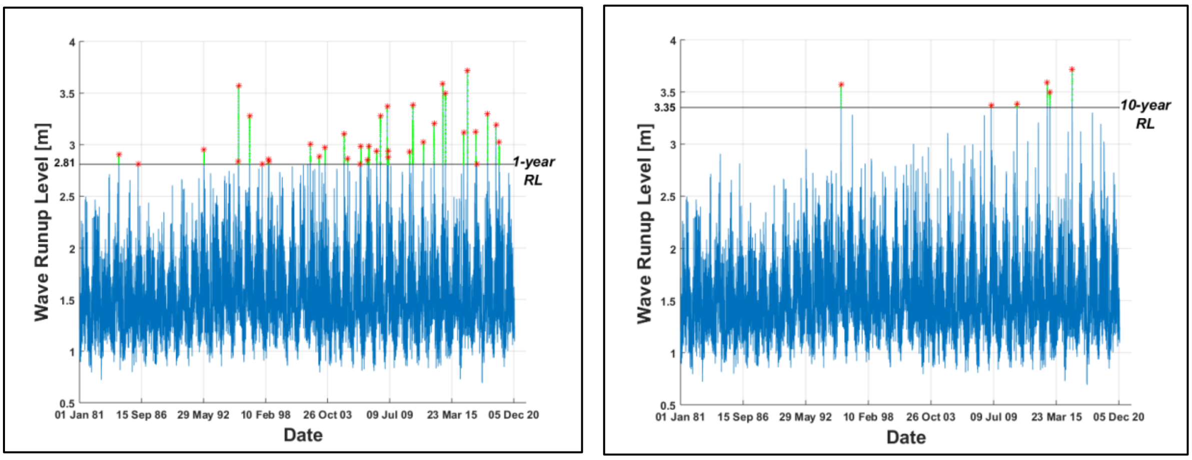

(a) (b)

*Figure 0-9: Inter-annual distribution of occurrences of extreme wave runup ≥ 1-year return level **(a)** and ≥ 10-year return level **(b)** over the period 1981–2020 at Sogefiha. The red asterisks are the clustering peak exceedances, while the green dots represent the other exceedances within each cluster of 72 hours. "RL" stands for Return Level.*

3.3.2. Present-day ESLs

This section presents the outcome of the joint probability analysis. To get the present-day ESLs, extreme wave runup was combined with extreme storm tide, assuming independence between them. Multiple combinations of these two components could be envisaged for the same ESL joint return period. For example, under the assumption of component independence, a 100-year joint return period of ESL can be obtained from the following combinations of individual return periods: 100 years and 1 years, 50 years and 2 years, 20 years and 5 years, 10 years and 10 years, with each combination having the same chance of occurring. However, only the worst-case results (the combinations that offer the maximum joint return values) are significant to the present study. They are provided with their 95% confidence intervals (in brackets) in Table 3-3. These maximum joint return values all correspond to the combination of the highest contribution of wave runup with the smallest contribution of Storm tide in each case. The current ESLs ≥ 4 m are reached from the joint return periods of 12 years, 2 years and 8 years, respectively, in Vridi, Petit-Bassam and Sogefiha. Given the local topographic conditions, these ESL ≥ 4 m, are susceptible to cause flooding in some areas of the coast. It is important to mention that the minimal fluctuations in storm tide imply that the changes in present-day ESLs between the different neighborhoods are similar to the results obtained from the analysis of extreme wave runup.

Table 3-3: Present-day Extreme Sea Levels (ESLs) deduced from the Joint Probability Method

Joint Return Period	**Joint Return Levels (in meter)**		
	Vridi	Petit-Bassam	Sogefiha
1-year	3.40 [3.34 – 3.46]	3.86 [3.78 – 3.92]	3.51 [3.44 – 3.56]
5- year	3.78 [3.65 – 3.91]	4.30 [4.15 – 4.44]	3.90 [3.76 – 4.02]
10- year	3.93 [3.74 – 4.12]	4.47 [4.27 – 4.70]	4.05 [3.87 – 4.25]
25- year	4.12 [3.84 – 4.43]	4.68 [4.39 – 5.07]	4.23 [3.97 – 4.57]
50- year	4.25 [3.89 – 4.68]	4.83 [4.45 – 5.36]	4.36 [4.02 – 4.83]
100- year	4.37 [3.94 – 4.96]	4.97 [4.51 – 5.66]	4.48 [4.08 – 5.09]

3.3.3. Future ESLs

The future ESLs were calculated by adding the projected regional sea level rise (SLR) to the present-day ESLs as stated in the approach overview. The use of this regional SLR projection did not allow the differentiation of SLR at the local scale for Vridi, Petit-Bassam and Sogefiha. The results for the 100-year return level are displayed in figure 3-10.

Additional outcomes regarding other future ESL return levels are provided in Annex A. All these projections illustrate how ESLs will be impacted by climate change in the future. The results show that the ESL elevations will increase in the future as the climate keeps changing. The average future ESL increase will be 0.11 m in the next decade. This increase could reach 0.22 to 0.26 m by 2050. By the end of the century, it is predicted that the future ESL elevations will be different from those of 2020 by 0.49, 0.62 and 0.84 m on average, respectively, under SSP1-2.6, SSP2-4.5 and SSP5-8.5 scenarios. The end-century 100-year ESL at Vridi, Petit-Bassam and Sogefiha under the high emissions scenario would be 5.21 m, 5.81 m and 5.32 m, respectively.

While it is interesting to demonstrate the impact of SLR on future ESL elevations, relying solely on such data for coastal management and planning without considering the potential changes in ESL frequencies could be limiting. Therefore, we analyzed changes over time and under SSPs in the current 100-year return period, as illustrated in Figure 3-11. This figure shows that in Port-Bouët Bay, the current 100-year return period will decrease in all neighborhoods.

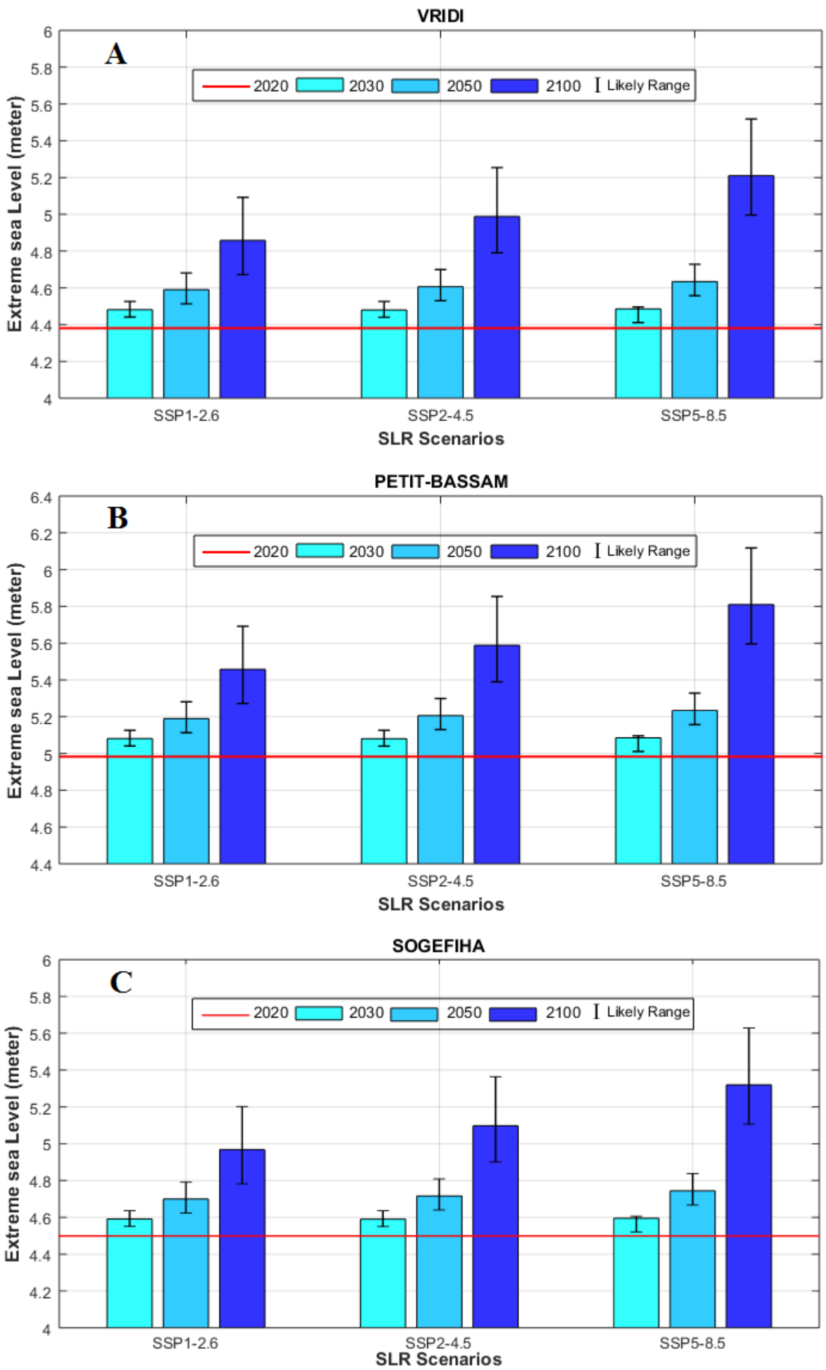

Figure 0-10: Future of the present-day 100-year return level under different SLR Scenarios at Vridi (A), Petit-Bassam (B) and Sogefiha (C). Red horizontal lines represent the present-day 100-year return level (2020). The vertical error bars represent the 17th - 83rd percentiles (likely range) for the years 2030, 2050 and 2100.

Over the next decade, today's 100-year ESLs will have return periods ranging from 52 to 63 years. This could decrease to between 24 and 37 years, i.e., more than doubling the current frequency by mid-century. By 2100, the current once-a-century ESLs in Port-Bouët Bay will occur nearly every 2 years under SSP5-8.5, and between 8 to 12 years under SSP1-2.6 and 5 to 7 years under SSP2-4.5. The neighborhood of Vridi is likely to be the most vulnerable in terms of future ESL frequency, followed by Sogefiha and Petit-Bassam in that order. This analysis allows understanding that even minor, short-term changes in SLR could significantly affect ESL frequencies. By the end of the century, ESLs that are currently infrequent in Port-Bouët Bay will become relatively common, regardless of the climate change scenario.

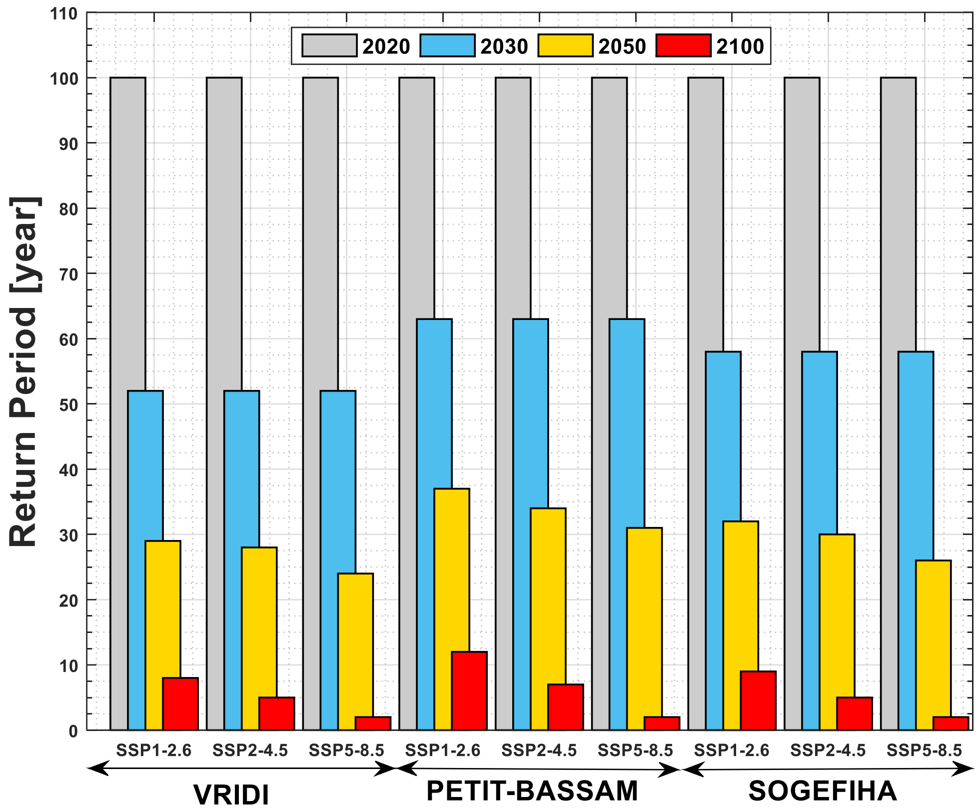

Figure 0-11: Evolution of the return period for the current 100-year return level over time under the different climate change scenarios for each neighborhood in Port-Bouët Bay.

3.4. Discussion

This study used a step-by-step methodological approach that includes different modelling techniques and statistical methods to assess the spatial and temporal evolution of extreme sea levels (ESLs) along the coastline of Port-Bouët Bay. The findings demonstrate that present-day ESLs are already high and will worsen in frequency and intensity due to the impacts of climate change in the future. This implies a greater likelihood of increasing coastal hazards in the area. The ESL scenarios generated by this study provide crucial data for evaluating the exposure and risks associated with coastal flooding and devising strategies for adaptation.

The current research represents an initial attempt to study local-scale ESLs along the Ivorian coastline. Compared to previous global-scale studies by Vousdoukas et al. (2018b) and Kirezci et *al*. (2020), our findings estimate much greater ESLs. The main difference in the determination of ESLs between these studies is the wave contribution, which was accounted for through the wave setup parameter in the above-mentioned studies, and is about 2.5 times smaller than the wave runup on reflective coasts (Roberts et al., 2020). This study's estimates of extreme storm tide elevation are in agreement with those of the global-scaled study by (Muis et al., 2016), with present-day extreme storm tide being between 0.5 and 1 m along the coast of Port-Bouët. However, unlike the global-scale approach, the adopted local-scale approach enables the examination of spatial variations in ESLs within the bay, with a resolution of approximately 2 km.

In the West African context, similar studies by Cisse et al. (2022a, 2022b) in Dakar and Saint Louis in Senegal have shown minimal contributions of storm surge components to total ESLs. This weak storm surge contribution to ESLs is due to easterly winds carrying storms away from land (Almar et al., 2019), which makes Atlantic tropical storms rarely make landfalls in this region of the globe. Instead, offshore meteorological conditions usually generate a strong swell climate (Almar et al., 2019; Prevosto et al., 2013), whose contributions to ESL and devastating impacts have been extensively highlighted in several studies across the region (e.g., Cisse et al., 2022; Cissé et al., 2022; Dahunsi et al., 2022; Osinowo & Popoola, 2021). Our study also highlights an increase in ESL frequencies in Port-Bouët Bay, which is consistent with global-scale findings (Tebaldi et al., 2021; Vitousek et al., 2017), but provides greater insight into the local variability for better adaptation.

In general, the accuracy of results in ESL studies may depend on data choices and assumptions in the methodology, which need to be discussed to raise uncertainties and/or find directions for further research. In this work, data choices and assumptions are mainly related to the selection of the dataset length for extreme value analysis (EVA), the determination of the representative beach slopes, and assumptions of independence between ESL components.

- ***Selection of dataset length***

Indeed, the choice of the length of the dataset to be considered in the EVA is decisive for the consistency of results. In general, analyses conducted using datasets that are too short yield less accurate return level estimates than those using longer datasets. However, there is no practical standard for the exact length of data to be used. According to Roberts et *al*. (2020),, using at least ten years of data could provide a reliable basis for estimating up to 100-year return values via the GPD-POT method. Arns et *al*. (2013) are more in favour of using 30 years of data for estimating 100-year return values. Nevertheless, based on his data length sensitivity analysis, Watson (2022) recommended the use of a much longer dataset if available, arguing that a longer dataset is more likely to contain key information on the major extreme events that have affected the study area, thus allowing for more optimal estimates. In light of the above, the 40 years of modelled datasets used in this work can be considered sufficient for the range of estimations performed, although it is expected that accuracy will improve as more quality in situ measurements become available.

- ***Determination of representative beach slopes***

In this study, it was observed that ESLs (Extreme Sea Levels) are very sensitive to beach morphology (beach slope). The fact of considering the beach face for the determination of the slopes, as suggested by Ruggiero et *al*. (2004) and Stockdon et *al*. (2006), allows for obtaining relatively high slopes that were stable and realistic for extreme conditions. Additionally, the use of historical cross-shore beach profiles helped to account for the seasonal variations of slopes. However, the irregularity of the collected profiles and their availability over a relatively short period could have an impact on the selection of representative slopes and, thus, on the quality of the estimates. It would therefore be necessary to have regular follow-ups of the morphology of the beaches in Port-Bouët.

- ***Independence between ESL components***

This work considers two assumptions of independence between ESL components. The first assumption is the independence between SLR and present-day ESL parameters, meaning that the current ESL components will be kept constant in the future. The second assumption is the independence between storm tide and wave runup, i.e., the occurrence of an extreme storm tide event will have no effect on the chance of extreme wave runup occurring (Petroliagkis et *al*., 2016). While these assumptions simplify our understanding of ESL, it is crucial to note that they are not always valid. Recent studies have shown that the predicted SLR could significantly influence each of the parameters composing present-day ESL (Cagigal et al., 2020; Morim et al., 2019; Pickering et al., 2017). Regarding the independence between storm tide and wave runup, while the tide component of the storm tide is of astronomical origin and the wave is of meteorological origin, and hence independent, it is essential to note that the storm surge component of the storm tide may be dependent on the wave, as both are driven by the same meteorological processes. Therefore, further studies should investigate these dependence aspects to generate more practical ESL scenarios.

3.5. Conclusion

The present section of the work focused on determining the evolution of extreme sea level elevation at the three neighborhoods located along Port-Bouët Bay. The analysis is based on validated modelled historical data from 1981 to 2020, which was built within the framework of this study to overcome the limitations related to data scarcity in this study area. These modelled datasets served to estimate the frequency and magnitude of present-day ESLs. The recent IPCC projections of sea level rise were also integrated to provide future ESLs till the end of the century.

The study results suggest that ESLs have been more intense and frequent these recent years, making the estimated present-day ESL to be relatively high. It was also observed that the current elevations will keep increasing in the future as the mean sea level continue to rise under climate change effects. The analysis also permits us to understand the role played by local coastal morphologies (beach slopes) on the spatial distribution of ESL, as demonstrated by the steepest slopes having the largest ESL elevations and the lowest slopes having the lowest ESL estimates.

These findings were possible by the application of two complementary statistical methods: the Generalized Pareto Distribution fitted to the peaks-over-thresholds approach (GPD-POT) and the joint probability method (JPM). The GPD-POT helped to estimate return values associated with return periods of individual ESL components. The JPM were used in addition to combining the individual likelihood of occurrences to obtain their joint return period/values.
The analysis and results presented in this study provide valuable insights into the current and growing threat of coastal inundation resulting from the increasing magnitude of ESLs along the neighborhoods of Port-Bouët Bay. The obtained ESL information can be useful in decision-making, planning, and emergency response efforts related to coastal flooding and others impacts. As such, these estimates can benefit a wide range of stakeholders, including coastal communities, infrastructure planners, environmental organizations, and researchers. Coastal communities can use this information to prepare for and mitigate the impacts of ESLs, while engineers can use the data to design resilient coastal protection structures. Environmental organizations can advocate for policies that address sea level rise, and researchers can make informed decisions.

Nevertheless, we strongly encourage comprehensive assessments of coastal risks associated with these ESL scenarios, particularly those related to coastal inundation and proactive actions to manage these risks in Port-Bouët Bay. Lastly, we suggest updating these projections when more consistent and accurate in situ data become available.

COASTAL FLOOD MAPPING AND EXPOSURE ASSESSMENT

Most contents of this chapter have been published in the article:

Kouakou, M., Tiémélé, J.A., Djagoua, E., Gnandi, K. (2023). Assessing potential coastal flood exposure along the Port-Bouët Bay in Côte d'Ivoire using the enhanced bathtub model. Environmental Research Communications, 5, 105001. https:// doi.org/10.1088/2515-7620/acfdfa

4.1. Introduction

Globally, it is well recognized that under climate change effects, extreme sea levels have increased at most locations of the globe and that has led to more intense and frequent coastal flood events these recent decades (Vousdoukas et *al*., 2018a). Most researchers agree that these observed increases are largely cause by climate-induced sea-level rise (Vitousek et *al*., 2017; Wahl et *al*., 2017), though it's worth noting that other factors such as land subsidence (Bagheri-Gavkosh et al., 2021) and continued socioeconomic development in coastal zones could also play a role (Vousdoukas et *al*., 2018b). Unluckily, all the projections of the Intergovernmental Panel on Climate Change (IPCC, 2021) predict continued rise in mean sea level, even with a considerable reduction in future CO_2 emissions. This shows that current flooding impacts could become increasingly worse in the future i.e., more places, people and assets could be threatened by the phenomenon. The situation has raised concerns about coastal flood exposure, as coastal communities and authorities are becoming increasingly eager to know about the vulnerability of their properties and infrastructure to coastal flood events.

As a key component of the coastal flood risk assessment, exposure estimates help providing vital information about populations and assets, which are located within the areas at risk of flooding or the flood prone areas. Generally, the information from exposure assessment are important and useful to coastal communities and decision-makers as basis for plans and interventions on preparedness, early warning, response recovery, and mitigation (HARPIS-SL, 2022). Such an assessment helps to generate ideas on the potential impacts of coastal flooding. Exposure analysis goes with flood mapping process. Coastal flood mapping is important for detecting the areas likely to be flooded and categorizing them for more effective analysis.

The Port-Bouët Bay is particularly exposed to the impact of coastal flood hazards (IMDC, 2017; Nicholls et *al*., 2007; World Bank, 2020) as a result of a growing demography, expansion of economic activities and limited investment in coastal protection infrastructures. That probably explains why it has suffered several damages from this hazard in the past. Despite this fact, limited information is available on the current coastal flood exposure as testified by the absence of coastal flood maps of past events. This lack of knowledge on local coastal flood exposure could strongly compromised the success of local adaptation and mitigation plans. In this part of the work, we have the objective of firstly identifying flood prone areas and secondly inventorying the exposed elements. The aim is to contribute at improving the understanding of the changing risk trend of this hazard in the Port-Bouët Bay.

In this chapter, we describe the methods and data used for creating the coastal flood maps and associated numbers over exposed elements. We show results on exposed buildings and populations for a variety of extreme sea level scenarios. Furthermore, we show how these results vary with time for different categories of land use. The discussion provides implications of the results, examines the accuracy and reliability of the maps and addresses some issues for further results improvement.

4.2. Data and Methodology

This study follows a two-step methodology that encompasses coastal flood modelling and exposure analysis. The first step involves generating flood maps using the enhanced Bathtub Model (eBTM), which integrates extreme sea level (ESL) conditions with the local morphological features. The second step involves overlaying the flood maps generated in the first step with the land use and population maps of the study site. This enables the estimation of coastal flood exposure, which is the number of people and assets at risk due to flooding. Figure 4-1 provides a schematic representation of the methodology shortly described above. In the following paragraphs, a more detailed description of each of the two steps is provided.

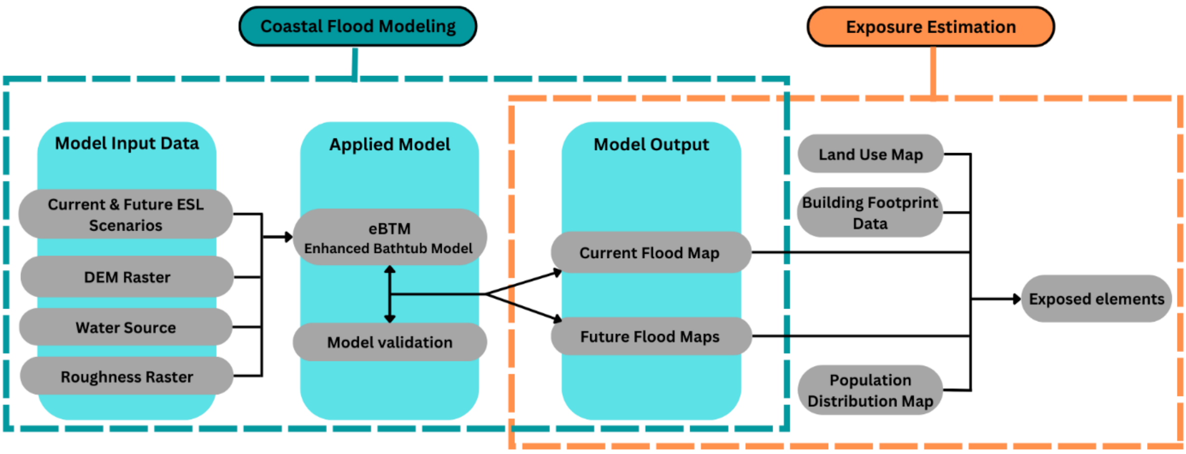

Figure 0-1: Flow chart showing the general research methodology

4.2.1. Coastal flood Modelling

4.2.1.1. Modelling Approach

Models can offer a comprehensive view of the flooding extends and depths at different spatial and temporal scales. In recent decades, many models have been developed and applied for coastal flood simulations. Two modeling approaches frequently used in the literature are the bathtub model (BTM) and the hydrodynamic model (HDM) (T. Neumann & Ahrendt, 2013). Each of these two types of models has its own strengths and limitations. But the choice of which approach to be used largely depends on the intended purpose and data availability. The BTMs are based on a hydrostatic approach in which, it is simply assumed that flooding occurs only when the land surface elevation is below the flood water level and hydrologically connected to the flooding source (Fereshtehpour & Karamouz, 2018; Poulter & Halpin, 2008). They are computationally efficient and very helpful to quickly obtain the flood-prone areas for a corresponding flood water level. Generally, BTMs use geographical information systems (GIS) as the basic working tool (Seenath et *al*., 2016) and can easily be executed through raster calculations. On the other hand, within the hydrodynamic modeling (HDM), coastal flood simulations are performed by solving mathematical equations e.g., the 2D /3D shallow water equations. This approach includes the dynamic aspect of the physical processes leading to flooding. It therefore requires detailed input conditions as well as specialized software and skills. HDMs can be complex and may result in longer computational times (Amante, 2018). They are commonly used for flood forecasting (Gallien et *al*., 2014) and the planning and implementation of flood protection measures (Ward et al., 2011).

In this study, since the purpose of is to map coastal flood extent, the GIS-based bathtub approach is considered to be fitting. Two methods arise from this approach: the simple bathtub model (sBTM) and the enhanced bathtub model (eBTM), which is an improvement to the sBTM by taking into consideration the beach slope and the surface roughness, two parameters that play a key role in result accuracy. The eBTM will therefore serve as the framework for conducting the various flood simulations in this work. The model was conceptualized by Williams (2019) and developed in ESRI ArcGIS software, aims to address temporary coastal inundation and the lack of easily accessible, user-friendly tools (Williams & Lück-Vogel, 2020). It is important to note that the eBTM, being a GIS-based model, focuses on capturing the dynamics within its scope, and while it may not encompass all aspects of physics like more advanced hydrodynamic models, it offers a valuable approach for understanding and assessing coastal flood scenarios. The model as tested and validated in Strand, a municipality in Cape Town, South Africa, is the eBTM module with homogeneous roughness (Williams & Lück-Vogel, 2020). However, a module with roughness raster (non-homogeneous) is also provided in the toolbox. This latter module, which reflects a growing body of GIS tools applicable to the coast, will be used in the context of this study. To conduct flooding simulations using the eBTM, four input datasets are essential: the digital elevation model (DEM), water source, surface roughness, and flood water level. The next section provides a detailed description of each of these crucial datasets.

4.2.1.2. Model input data

- *Digital Elevation Model (DEM)*

For reliable coastal flood modelling, a high-resolution DEM is crucial. In our analysis, the Digital Elevation Model (DEM), specifically the digital terrain model (DTM), was obtained from topographic survey data collected in 2013 as part of the ‘‘Digital Topographic Mapping Project for Urban Infrastructure Development’’ (JICA, 2015). The DTM represents the bare earth elevation, excluding any aboveground features (buildings and vegetation). The data was initially collected in point file format and covered 931 measurement points over the study site, with one point for every 11-12 m^2. To obtain a continuous regular terrain elevation, this relatively coarse dataset was later interpolated to fill the gaps. The resulting DEM has a resolution of 10 × 10 m and uses as vertical datum, the Abidjan mean sea level, which serves as the reference point for the port of Abidjan. While the resolution might seem coarse for coastal inundation modelling, it is important to recognize the data scarcity in the study area, compelling us to optimize the available DEM resources. Figure 4-2 provides a visual representation of the obtained Digital Terrain Model (DTM).

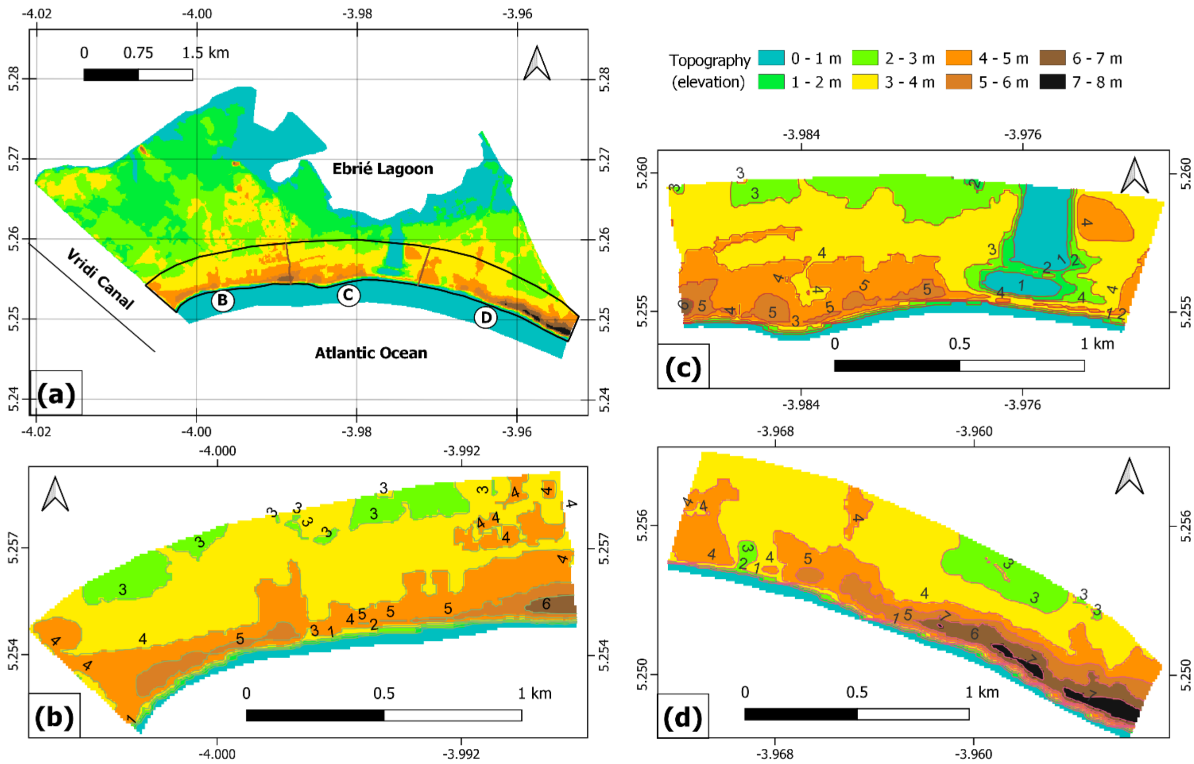

Figure 0-2: Digital Terrain Model (DTM) of the study area: (a) provides an overview of the DTM for Port-Bouët Bay. (b), (c), and (d) offer detailed views of the DTM around the coastlines in Vridi, Petit-Bassam, and Sogefiha respectively. Elevations in the study area range from 0 to 8m, with the majority of high-elevated locations located along the coastline. The vertical datum is the Abidjan Mean Sea Level.

- *Surface Roughness*

As eBTM is a GIS-based model, it should be noted that it does not directly address the detailed physics as a hydrodynamic or numerical model would. This means that certain factors, like wind-push effects, remain unaccounted for in this approach, unlike more sophisticated models. However, the model incorporates the roughness parameter of the terrain to address terrain slope's influence on water movement across the landscape. The eBTM offers two options for roughness input: a single-value roughness for the entire study site, used in the homogeneous roughness module, and space-varying values, used in the roughness module. However, in both cases, roughness values fluctuate between a minimum of 0 for smooth surfaces and a maximum of 1 for rough surfaces (Williams, 2020). For this analysis, the roughness raster was used. The roughness raster file of the study area (see figure 4-3) was generated with the same resolution as the input DTM. As illustrated in figure 4-3, rough areas are prominently located along the coastline.

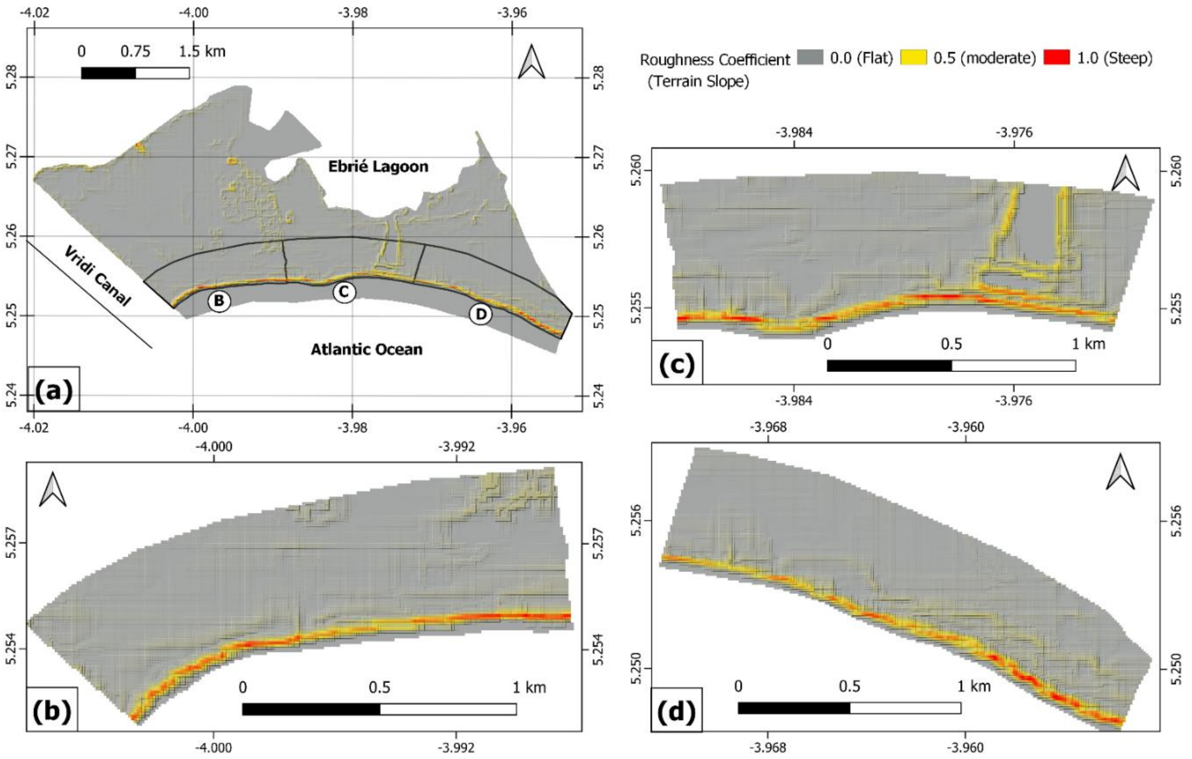

Figure 0-3: Surface Roughness Distribution across the Study Area: (a) presents an overview of surface roughness across the entire Port-Bouët Bay region. (b), (c), and (d) offer focused perspectives on roughness variations along the coastlines of Vridi, Petit-Bassam, and Sogefiha respectively. A roughness value of 0 represents a smooth, flat terrain with minimal elevation changes, while a value of 1 indicates a rough, steep terrain with significant elevation variations. A roughness value of 0.5 can be considered "moderate" or "intermediate," implying a surface roughness level between complete smoothness and high roughness.

- *Water Source*

In eBTM modeling, the water source represents the initial position of the floodwater, establishing hydrological connectivity to the coast and providing a starting point for the water's inward propagation (Williams & Lück-Vogel, 2020). To obtain the water source for this analysis, the zero-altitude shoreline along the coast was digitized from the input DEM (saved as a shapefile), ensuring that the water source intercepts the DEM to maintain hydrological connectivity to the coast (Williams, 2020).

- *Flood water Level scenarios*

To assess which land areas would be flooded during a coastal flood event, flood water level must be specified in the model. In this research project, several scenarios were considered. These scenarios were estimated from extreme sea level (ESL) conditions, which result from the combined effects of tide, storm surge, wave runup and the projected relative sea level rise

(SLR). ESLs were retrieved from the published work of Kouakou et al. (2023) in which values are provided by neighborhood for three climate change scenarios based on SSPs (see Table 4-1). The present-day ESLs were based on statistical 100-year joint return values of storm tide (tide + storm surge) and wave runup. Future ESLs were predicted by integrating the present-day ESLs with the recent SLR projections based on shared socioeconomic pathways (SSPs) (see Fox-Kemper et *al*., 2021; Garner et *al*., in prep., 2021).

Table 4-1: Values of Extreme Sea Level (ESL) for different SSP scenarios used to run the eBTM model (Kouakou et al., 2023)

Location	Scenarios	YEARS			
		Present-days	2030	2050	2100
Vridi	SSP1-2.6	4.37 m	4.481 m	4.590 m	4.858 m
	SSP2-4.5		4.48 m	4.606 m	4.988 m
	SSp5-8.5		4.485 m	4.634 m	5.210 m
Petit-Bassam	SSP1-2.6	4.97 m	5,081 m	5.190 m	5.458 m
	SSP2-4.5		5.080 m	5.206 m	5.588 m
	SSp5-8.5		5.085 m	5. 588 m	5.810 m
Sogefiha	SSP1-2.6	4.48 m	4.591 m	4.700 m	4.968 m
	SSP2-4.5		5. 590 m	4.716 m	5.098 m
	SSp5-8.5		4.595 m	4.744 m	5.320 m

4.2.1.3. Model setup and validation

The model was configured with the assumption that input datasets such as topography, surface roughness, and water source will remain constant in the future, with only the flood water level changing over time. Since the input datasets are available for each coastline segment of the Port-Bouët Bay, the model simulations were executed individually for each neighborhood to produce the outputs for the corresponding periods. This approach of running separate models for each neighborhoods helps ensure accurate representation and assessment of flood impacts for each distinct location. The output from each simulation was provided as a flood raster layer that is connected to the coast, indicating the water depths relative to the input DTM for each pixel. The flood layers were carefully reviewed to ensure that the working resolution is capable of producing results that align with the local flood patterns.

After the model was set up and the initial outputs were checked, the next step was to evaluate the accuracy of the results. To achieve this, the model results were compared with GPS coordinates of areas that were recently flooded. During a ground survey, local residents were asked to indicate coastal flood limits for recent years or show the locations where they had personally experienced flooding. The GPS coordinates of these locations were collected and compared with the present-day modeled flood layer to determine any overlap. Twenty GPS points were collected for events that occurred between 2014 and 2020.

4.2.2. Exposure estimation

To assess the potential impact of floods on the urbanized area of port-Bouët Bay, it is necessary to determine the exposed elements (assets, populations and land-uses). This requires detailed data on these elements in a Geoinformatics format, along with coastal flood layers (Percival & Teeuw, 2019). In this study, the used datasets were partially completed and needed some additional arrangements. The population data was downloaded from the "Data for Good" platform (FCL and CIESIN, 2022). This database provides global raster files of population estimates within 30-meter grid cells for the year 2020 using AI, satellite imagery, and census data. The development of these high-resolution maps relies on high-resolution identification of populated areas and a thorough understanding of the underlying population distribution patterns. To streamline the analysis, the initially collected population raster file for the entire country was clipped to match the study area's extent, and subsequently disaggregated to align with the resolution of the flood raster files (10 × 10 m). For simplicity purpose, the disaggregation process used the uniform disaggregation method, equally distributing population counts from the coarse grid to the finer grid cells. Since the acquired data represents the 2020 population count, which pertains to the present-day, future population data was derived through projections using equation 4-1.

$$\boldsymbol{P_f = P_p \times (1 + R_m)^t} \qquad \textit{(Equation 4-1)}$$

Where $\boldsymbol{P_f}$ is the future population; $\boldsymbol{P_p}$ is the present population; $\boldsymbol{R_m}$ is the average annual growth rate, and $\boldsymbol{t}$ is the projected number of years. The value of $\boldsymbol{R_m}$ was calculated using historical population data from CIESIN (2018), which provides past population estimates every five years from 2000 to 2020, along with equation 4-2, where $\boldsymbol{P_i}$ and $\boldsymbol{P_{i-1}}$ are respectively the ending and starting population count over the five-year period.

$$\boldsymbol{R_m = \left. \sum \frac{P_i - P_{i-1}}{5 \times P_{i-1}} \middle/ n \right.} \qquad \textit{(Equation 4-2)}$$

In order to evaluate the potential number of buildings at risk of flooding, building footprints were incorporated into the exposure analysis using the "open building" database (Sirko et *al*., 2021). This database offers one of the most extensive building maps for the region. Additionally, each footprint in this database is assigned a confidence level, enabling manual adjustments for low-confidence footprints to achieve the most accurate real-world representation. In evaluating potential flood impacts on various occupations within the area, the land-use map was created by digitizing the different occupations within the study site. This process involved satellite imagery from OpenStreetMap and conducting guided field surveys to validate the accuracy of the data. The resulting occupations were then categorized into seven specific land use classes (refer to Figure 4-4), including open area class that corresponds to unoccupied spaces. Noteworthy that in Figure 4-4, land-use types are assigned based on predominant occupations.

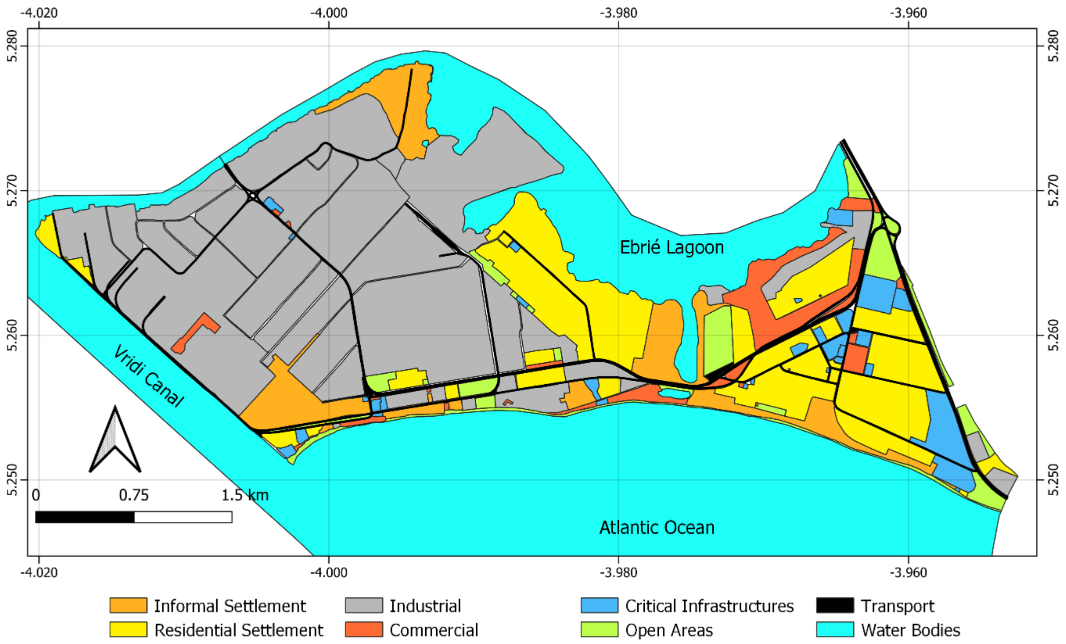

Figure 0-4: Land use map of the study area based on satellite imagery and ground-truthing. It comprises seven major classes that summarize all the occupations that are located in the area. The colour coding of this land use map is consistent with the recommendations of Jeer and Bain (1997).

The exposure analysis for each scenario involved overlaying the respective flood layer with the population, building, and land use distribution maps of the study area. This allowed us to determine the number of people and buildings at risk, identify the likely affected land-use categories and estimate the flooded surface per land use. To conduct this analysis, we employed the zonal statistics approach, which involves aggregating data within flooded zones to gain insights into various attributes or characteristics. This technique provides a deeper understanding of how data is distributed and interacts within the flooded areas, contributing to a comprehensive evaluation of flood impacts for each neighborhood within our study area.

4.3. Results

4.3.1. Coastal flood mapping

Before presenting and commenting on the findings, the eBTM output for the present day was compared to the GPS coordinates of recently flooded areas, as described in the model validation section. The twenty collected observation points are plotted against the model output in Figure 4-5. It emerged from this comparison that, the model results match with about two-thirds of the observations. In the remaining one-third, the modeled coastal flood is underestimated. However, the spatial differences between the model and observations outside of the modeled flood extent were mostly less than 10 meters, i.e., an underestimation of just one pixel. Only two observations (point number 8 and 20) were found to be distant from the modeled flood limit by more than 10 meters (14 and 16 meters, respectively). After analyzing the simulation's resolution, it can be inferred that the observed distribution of coastal floods and the model results for the present day exhibit a general consistency. Consequently, the validity of the input datasets and the eBTM simulation in the Port-Bouët Bay can then be established.

Figure 4-6 and Table 4-2 present a comprehensive overview of the simulation results across different climate change scenarios and years, illustrating the extent of the flooded areas within the Port-Bouët Bay. The visualizations in figure 4-6 offer clear evidence of the bay's vulnerability to flooding, primarily concentrated in areas adjacent to the shoreline. Currently, as of 2020, the simulations under the 100-year ESL return level reveal that the estimated flooded area is approximately 21.58 hectares (see Table 4-2). The simulations project varying degrees of increased flooding in the coming decades. Over the next 10 years, a projected 5-8% of additional land would periodically be flooded during extreme sea level events. Looking ahead to 2050, the coastal flood extent is anticipated to rise by 14-18% compared to the present state. Towards the end of the century, two specific scenarios, SSP1-2.6 and SSP2-4.5, may lead to flood increases of up to 27% and 37%, respectively. Particularly under SSP5-8.5, by the year 2100, Figure 4-6c of the flood map strikingly displays a significant surge in coastal flooding, distinctly surpassing current conditions. The analysis underscores the potential doubling of the current flood extent by 2100 under SSP5-8.5. The detailed values for the different neighborhoods, scenarios, and years are exhaustively presented in Table 4-2.

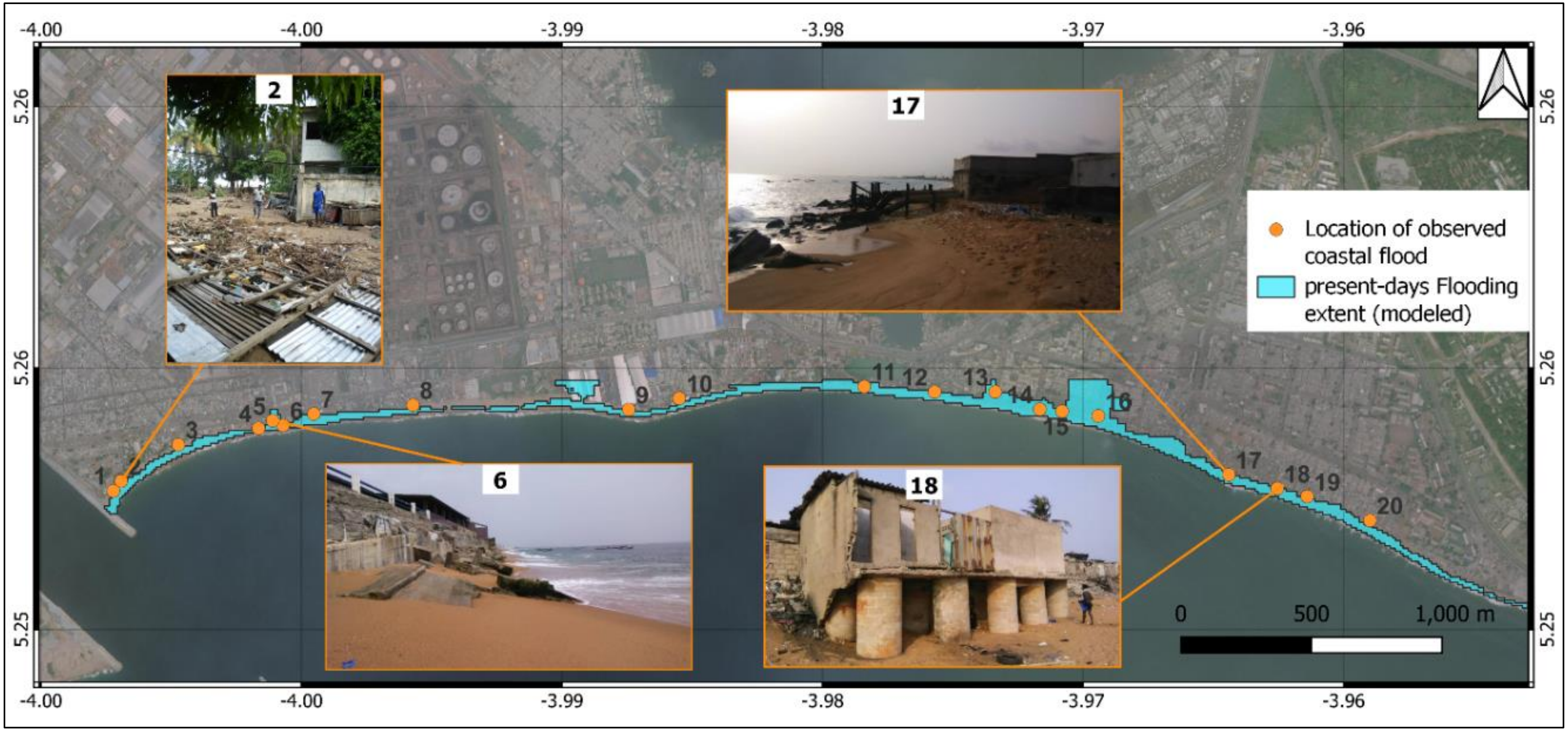

Figure 0-5: shows the locations of recent observed coastal flooding (orange dots) overlaid with modeled current flood extent (blue band) to ensure the validity of the eBTM simulations. These observations correspond to the period between 2014 and 2020. Pictures of some area are provided.

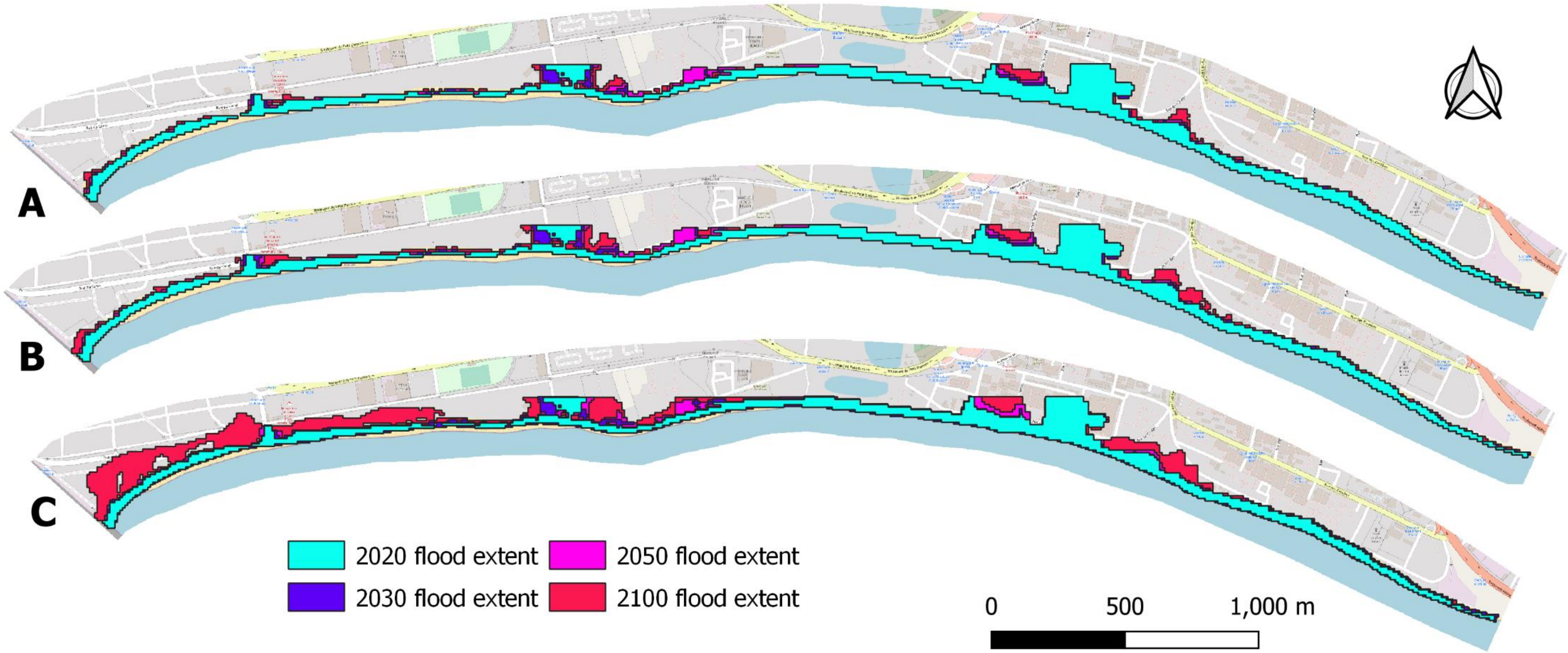

Figure 0-6: Maps showing the total flood extent for present and future situation for different climate change conditions along the Port-Bouët Bay. A – the SSP1-2.6 scenarios (low; B – the SSP2-4.5 scenario (intermediate); C – the SSP5-8.5 scenario (high). Background outlines are from OpenStreetMap standard. The area shown for each scenario is 5.5 km × 0.45 km.

Table 4-2: Estimates of total flooded area (in hectares) per neighbourhood and per scenario.

Location	Scenarios	Years			
		2020	2030	2050	2100
Vridi	SSP1-2.6	4.47 ha	4.63 ha	4.93 ha	5.64 ha
	SSP2-4.5		4.57 ha	5.03 ha	6.58 ha
	SSP5-8.5		4.84 ha	5.07 ha	18.62 ha
Petit-Bassam	SSP1-2.6	6.11 ha	6.82 ha	8.00 ha	6.11 ha
	SSP2-4.5		6.77 ha	8.00 ha	9.19 ha
	SSP5-8.5		7.14 ha	8.23 ha	10.76 ha
Sogefiha	SSP1-2.6	11.00 ha	11.43 ha	11.83 ha	13.06 ha
	SSP2-4.5		11.41 ha	11.89 ha	13.87 ha
	SSP5-8.5		11.47 ha	12.12 ha	15.24 ha

The information provided in Table 4-2 provides evidence that the neighborhoods of Vridi, Petit-Bassam, and Sogefiha experience varying degrees of exposure to coastal flooding under different climate change scenarios and years. Among these neighborhoods, Vridi consistently exhibits the least exposure to coastal flooding across the scenarios and years. Notably, the SSP5-8.5 scenario for the year 2100 shows a significant increase in the flooded area, indicating the highest level of exposure under this particular climate change trajectory and year. In the case of Petit-Bassam, there is a moderate level of exposure to coastal flooding. While the projections for flooded areas increase across scenarios and years, the growth appears gradual, suggesting a steadier rise in flooding over time. Conversely, Sogefiha is consistently projected to experience the highest degree of exposure to coastal flooding among the three neighborhoods. The neighborhood's initial larger flooded area and its consistent expansion across all scenarios and years point to a heightened susceptibility to rising sea levels. Overall, this analysis suggests that Sogefiha is the most exposed neighborhood, followed by Petit-Bassam, and then Vridi.

4.3.2. Coastal Flood Exposure

4.3.2.1. Exposed populations and Buildings

Based on the coastal flood extent discussed earlier, we have identified the population and buildings exposed to floodwaters. Figure 4-7 shows the results for various climate change scenarios. From figure 4-7a, around 2465 people are currently exposed to the once-a-century flood water level, with this number expected to increase due to demographic growth. By 2030, the increase will be between 42% and 45%, while by mid-century, it could reach 82% to 85%. Assuming that population growth remains the same, by 2100, the number of exposed individuals may be 24.93, 27.03, and 40.78.3 thousand under SSP1-2.6, SSP2-4.5, and SSP5-8.5, respectively.

Figure 4-7b indicates that roughly 544 buildings in the study area are exposed to coastal floods, with the majority being fully within the inundated zones. However, a subset of these buildings, situated at the outskirts of flood zones, would only experience partial exposure. Regardless of the scenario, the number of exposed buildings is expected to slightly increase from 2020 to 2050 under future climate change conditions. By end-century, under SSP1-2.6 and SSP2-4.5, the percentage of increase in flood-affected buildings would be 43% and 62% higher than the current scenario, respectively. However, under SSP5-8.5, the number of affected buildings could be almost three times more than the current scenario.

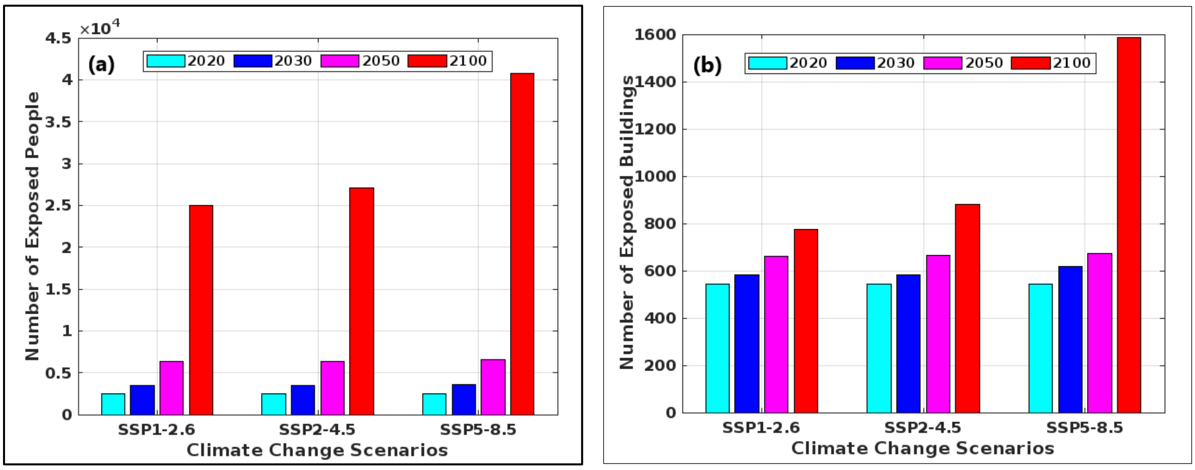

Figure 0-7: Number of population (a) and buildings (b) exposed to coastal flood events along the Port-Bouët Bay under different climate change scenarios for present and future periods.

The analysis of exposed elements in each neighbourhood reveals distinct spatial patterns across scenarios (refer to figure 4-8). In Vridi, the current count of exposed population of 285 people gives way to divergent trajectories over time. By 2030, exposure increases by around 44-51% compared to the baseline, with further escalation by 2050 (145-163%). By the century's end, the exposed population reaches a significant magnitude, becoming nearly 46 times greater than the count in 2020 under scenario SSP5-8.5. In Petit-Bassam, the 817 people currently exposed rises by approximately 50-53% by 2030, and projections for 2100 reaching 10 to 13 times higher. A parallel trend emerges in Sogefiha, where exposure climbs by about 36-39% by 2030, rising to around 140-146% by 2050 and may reach 8 to 11 times higher by the end of the century. Shifting focus to exposed buildings, noteworthy trends emerge. In Vridi, the initial building exposure count of 33 in 2020 experiences slight upticks by 2030 and 2050, followed by a significant surge by 2100. It is worth noting that the number of buildings exposed to flooding could reach a staggering 670 by 2100 under the SSP5-8.5 scenario. Similarly, in Petit-Bassam, where exposure begins at 141 buildings, reaching 158 to 185 by 2030 and ascending to 221- 278 by 2100. Likewise, in Sogefiha, building exposure starts at 370, remains steady at 392 by 2030, and increases to 43- 426 by 2050, culminating at 498- 637 by the close of the century.

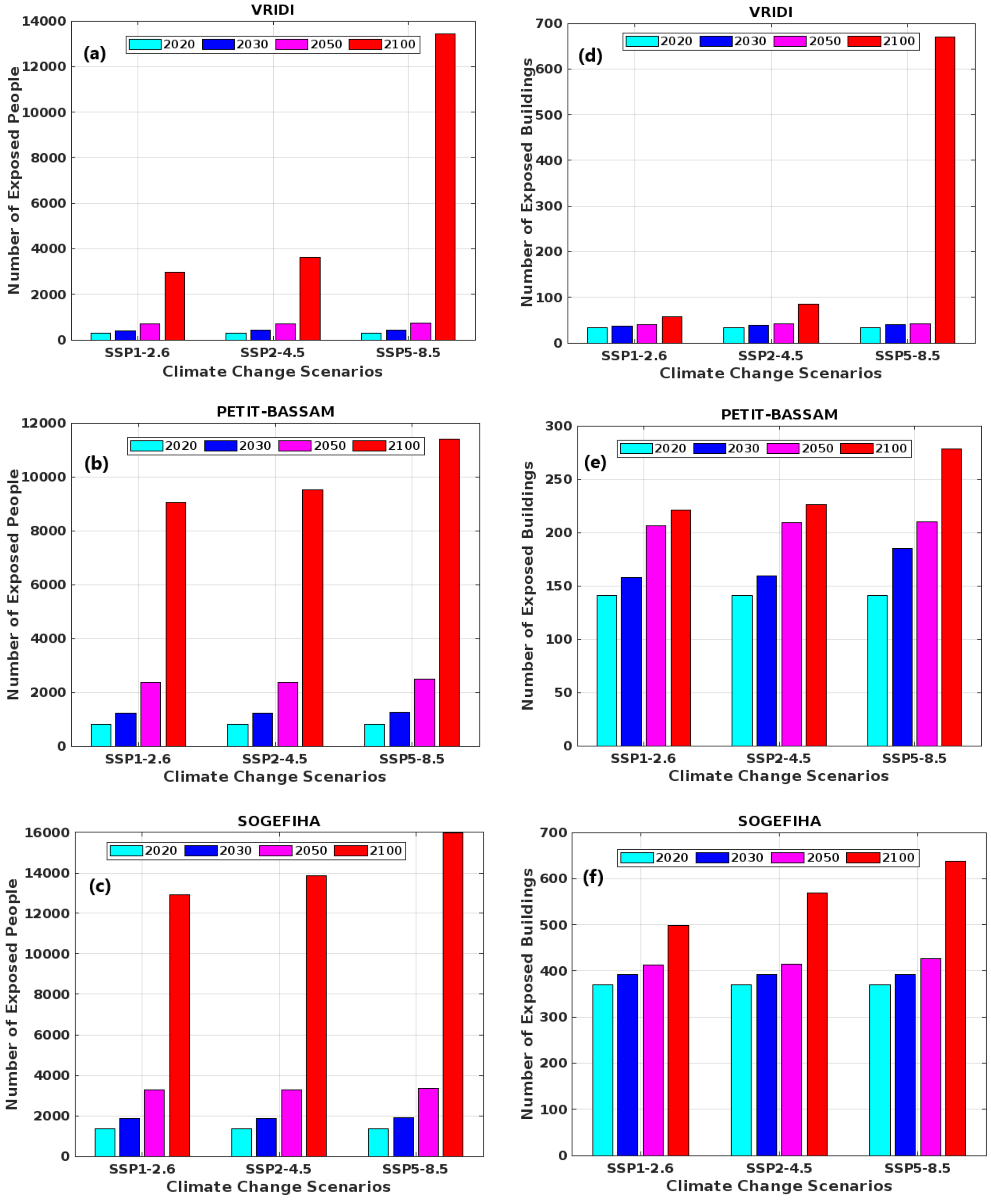

Figure 0-8: Population and Building Exposure in Port-Bouët's Neighborhoods under Various Climate Change Scenarios for the Present and Future periods. Exposed Population in Vridi (A), Petit-Bassam (B), and Sogefiha (C). Exposed Buildings in Vridi (D), Petit-Bassam (E), and Sogefiha (F).

4.3.2.2. Land use in flooded areas

In this subsection, we evaluated the distribution of land use in the flooded zones for each of the scenarios. Our findings reveal that, for the present-day 100-year return period of extreme sea level, the most exposed land use class is the open area (11.98 ha), followed by informal settlement (5.44 ha), residential settlement (1.82 ha), commercial (1.36 ha), industrial (0.74 ha), critical infrastructure (0.2 ha) and transport (0.02 ha), in that order. These distributions are primarily based on the dominant occupations within the flooded zones. Noteworthy, the significant proportion of exposed "open areas" helps to mitigate the potential impacts of today's coastal flood, as there are no significant assets in this land use class.

Under future climate change scenarios, as the flooded surface per land use increases, the ranking of occupations most or least exposed would remain similar to the current situation (see figure 4-9). This indicates that the exposure of all land use type would increase proportionally to the flooded surface. However, we note a negative trend (decrease) of the future flooded surface of "open areas" over time, while the other land uses have a positive trend of flooded surface (increase). For instance, under SSP5-8.5 (see Figure 4-9f), the relative share of “open areas” decreases from 55.5% in 2020 to 35.2% in 2100, a decrease of about 20.3%, while there is an increase of 4.6% for “Industrial" (from 3.5% to 8.1%), 4.5% for informal settlements (from 25.2% to 29.7%), 3.7% for "critical infrastructures" (from 0.9% to 4.6%), 3% for "Commercial" (from 6.3% to 9.3%), 2.7% for "Residential settlement" (from 8.5% to 11.2%), and 1.8% for "Transport" (from 0.1% to 1.9%).

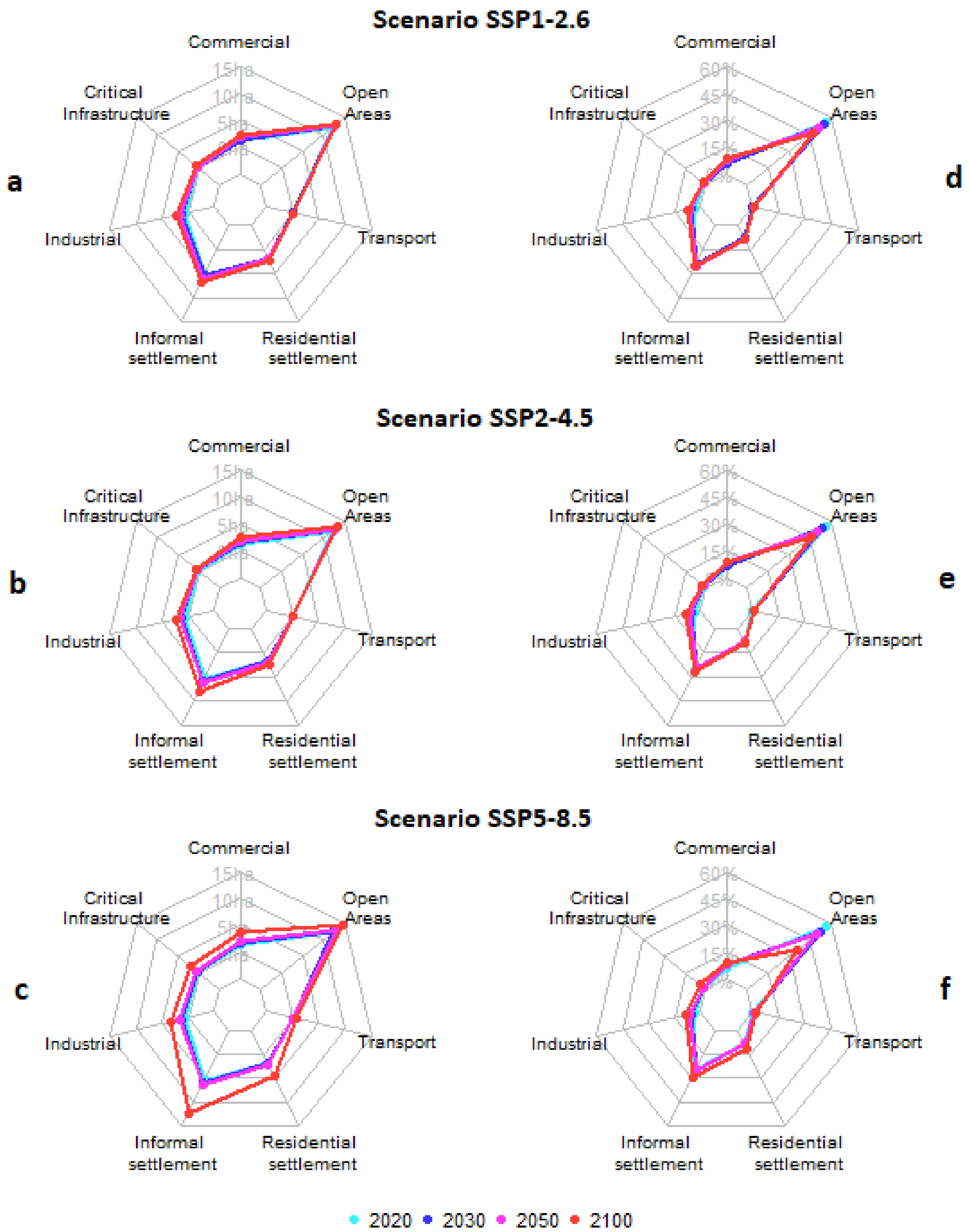

Figure 0-9: Land use exposure to coastal flooding in the Port-Bouët Bay for different climate change scenarios SSP1-2.6, SSP2-4.5 and SSP5-8.5. ***a***, ***b*** *and* ***c*** *show the flooded area per land use (in ha).* ***d***, ***e*** *and* ***f*** *display the distribution of affected land use as percentage (%) of the total flooded area.*

The changes in exposed land-uses suggest that coastal flood impacts could be increasingly severe in the coming decades. Furthermore, it is crucial to underscore that the affected housing areas, encompassing both informal settlements and residential settlements – the two predominant categories following "open areas", are likely to suffer most from flood damage, as they are located in most cases in the first line along this coastline. A closer look at the distribution of affected housing areas across coastal neighborhoods of the Port-Bouët Bay is shown in figure 4-10. As it can be observed, Sogefiha currently stands out as the most exposed neighborhood accounting for 86% of the housing surface exposure, trailed by Petit-Bassam (11%) and Vridi (3%). This pattern is anticipated to persist both over time and across various climate change scenarios, barring one notable exception in the year 2100 under the SSP5-8.5 scenario, where projected flooding in Vridi would lead to the inundation of substantial housing surfaces. Consequently, this would elevate Vridi to the position of the second-most exposed neighborhood, closely trailing Sogefiha in terms of housing exposure for this particular scenario.

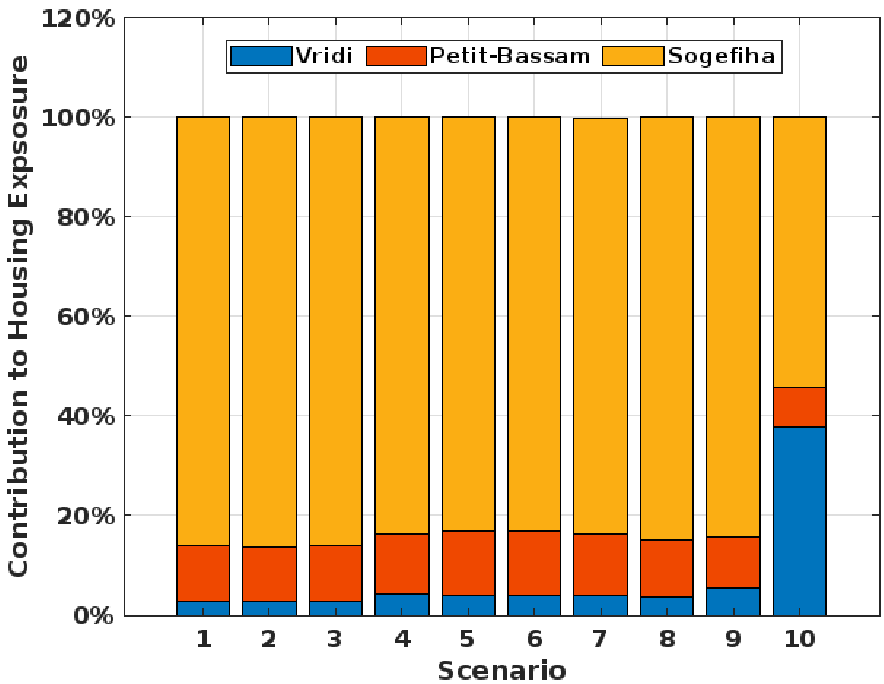

Figure 0-10: Contribution of Housing Exposure by Neighbourhood in Port-Bouët Bay. The calculation considers the combined surfaces of informal settlements and residential areas. The x-axis depicts a range of climate change scenarios, spanning different timeframes and representative concentration pathways: Scenario 1 (2020), Scenario 2 (2030; SSP1-2.6), Scenario 3 (2030, SSP2-4.5), Scenario 4 (2030, SSP5-8.5), Scenario 5 (2050; SSP1-2.6), Scenario 6 (2050, SSP2-4.5), Scenario 7 (2050, SSP5-8.5), Scenario 8 (2100, SSP1-2.6), Scenario 9 (2100, SSP2-4.5), and Scenario 10 (2100, SSP5-8.5).

4.4. Discussions

4.4.1. Insights

Using a GIS-based approach, the present study evaluates the current and future exposure to coastal flood hazard in the Port-Bouët Bay. This kind of assessment is critical in managing and mitigating the risks associated with coastal flooding (Sarica et *al*., 2021). The study used the enhanced bathtub model (eBTM), which is a simple yet effective mapping method that yielded significant outcomes. To achieve this, we incorporated into the eBTM, a 10-meter resolution DTM and robust time-dependent extreme sea level (ESL) scenarios. This DEM, generated from the topographical data of JICA (2015), is one of the most accurate available for the area. Noteworthy, those open-source DEMs with resolutions of 30-90 meters can impede mapping the extent of coastal flooding due to various errors (Wechsler, 2007). As for the time-dependent ESL scenarios, they help demonstrate the significance of climate change effects on coastal flooding and their potential impacts at the different time scales considered in this study. The simulations not only provide insights on the area likely to be flooded in different climate change scenarios but also to facilitate the estimations of the number of people, buildings and surface of land-uses that could be affected in each of these scenarios

The study's results showed that the Port-Bouët Bay is currently exposed to coastal flood phenomenon with projections showing increasing inundation surfaces and potential doubling of flood extent by 2100 under climate change scenario SSP5-8.5. This is particularly due to topographical characteristics of the area and the unprotected coastline. Noteworthy that the flood maps obtained under current and future sea-level conditions reveal a relatively constrained flooding extent, primarily within the first 200 meters from the coastline. This flooded area, which represents only 2-4% of the entire study area, holds particular importance due to the potential implications for coastal communities and land use. By intersecting the flood extent with population, building, and land-use data, the study provides a better understanding of the potential exposure to coastal flood hazards in Port-Bouët Bay. The examination of population and building exposure to coastal floods revealed that Port-Bouët Bay is currently exposed to a relatively significant number of people and buildings, with potential increases projected by 2030 and mid-century, and substantial rises by 2100. This increasing flood exposure can be attributed to the dense population and building concentration along the coastline, making the area particularly susceptible to such hazards and their potential consequences. The land-use exposure analysis indicates the predominance of exposed housing areas (both informal and residential land-use), representing 76% of the exposed land-use excluding open spaces. These findings corroborate the outcomes of larger-scale studies conducted by IMDC (2017), Muis et *al*. (2017), Nicholls et *al*. (2007), World Bank, (2022). The spatial distribution of this coastal flood exposure across neighborhood indicated that the Sogefiha is the most exposed neighborhoods followed by petit-bassam and Vridi. However, a significant surge in coastal flooding in Vridi by 2100 under the SSP5-8.5 scenario could result in substantial exposure, potentially changing this above order.

4.4.2. Limitations

Given the potential for uncertainty in the study's estimations, it is vital to discuss them to acknowledge limitations and pinpoint areas for future research and improvements. In this work, uncertainties may rise from various sources: One such source is the non-variation over time in certain input datasets, such as topography, roughness, water source, and land use distribution. Though these assumptions may be valid in the short-term basis, there can introduce some uncertainties in the long-term estimations coastal flood exposure. Nevertheless, these assumptions helped to simplify the understanding of the coastal environment of Port-Bouët Bay as these types of data were not accurately available for the area.

Another source of uncertainty may arise from the model validation process. The validation of coastal flood simulations requires data on flooding characteristics collected in a safe and effective way, very shortly after flood occurrence (Molinari et al., 2018; OPW, 2019). Unfortunately, in many coastal regions, such data is rarely available since occurrences of coastal flooding are infrequent and related information is often not documented following flood incidents, as stated by Bates (2004). In this study, model outputs were validated against observed data on coastal flood extent that were collected through surveys. However, the reliability of such validation data remains low due to the time lag between the flood occurrence and the survey. Therefore, to complement existing validation methods, it is advisable for competent authorities to explore newer data capture methods, such as citizen science (public participation in scientific research), especially during extreme events. Additionally, it is recommended to conduct regular post-coastal flood data collection and create a database to gather temporal and spatial information about historical events. Implementing these approaches can enhance model validation and minimize uncertainties in coastal flood studies along the Ivorian coasts (Bates, 2004; Molinari et al., 2018; OPW, 2019; Tavares et al., 2021).

In the course of our study, we employed the uniform disaggregation method for population distribution, evenly allocating population counts from a coarse grid to finer grid cells. Worth noting is that the obtained 30x30m resolution population maps from the "data for goods database" already relied on high-resolution identification of inhabited areas and a comprehensive understanding of underlying population distribution patterns. This uniform disaggregation method, serving as a simplification approach to transition from 30x30m to 10x10m resolution, effectively fulfilled the purpose of this study. However, we strongly recommend exploring alternative methods including machine-learning techniques for enhancing the accuracy and granularity of population disaggregation in future coastal flood exposure assessments. Generally, flood exposure in urban areas can be associated with flood characteristics such as flood frequency, duration, depth, extent and velocity (De Moel et al., 2009). But, the specific flood characteristics to be taken into account in exposure assessments may vary according to research objectives, methodological approach, and data quality. For Merz et al. (2007) and Zhu et *al*. (2019), flood depth is the main driver of urban flood exposure. On the other hand, DCLG (2009) suggested that flood extent alone could be adequate to identify the exposed elements to floods for spatial planning purposes. In the case of the current research, only flood extent was considered in the exposure analysis though both flood depth and extent were provided as outputs from the eBTM. This consideration is consistent with several studies recently carried out in the field of flood management (Dandapat & Panda, 2018; Hadipour et al., 2020; Jafarzadegan et al., 2022; Stephens et al., 2017). In this study, the omission of flood depth was based on two main factors: the unreliability of the flood depth outputs, which were not validated, and the resolution of the DEM used in the analysis, potentially affecting flood depth accuracy. Due to these limitations, we focused on other flood-related parameters confidently derived from available data. Including flood depths may require precise and current coastal land elevation data (Ward et al., 2011), which was unavailable as the DEM used dates back to 2013. This outdated data could introduce uncertainty in the analysis. However, it is essential to recognize that incorporating water depths could have assisted in determining exposure severity. It is important to acknowledge that the present work represents an initial attempt to approximate the issue of coastal flood exposure along the Ivorian coastline. Thus, as more and accurate data becomes available, there is the potential for further improvements and considerations in this issue. To further achieve this, Ward et al. (2011) suggests that the acquisition of LiDAR data, along with regular field campaigns, would be necessary to enhance mapping outcomes and explore other aspects of coastal flood exposure in Port-Bouët Bay. LiDAR-based high-resolution DEMs have demonstrated superior mapping capabilities for coastal flood-prone areas in comparison to other types of DEMs (Gesch, 2009; Poulter & Halpin, 2008). DEMs can be divided into digital terrain models (DTMs), also known as "bare-earth" DEMs, and digital surface models (DSMs), which capture the heights of objects on the Earth's surface such as buildings and vegetation (Guth et *al*., 2021; Rogers et *al*., 2020). This study makes used of DTM data. However, Williams & Lück-Vogel (2020) recommend DSMs as they are based on the principle that solid structures such as buildings and walls may influence water flow patterns in urban landscapes, thereby offering protection to other structures. DSMs assist in identifying water pathways during flood events. In this context, eBTM performs better with DSMs than with DTM, as a DTM represents an unobstructed environment for water movement. Therefore, it clearly appears that LiDAR-derived high-resolution DSM, when available and accessible, could greatly improve the present study's results. Such data could also assist in predicting future topographical changes (Zhang et *al*., 2005), which is critical for estimating future coastal flood exposure.

4.5. Conclusions

This section of the work has presented an assessment of the potential trend of exposure to coastal flooding in Port-Bouët Bay under three climate change scenarios. Despite the simplicity of the methodology employed, it has provided a preliminary yet informative overview of flood-prone areas, the populations, buildings, and land use categories exposed to extreme sea level conditions, along with their distribution across the coastal neighbourhoods.

In the face of some data constraints, particularly in terms of future scenarios, specific assumptions were leveraged to address these challenges while highlighting opportunities for improving data quality and model validation. Our study's results reveal a gradual increase in flood extent and exposed elements (populations, buildings and land-uses) from the present day to the close of the century. This suggests the likelihood of heightened damages and losses resulting from coastal flood hazards, particularly within informal settlements and residential areas, identified as the most exposed land use categories. Consequently, coastal flood hazards would emerge as the most substantial climate change impact in the study area in the forthcoming decades.

The findings of this study are very useful to be applied in adaptation strategies. They can provide researchers and decision-makers with insights into the potential impacts of coastal flooding both in the present and in the future conditions. This information not only holds potential for revising and planning future adaptation programs but also serves as a foundational baseline for upcoming studies, potentially inspiring the pursuit of enhanced data collection and analysis. By identifying exposed areas and assets exposed to coastal flooding, we can raise awareness and readiness levels across various decision-making tiers, including residents, emergency responders, and stakeholders. This proactive approach might involve promoting the implementation of flood protection measures and the development of comprehensive emergency response plans for flood-related disasters. Furthermore, the spatial disaggregation of findings down to the neighbourhood scale offers the advantage of tailored risk management and targeted interventions, thus enhancing local resilience.

ASSESSMENT OF COASTAL FLOOD RISK IN A CHANGING CLIMATE

5.1. Introduction

The Port-Bouët Bay has been facing an increasing threat of coastal flooding, resulting in significant damage to infrastructure, loss of livelihood, and environmental disruption over the past few decades (Konan et al., 2016; Sadia, 2014). With the ongoing effects of climate change, coastal flood hazards are projected to worsen, leading to higher and more frequent extreme sea-level (ESL) occurrences (Kouakou et al., 2023). Consequently, exposure to flooding will also increase, with more people and assets at risk due to dense urbanization and a growing population in the area. It is evident that future coastal flood events will have more consequences if the issue is not addressed. Therefore, it is crucial to comprehend the risks associated with coastal flooding and to compute them at appropriate spatial and temporal scales to devise effective measures for reducing their impacts and ensuring their usefulness in decision-making and planning processes.

Understanding coastal flood risk goes beyond supporting decision-makers in disaster risk management. It also contributes to the sustainable development of coastal areas. Although risk management is not directly included in any of the 17 Sustainable Development Goals (SDGs) of the United Nations' 2030 Agenda for Sustainable Development. It is relevant to several SDGs, such as human well-being (SDG-3), water management (SDG-6), resilient infrastructure (SDG-9), climate action (SDG-13), sustainable cities and communities (SDG-11), and sustainable use of terrestrial ecosystems (SDG-15) (Binns, 2022; United Nations, 2022). Therefore, knowledge of coastal flood risk is crucial for better community engagement, awareness, and resilience, which are vital for sustainable flood risk management. It also offers opportunities to combine different aspects of risk management to develop sustainable solutions that can mitigate vulnerabilities and risks and increase human well-being in both the present and future.

Coastal flood risk (CFR) is a complex concept, and its understanding is often challenging due to its multifaceted, multidimensional, and temporal nature. As a result, there has been a lack of exploration of the risk, with many studies focusing only on certain aspects of the CFR concept. Specifically, more research has concentrated on either the natural factors (hazard) or human factors (exposure and vulnerability) instead of integrating all factors for a more comprehensive analysis. Moreover, most studies have focused on the current risk rather than including the potential risk, limiting a full understanding of the CFR. Additionally, the topic is frequently approached subjectively, further complicating comprehension. In the Port-Bouët Bay area, there is a limited number of studies on CFR, despite the region's vulnerability to coastal flooding. To address these concerns, the present part of the project aims to provide a comprehensive assessment of CFR at a local scale under both present and future climate change conditions, filling gaps in knowledge and understanding.

The chapter consists of five sections, including this introductory section. Section 2 describes the methodology used, while Section 3 presents the results. Section 4 contains the discussion, and finally, the conclusions are presented in Section 5.

5.2. Methodology

The concept of risk in the context of climate change, as defined in the Intergovernmental Panel on Climate Change (IPCC) Sixth Assessment Report (AR6), is the outcome of dynamic interactions between climate-related hazard, exposure and vulnerability of those affected (Reisinger et al., 2020). These three terms "Hazard – Exposure – Vulnerability" thus constitute the risk components. According to the IPCC (2019), hazard refers to the potential occurrence of an event or trend that may result in losses, damages and disruptions of services. Exposure is the presence of people and their assets in areas and environments that may suffer adverse effects. Vulnerability describes the propensity or predisposition to be negatively impacted. In accordance with this framework, the objective of this study is to derive present and future coastal flood risk indices from indices of risk components mentioned above calculated for the neighbourhoods of the Port-Bouët Bay. The methodological approach is presented in figure 5-1 and can be summarised as follows. First, the indicators for each of the risk components are selected and validated based on an extensive review of the literature, local expert opinion and other scientific considerations. The data for these indicators are collected, pre-processed, and processed to obtain the component indices. These indices are aggregated to derive coastal flood risk indices including risk trends for each neighbourhood in the study site under climate change scenarios (SSP1-2.6, SSP2-4.5, and SSP5-8.5). Detailed information about the data and methods used at each stage of the workflow is presented in the subsequent sections.

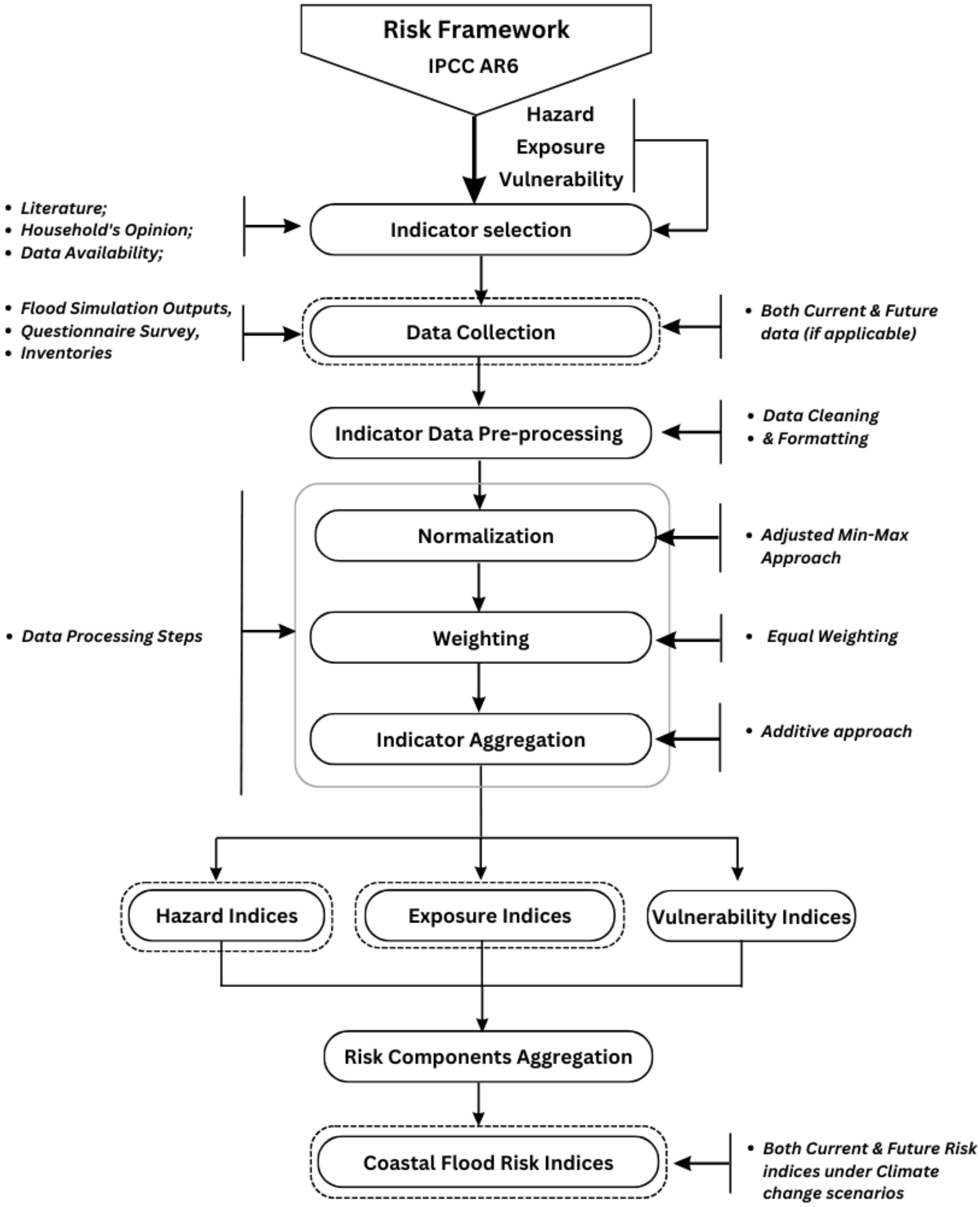

Figure 0-1: The adopted workflow of the study

5.2.1. Hazard Component

In most previous studies, the term "hazard" is used to describe the climatic and morphological factors of coastal flood risk which may include sea level rise (SLR), coastal land elevation and other triggers such tidal range, wave height, storm surge etc... (Ferreira et al., 2021; Hadipour et al., 2020; Martinelli et al., 2010). However, flood characterising parameters such as flood frequency, duration, depth, extent and velocity, could also be used to assess coastal flood hazard as they effectively depict the severity and likelihood of a flood event in a given location (Dandapat & Panda, 2018; Stephens et al., 2017).

Prior works in this ongoing research project have mainly focused on characterizing the hazard. This initially made it possible to analyse and combine the sea level components in order to deduce the resulting extreme sea level (ESLs) values (see Chapter 3). Then, in a second step, to use the estimated 100-year ESLs to simulate flooding situations in the Port-Bouët Bay using a GIS-based modelling (eBTM) that additionally takes into account data such as the topography, terrain roughness and water source (see chapter 4). Flood depth and flood extent information were thus obtained from these simulations. So, they have been taken into consideration as hazard indicators for coastal flood risk in this study. The choice of these indicators is consistent with the various sources listed in Table 5-1. For each of these two indicators, estimations are provided for the current period i.e., year 2020 (considered as the reference scenario) and for future periods i.e., 2030, 2050 and 2100 under SSP1-2.6, SSP2-4.5 and SSP5-8.5 (see section 4.3.1 in chapter 4). All these scenarios were considered in order to addresses high uncertainties associated with flood risk projections in the future (Muis et al., 2015).

Table 5-1: Description of the selected hazard indicators and their impacts on coastal flood risk index

Risk Component	Indicator	Description & Justification	Impact	References
Hazard	Flood extent	Spatial coverage of 100-year coastal flooding *A larger flood extent indicates a higher hazard level and an increased risk of damage to coastal communities, infrastructure, and ecosystems.*	+	(Wu, 2021)
	Flood depth	Maximum flood depth value reached by flooding. *A greater flood depth indicates a higher hazard level and an increased risk of damage to properties, infrastructure, and the environment.*	+	(Hadipour et al., 2020; Paranunzio et al., 2022; H. Xu et al., 2022);

5.2.2. Exposure Component

To understand and evaluate the exposure to coastal flooding in Port-Bouët Bay, the inundation layers obtained from the hazard simulations were superimposed on the spatial distribution of the population and assets in order to obtain estimates of the different exposed elements (see Chapter 4). In this context, the calculation of the exposure index in this study will obviously take into account two indicators, namely the affected population and the assets. These two indicators have already been accounted in similar works whose sources are provided in table

5-2. As for the hazard component of the risk, data regarding exposure variables is available for each neighbourhood and for both current and future periods. In this project, population and buildings data were obtained from CIESIN (2018) and Sirko et al. (2021) respectively. Note that the projected exposed population accounts for local population growth calculated over the period 2000 – 2020. For the projection of exposed assets, we assumed the total number of building unchanged over time. This is because of the high rate of urbanisation.

Table 5-2 Description of the selected exposure indicators and their impacts on coastal flood risk index

Risk Component	Indicator	Description & Justification	Impact	References
Exposure	Number of affected people	Number of individuals living within the flooded areas *As this number increases, the exposure will get higher and the risk of injury, displacement and loss of livelihoods increases.*	+	(Hinkel et al., 2014; Hauer et al., 2021; Neumann et al., 2015)
	Number of affected assets	Number of buildings within the flooded areas *As the number of affected structures rises, exposure and risk of damage and significant economic losses increases*	+	(Buchanan et al., 2020; Kebede & Nicholls, 2011)

5.2.3. Vulnerability Component

Vulnerability to coastal flooding can be multifaceted (Cardona et al., 2012). It encompasses both susceptibility and coping capacity with which it is positively and negatively correlated respectively (IPCC, 2019). As previously mentioned, vulnerability has several dimensions that should be taken into account to obtain a complete understanding of the vulnerability. However, given that the current study is aimed at informing policy decisions regarding coastal flood management planning in the urbanized Port-Bouët Bay area, we will give greater priority to analysing socio-economic vulnerability as a key dimension. Our vulnerability assessment is based on a questionnaire survey. The design of the survey, which includes steps such as the selection of indicators, the calculation of the sample size, the definition of the collection method and the implementation of the field campaign are explained in detail below.

5.2.3.1. Indicators selections

The process of selecting relevant indicators for vulnerability assessment in this study involved two steps, which followed the procedure outlined in Jhan et al. (2020) and Vandermeulen (1998). In the first step, a broad list of indicators commonly used in coastal flood vulnerability studies was created by searching in relevant publications using academic databases and key words such as coastal flood indicators, vulnerability indicators, and socio-economic indicators. The criteria used to identify relevant literature included relevance to coastal flooding, applicability to urban contexts, and recency (a focus on literatures within the last two decades). This resulted in a set of 21 potential indicators that characterize the susceptibility and coping capacity of communities related to coastal flooding.

In the second step, the suitability of the potential indicators for application in Port-Bouët Bay was assessed since the potential indicators are associated with various external contexts that may differ significantly from the study area. A questionnaire for a pre-test survey was built using the potential indicators and some indicators were skipped due to difficulties in collecting information from the population, such as “past flooding experiences”, “household income”, “local networking”, and others. Finally, 13 vulnerability indicators were selected for this study, which cover both the susceptibility and coping capacity sub-components and are highly related to the coastal flood issues. Table 5-3 describes these selected vulnerability indicators and their respective impacts on risk. The actual survey was conducted using these selected indicators. It is important to note that the indicators selected in this study are not exhaustive but rather sufficient to provide a qualification of the socioeconomic situation in the study area (Moss et al., 2001).

Table 5-3: Description of the selected vulnerability indicators and their impacts on coastal flood risk index

Risk Component	Indicator	Description & Justification	Impact	References
Vulnerability	% Disabled people	Disabled residents as a percentage of all residents: *People with disabilities may have limited mobility and communication barriers that may prevent them to evacuate quickly or understand warning or evacuation orders in an event of coastal flood. The higher the percentage, the higher the vulnerability*	+	(Balica et al., 2012; Okaka & Odhiambo, 2019)
	% Long-term sick people	Residents suffering from limiting long-term illness as a percentage of all residents: *As disabled people, long-term sick residents may have low mobility and may be dependent on caregivers or medical equipment. Their safety and well-being may heavily be impacted during coastal flooding events. The higher the percentage, the higher the vulnerability*	+	(Garbutt et al., 2015; Okaka & Odhiambo, 2019)
	Elderly and child rate	Residents aged ≥ 65 or ≤ 10 as a percentage of all residents: *Both elderly and child residents may have limited mobility, dependence on family members and may be susceptible to injuries, drowning and other accidents during a flooding event. Higher rate will increase the vulnerability*	+	(Connor & Hiroki, 2005; Meur-ferec et al., 2020)
	Proportion of female	Residents who are female as a percentage of all residents *Like elderly and disabled residents, female residents may have limited mobility and may require assistance with evacuations or other necessary tasks during a flood event, especially if they are pregnant or with childcare responsibilities. The greater the proportion, the higher the vulnerability related to coastal flooding*	+	(Garbutt et al., 2015; Kirby et al., 2019; Tate et al., 2021)
	% Households with low income	*Low-income households may have limited financial resources and may be less likely to have access to flood risk information or emergency preparedness measures, which can make it more difficult to prepare for or recover from a coastal flood event. Vulnerability increases with higher percentage of low-income households*	+	(Garbutt et al., 2015; Kirby et al., 2019)

	Dependency ratio	Proportion of the population that are not working and thus dependent on working people for support: *The higher the ratio, the greater the vulnerability.*	+	(Karunarathne & Lee, 2020; Rana & Routray, 2018)
	Household size	*Households with larger numbers of individuals may be more vulnerable to the impacts of coastal flooding.*	+	(Okaka & Odhiambo, 2019; Rana & Routray, 2018)
	% Households with precarious building condition	*Buildings that are poorly maintained or constructed with inadequate materials may be more vulnerable to the impacts of flooding.*	+	(Müller et al., 2011; Stephenson & D'Ayala, 2014)
	Literacy rate	Percentage of population with higher education: *This provides insight into a community's ability to access and understand warning and emergency information and respond to flood events effectively. Higher literacy rate.*	-	(Kablan et al., 2017; Pakhtunkhwa & Nazeer, 2019)
	% Households sensitized on coastal flooding	*Sensitization efforts can help educate households about the specific risks posed by coastal flooding. The higher the household are sensitized, the lower the vulnerability.*	-	(Müller et al., 2011)
	% Households with access to warning system	*Access to a warning system can enable to better prepare for a flooding event and respond quickly. The higher the percentage, the lower the vulnerability.*	-	(Balica et al., 2012)
	% Households with means of evacuation	*The more the households have proper evacuation resources (routes, transportation, shelters, etc.), the lower the vulnerability and risk.*	-	(Birkmann et al., 2013)
	% Household taking private flood protection initiatives	*The more the household are private taking initiatives to protect their property (e.g., sandbags et others), the lower the vulnerability*	-	(Müller et al., 2011)

5.2.3.2. Sample Size Calculation

A sample size represents the portion of the population or household chosen for the survey. For the survey outcomes to be sufficiently representative, the sample size needs to be wisely determined. several approaches exist to calculate the sample size of a given population (Memon et al., 2020; Nanjundeswaraswamy & Divakar, 2021). In this work, the sample size calculation follows the Cochran (1977) approach for a smaller population. The choice of this approach is also lies in the fact that the survey was planned to be taken place in the area of influence of the coastal flood hazard that is a relatively small area (within the 500m zone from the coastline). According to this method, the sample size should be determined using equation 5-1.

$$n = \frac{n_0}{1+\frac{(n_0-1)}{N}} \qquad \textit{(Equation 5-1)}$$

In which n is the sample size, n_0 is the Cochran's sample size recommendation and N is the total population size, here taken as the total number of households. The total household number was estimated based on the total population living in this zone and the average household size of the city which is 4.2 according to (INS, 2021). The Cochran's sample size recommendation is obtained through equation 5-2.

$$n_0 = \frac{S^2 p(1-p)}{e^2} \qquad \textit{(Equation 5-2)}$$

In which:

- S is the level of confidence desired for the survey results. Here, 95% confidence is considered. So, $S = 1.96$
- p is the estimated population or household proportion which has the attribute in question. Here taken as 50% i.e., 0.5
- e is the margin of error for the survey results. The smaller e, the more precise the study, so we consider e equals 5% i.e., 0.05

After completing all calculations, it was determined that the minimum sample size required would be 357 households, which is considered sufficient for the selected area. However, to accommodate the non-responses in the survey, a non-response rate of 10% was assumed, and as a result, the minimum sample size was established as 392 households. This sample size was equally distributed to the three local units of the study, which are Vridi, Petit-Bassam and Sogefiha.

5.2.3.3. Collection mode and Sampling method

It is a face-to-face cross-sectional survey. The selection of households to be surveyed was based on random sampling procedure. Under this procedure, all households in a given neighbourhood have an equal chance of being selected to participate in the survey. According to Noor et al. (2022), this sampling technique is unbiased and increase the generalizability of the results. Additionally, for the survey results to be reliable and valid the targeted respondent for each randomly selected household was either the father, mother or adult child; all having been in the area for subsequent period.

5.2.3.4. Implementation of the field Campaign

The survey took place over six days, from January 31 to February 5, 2022. Prior to the data collection phase, a pre-survey was conducted on January 28 to allow the interviewers to test the questionnaire and collection tools for possible adaptations or corrections. For the survey, two teams of three people each were formed to cover the entire area. In the field, the teams worked together and moved sector by sector. Each team consisted of two interviewers and one guide who was actually a local resident in charge of facilitating contact with the households. The questionnaire was administered mainly through smartphones via the Kobo Collect application, which is a module of Kobo toolbox (https://www.kobotoolbox.org). Indeed, Kobo toolbox is an open-source set of tools for questionnaire set-up, data collection, management and analysis and visualization. Through this toolbox, the data collected in the field were directly submitted to the server (with or without internet connection) at the time of collection. This technology also offers the advantages of:

- Comprehending the questionnaire for better administration
- Supervising the data collection remotely
- Saving collected data online to limit potential losses
- Downloading all the data immediately after the data collection is completed
- Reducing data entry and cleaning efforts

However, some printed versions of the questionnaire were available to address challenges such as unexpected smartphone malfunctions, battery depletion issues or even respondent discomfort related to the use of smartphones. Figure 5-2 illustrates an interview with a local resident using printed questionnaire. Note that at the request of some respondents, the interview session was followed by a short field visit to observe the damage caused by past coastal flooding on their property. The major challenges during this field campaign were (i) the accessibility of households, (ii) the unavailability of respondents due to suspicions of espionage and (iii) the security of the teams, especially in the precarious areas of the different neighbourhoods.

Figure 0-2: Picture of an interview session in a precarious place of the neighbourhood of Sogefiha (Photo credit: K.M.D.P. KOUAKOU on the 2022-02-05)

5.2.4. Risk assessment

The overall result of the current risk assessment is to obtain risk indices. A risk index is a numerical value or score calculated from a set of selected indicators and used to assess the level of risk associated with a particular hazard. Indices also help to better communicate the complex hazard risk information to the general public (Bao et al., 2018). This section of the methodology describes the process for calculating coastal flood risk index. This generally involves the standardization of indicators, the weighting and aggregation of indicators, and the aggregations of risk components to risk.

5.2.4.1. Normalization of indicator data

Normalization is an important step in risk assessment as it allows for a consistent integration of indicators that may be in different units, scales or magnitudes. Different approaches exist to rescale and remove the dimensional units of indicators values (Patro & sahu, 2015; Vafaei et al., 2018). In this work, the linear min-max normalization technique is considered. Traditionally, normalized indicator, using this technique, fall between 0 and 1, where 1 represents high risk and 0 low risk to coastal flood hazard (Percival, 2016). However, in order to avoid that the calculation of risk is biased by the extreme values of indicators, a new threshold was defined during the scaling process. This adjusted method is also known as the threshold-based min-max normalisation and is particularly suitable for enhancing scaling accuracy (Aksu et al., 2019; Yavuz & Deveci, 2012). For the implementation of the method, all the data were normalized between 0.1 and 0.9. To rescale to that range, the equations 5-3 and 5-4 below were used. The use of one or the other of these equations really depends on the correlation that the considered indicator has with the risk (see table 5-1, 5-2 and 5-3). Thus, for indicators that have a positive correlation with risk, equation 5-3 is used while equation 5-4 is used for indicators that are negatively correlated with the risk.

$$X_j = 0.8 \times \frac{X_i - X_{min}}{X_{max} - X_{min}} + 0.1 \qquad \textit{(Equation 5-3)}$$

$$X_j = 0.8 \times \frac{X_{max} - X_i}{X_{max} - X_{min}} + 0.1 \qquad \textit{(Equation 5-4)}$$

X_j and X_i are respectively the normalized value and the actual value of a given indicator in a given neighbourhood. While, X_{max} and X_{min} respectively represent the maximum value and the minimum value of the given indicator across all the neighbourhoods and years. The scaling factor of 0.8 is the range between the thresholds 0.1 and 0.9.

5.2.4.2. Weighting and Aggregation of Indicators

The process of indicator weighting involves assigning varying degrees of importance to each indicator in the analysis, based on their perceived or calculated significance. These weights can be assigned using a variety of approaches, including expert opinion, statistical analysis or stakeholder input (Gan et al., 2017). Nevertheless, this work considers equal weights for all indicators. The purpose of applying equal weights is first to initiate this risk analysis in a more simplistic way by overcoming the limitations related to the lack of prior knowledge about the selected indicators in the area while removing the need for subjective weighting. Second, to balance the multiple existing competing interests to avoid misleading of end-users.

The aggregation of the indicators allows integrating indicators values to an overall value that represents the index of the risk component (hazard, exposure and vulnerability). In this study, the aggregation method used is the additive approach, whereby the aggregated value is obtained by adding up the normalized values of individual indicator each of them multiplied by its corresponding weights (Langhans et al., 2014; Machado & Ratick, 2017). However, as we consider no variation in weight, normalized values X_j of indicators, here, are simply averaged to get the risk component index (RCI) as shown in equation 5-5.

$$RCI = \frac{\sum_{j=1}^{n} X_j}{n} \quad \textit{(Equation 5-5)}$$

5.2.4.3. Aggregating risk components to risk

This final step of the process focusses on consolidating individual risk components into a comprehensive risk index. In this work, building on Hadipour et al. (2020) and Paranunzio et al. (2022) approaches, the risk index (RI) was formulated as the product of hazard [H], exposure [E], and vulnerability [V] as indicated by equation 5-6. This formulation is in line with the IPCC AR6 risk concept. The risk component indices derived from equation 5-5 will be used as inputs for equation 5-6 to obtain the coastal flooding risk index.

$$RI = H \times E \times V \quad \text{(Equation 5-6)}$$

To assess the risk trend i.e., the temporal evolution of the coastal flood risk index across the study area, each term of the above equation should be varied in time. However since the vulnerability data only refer to the current situation, changes in risk in the future are only based on changes in the exposure and hazard components as consider by Paranunzio et al. (2022). Equation 5-6 can therefore be reformulated for future risk index as shown below (equation 5-7) where t represents the future years for which hazard and exposure information has been provided in accordance with the three different scenarios considered namely SSP1-2.6, SSP2-4.5 and SSP5-8.5.

$$RI_k(t) = H_k(t) \times E_k(t) \times V \quad \text{(Equation 5-7)}$$

To effectively communicate the likelihood and the potential implication of indices, both the risk component indices (RCI) and the risk indices (RI) were categorized into meaningful number of classes, using equal interval classification. The equal interval technique involves dividing the range of index values into sub-ranges of equal size and is particularly to highlight the significance of an index value in comparison to the other (Osaragi, 2002)

5.3. Results

5.3.1. Hazard, Exposure and Vulnerability Levels in Port-Bouët Bay

5.3.1.1. Hazard Levels

After normalizing and aggregating the indicators, hazard indices for each neighbourhood in the different periods were obtained. Figure 5-3 presents the spatial and temporal distribution of hazard levels in the Port-Bouët Bay. The analysis of this distribution shows that over the considered time period (from 2020 to 2100), the hazard level varies from very low to very high. For the current period, the hazards at Petit-Bassam and Sogefiha are low while at Vridi it is very low. The current hazard level at Vridi could remain until mid-century regardless of the climate change scenario. However, at Petit-Bassam and Sogefiha, between 2020 and 2030, it could move from low to medium and remain so until 2050. In 2100, the hazard levels display greater variability under the climate change scenario. Under SSP1-2.6 and SSP2-4.5, the hazard levels in Petit-Bassam and Sogefiha increase to high while that of Vridi increases to low. But, under SSP5-8.5, all coastal flood hazard levels in the Port-Bouët Bay could be very high.
A closer look at the indices of the different factors contributing to the hazard, namely the flood extent of flood depth, allows us to understand the variability of the hazard observed at the different neighbourhoods. Indeed, the great variability of the hazard level in Petit-Bassam and Sogefiha can be explained by the fact that these two neighbourhoods have maximum index values respectively for flood depth of flood extent. The lower hazard in Vridi comes from minimal indices in both flood extent and depth. However, the predicted extreme sea level (ESL) at Vridi in 2100 under SSP5-8.5 could create an unprecedented flooding extent that could explain the increase from low hazard in 2050 to very high hazard in 2100 under SSP5-8.5.

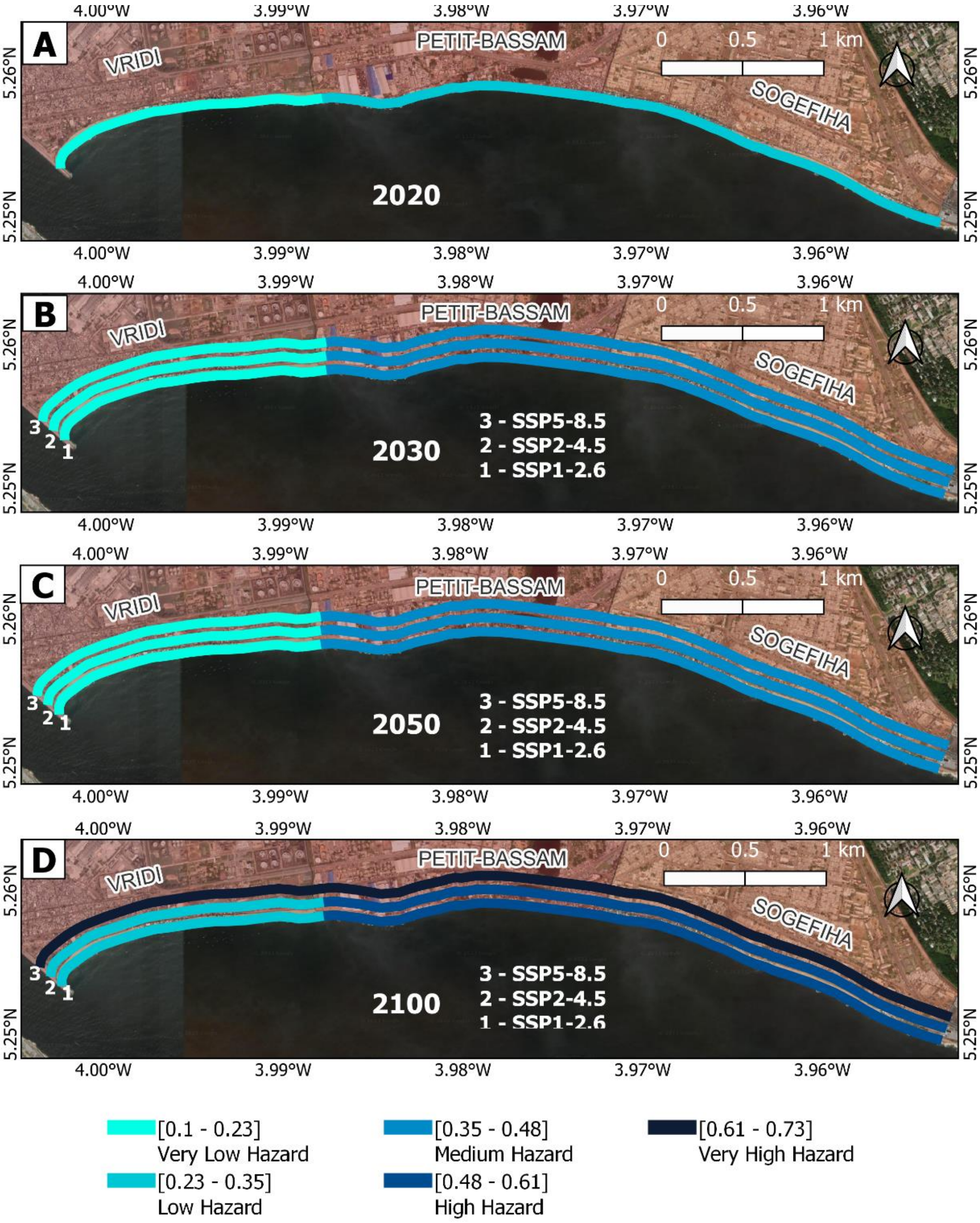

Figure 0-3: Maps showing the spatial and temporal distribution of coastal flood hazard index in the Port-Bouët Bay

5.3.1.2. Exposure Levels

The coastal flood exposure level in the Port-Bouët Bay is here determined based on the normalized number of population and building found in the simulated flooded areas. It was then classified into five categories from very low to very high, which are shown in Figure 5-4.

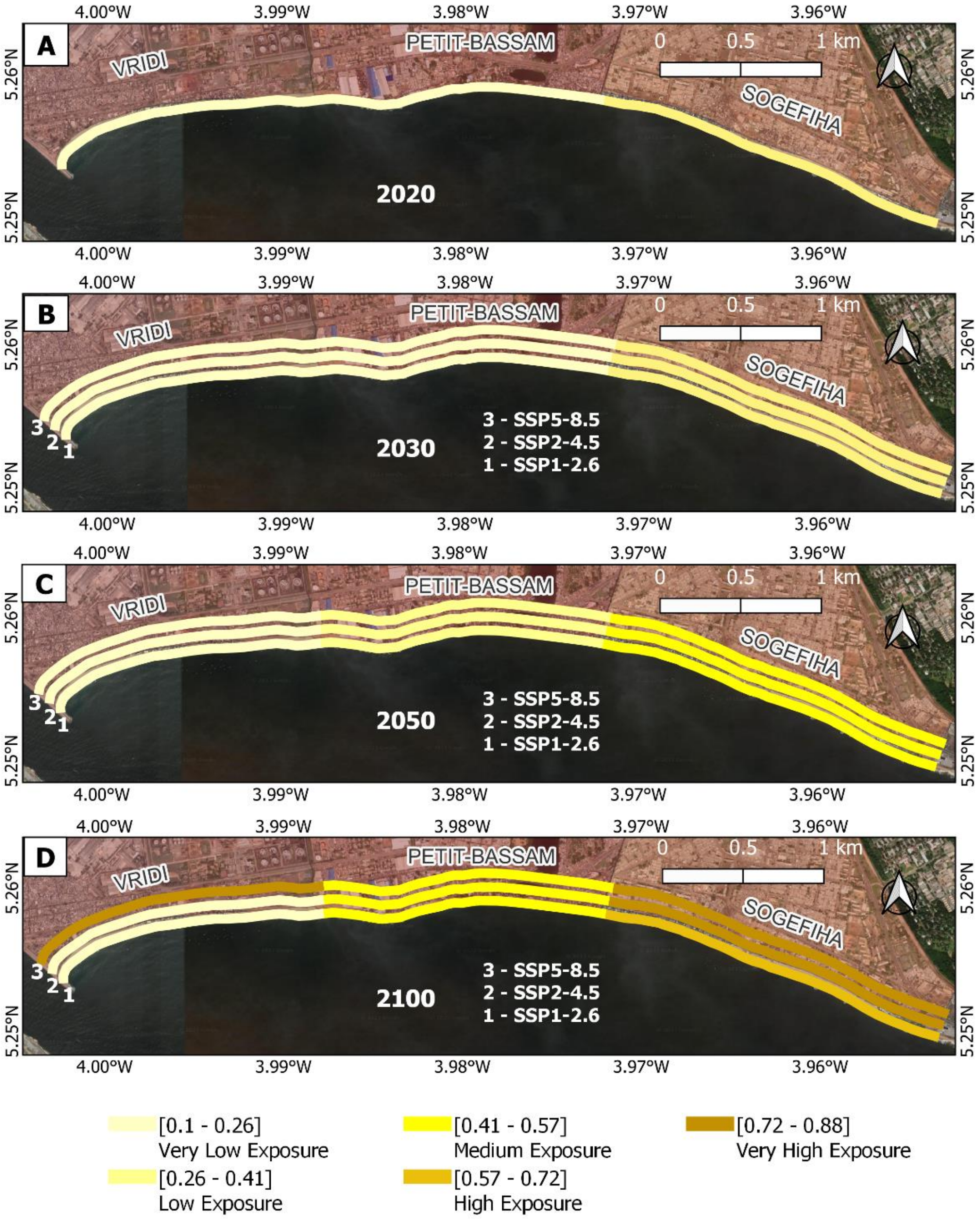

Figure 0-4: Maps showing the spatial and temporal distribution of coastal flood exposure index in the Port-Bouët Bay.

Under the reference scenario (2020), the exposure at Vridi and Petit-Bassam are very low while the level at Sogefiha is Low. Sogefiha has a higher exposure than the two other neighbourhoods do, as more people and buildings are located within the flooded area. This tendency would remain the same until 2030. In the middle of the century, exposure levels at Petit-Bassam are projected to shift from very low to low, and at Sogefiha, they are expected to transition from low to moderate (medium). Meanwhile, Vridi's exposure level is anticipated to continue being very low. By the end of the century, the anticipated exposure levels are expected to vary significantly across scenarios in both Vridi and Sogefiha, while for Petit-Bassam, the exposure level would be moderate for all scenarios. In Vridi, exposure levels under SSP1-2.6 and SSP2-4.5 are projected to be very low, while under SSP5-8.5, this level may become very high. In Sogefiha, the exposure level under SSP1-2.6 is expected to be high and very high under scenarios SSP2-4.5 and SSP5-8.5.

5.3.1.3. Vulnerability Levels

The aggregation of the 13 vulnerability indicators selected in this study made it possible to obtain vulnerability indices for the neighbourhoods of Port-Bouët Bay. Since vulnerability is very challenging to model and predict future, we only determine it for the current situation. The outcomes of vulnerability index mapping are displayed in figure 5-5, in which vulnerability indices are classified into three classes ranging from low to high. This smaller number of vulnerability classes compared to the hazard and exposure classification is mainly because of the smaller range of indices. Figure 5-5 shows low vulnerabilities at both Vridi (V=0.43) and Petit-Bassam (V= 0.44) and high vulnerability at Sogefiha. This spatial distribution of coastal flood vulnerability clearly reflects the reality on the ground since all along the Sogefiha area, vulnerable precarious housing predominantly occupies the first lines of the coast (B. Touré et al., 2012a), which is to a lesser extent at Vridi and Petit-Bassam.

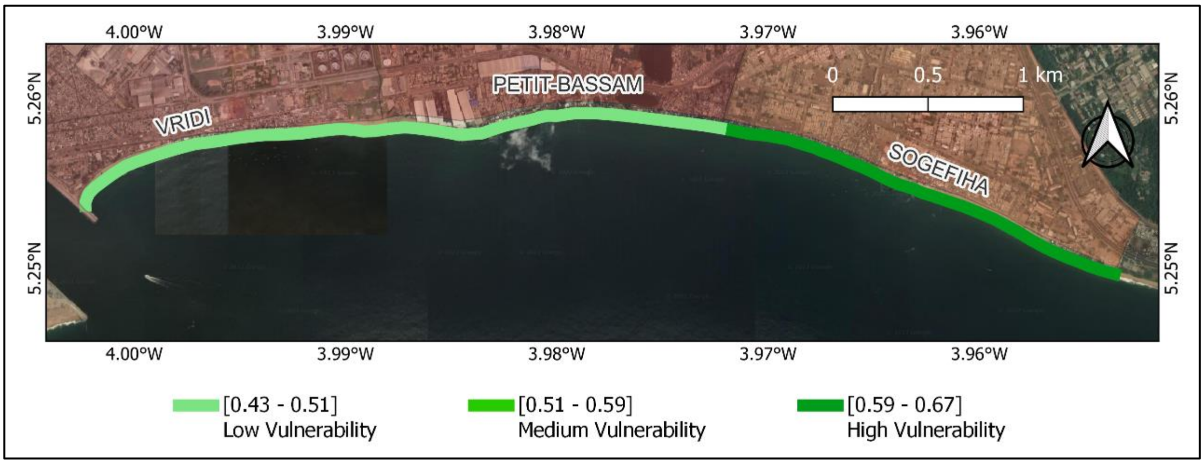

Figure 0-5: Map showing the spatial variation of coastal flood vulnerability index for the current period in the Port-Bouët Bay (this present-days tendency is assumed constant over time).

To further understand the underlying reasons for this distribution of the aggregated values of vulnerability, an analysis of the individual indicator values at the three neighbourhoods was performed and plotted in the spider chart below (figure 5-6). With one glance at this chart, it can be seen that the higher vulnerability at Sogefiha is mainly due to the high (1) percentage of disabled people, (2) elderly and child population rate, (3) ratio of female, (4) household size, and (5) proportion of households with precarious building conditions. Sogefiha possesses the maximum normalized value for each of these above indicators that all have a positive impact on vulnerability, i.e., sensitivity indicators (see table 5-3). Out of the 13 selected vulnerability indicators, Vridi and Petit-Bassam obtained the maximum normalized value in four indicators each, as shown in the plot. Note that most of the indicators in which Petit-Bassam excels have a negative correlation with vulnerability, i.e., coping capacity indicators."

Figure 5-0-6: Spider diagram of vulnerability normalized indicator values for Vridi, Petit-Bassam and Sogefiha.

The above analysis indicates that to reduce vulnerability to coastal flooding in Port-Bouët Bay, Sogefiha requires measures to reduce sensitivity, while Petit-Bassam would need increased adaptation efforts. As for Vridi a balance between measures for reducing sensitivity (decrease household income dissatisfaction and dependency ratio) and increasing coping capacity (increase sensitisation on coastal flood risk and evacuation resources) would probably be beneficial for reducing coastal flood vulnerability.

5.3.2. Coastal Flood Risk Trends

The hazard, exposure, and vulnerability levels described in the previous sections represent the key components of overall coastal flood risk. To gain a more comprehensive understanding of and address this risk, these component indices were combined using Equation 5-7. The resulting risk indices were then used to map the evolving spatial and temporal trends of risk across Port-Bouët Bay (refer to Figure 5-7).

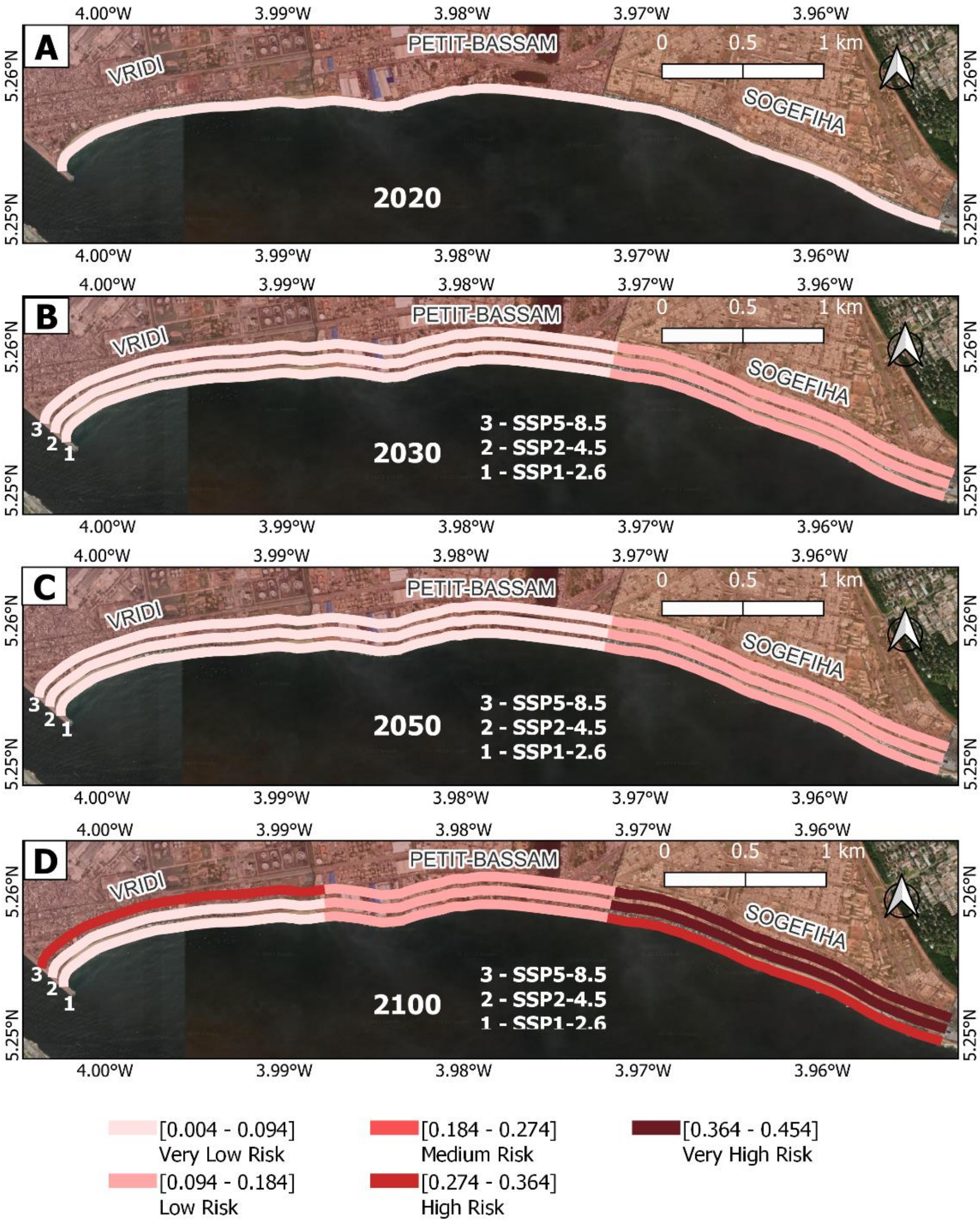

Figure 0-7: Map showing the spatial and temporal distribution of coastal flood risk index under climate change scenarios in the Port-Bouët Bay.

The risk indices have been categorized into five classes, ranging from very low to very high risk. As shown in Figure 5-7, the current coastal flood risk in all neighborhoods of Port-Bouët Bay is very low. Vridi and Petit-Bassam are expected to maintain minimal risk levels until mid-century. However, the risk level in Sogefiha is projected to increase to a low by 2030 and remain at that level until 2050. Notably, there will be no significant variations in risk levels across climate change scenarios in each neighborhood from the present day to the middle of the century. By 2100, some divergences can be observed, except in Petit-Bassam, where the risk level is predicted to remain low regardless of the SSP. In Vridi, the end-of-century risk level is expected to remain very low under SSP1-2.6 and SSP2-2.5, but it rises to a high-risk level under SSP5-8.5. In Sogefiha, the end-of-century risk level is projected to be high under SSP1-2.6 and very high under both SSP2-4.5 and SSP5-8.5.

5.3.3. Contributions to the overall coastal flood risk in Port-Bouët Bay

5.3.3.1. Contributions of the risk components

Further exploration of the risk components was conducted to enhance the understanding of their relative individual importance in determining the overall risk index and provide stakeholders and decisions-makers key information regarding the underlying factors of the coastal flood risk in the study area. To do this, the risk components indices were averaged across the different periods, and then compared to identify the largest contributor over time (see figure 5-8). The findings indicate that the temporal evolution of risk components' contribution to the total risk in Vridi and Sogefiha follows a similar pattern from 2020 to 2050 with vulnerability being the main contributor. By 2100, the hazard is projected to become the most significant contributing factor at Vridi, while exposure is predicted to become the primary contributor at Sogefiha. In Petit-Bassam, vulnerability is expected to be the primary contributor to present-day risk, but it is anticipated that the hazard component will become the most significant contributor from 2030 until the end of the century. These results provide valuable insight into the changing nature of risk components and can aid in developing effective risk management strategies over time.

5.3.3.2. Contribution of the neighbourhoods

By analysing the spatial and temporal trends of the risk and averaging of the indices, we determined the contribution of each neighbourhood to the total coastal flood risk in the study area. The percentage contributions of each neighbourhood to the risk are presented in Figure 5-9, where Sogefiha, Petit-Bassam, and Vridi are ranked as the top contributors to the risk, respectively. This information is crucial in guiding the identification of priority intervention areas for integrated coastal flood risk management.

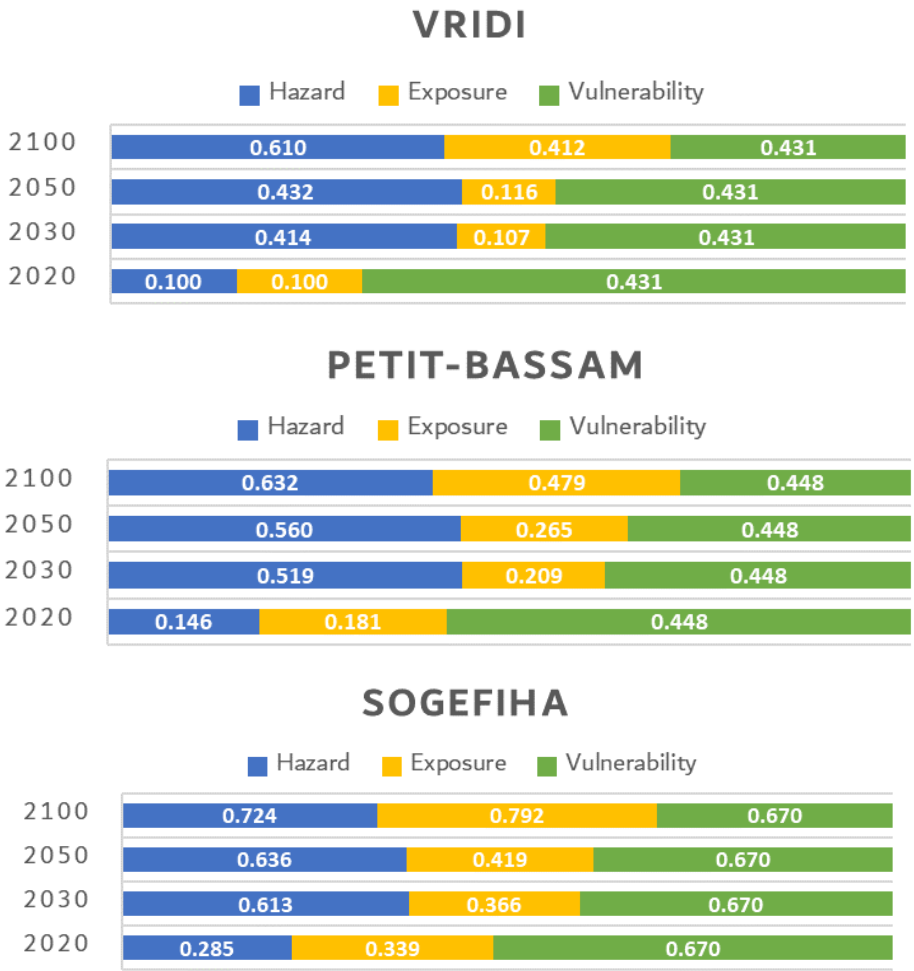

Figure 0-8: Contribution of the risk Components (Hazard; Exposure and Vulnerability) to the overall coastal flood risk in each Neighbourhood (Vridi, Petit-Bassam and Sogefiha) in Port-Bouët Bay

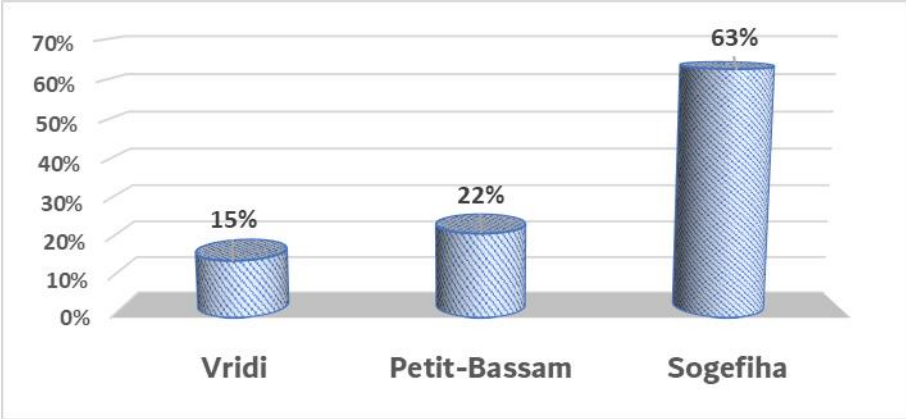

Figure 0-9: Contributions of the neighbourhoods to the overall coastal flood risk in Port-Bouët Bay

5.4. Discussion

5.4.1. Insights

This section of the work involved determining the spatial and temporal trends in coastal flood risk indices along the Port-Bouët Bay using both the IPCC AR6 risk-centred approach (IPCC, 2019; Reisinger et al., 2020) and an indicator-based approach. The first approach considers all three aspects that contribute to defining coastal flood risk, namely hazard, exposure, and vulnerability - while the latter permitted a meticulous selection of indicators based on their relevance to coastal flood phenomenon and their applicability to the local context. . To account for different sea-level rise projections, the study employed the SSP scenario, notably the SSP1-2.6, SSP2-4.5 and SSP5-8.5 which refer as the low, intermediate and high scenarios of Greenhouse Gas emissions respectively (Fox-Kemper et al., 2021; Garner et al., In prep., 2021). The methodology employed in this study follows to the standard principles of risk analysis. The different steps involved have been thoroughly explained to ensure that it is understandable and can be replicated in other contexts. The study's focus was to calculate risk indices by deriving them from the individual indices of the different components, which were obtained using selected indicators from indices of its different components whose indices were obtained from the selected indicators.

The calculated indices for each risk component reveal varying levels of hazard, exposure, and vulnerability across neighbourhoods, indicating relative disparities between these locations. Climate change could lead to a significant increase in hazard levels by the end of the century, subsequently amplifying the exposure. Regarding the resulting coastal flood risk, although the current risk is relatively very low (as depicted in Figure 5-7), it already poses challenges to the communities residing along the Port-Bouët Bay (Konan et al., 2016; Sadia, 2014). The projections of risk indicate that under all SSP scenarios, there will be an increase in the risk indices for all neighbourhoods, with the neighbourhood of Sogefiha being identified as the most at risk by the year 2100. When analysis the contribution of the different components to the overall risk, it appears, that vulnerability is the predominant contributor to the current level of risk. However, if vulnerability levels remain the same as they are today, the current predominance of vulnerability is expected to gradually diminish and give way to hazard and exposure by 2100.

Noteworthy that the approaches employed in this study helped provide significant information on the risk factors, including hazard, exposed elements, and the vulnerability of people and assets, for more targeted responses to the issue. Calculation and presentation of the index at the neighbourhood scale also facilitated identification of the neighbourhoods most at risk, informing prioritization of adaptation efforts. Thus, this study provides valuable insights on coastal flooding in an area where research on the topic has been very limited. Previous studies along the Ivorian coastline mostly focused on broader concerns, such as “coastal risk” and “coastal vulnerability” (Robin et al., 2004; Tano et al., 2016, 2018). Nonetheless, the present study aims to draw attention to the issue of coastal flooding, which has been overshadowed by coastal erosion, even though both pose serious threats to the communities along the Port-Bouët Bay. In terms of implications, the computed risk trends indicate an urgent need for tailored strategies to mitigate and adapt to minimize coastal flood risk. Additionally, with these outcomes, decision-makers could prioritize their interventions based on the specific challenges faced by different locations.

5.4.1. Limitations

In this work, there may be several potential limitations to consider, which could arise from the estimated extreme sea levels, flood mapping, exposure assessments, vulnerability indicator selection, data collection method, applied weighting method, and the considerations made in the risk assessment. While the first three points have been discussed extensively in chapters 3 and 4, this section will focus on the remaining points to complete highlighting all the possible limitations to this study.

- ***Vulnerability Indicators selection***

The vulnerability assessment in this study used a set of 13 indicators. It is important to note that, in such evaluations, the number of indicators is not as critical as their quality, impact, and relevance. For example, in similar coastal flood vulnerability assessments, Hadipour et al. (2020) used four (04) indicators, Ferreira et al. (2021) considered ten (10) indicators, Paranunzio et al. (2022) selected twelve (12) indicators, and Wu (2021) employed thirty (30) indicators. In our case, the chosen indicators were carefully selected and validated based on the opinions of the households involved. However, it is essential to acknowledge that there are other validation methods available for indicators, including expert judgment, stakeholder engagement, and statistical analysis (source). We recommend exploring the proposed alternative methods in future research to identify more relevant indicators for a more comprehensive assessment of coastal flood vulnerability within the specific local context.

- ***Survey Data Collection Method***

About the survey data collection method, it is important to note that some households within the survey coverage area are facing the threat of eviction from communal authorities due to their high exposure to coastal hazards. This situation can potentially influence individuals' responses, leading them to align with societal expectations or perceived social norms instead of being completely honest or transparent. This phenomenon is related to the concept of social desirability bias (Grimm, 2010). To minimize the impact of potential social desirability bias on the collected data, the questionnaire was designed with careful consideration to be non-judgmental and provide the option for anonymity. These measures aimed to create a safe environment for respondents to share their true thoughts, beliefs, and experiences.

However, it is worth noting that further studies should explore additional strategies to mitigate social desirability bias more effectively. The recommendations provided by (Ried et al., 2022) can serve as valuable guidance in this regard. By implementing these suggestions, future research works can improve the accuracy and reliability of the collected data, allowing for a more comprehensive understanding of the situation at hand.

- ***Weighting Method***

Assigning appropriate weights to the available input variables is a critical factor in the calculation of a indices, as the impact of different feature weights can significantly influence the final outcome (Papathoma-köhle et al., 2019). The choice of weighting methods is very often a subject of critique in the development of risk calculation indices, as it can lead to varying index values depending on the technique employed (Tsesmelis et al., 2019). In the present study, the equal weights method was used to avoid issues with overweighting and underweighting. However, this method may not accurately reflect reality (OECD, 2008). To address this limitation, alternative statistical or empirical approaches, such as principal component analysis (PCA) and analytical hierarchy process (AHP) and others, could be explored and even combined with expert judgements (Bucherie et al., 2022; Sekovski et al., 2020; Wu, 2021) to further enhance the accuracy and robustness of the indices.

- ***Risk index calculation***

In the work, the calculation of future coastal flood risk indices did not incorporate the dynamic nature of vulnerability component. This approach was necessary due to the limitations of the collected vulnerability data, which solely pertained to the current situation, and the lack of sufficient data to project vulnerability in the study area for the future. It is worth mentioning that previous researchers have also encountered similar challenges (e.g., Hadipour et al., 2020; Paranunzio et al., 2022). As a result, the conclusions drawn from these indices are valid only under the assumption that future vulnerability levels remain relatively unchanged compared to the current situation. This show the urgent need to undertake effective actions to reduce vulnerability for if vulnerability were to increase in the future, it would significantly elevate the overall coastal flood risk levels. However, it is must be acknowledged that incorporating future vulnerability data regarding the population and properties within flood-prone areas would have significantly enhanced the value of the framework and provide more precise and comprehensive risk assessments. By considering future vulnerability aspects, the risk projections presented in this study would offer a more accurate depiction of potential risks and contribute to an improved overall assessment.

- ***Index classification and Representation***

Various classification methods for indices are available, including natural breaks (Jenks), equal interval, quantile (equal counts), and standard deviation, with the selection of each method closely tied to the aim of the assessment (Papathoma-köhle et al., 2019). In general, indices can be visualized through tables, bar or line charts, or trend diagrams (OECD, 2008). In this study, considering the geographical nature of the analysis and the need to effectively communicate information to the different end-users in a simplified manner, the use of GIS maps was deemed the most appropriate approach for representation. The outcomes of the index calculations were presented using equal interval classes. However, it is important to note that relying solely on class-based representation can be misleading, as neighbourhoods falling within the same risk class may not experience equal levels of impact, exposure, or vulnerability to coastal flooding. For instance, when comparing the current situation to mid-century, both the Vridi and Petit-Bassam neighbourhoods are projected to remain in the same risk class (very low). However, in terms of the index, the flood risk in both neighbourhoods is expected to double during that period. This discrepancy between the risk class and index values may have emerged because of the use of the equal interval classification method. However, it highlights the significance of rather focusing on the specific factors that contribute to the index values.

While acknowledging the identified limitations, the findings in this study offer a valuable foundation for community-level strategies, planning, and support for coastal resilience projects. For example, the study can contribute to initiatives like the West African Coastal Area Resilience Investment Program (WACA-ResIP), a World Bank-funded project aiming at enhancing the resilience of targeted communities and coastal areas against erosion and flooding in six (6) West African countries. However, it is important to note that the risk indices were calculated at the neighbourhood level, and therefore should not be used to draw conclusions at a smaller scale (household level) or larger scale (regional level) without further assessment due to the limitations of the data and methods used. To upscale or downscale the current results, flood risk estimates will require a combination of these and other methods, tailored to the specific characteristics and needs of the study area. It is important to note that downscaling the risk indices to smaller scales, such as the household or individual level, will pose greater challenges than upscaling due to the need for more precise data and the increased possibility of uncertainties in the estimates.

5.6. Conclusion

This chapter has provided valuable insights and information on how the risk of coastal flooding due to climate change will evolve along the Port-Bouët Bay until the end of the century. The research employed the IPCC-AR6 risk framework and calculated risk indexes based on locally relevant indicators. Additionally, the study considered low, intermediate, and high SLR scenarios to anticipate the future trajectories of climate change. The findings of the study serve as a screening tool, offering estimates and suggestions for initiating discussions among stakeholders and researchers regarding the topic of coastal flood risk. The integration of these findings into coastal flood risk management planning can help achieve several key objectives:

- Assist policy and decision makers in developing climate resilience measures,
- Prioritize and target adaptation measures effectively,
- Increase awareness among various stakeholders and the public about coastal flood risk under different climate and environmental scenarios, thereby enhancing the management of the impacts of sea-level rise and changes in storm patterns.

Of course, this study has limitations that could be addressed in future research. To produce more accurate and customized results, further studies could consider additional relevant indicators of exposure and socio-economic vulnerability. Although this research solely focused on socio-economic vulnerability, we recommend linking physical or ecological dimensions to socio-economic vulnerability for efficient reduction strategies of flood risk.

RECOMMENDATIONS & CONCLUDING REMARKS

Recommendations

The analysis of the evolution of the risk of coastal flooding along the Port-Bouët Bay highlights the need for extensive efforts to mitigate coastal flood impacts and improve the resilience of the coastal communities. In other words, local and government authorities, together with all stakeholders need to develop plans and measures aiming at mitigating the potential impacts and facilitating population adaptation. In the following section, we will outline the most relevant plans and measures adapted to the urban environment of Port-Bouët Bay. They have been categorised into three groups: measures that either manage hazard, exposure, or vulnerability. Of course, these measures can be combined for sustainable and integrated risk management. Moreover, a measure from one group could influence and modify another component of the risk (Mortensen et al., 2023), hence the need to carry out feasibility studies before choosing or implementing measures from the current proposal.

Hazard Reduction

Managing coastal flood hazards involves reducing the impacts of floods through coastal protection measures. To protect the coast and prevent damage to inland areas, different options are available, including structural and non-structural measures.

- **Structural measures** also known as “hard solutions” include constructing seawalls, sea dikes, and coastal levees made from diverse materials and designed to a sufficient height to contain expected floodwater. The height of the structure is determined by the allowable risk, which is usually based on economic optimization or the availability of funds. While hard solutions can provide effective coastal flood protection, they can also be vulnerable to overtopping or failure specially in the face of constant increasing of extreme sea level under climate change effects as demonstrated in this work. In addition to their high cost and the heavy engineering works required, these solutions can also raise aesthetic, social and environmental concerns. Furthermore, opting for structural protection can result in costly repairs if the structures sustain damages, which can sometimes exceed the cost of the initial construction cost itself. Considering the limitations mentioned above, we strongly recommend that structural measures be used as a last resort for reducing coastal flood hazards in Port-Bouët Bay. In addition, it is important to conduct more in-depth feasibility studies to not only determine the optimal design but also to avoid potential issues that may arise from these structural measures.

- **The use of non-structural measures** also known as “nature-based solutions” is becoming more popular in recent years. As such, increasing importance is given to dune reinforcement and stabilization as one of the main solutions to cope with coastal floods. Coastal dune reinforcement and stabilization involves using various techniques and materials to protect and strengthen sand dunes along the coast, which in turn can help reduce the impacts of coastal erosion and flooding. These techniques include planting vegetation, installing sand fencing, and using geotextiles to reinforce the dune structure and promote their natural growth and stability while enhancing their ability to resist extreme sea level elevations. An additional measure that goes with this is to prohibit and enforce regulations against sand mining to preserve the natural protective features of the coastline and ensure the safety of local communities.

Exposure Reduction

Whether it is decided to fully protect, partially protect, or not protect the coast of Port-Bouët Bay in the future, it is crucial to inform both current and future residents about their potential exposure to coastal flooding and the possible ways to mitigate such exposure. This will ensure that residents are aware of their responsibilities and can make informed decisions. To modify the current and anticipate future exposure to coastal flood hazard in Port-Bouët Bay, the following measure could be suggested:

- **Spatial planning and controlled urbanisation** with a focus in setting up the appropriate governance arrangements needed to guarantee that the appropriate spatial planning and controlled urbanisation systems will be put in place, implemented and will be sustained over the several decades. This could involve implementing zoning regulations, building codes, or incentives for green infrastructure.

- **Creating coastal setbacks** by retreating and prohibiting development in flood-prone zones along the coast, which can reduce the risk of damage from coastal flooding. This approach can also establish natural buffers that absorb wave energy and protect inland areas (Sanò et al., 2011).

- **Building floodable spaces** by designing buildings and public spaces that can be intentionally be flooded during a flood event. This can help reduce the damage from flooding and ensure that they are usable after a flood. Floodable spaces can also provide recreational opportunities for the community during non-flood periods. An example of the concept being discussed is already being implemented in Eastern Port-Bouët: the seafront Promenade of Gonzagueville.
- **Promote flood-resistant adaptations for buildings** in flood-prone areas. These adaptations can be divided into two categories: "dry proofing," which includes measures such as elevated foundations, stilt housing, and local protection, and "wet proofing," which involves reducing damage by making buildings waterproof up to a certain level.
- **Developing evacuation plans** in extreme cases and in case when none of the above proposed measures is envisioned. However, such plans require further researches and data e.g., cost-benefit analysis.

Vulnerability Reduction

Coastal communities are often confronted with various challenges that heighten their vulnerability to coastal flooding, necessitating the need for adaptation and resilience measures to mitigate the associated risks. Based on the recommendations from Zanuttigh (2011), we suggest that the vulnerability of the Port-Bouët Bay to coastal flooding can be addressed by implementing the following measures:

- **Risk communication and education** to improve resilience to current and future risks associated with climate change. To be effective, it is crucial to conduct preliminary investigations of coastal risk perception, engaging local communities and stakeholders involved in flood mitigation, planning, and knowledge dissemination. This will enable the development of best practices for communicating flood risk and promoting preparedness, contributing to effective multilevel governance systems critical for enhancing adaptive capacity to deal with disturbance and build preparedness for living with change and uncertainty.
- **Hazard Monitoring and Developing early warning systems** can help individuals and communities take proactive measures to prepare for coastal flood events, including evacuating vulnerable areas and moving valuable assets to safer locations.

- **Effective multilevel governance systems**. These are essential for enhancing adaptive capacity and preparedness in dealing with disturbances and building resilience to cope with change and uncertainty.
- **Establishing insurance systems** can aid in the economic and social recovery process after a disaster while also limiting the impact of future disasters by implementing pricing or coverage restrictions to discourage development in areas prone to hazards.
- **Establishing post-crisis units** with trained personnel to provide psychological support for those affected by disasters

Concluding Remarks

Coastal floods phenomenon poses a significant threat to the Port-Bouët Bay area, but due to the limited number of studies, its impacts and risks is poorly understood within the local context. In order to address this question, the present thesis proposed to assess the current coastal flood risk and its future evolution under climate change effects at the local scale within the bay. To achieve this, the study employed a range of approaches including numerical modelling, GIS-based modelling, empirical methods, statistical analyses, and index calculations. These methods enabled the assessment to incorporate all the coastal flood drivers and comprehensively analysing all risk components, offering a more thorough understanding of the risk. After conducting several analyses, the main findings suggest that:

- Current coastal flood events are associated with high extreme sea level conditions. As mean sea level continues to rise due to the effects of climate change, these current extremes will become even higher, with shorter return periods. This will result in more severe and frequent future coastal flood events in all neighbourhoods within the Bay.
- Present-day coastal floods are likely to flood approximately 21.58 ha of coastal land, exposing a significant number of people and assets. With future climate change, the flooding coverage is expected to gradually increase, almost doubling by the end of the century in the worst-case scenarios. This will result in a higher exposure to flooding.
- In terms of land use exposure, informal settlements are the most exposed, followed by residential settlements, commercial areas, and industrial land, in that order.
- Due to its high susceptibility, Sogefiha is more vulnerable to coastal flood damage compared to Vridi and Petit-Bassam, which currently have low vulnerability levels.

- The combination of risk component indices indicates that the current coastal flood risk is relatively very low. However, the future risk trend will vary across neighbourhoods. By 2100, Vridi may still have very low risk, but a shift to high risk is possible under SSP5-8.5. Petit-Bassam will have low risk under all SSPs, while Sogefiha will have high risk under SSP1-2.6 and SSP2-4.5, with a possibility of reaching very high levels under SSP5-8.5.

This study enhances understanding of risk factors and can aid in developing effective strategies for mitigating and adapting to coastal flood risk in the Port-Bouët Bay area. In this regard, a certain number of proposed measures have been drafted here to proactively address the issue.

REFERENCES

Abé, J. (2005). *Contribution a la connaissance de la morphologie et de la dynamique du littoral ivoirien (Cas du littoral d'Abidjan) Essai de modelisation en vue d'une gestion rationnelle*. Université de Cocody.

Addo, K. A. (2013). *Shoreline morphological changes and the human factor . Case study of Accra Ghana*. 85–91. https://doi.org/10.1007/s11852-012-0220-5

Adingra, A., & Kouassi, M. A. (2011). Pollution en lagune ebrié et ses impacts sur l'environnement et les populations riveraines. *Fiche Technique et Document de Vulgarisation Du Centre de Recherches Océanologiques, d'Abidjan (Côte d'Ivoire)*, 48–53. http://hdl.handle.net/1834/5812

Aksu, G., Güzeller, C. O., & Eser, M. T. (2019). The Effect of the Normalization Method Used in Different Sample Sizes on the Success of Artificial Neural Network Model. *International Journal of Assessment Tools in Education*, *6*(2), 170–192. https://doi.org/10.21449/ijate.479404

Alam, E., Khan, M. S., & Salam, R. (2022). Vulnerability assessment based on household views from the Dammar Char in Southeastern Bangladesh. *Natural Hazards*, *113*(1), 329–344. https://doi.org/10.1007/s11069-022-05302-1

Almar, R., Kestenare, E., & Boucharel, J. (2019). On the key influence of remote climate variability from tropical cyclones, north and south atlantic mid-latitude storms on the senegalese coast (West africa). *Environmental Research Communications*, *1*(7). https://doi.org/10.1088/2515-7620/ab2ec6

Almar, R., Ranasinghe, R., Bergsma, E. W. J., Papa, F., Vousdoukas, M., Athanasiou, P., Almeida, L. P., Kestenare, E., Diaz, H., & Melet, A. (2021). A global analysis of extreme coastal water levels with implications for potential coastal overtopping. *Nature Communications*, 1–9. https://doi.org/10.1038/s41467-021-24008-9

Alves, B., Angnuureng, D. B., Morand, P., & Almar, R. (2020). A review on coastal erosion and flooding risks and best management practices in West Africa: what has been done and should be done. *Journal of Coastal Conservation*, *24*(3). https://doi.org/10.1007/s11852-020-00755-7

Amani, E. M. E., Akobe, A. C., Diangone, T. E., & Monde, S. (2019). Etude des Paramètres Hydrologiques par Analyse en Composante Principale (ACP), de la Baie de Biétry , Lagune Ebrie (Côte d ' Ivoire). *European Journal of Scientific Research*, *154*(1), 112–118.

Amante, C. (2018). *Consideration of Elevation Uncertainty in Coastal Flood Models*. https://doi.org/10.13140/RG.2.2.11549.15848

Ankrah, J., Monteiro, A., & Madureira, H. (2023). Shoreline Change and Coastal Erosion in West Africa: A Systematic Review of Research Progress and Policy Recommendation. *Geosciences (Switzerland)*, *13*(2). https://doi.org/10.3390/geosciences13020059

Arfi, R., & Guiral, D. (1994). Un écosystème estuarien eutrophe : la baie de Biétri. In J.-R. Durand, P. Dufour, D. Guiral, & S. G. F. Zabi (Eds.), *Environnement et ressources* *aquatiques en Côte d'Ivoire : 2. Les milieux lagunaires* (Vol. 2, pp. 335-363 ISBN 2-7099-1136–1). ORSTOM, Paris (France).

Arias, P. A., Bellouin, N., Coppola, E., Jones, R. G., Krinner, G., Marotzke, J., Naik, V., Palmer, M. D., Plattner, G. K., Rogelj, J., & et al. (2021). Technical Summary. In V. Masson-Delmotte, P. Zhai, A. Pirani, S. . L. Connors, C. Péan, S. Berger, N. Caud, Y. Chen, L. Goldfarb, M. I. Gomis, & et al. (Eds.), *Change 2021: The Physical Science Basis. Contribution of Working Group I to the Sixth Assessment Report of the Intergovernmental Panel on Climate Change* (p. 33−144). Cambridge University Press. https://doi.org/https://doi.org/10.1017/9781009157896.002

Arns, A., Wahl, T., Haigh, I. D., Jensen, J., & Pattiaratchi, C. (2013). Estimating extreme water level probabilities : A comparison of the direct methods and recommendations for best practise. *Coastal Engineering*, *81*, 51–66. https://doi.org/10.1016/j.coastaleng.2013.07.003

Aubrecht, C., Dilek, Ö. A., Joachim, K., & Sérgio, F. (2013). Future-oriented activities as a concept for improved disaster risk management. *Disaster Advances*, *6*(12), 1–10.

Bagheri-Gavkosh, M., Hosseini, S. M., Ataie-Ashtiani, B., Sohani, Y., Ebrahimian, H., Morovat, F., & Ashrafi, S. (2021). Land subsidence: A global challenge. *Science of the Total Environment*, *778*(146193), 1–17. https://doi.org/10.1016/j.scitotenv.2021.146193

Bahino, J. (2018). Analyse de la qualité de l'air dans les zones urbaines en Afrique: Caracterisation de la pollution gazeuse des especes chimiques NO2, SO2, HNO3, NH3 et O3 à Abidjan et Cotonou. In *Revue Teledetection*. Université Félix Houphouët-Boigny.

Balica, S. F., Wright, N. G., & van der Meulen, F. (2012). A flood vulnerability index for coastal cities and its use in assessing climate change impacts. In *Natural Hazards* (Vol. 64, Issue 1). https://doi.org/10.1007/s11069-012-0234-1

Ballu, V., Bouin, M. N., Siméoni, P., Crawford, W. C., Calmant, S., Boré, J. M., Kanas, T., & Pelletier, B. (2011). Comparing the role of absolute sea-level rise and vertical tectonic motions in coastal flooding, Torres Islands (Vanuatu). *Proceedings of the National Academy of Sciences of the United States of America*, *108*(32), 13019–13022. https://doi.org/10.1073/pnas.1102842108

Bao, S., Gayes, P., & Pietrafesa, L. (2018). The Need and Rationale for a Coastal Flood Risk Index. *OCEANS 2018 MTS/IEEE Charleston*, 1–4. https://doi.org/10.1109/OCEANS.2018.8604927

Basan, P. B., Biggs, R. B., Boothroyd, J. C., Chrzastowski, M. J., Davis, R. A., Fox, W. T., Frey, R. W., Goldsmith, V., Hopkins, T. S., Klein, G. de V., Kraft, J. C., Nichols, M. M., Niedoroda, A. W., Swift, D. J. P., & Wright, L. D. (1985). *Coastal Sedimentary Environments* (R. A. Davis (ed.)). Springer-Verlag.

Bates, P. D. (2004). Remote sensing and flood inundation modelling. *Hydrological Processes*, *18*, 2593–2597. https://doi.org/10.1002/hyp.5649

Berkes, F., & Ross, H. (2016). Panarchy and community resilience: Sustainability science and policy implications. *Environmental Science and Policy*, *61*, 185–193. https://doi.org/10.1016/j.envsci.2016.04.004

Berkowitz, B., & Galocha, A. (2022). *What is storm surge*. Washington Post. https://www.washingtonpost.com/weather/2022/09/26/what-is-storm-surge/

Binns, A. D. (2022). Sustainable development and flood risk management. *Journal of Flood Risk Management*, *15*(2), 3–5. https://doi.org/10.1111/jfr3.12807

Birkmann, J. (2007). Risk and vulnerability indicators at different scales:. Applicability, usefulness and policy implications. *Environmental Hazards*, *7*(1), 20–31. https://doi.org/10.1016/j.envhaz.2007.04.002

Birkmann, J., Cardona, O. D., Carreño, M. L., Barbat, A. H., Pelling, M., Schneiderbauer, S., Kienberger, S., Keiler, M., Alexander, D., Zeil, P., & Welle, T. (2013). Framing vulnerability, risk and societal responses: The MOVE framework. *Natural Hazards*, *67*(2), 193–211. https://doi.org/10.1007/s11069-013-0558-5

Birkmann, J., & von Teichman, K. (2010). Integrating disaster risk reduction and climate change adaptation: Key challenges-scales, knowledge, and norms. *Sustainability Science*, *5*(2), 171–184. https://doi.org/10.1007/s11625-010-0108-y

BNETD. (2018). *Amenagement du Carrefour AKWABA dans la commune de Port-Bouet (Abidjan) - Etude d'Impact Environnemental et Social (EIES)* (pp. 1–249). Ministere des Infrastructures Éconmiques.

Brière, C., Chatelain, J. A. M., Hoekstra, R., Nederhoff, K., Swinkels, C., & Zwaag, J. van der. (2015). *Etude de faisabilité de l'ouverture de l'embouchure du fleuve Comoé à Grand Bassam (Côte d'Ivoire) : Etudes par modèles numériques. Deltares report 1209601-000-HYE-0003*.

Bruno, M. F., Molfetta, M. G., Totaro, V., & Mossa, M. (2020). Performance Assessment of ERA5 Wave Data in a Swell Dominated Region. *Journal of Marine Science and Engineering*, *8*(214). https://doi.org/10.3390/jmse8030214

Buchanan, M. K., Kulp, S., Cushing, L., Morello-Frosch, R., Nedwick, T., & Strauss, B. (2020). Sea level rise and coastal flooding threaten affordable housing. *Environmental Research Letters*, *15*(12). https://doi.org/10.1088/1748-9326/abb266

Bucherie, A., Hultquist, C., Adamo, S., Neely, C., Ayala, F., Bazo, J., & Kruczkiewicz, A. (2022). A comparison of social vulnerability indices specific to flooding in Ecuador: principal component analysis (PCA) and expert knowledge. *International Journal of Disaster Risk Reduction*, *73*(February), 102897. https://doi.org/10.1016/j.ijdrr.2022.102897

Butler, A., Heffernan, J. E., Tawn, J. A., Flather, R. A., & Horsburgh, K. J. (2007). Extreme value analysis of decadal variations in storm surge elevations. *Journal of Marine Systems*, *67*, 189–200. https://doi.org/10.1016/j.jmarsys.2006.10.006

Cagigal, L., Rueda, A., Castanedo, S., Cid, A., Perez, J., Stephens, S. A., Coco, G., & Méndez, F. J. (2020). Historical and future storm surge around New Zealand: From the 19th century to the end of the 21st century. *International Journal of Climatology*, *40*(3), 1512–1525. https://doi.org/10.1002/joc.6283

Caires, S. (2011). *Extreme Value Analysis: Still Water Level. JCOMM Technical Report No. 58*.

Caires, S., & Bos, C. (2009). *ORCA: Spatial Statistical Analysis; Sub-Project of Loads and Strenghts (9.1a, Salt). Deltares Report 1200266-003-HYE-0003.*

Cañellas, B., Orfila, A., Méndez, F. J., Menéndez, M., & Tintoré, J. (2007). Application of a POT model to estimate the extreme significant wave height levels around the Balearic Sea (Western Mediterranean) Application of a POT model to estimate the extreme significant wave height levels around the Balearic Sea (Western Mediter. *Proceedings of the 9th International Coastal Symposium*, *SI 50*(ICS2007), 1–6.

Cardona, O. D., Van Aalst, M. K., Birkmann, J., Fordham, M., Mc Gregor, G., Rosa, P., Pulwarty, R. S., Schipper, E. L. F., Sinh, B. T., Décamps, H., Keim, M., Davis, I., Ebi, K. L., Lavell, A., Mechler, R., Murray, V., Pelling, M., Pohl, J., Smith, A. O., & Thomalla, F. (2012). Determinants of risk: Exposure and vulnerability. In *Managing the Risks of Extreme Events and Disasters to Advance Climate Change Adaptation: Special Report of the Intergovernmental Panel on Climate Change* (Field, C.B, Vol. 9781107025, pp. 65–108). https://doi.org/10.1017/CBO9781139177245.005

Carter, W. N. (2008). Disaster Management: A Disaster Manager's Handbook. In *in: Oceans '77 Conf. Record, Third Annual Conf. on Oceanic Engng., (Los Angeles, U.S.a.: Oct.17-19, 1977)* (Vols. 2, New Yo). Asian Development Bank. https://doi.org/10.1109/oceans.1977.1154316

Cerveny, R. S., Bessemoulin, P., Burt, C. C., Cooper, M. A., Cunjie, Z., Dewan, A., Finch, J., Holle, R. L., Kalkstein, L., Kruger, A., Lee, T.-C., Martínez, R., Mohapatra, M., Pattanaik, D. R., Peterson, T. C., Sheridan, S., Trewin, B., Tait, A., & Abdel, W. M. M. (2017). WMO Assessment of Weather and Climate Mortality Extremes: Lightning, Tropical Cyclones, Tornadoes, and Hail. *WEATHER, CL IMATE , AND SOCIETY*, *9*, 487–497. https://doi.org/10.1175/WCAS-D-16-0120.1

Chang, H., Pallathadka, A., Sauer, J., Grimm, N. B., Zimmerman, R., Cheng, C., Iwaniec, D. M., Kim, Y., Lloyd, R., Mcphearson, T., Rosenzweig, B., Troxler, T., Welty, C., Brenner, R., & Herreros-cantis, P. (2021). Assessment of urban flood vulnerability using the social-ecological-technological systems framework in six US cities. *Sustainable Cities and Society*, *68*(October 2020), 102786. https://doi.org/10.1016/j.scs.2021.102786

Chauveau, E., Chadenas, C., Comentale, B., Pottier, P., Blanloeil, A., Feuillet, T., Mercier, D., Pourinet, L., Rollo, N., Tillier, I., & Trouillet, B. (2011). Xynthia: lessons learned from a catastrophe. *Journal of Geography: Environnement, Nature, Paysage*, *538*, 1–21. https://doi.org/https://doi.org/10.4000/cybergeo.28032

Cheng, Y., & Andersen, O. B. (2009). Improvement in global ocean tide model in shallow water regions. Poster Number: SV.1-68 45. *Altimetry for Oceans and Hydrology OST-ST Meeting*, 1–2. https://doi.org/10.1029/2008JC005179.Munk

Church, J. A., & White, N. J. (2011). *Sea-Level Rise from the Late 19th to the Early 21st Century*. 585–602. https://doi.org/10.1007/s10712-011-9119-1

CIESIN. (2018). *Documentation for the Gridded Population of the World, Version 4 (GPWv4), Revision 11 Data Sets*. https://doi.org/https://doi.org/10.7927/H45Q4T5F

Cissé, C. O. T., Almar, R., Youm, J. P. M., Jolicoeur, S., Taveneau, A., Sy, B. A., Sakho, I., Sow, B. A., & Dieng, H. (2022). Extreme Coastal Water Levels Evolution at Dakar (Senegal, West Africa). *Climate*, *11*(1), 6. https://doi.org/10.3390/cli11010006

Cisse, C. O. T., Brempong, E. K., Taveneau, A., Almar, R., Sy, B. A., & Angnuureng, D. B. (2022). Extreme coastal water levels with potential flooding risk at the low-lying Saint Louis historic city, Senegal (West Africa). *Frontiers in Marine Science*, *9*(December), 1–12. https://doi.org/10.3389/fmars.2022.993644

Clark, P. U., Shakun, J. D., Marcott, S. A., Mix, A. C., Eby, M., Kulp, S., Levermann, A., Milne, G. A., Pfister, P. L., Santer, B. D., Schrag, D. P., Solomon, S., Stocker, T. F., Strauss, B. H., Weaver, A. J., Winkelmann, R., Archer, D., Bard, E., Goldner, A., … Plattner, G. K. (2016). Consequences of twenty-first-century policy for multi-millennial climate and sea-level change. *Nature Climate Change*, *6*(4), 360–369. https://doi.org/10.1038/nclimate2923

Cochran, W. G. (1977). *Sampling Techniques, 3rd Edition*.

Coles, S. (2001). *An Introduction to Statistical Modeling of Extreme Values*. Springer-Verlag. https://doi.org/https://doi.org/10.1007/978-1-4471-3675-0

Connor, R. F., & Hiroki, K. (2005). Development of a method for assessing flood vulnerability. *Water Science and Technology*, *51*(5), 61–67. https://doi.org/10.2166/wst.2005.0109

Coppola, D. P. (2015). Introduction to International Disaster Management. In *Elsevier Inc*. https://doi.org/10.1016/C2014-0-00128-1

Coquet, M., Mercier, D., & Fleury-Bahi, G. (2018). Individuals' perceptions of areas exposed to coastal flooding in four French coastal municipalities: the contribution of sketch mapping. *Geoenvironmental Disasters*, *5*(1). https://doi.org/10.1186/s40677-018-0107-3

Coulibaly, L., Diomandé, D., Coulibaly, A., & Gourène, G. (2004). Utilisation des ressources en eaux, assainissement et risques sanitaires dans les quartiers précaires de la commune de Port-Bouët (Abidjan; Côte d'Ivoire). *VertigO*, *Volume 5 Numéro 3*. https://doi.org/10.4000/vertigo.3299

Cowell, P. J., & Thom, B. G. (1994). Morphodynamics of coastal evolution. In B. Carter, R. W. G. Carter, & C. D. Woodroffe (Eds.), *Coastal Evolution: Late Quaternary Shoreline Morphodynamics* (pp. 33–86). Cambridge University Press.

Creel Liz. (2003). Ripple Effects: Population and Coastal Regions. In *Population Reference Bureau*. https://pdf.usaid.gov/pdf_docs/Pnadd169.pdf

D'Arcy, E., Tawn, J. A., & Sifnioti, D. E. (2022). Accounting for Climate Change in Extreme Sea Level Estimation. *Water (Switzerland)*, *14*(19), 1–21. https://doi.org/10.3390/w14192956

Dahunsi, A. M., Bonou, F., Dada, O. A., & Baloïtcha, E. (2022). Spatio-Temporal Trend of Past and Future Extreme Wave Climates in the Gulf of Guinea Driven by Climate Change. *Journal of Marine Science and Engineering*, *10*(11). https://doi.org/10.3390/jmse10111581

Dandapat, K., & Panda, G. K. (2018). A geographic information system-based approach of flood hazards modelling, Paschim Medinipur district, West Bengal, India. *Jamba: Journal of Disaster Risk Studies*, *10*(1), 1–7. https://doi.org/10.4102/jamba.v10i1.518

DCLG. (2009). *Planning Policy Statement 25: Development and Flood Risk Practice Guide*.
De Moel, H., Van Alphen, J., & Aerts, J. C. J. H. (2009). Flood maps in Europe - Methods, availability and use. *Natural Hazards and Earth System Science*, *9*(2), 289–301. https://doi.org/10.5194/nhess-9-289-2009
Deltares. (2015a). *1D/2D/3D Modelling suite for integral water solutions Delft3D Flexible Mesh Suite: D-Flow Flexible Mesh Technical Reference Manual Version 1.1.148*.
Deltares. (2015b). *1D/2D/3D Modelling suite for integral water solutions Delft3D Flexible Mesh Suite: D-Flow Flexible Mesh User Manual Version 1.1.148*.
Diaw, T. (2018). *A peninsula in coastal erosion ? Dakar , the Senegalese capital city facing the sea level rise in the context of climate change Une presqu ' île en érosion côtière ? Dakar , la capitale sénégalaise face à l ' avancé e de la mer dans le contexte du changem*. *2*(1), 91–108.
Djagoua, E., Bakayoko, F., Kouadio, J. M., Kassi, J.-B., Mobio, B. H., Adonis, K. K., Tiemélé, J. A., & Yavo, P. (2016). Cartographie De La Dynamique Du Trait De Cote A Grand-Lahou : Utilisation De L ' outil « Digital Shoreline Analysis System (Dsas)». *European Scientific Journal*, *July 2017*. https://doi.org/10.19044/esj.2016.v12n36p327
Dodman, D., Brown, D., Francis, K., Hardoy, J., Johnson, C., & Satterthwaite, D. (2013). *Understanding the nature and scale of urban risk in low- and middle-income countries and its implications for humanitarian preparedness , planning and response Understanding the nature and scale of urban risk in low- and middle-income countries and its im* (Issue March). http://pubs.iied.org/10624IIED.html%0ADisclaimer:
Durand, J.-R., & Guiral, D. (1994). Hydroclimat et hydrochimie. *Environnement et Ressources Aquatiques En Côte d'Ivoire : 2. Les Milieux Lagunaires.*, 59–90.
EEA. (2013). *Balancing the future of Europe's coasts — knowledge base for integrated management* (Issue 12). https://doi.org/10.2800/99116
Engle, N. L., de Bremond, A., Malone, E. L., & Moss, R. H. (2014). Towards a resilience indicator framework for making climate-change adaptation decisions. *Mitigation and Adaptation Strategies for Global Change*, *19*(8), 1295–1312. https://doi.org/10.1007/s11027-013-9475-x
Fang, J., & Shi, P. (2021). Research progress and prospect of coastal flood disaster risk assessment against global climate change. *Journal of Geography and Cartography*, *4*(2), 102–116. https://doi.org/10.24294/jgc.v4i2.1311
Fassardi, C. (2007). *the Definition of Wave Setup and Runup Using a Response Based Approach*. *April 2007*, 1800–1811. https://doi.org/10.1142/9789812709554_0152
Fawcett, D., Pearce, T., Ford, J. D., & Archer, L. (2017). Operationalizing longitudinal approaches to climate change vulnerability assessment. *Global Environmental Change*, *45*(May), 79–88. https://doi.org/10.1016/j.gloenvcha.2017.05.002
FCL and CIESIN. (2022). *High resolution settlement layer (HRSL) Source imagery for HRSL, Maxar*.
Fekete, B., Vörösmarty, C., & Grabs, W. (2002). *Global composite runoff fields Version 1.0 / Comoe Basin Station: Aniassue*. University of New Hampshire, and Global Runoff Data

Centre, Koblenz, Germany. https://www.compositerunoff.sr.unh.edu/html/Polygons/P1428400.html

FEMA. (2018). *Guidance for Flood Risk Analysis and Mapping: Coastal Wave Runup and Overtopping*.

Fereshtehpour, M., & Karamouz, M. (2018). DEM Resolution Effects on Coastal Flood Vulnerability Assessment: Deterministic and Probabilistic Approach. *Water Resources Research*, *54*(7), 4965–4982. https://doi.org/10.1029/2017WR022318

Ferreira, J. C., Cardona, F. S., Santos, C. J., & Tenedório, J. A. (2021). Hazards, vulnerability, and risk analysis on wave overtopping and coastal flooding in low-lying coastal areas: The case of costa da caparica, Portugal. *Water (Switzerland)*, *13*(2). https://doi.org/10.3390/w13020237

Flather, R. A. (2003). Air–Sea Interaction / Storm Surges. *Encyclopedia of Atmospheric Sciences, Academic Press*, 109–118. https://doi.org/10.1016/B0-12-227090-8/00067-1

Foli, B. A. K., Addo, K. A., Ansong, J. K., & Wiafe, G. (2021). Evaluation of ECMWF and NCEP Reanalysis Wind Fields for Long-Term Historical Analysis and Ocean Wave Modelling in West Africa. *Remote Sensing in Earth Systems Sciences*. https://doi.org/https://doi.org/10.1007/s41976-021-00052-3

Ford, J. D., Pearce, T., McDowell, G., Berrang-Ford, L., Sayles, J. S., & Belfer, E. (2018). Vulnerability and its discontents: the past, present, and future of climate change vulnerability research. *Climatic Change*, *151*(2), 189–203. https://doi.org/10.1007/s10584-018-2304-1

Fox-Kemper, B., Hewitt, H. T., Xiao, C., Aðalgeirsdóttir, G., Drijfhout, S. S., Edwards, T. L., Golledge, N. R., Hemer, M., Kopp, R. E., Krinner, G., & Al., E. (2021). Ocean, Cryosphere and Sea Level Change. In V. Masson-Delmotte, P. Zhai, A. Pirani, S. L. Connors, C. Péan, S. Berger, N. Caud, Y. Chen, L. Goldfarb, M. I. Gomis, & et al. (Eds.), *Climate Change 2021: The Physical Science Basis. Contribution of Working Group I to the Sixth Assessment Report of the intergovernmental Panel on Climate Change* (In press). Cambridge University Press.

Frederikse, T., Buchanan, M. K., Lambert, E., Kopp, R. E., Oppenheimer, M., Rasmussen, D. J., & Wal, R. S. W. Van De. (2020). Antarctic Ice Sheet and emission scenario controls on 21st-century extreme sea-level changes. *Nature Communications*, *390*, 1–11. https://doi.org/10.1038/s41467-019-14049-6

Gallien, T. W., Sanders, B. F., & Flick, R. E. (2014). Urban coastal flood prediction: Integrating wave overtopping, flood defenses and drainage. *Coastal Engineering*, *91*, 18–28. https://doi.org/10.1016/j.coastaleng.2014.04.007

Gan, X., Fernandez, I. C., Guo, J., Wilson, M., Zhao, Y., Zhou, B., & Wu, J. (2017). When to use what: Methods for weighting and aggregating sustainability indicators. *Ecological Indicators*, *81*(May), 491–502. https://doi.org/10.1016/j.ecolind.2017.05.068

Garbutt, K., Ellul, C., & Fujiyama, T. (2015). Mapping social vulnerability to flood hazard in Norfolk, England. *Environmental Hazards*, *14*(2), 156–186. https://doi.org/10.1080/17477891.2015.1028018

Garner, G. G., Hermans, T., Kopp, R. E., Slangen, A. B. A., Edwards, T. L., Levermann, A., Nowikci, S., Palmer, M. D., Smith, C., B., F.-K., & et al. (2021). *IPCC AR6 Sea-Level Rise Projections Version 20210809*.

Garner, G. G., Kopp, R. E., Hermans, T., Slangen, A. B. A., Koubbe, G., Turilli, M., Jha, S., Edwards, T. L., Levermann, A., Nowikci, S., Palmer, M. D., & Smith, C. (n.d.). *Framework for Assessing Changes to Sea-level (FACTS)*.

GEBCO Company Group. (2021). *GEBCO 2021 Grid*. https://doi.org/https://doi.org/10.5285/c6612cbe-50b3-0cff-e053-6c86abc09f8f

GEF LME LEARN. (2020). *Coastal Hazard and Risk Mitigation: Taking an integrated approach to protect people and places*. https://iwlearn.net/: https://iwlearn.net/

Gesch, D. B. (2009). Analysis of Lidar Elevation Data for Improved Identification and Delineation of Lands Vulnerable to Sea-Level Rise. *Journal of Coastal Research*, *SI*(53), 49–58. https://doi.org/10.2112/SI53-006.1

Gomes da Silva, P., Coco, G., Garnier, R., & Klein, A. H. F. (2020). On the prediction of runup, setup and swash on beaches. *Earth-Science Reviews*, *204*, 103148. https://doi.org/10.1016/j.earscirev.2020.103148

Gomez, L. M. A., Janet, O., & Ntajal, J. (2020). Vulnerability to coastal erosion in The Gambia : Empirical experience from Gunjur. *International Journal of Disaster Risk Reduction*, *45*, 101439. https://doi.org/10.1016/j.ijdrr.2019.101439

Gourlay, M. R. (2011). Waves and Wave-Driven Currents. In *Encyclopedia of Modern Coral Reefs. Encyclopedia of Earth Sciences Series.: Vol. Part 2* (Issue 1842, pp. 1174–1180). Springer. https://doi.org/10.1007/978-90-481-2639-2_32

Grases, A., Gracia, V., Garc, M., & Lin-ye, J. (2020). Coastal Flooding and Erosion under a Changing Climate : Implications at a Low-Lying Coast(Delta, Ebro). *Water*, *12*(346), 1–26. https://doi.org/doi:10.3390/w12020346

Gravley, D. (2001). Risk, Hazard, and Disaster. *Most*, 1990–1996.

Grimm, P. (2010). Social Desirability Bias. *Wiley International Encyclopedia of Marketing.*, pp1.

Guerrera, F., Mart, M., Tramontana, M., Nimon, B., & Essotina, K. (2021). *Shoreline Changes and Coastal Erosion : The Case Study of the Coast of Togo (Bight of Benin , West Africa Margin)*.

Guth, P. L., Van Niekerk, A., Grohmann, C. H., Muller, J. P., Hawker, L., Florinsky, I. V., Gesch, D., Reuter, H. I., Herrera-Cruz, V., Riazanoff, S., López-Vázquez, C., Carabajal, C. C., Albinet, C., & Strobl, P. (2021). Digital elevation models: Terminology and definitions. *Remote Sensing*, *13*(18), 1–19. https://doi.org/10.3390/rs13183581

Hadipour, V., Vafaie, F., & Deilami, K. (2020). Coastal flooding risk assessment using a GIS-based spatial multi-criteria decision analysis approach. *Water (Switzerland)*, *12*(9). https://doi.org/10.3390/W12092379

Hall, J. W., Sayers, P. B., Walkden, M. J. A., & Panzeri, M. (2006). Impacts of climate change on coastal flood risk in England and Wales: 2030-2100. *Philosophical Transactions of the Royal Society A: Mathematical, Physical and Engineering Sciences*, *364*(1841), 1027–

1049. https://doi.org/10.1098/rsta.2006.1752
Hallegatte, S., Green, C., Nicholls, R. J., & Corfee-morlot, J. (2013). Future flood losses in major coastal cities. *Nature Climate Change*, *3*(9), 1–5. https://doi.org/10.1038/nclimate1979
HARPIS-SL. (2022). *Flood Exposure, Vulnerability and Risk*. INTEGREMS. https://www.harpis-sl.website/index.php/hazard-assessment/natural/flood/fldexposure-vulnerability-and-risk-assessment
Hauer, M. E., Hardy, D., Kulp, S. A., Mueller, V., Wrathall, D. J., & Clark, P. U. (2021). Assessing population exposure to coastal flooding due to sea level rise. *Nature Communications*, *12:6900*, 1–9. https://doi.org/10.1038/s41467-021-27260-1
Hawkes, P. J. (2005). *Use of Joint Probability Methods in Flood Management - A Guide to Best Practice R&D Technical Report FD2308/TR2*.
Hegerl, G. C., Zwiers, F. W., Braconnot, P., Gillett, N. P., Luo, Y., Marengo Orsini, J. A., Nicholls, N., Penner, J. E., & Stott, P. A. (2007). Understanding and attributing climate change. In S. Solomon, D. Qin, M. Manning, Z. Chen, M. Marquis, K. B. Averyt, M. Tignor, & H. L. Miller (Eds.), *IPCC, 2007: Climate Change 2007: the physical science basis. contribution of Working Group I to the Fourth Assessment Report of the Intergovernmental Panel on Climate Change* (pp. 663–746). Cambridge University Press. https://doi.org/http://hdl.handle.net/102.100.100/124109?index=1
Hemer, M. A., Fan, Y., Mori, N., Semedo, A., & Wang, X. L. (2013). Projected changes in wave climate from a multi-model ensemble. *Nature Climate Change*, *3*(5), 471–476. https://doi.org/10.1038/nclimate1791
Hersbach, H., Bell, B., Berrisford, P., Biavati, G., Horányi, A., Sabater, J. M., Nicolas, J., Peubey, C., Radu, R., Rozum, I., Schepers, D., Simmons, A., Soci, C., Dee, D., & Thépaut, J.-N. (2018). ERA5 hourly data on single levels from 1979 to present. *Copernicus Climate Change Service (C3S) Climate Data Store (CDS)*. https://doi.org/https://doi.org/10.24381/cds.adbb2d47
Hicks, S. D. (2006). Understanding tides. *Center for Operational Oceanographic Products and Services*, 1–83. https://tidesandcurrents.noaa.gov/publications/Understanding_Tides_by_Steacy_finalFINAL11_30.pdf
Hinkel, J., Lincke, D., Vafeidis, A. T., Perrette, M., Nicholls, R. J., Tol, R. S. J., Marzeion, B., Fettweis, X., Ionescu, C., & Levermann, A. (2014). Coastal flood damage and adaptation costs under 21st century sea-level rise. *Proceedings of the National Academy of Sciences of the United States of America*, *111*(9), 3292–3297. https://doi.org/10.1073/pnas.1222469111
Holthuijsen, L. H. (2007). Waves in oceanic and coastal waters. In *Cambridge University Press*.
Howard, T., & Palmer, M. D. (2019). Contributions to 21st century projections of extreme sea-level change around the UK Contributions to 21st century projections of extreme sea-level change around the UK. *Environmental Research Communications, 1*(095002). https://doi.org/https://doi.org/10.1088/2515-7620/ab42d7

Idier, D., Rohmer, J., Pedreros, R., Le Roy, S., Lambert, J., Louisor, J., Le Cozannet, G., & Le Cornec, E. (2020). Coastal flood: a composite method for past events characterisation providing insights in past, present and future hazards—joining historical, statistical and modelling approaches. In *Natural Hazards* (Vol. 101, Issue 2). Springer Netherlands. https://doi.org/10.1007/s11069-020-03882-4

Iftekhar, A., & Charlesworth, E. (2014). *Urban Disaster Management Toolkit: An Assessment-Based Approach to World Vision's Disaster Management Dimensions*.

IMDC. (2017). *Coût de la dégradation environnementale, évaluation du risque multi-aléas et analyse coût-bénéfice des solutions pour la zone côtière. D7d: Analyse coût-bénéfice des options de RRC et ACC sélectionnées pour la Côte d'Ivoire – secteur CI5 Port Bouët*.

INS. (2021). *Resulats Globaux Recensement général de la population et de l'habitat (R.G.P.H.) 2021*. 1–37.

IPCC. (2012). *Managing the Risks of Extreme Events and Disasters to Advance Climate Change Adaptation. A Special Report of Working Groups I and II of the Intergovernmental Panel on Climate Change* (C. B. Field, V. Barros, T. F. Stocker, D. Qin, D. J. Dokken, K. L. Ebi, M. D. Mastrandrea, K. J. Mach, G.-K. Plattner, S. K. Allen, M. Tignor, & and P. M. Midgley (eds.)). Cambridge University Press.

IPCC. (2019). Annex I: Glossary. In N. M. Weyer (Ed.), *Special Report on the Ocean and Cryosphere in a Changing Climate Glossary (September 2019): SROCC* (In Press, pp. 541–562). H.-O. Pörtner, D.C. Roberts, V. Masson-Delmotte, P. Zhai, M. Tignor, E. Poloczanska, K. Mintenbeck, A. Alegría, M. Nicolai, A. Okem, J. Petzold, B. Rama, N.M. Weyer. http://journal.um-surabaya.ac.id/index.php/JKM/article/view/2203

IPCC. (2021). *Climate Change 2021 The Physical Science Basis Climate Change 2021 Contribution of Working Group I to the Sixth Assessment Report of the Intergovernmental Panel on Climate Change* (V. Masson-Delmotte, P. Zhai, A. Pirani, S. L. Connors, C. Péan, S. Berger, N. Caud, Y. Chen, L. Goldfarb, M. I. Gomis, M. Huang, K. Leitzell, E. Lonnoy, J. B. R. Matthews, T. K. Maycock, T. Waterfield, O. Yelekçi, & & B. Z. R. Yu (eds.); In press). Cambridge University Press. https://doi.org/https://doi.org/10.1017/9781009157896

Jafarzadegan, K., Muñoz, D. F., Moftakhari, H., Gutenson, J. L., Savant, G., & Moradkhani, H. (2022). Real-time coastal flood hazard assessment using DEM-based hydrogeomorphic classifiers. *Natural Hazards and Earth System Sciences*, *22*(4), 1419–1435. https://doi.org/10.5194/nhess-22-1419-2022

Jeer, S., & Bain, B. (1997). Traditional Color Coding for Land Uses. *American Planning Association*, 4–5. http://gsd.harvard.edu/gis/manual/style/ColorConventions.pdf

Jevrejeva, S., Moore, J. C., Grinsted, A., & Woodworth, P. L. (2008). Recent global sea level acceleration started over 200 years ago ? *GEOPHYSICAL RESEARCH LETTERS*, *35*(L08715), 1–4. https://doi.org/10.1029/2008GL033611

Jhan, H. T., Ballinger, R., Jaleel, A., & Ting, K. H. (2020). Development and application of a socioeconomic vulnerability indicator framework (SVIF) for local climate change adaptation in Taiwan. *Sustainability (Switzerland)*, *12*(4).

https://doi.org/10.3390/su12041585
Jia, H., Chen, F., & Du, E. (2021). Adaptation to disaster risk—An overview. *International Journal of Environmental Research and Public Health*, *18*(21). https://doi.org/10.3390/ijerph182111187
JICA. (2015). *The Republic of Côte d ' Ivoire Digital Topographic Mapping Project for Urban Infrastructure Development (A Fast Track Project)*. https://openjicareport.jica.go.jp/pdf/12247441_01.pdf
Jones, R. N., & Preston, B. L. (2011). Adaptation and risk management. *Wiley Interdisciplinary Reviews: Climate Change*, *2*(2), 296–308. https://doi.org/10.1002/wcc.97
Kablan, M. K. A., Dongo, K., & Coulibaly, M. (2017). Assessment of social vulnerability to flood in urban Côte d'Ivoire using the MOVE framework. *Water (Switzerland)*, *9*(4), 1–19. https://doi.org/10.3390/w9040292
Kang, J. L., Su, M. D., & Chang, L. F. (2005). Loss functions and framework for regional flood damage estimation in residential area. *Journal of Marine Science and Technology*, *13*(3), 193–199. https://doi.org/10.51400/2709-6998.2126
Karunarathne, A. Y., & Lee, G. (2020). Developing a multi-facet social vulnerability measure for flood disasters at the micro-level assessment. *International Journal of Disaster Risk Reduction*, *49*, 101679. https://doi.org/10.1016/j.ijdrr.2020.101679
Kebede, A. S., & Nicholls, R. (2011). Population and Assets Exposure to Coastal Flooding in Dar es Salaam (Tanzania): Vulnerability to Climate Extremes. *Regional Environmental Change*, 1–26.
Kirby, R. H., Reams, M. A., Lam, N. S. N., Zou, L., Dekker, G. G. J., & Fundter, D. Q. P. (2019). Assessing Social Vulnerability to Flood Hazards in the Dutch Province of Zeeland. *International Journal of Disaster Risk Science*, *10*(2), 233–243. https://doi.org/10.1007/s13753-019-0222-0
Kirezci, E., Young, I. R., Ranasinghe, R., Muis, S., Nicholls, R. J., Lincke, D., & Hinkel, J. (2020). Projections of global-scale extreme sea levels and resulting episodic coastal flooding over the 21st Century. *Scientific Reports*, *10*(1), 1–12. https://doi.org/10.1038/s41598-020-67736-6
Koffi, K. P. (2017). *Etude de l'évolution morpho-sédimentaire du littoral ivoirien : remaniement sédimentaire à l'échelle multi-temporelle*. Université Felix Houphouët Boigny Abidjan.
Koffi, K. P., Affian, K., & Abé, J. (1993). Contribution à l'étude des caractéristiques morphologiques de l'unité littorale de Côte d'Ivoire, Golfe de Guinée: cas du périmètre littoral de Port-Bouet. *Journal Ivoirien d'Océanologie et de Limnologie*, *2*(1), 43–52.
Kohno, N., Dube, S. K., Entel, M., Fakhruddin, S. H. M., Greenslade, D., Leroux, M. D., Rhome, J., & Thuy, N. B. (2018). Recent Progress in Storm Surge Forecasting. *Tropical Cyclone Research and Review*, *7*(2), 128–139. https://doi.org/10.6057/2018TCRR02.04
Kohno, N., Kamakura, K., Minematsu, H., Yorioka, Y., Hisashige, K., Shimizu, E., Fukunaga, A., Taniwaki, Y., Tanijo, S., Kishimoto, K., Nishigaki, T., Nishimura, S., & Terasaka, Y. (2007). The Mechanism of the Storm Surges in the Seto Inland Sea Caused by Typhoon

Chaba. *Tenki*, *9*(9), 1–18.
Komar, P. D. (1998). *Beach Processes and Sedimentation. 2nd Edition*. Englewood-Cliffs.
Konan, K. E. (2012). *Etude morpho-dynamique et sensibilité aux événements « exceptionnels » du cordon littoral sableux ivoirien à l'Est d'Abidjan (Abidjan-Aforenou)*. Université Félix Houphouët Boigny Abidjan.
Konan, K. E. (2014). *Relations entre les points critiques d ' érosion et le transit littoral en Côte d ' Ivoire The relation between erosion hotspots and the littoral drift in Côte d ' Ivoire Relations entre les points critiques d ' érosion et le transit littoral en Côte d ' . January*.
Konan, K. E., Abe, J., Aka, K., Neumeier, U., Nyessen, J., & Ozer, A. (2016). Impacts des houles exceptionnelles sur le littoral ivoirien du Golfe de Guinée. *Géomorphologie : Relief, Processus, Environnement*, *22*(1). https://doi.org/10.4000/geomorphologie.11241
Kouakou, M., Bonou, F., Gnandi, K., Djagoua, E., Idrissou, M., & Abunkudugu, A. (2023). Determination of Current and Future Extreme Sea Levels at the Local Scale in Port-Bouët Bay (Côte d'Ivoire). *Journal of Marine Science and Engineering*, *11*(4), 756. https://doi.org/https:// doi.org/10.3390/jmse11040756
Kuhlicke, C., Scolobig, A., Tapsell, S., Steinführer, A., & de Marchi, B. (2011). Contextualizing social vulnerability: Findings from case studies across Europe. *Natural Hazards*, *58*(2), 789–810. https://doi.org/10.1007/s11069-011-9751-6
Lamothe, M. de N. de, & Rognon, F. (1975). L'hybride Port-Bouet 121: Nouveau resulats. *Oléagineux*, *30*(11), 457–465.
Lang, M., Coeur, D., Bard, A., Bacq, B., Becker, T., Bignon, E., Blanchard, R., Bruckmann, L., Delserieys, M., Edelblutte, C., & Merle, C. (2013). Les inondations remarquables en France: premiers éléments issus de l'enquête EPRI 2011. *Houille Blanche*, *5*, 37–47. https://doi.org/10.1051/lhb/2013041
Langhans, S. D., Reichert, P., & Schuwirth, N. (2014). The method matters: a guide for indicator aggregation in ecological assessments. *Ecological Indicators*, *45*, 494–507. https://doi.org/https://doi.org/10.1016/ j.ecolind.2014.05.014
Lemasson, L., & Rebert, J.-P. (1968). *Observations de courants sur le Plateau Continental Ivoirien: Mise en evidence d'un sous-courant*.
Lemasson, L., & Rebert, J.-P. (1973). Circulation dans le Golfe de Guinée de la région d'origine du sous-courant Ivoirien. *Cah. O.R.S.T.O.M Sér. Océonogr.*, *XI*(3), 303–316.
Li, C., Cai, R., & Yan, X. (2023). *Assessment of the Future Changes in the Socio-Economic Vulnerability of China ' s Coastal Areas*.
Li, C., Held, H., Hokamp, S., & Marotzke, J. (2020). Optimal temperature overshoot profile found by limiting global sea level rise as a lower-cost climate target. *Science Advances*, *6*(2), 1–8. https://doi.org/10.1126/sciadv.aaw9490
Lincke, D., Hinkel, J., Mengel, M., & Nicholls, R. J. (2022). Understanding the Drivers of Coastal Flood Exposure and Risk From 1860 to 2100. *Earth's Future*, *10*(12). https://doi.org/10.1029/2021EF002584
Machado, E. A., & Ratick, S. (2017). Implications of indicator aggregation methods for global change vulnerability reduction efforts. *Mitigation and Adaptation Strategies for Global*

Change, *23*(7), 1109–1141. https://doi.org/10.1007/s11027-017-9775-7

Magnan, A. K., Schipper, E. L. F., Burkett, M., Bharwani, S., Burton, I., Eriksen, S., Gemenne, F., Schaar, J., & Ziervogel, G. (2016). Addressing the risk of maladaptation to climate change. *Wiley Interdisciplinary Reviews: Climate Change*, *7*(5), 646–665. https://doi.org/10.1002/wcc.409

Manyena, B., Machingura, F., & O'Keefe, P. (2019). Disaster Resilience Integrated Framework for Transformation (DRIFT): A new approach to theorising and operationalising resilience. *World Development*, *123*, 104587. https://doi.org/10.1016/j.worlddev.2019.06.011

Marcos, M., Rohmer, J., Vousdoukas, M. I., Mentaschi, L., Cozannet, G. Le, & Amores, A. (2019). Increased Extreme Coastal Water Levels Due to the Combined Action of Storm Surges and Wind Waves Geophysical Research Letters. *Geophical Research Letters*, *46*, 4356–4364. https://doi.org/10.1029/2019GL082599

Martin, L. (1974). *Le trou-sans-fond, canyon sous-marin de la côte d'ivoire*. *VI*, 67–76.

Martinelli, L., Zanuttigh, B., & Corbau, C. (2010). Assessment of coastal flooding hazard along the Emilia Romagna littoral, IT. *Coastal Engineering*, *57*(11–12), 1042–1058. https://doi.org/10.1016/j.coastaleng.2010.06.007

Mascle, J. ., Basile, C. ., Bouillin, J.-P. ., Mascle, G. ., Cousin, M. ., Durand, M. ., Dejax, J., & Moullade, M. (1997). A geological field trip to the Cote d'Ivoire- Ghana transform margin. *Oceanologica Acta*, *21*(1), 1–20. https://doi.org/https://doi.org/10.1016/S0399-1784(98)80045-5

Maul, G. A., & Duedall, I. . (2019). Demography of Coastal Populations. In C. W. Finkl & C. Makowski (Eds.), *Encyclopedia of Coastal Science. Encyclopedia of Earth Sciences Series*. Springer, Cham. https://doi.org/https://doi.org/10.1007/978-3-319-93806-6_115

Mcfall, B. C. (2019). The Relationship between Beach Grain Size and Intertidal Beach Face Slope. *Journal of Coastal Research*, *35*(5), 1080–1086. https://doi.org/10.2112/JCOASTRES-D-19-00004.1

Meehl, G. A., Hu, A., Tebaldi, C., Arblaster, J. M., Washington, W. M., Teng, H., Sanderson, B. M., Ault, T., Strand, W. G., & White, J. B. (2012). Relative outcomes of climate change mitigation related to global temperature versus sea-level rise. *Nature Climate Change*, *2*(8), 576–580. https://doi.org/10.1038/nclimate1529

Melby, J. A., Nadal-Caraballo, N. C., & Kobayashi, N. (2012). Wave Runup prediction for flood mapping. *Coastal Engineering Proceedings*, *1*, 1–15. https://doi.org/https://doi.org/10.9753/icce.v33.management.79

Memon, M. A., Ting, H., Cheah, J.-H., Thurasamy, R., Chuah, F., & Cham, T. H. (2020). Sample Size for Survey Research: Review and Recommendations. *Journal of Applied Structural Equation Modeling*, *4*(2), i–xx. https://doi.org/10.47263/jasem.4(2)01

Mentaschi, L., Vousdoukas, M. I., Voukouvalas, E., Dosio, A., & Feyen, L. (2017). Global changes of extreme coastal wave energy fluxes triggered by intensified teleconnection patterns. *Geophysical Research Letters*, *44*(5), 2416–2426. https://doi.org/10.1002/2016GL072488

Merz, B., Thieken, A. H., & Gocht, M. (2007). Flood risk mapping at the lcal scale: Concepts and Challenges. In S. Begum & et al. (Eds.), *Flood Risk Management in Europe* (Vol. 23, pp. 231–251). Springer. https://doi.org/10.1007/978-1-4020-4200-3

Meur-ferec, C., Berre, I. Le, Cocquempot, L., Guillou, É., Henaff, A., Lami, T., Dantec, N. Le, Letortu, P., & Noûs, C. (2020). flooding Une méthode de suivi de la vulnérabilité systémique à l ' érosion et la submersion marines. *Développement Durable et Territoires*, *11*(1), 0–23. https://doi.org/10.4000/developpementdurable.16731

Mohanty, P. C., Mahendra, R. S., Nayak, R. K., Manche, S. S., Joseph, S., Nair, T. M. B., & Srinivasa Kumar, T. (2023). Characteristics of astronomical tides and their modulation on sea level extremes along the Indian coast. *Ocean and Coastal Management*, *231*(November 2022), 106398. https://doi.org/10.1016/j.ocecoaman.2022.106398

Molinari, D., Bruijn, K. M. De, Jesica, T., Aronica, G. T., Bouwer, M., Molinari, D., Bruijn, K. M. De, Castillo-, J. T., Aronica, G. T., & Bouwer, L. M. (2018). Validation of flood risk models : Current practice and possible improvements. *International Journal of Disaster Risk Reduction*, 1–22. https://doi.org/10.1016/j.ijdrr.2018.10.022

Morgan, E. A., Nalau, J., & Mackey, B. (2019). Assessing the alignment of national-level adaptation plans to the Paris Agreement. *Environmental Science and Policy*, *93*(June), 208–220. https://doi.org/10.1016/j.envsci.2018.10.012

Morim, J., Hemer, M., Wang, X. L., Cartwright, N., Trenham, C., Semedo, A., Young, I., Bricheno, L., Camus, P., Casas-Prat, M., Erikson, L., Mentaschi, L., Mori, N., Shimura, T., Timmermans, B., Aarnes, O., Breivik, Ø., Behrens, A., Dobrynin, M., … Andutta, F. (2019). Robustness and uncertainties in global multivariate wind-wave climate projections. *Nature Climate Change*, *9*(9), 711–718. https://doi.org/10.1038/s41558-019-0542-5

Mortensen, E., Tiggeloven, T., Haer, T., Van Bemmel, B., Le Bars, D., Muis, S., Eilander, D., Weiland, F. S., Bouwman, A., Ligtvoet, W., & Ward, P. J. (2023). The Potential of Global Coastal Flood Risk Reduction Using Various DRR Measures. *Natural Hazards and Earth System Sciences*, *January*, 1–33. https://doi.org/10.5194/nhess-2022-284

Moss, R. H., Brenkert, A. L., & Malone, E. L. (2001). *Vulnerability to Climate Change: A Quantitative Approach* (Issue PNNL-SA-33642).

Muis, S., Güneralp, B., Jongman, B., Aerts, J. C. J. H., & Ward, P. J. (2015). Flood risk and adaptation strategies under climate change and urban expansion: A probabilistic analysis using global data. *Science of the Total Environment*, *538*, 445–457. https://doi.org/10.1016/j.scitotenv.2015.08.068

Muis, S., Verlaan, M., Nicholls, R. J., Brown, S., Hinkel, J., Lincke, D., Vafeidis, A. T., Scussolini, P., Winsemius, H. C., & Ward, P. J. (2017). Earth ' s Future A comparison of two global datasets of extreme sea levels and resulting flood exposure Earth ' s Future. *Earth's Future*, *5*, 379–392. https://doi.org/10.1002/eft2.197

Muis, S., Verlaan, M., Winsemius, H. C., Aerts, J. C. J. H., & Ward, P. J. (2016). A global reanalysis of storm surges and extreme sea levels. *Nature Communications*, *7*(11969), 1–11. https://doi.org/10.1038/ncomms11969

Müller, A., Reiter, J., & Weiland, U. (2011). Assessment of urban vulnerability towards floods using an indicator-based approach-a case study for Santiago de Chile. *Natural Hazards and Earth System Sciences*, *11*(8), 2107–2123. https://doi.org/10.5194/nhess-11-2107-2011

N'guessan, Y. A., Diangoné, E., Konan, E. K., Sékongo, R., & Wognin, V. (2018). Sedimentary Dynamics of the Coastline of the Vridi Canal in Port- Bouët , Abidjan (Côte D ' ivoire). *Journal of Environmental Science, Computer Science and Engineering & Technology*, *7*(1), 70–79. https://doi.org/10.24214/jecet.A.7.1.07079.

N'guessan, Y. A., Konan, K. E., Touré, M., Sékongo, R., Wognin, V., & Aka, K. (2017). Evolution of the Coastline and sedimentary dynamics in Port-Bouet Bay, Abidjan (Cote d'Ivoire). *American Journal of Scientific Research*, *109*, 87–96. http://www.americanjournalofscientificresearch.com

Nalau, J., Handmer, J., Dalesa, M., Foster, H., Edwards, J., Kauhiona, H., Yates, L., & Welegtabit, S. (2016). The practice of integrating adaptation and disaster risk reduction in the south-west Pacific. *Climate and Development*, *8*(4), 365–375. https://doi.org/10.1080/17565529.2015.1064809

Nanjundeswaraswamy, T. S., & Divakar, S. (2021). Determination of Sample Size and Sampling Methods in Applied Research. *Proceedings on Engineering Sciences*, *3*(1), 25–32. https://doi.org/10.24874/pes03.01.003

Nash, J. E., & Sutcliffe, J. V. (1970). River Flow Forecasting Through Conceptual Models - Part I - A Discussion of Principles. *Journal of Hydrology*, *10*(1970), 282–290. https://doi.org/10.1061/(asce)1084-0699(2006)11:6(597)

Ndour, A., Laïbi, R. A., Sadio, M., Degbe, C., Degbe, E., Anthony, E. J., Dussouillez, P., Diaw, A. T., Oy, L. M., Sambou, H., & Di, B. (2017). *Ocean & Coastal Management Management strategies for coastal erosion problems in west Africa : Analysis , issues , and constraints drawn from the examples of Senegal and Benin d e*. 1–15. https://doi.org/10.1016/j.ocecoaman.2017.09.001

Nelson, M. C., Ingram, S. E., Dugmore, A. J., Streeter, R., Peeples, M. A., McGovern, T. H., Hegmon, M., Arneborg, J., Kintigh, K. W., Brewington, S., Spielmann, K. A., Simpson, I. A., Strawhacker, C., Comeau, L. E. L., Torvinen, A., Madsen, C. K., Hambrecht, G., & Smiarowski, K. (2016). Climate challenges, vulnerabilities, and food security. *Proceedings of the National Academy of Sciences of the United States of America*, *113*(2), 298–303. https://doi.org/10.1073/pnas.1506494113

Nerem, R. S., Chambers, D. P., Choe, C., & Mitchum, G. T. (2010). *Estimating Mean Sea Level Change from the TOPEX and Jason Altimeter Missions Estimating Mean Sea Level Change from the TOPEX and Jason Altimeter Missions*. *0419*. https://doi.org/10.1080/01490419.2010.491031

Neumann, B., Vafeidis, A. T., Zimmermann, J., & Nicholls, R. J. (2015). Future coastal population growth and exposure to sea-level rise and coastal flooding - A global assessment. *PLoS ONE*, *10*(3). https://doi.org/10.1371/journal.pone.0118571

Neumann, T., & Ahrendt, K. (2013). Comparing the "Bathtub Method" with MIKE 21 HD

Flow Model for Modelling Storm Surge Indundation: Case Study Kiel Fjord. In *RADOST Report Series* (Issue 22). http://klimzug-radost.de/en/info/comparing-bathtub-method-mike-21-hd-flow-model-modelling-storm-surge-indundation-case-study-kie

Nicholls, R. J., Hanson, S., Herweijer, C., Patmore, N., Hallegatte, S., Corfee-Morlot, J., Chateau, J., & Muir-Wood, R. (2007). Ranking of the World's cities most exposed to coastal flooding today and in the future. In *OECD Environment Working Paper No. 1 (ENV/WKP(2007)1).* http://dpanther.fiu.edu/dpService/dpPurlService/purl/FI15061848/00001

Nicholls, R. J., Lincke, D., Hinkel, J., Brown, S., Vafeidis, A. T., Meyssignac, B., Hanson, S. E., Merkens, J. L., & Fang, J. (2021). A global analysis of subsidence, relative sea-level change and coastal flood exposure. *Nature Climate Change*, *11*(7), 634. https://doi.org/10.1038/s41558-021-01064-z

NOAA. (2023). *Tides and Water Levels: Types and Causes of Tidal Cycles – Diurnal, Semidiurnal, Mixed Semidiurnal; Continental Interference*. National Ocean Service. https://oceanservice.noaa.gov/education/tutorial_tides/tides07_cycles.html

Noor, S., Tajik, O., & Golzar, J. (2022). Simple Random Sampling. *International Journal of Education and Language Studies*, *1*(2), 78–82. https://doi.org/DOI: 10.22034/ijels.2022.162982

OECD. (2008). Handbook on Constructing Composite Indicators: Methodology and user fuide. In *Journal of the American Geriatrics Society*. OECD PUBLICATIONS. https://www.oecd.org/els/soc/handbookonconstructingcompositeindicatorsmethodologyanduserguide.htm

Okaka, F. O., & Odhiambo, B. D. O. (2019). Households' perception of flood risk and health impact of exposure to flooding in flood-prone informal settlements in the coastal city of Mombasa. *International Journal of Climate Change Strategies and Management*, *11*(4), 592–606. https://doi.org/10.1108/IJCCSM-03-2018-0026

ONU-Habitat. (2011). *Côte D ' Ivoire : Profil Urbain de Port-Bouet* (pp. 1–32). Programme des NatioNs UNies PoUr les ÉtablissemeNts HUmains.

OPW. (2019). *Food data collector's handbook: A practical guide to flood data collection*. The Stationery Office. https://www.gov.ie/en/collection/a06c18-flood-event-data-collection/

Osaragi, T. (2002). Classification Methods for Spatial Data Representation. *UCL Working Papers Series*, *44*(August), 1–19. www.casa.ucl.ac.uk%5Cnhttp//www.casa.ucl.ac.uk/paper40.pdf

Osinowo, A. A., & Popoola, S. O. (2021). Long-term spatio-temporal trends in extreme wave events in the Niger delta coastlines. *Continental Shelf Research*, *224*(August 2020), 104471. https://doi.org/10.1016/j.csr.2021.104471

Pakhtunkhwa, N. K., & Nazeer, M. (2019). Flood Vulnerability Assessment through Different Methodological Approaches in the Context of North-West Khyber Pakhtunkhwa, Pakistan. *Sustainability (Switzerland)*, *11*(6695), 18.

Pan, X., Rahman, A., Haddad, K., & Ouarda, T. B. M. J. (2022). Peaks-over-threshold model in flood frequency analysis: a scoping review. *Stochastic Environmental Research and*

Risk Assessment, *36*(9), 2419–2435. https://doi.org/10.1007/s00477-022-02174-6
Pandey, A. C., Singh, S. K., & Nathawat, M. S. (2010). Waterlogging and flood hazards vulnerability and risk assessment in Indo Gangetic plain. *Natural Hazards*, *55*(2), 273–289. https://doi.org/10.1007/s11069-010-9525-6
Papathoma-köhle, M., Schlögl, M., & Fuchs, S. (2019). Vulnerability indicators for natural hazards : an innovative selection and weighting approach. *Scientific Reports*, *9*(15026), 1–14. https://doi.org/10.1038/s41598-019-50257-2
Paranunzio, R., Guerrini, M., Dwyer, E., Alexander, P. J., & O'Dwyer, B. (2022). Assessing Coastal Flood Risk in a Changing Climate for Dublin, Ireland. *Journal of Marine Science and Engineering*, *10*(11). https://doi.org/10.3390/jmse10111715
Patro, S. G. K., & sahu, K. K. (2015). Normalization: A Preprocessing Stage. *Iarjset*, 20–22. https://doi.org/10.17148/iarjset.2015.2305
Pecher, A., & Kofoed, J. (2017). *Handbook of Ocean Wave Energy* (Ocean Engi). Springer Open. https://doi.org/10.1007/978-3-319-39889-1
Percival, S. (2016). *Portsmouth Coastal Flood Vulnerability and Risk : Assessment and Mapping of Impacts at Microscale: Vol. I* (Issue June). http://ludwig.lub.lu.se/login?url=https://search.ebscohost.com/login.aspx?direct=true&db=edsble&AN=edsble.714156&site=eds-live&scope=site
Percival, S., & Teeuw, R. (2019). A methodology for urban micro-scale coastal flood vulnerability and risk assessment and mapping. *Natural Hazards*, 1–23. https://doi.org/https://doi.org/10.1007/s11069-019-03648-7
Pescaroli, G., & Alexander, D. (2016). Critical infrastructure, panarchies and the vulnerability paths of cascading disasters. *Natural Hazards*, *82*(1), 175–192. https://doi.org/10.1007/s11069-016-2186-3
Petroliagkis, T. I., Voukouvalas, E., Disperati, J., & Bidlot, J. (2016). *Joint Probabilities of Storm Surge, Significant Wave Height and River Discharge Components of Coastal Flooding Events*. https://doi.org/https://doi.org/10.2788/677778
Philibert, K. K., & Sylvain, M. (2012). *IMPACT DE LA MAREE EXCEPTIONNELLE D ' AOUT 2011 SUR LE PERIMETRE LITTORAL PORTUAIRE DE SAN-PEDRO 1-Présentation du site et methodologie*. *15*(August 2011).
Pickering, M. D., Horsburgh, K. J., Blundell, J. R., Hirschi, J. J. M., Nicholls, R. J., Verlaan, M., & Wells, N. C. (2017). The impact of future sea-level rise on the global tides. *Continental Shelf Research*, *142*(September 2016), 50–68. https://doi.org/10.1016/j.csr.2017.02.004
PNGEC. (2015). *Stratégie de Gestion de l'Environnement Cotier en Cote d'Ivoire et Plan d'Action Natonal*.
Pollard, J. A., Spencer, T., & Brooks, S. M. (2019). The interactive relationship between coastal erosion and flood risk. *Progress in Physical Geography*, *43*(4), 574–585. https://doi.org/10.1177/0309133318794498
Poulter, B., & Halpin, P. N. (2008). Raster modellingof coastal from sea-level rise. *International Journal of Geographical Information Science*, *22*(2), 167–182.

https://doi.org/10.1080/13658810701371858

Prevosto, M., Ewans, K., Forristall, G. Z., & Olagnon, M. (2013). Swell genesis, modelling and measurements in West Africa. *Proceedings of the International Conference on Offshore Mechanics and Arctic Engineering - OMAE, June 9-14*. https://doi.org/10.1115/OMAE2013-11201

Prodger, S., Russell, P., & Davidson, M. (2016). Grain-size distributions on high energy sandy beaches and their relation to wave dissipation. *Sedimentology*, 1–14. https://doi.org/10.1111/sed.12353

Quelennec, R. E. (1984). Identification des problemes sur le littoral sableux de Cote d'Ivoire. Propositions d'actions prioritaires. *Documents Bureau de Recherches Geologiques et Minieres*.

Ramsdales, D. (2023). *Spering, Neap & Proxigean Tides*. Kent Coasts Sea Fishing Compendium. http://hagstone.net/springs.html

Rana, I. A., Asim, M., Aslam, A. B., & Jamshed, A. (2021). Disaster management cycle and its application for flood risk reduction in urban areas of Pakistan. *Urban Climate*, *38*(June), 100893. https://doi.org/10.1016/j.uclim.2021.100893

Rana, I. A., & Routray, J. K. (2018). Multidimensional Model for Vulnerability Assessment of Urban Flooding: An Empirical Study in Pakistan. *International Journal of Disaster Risk Science*, *9*(3), 359–375. https://doi.org/10.1007/s13753-018-0179-4

Reguero, B. G., Losada, I. J., Díaz-Simal, P., Méndez, F. J., & Beck, M. W. (2015). Effects of climate change on exposure to coastal flooding in Latin America and the Caribbean. *PLoS ONE*, *10*(7), 1–19. https://doi.org/10.1371/journal.pone.0133409

Reisinger, A., Howden, M., Vera, C., Garschagen, M., Hurlbert, M., Kreibiehl, S., Mach, K. J., Mintenbeck, K., O'neill, B., Pathak, M., Pedace, R., Pörtner, H.-O., Poloczanska, E., Rojas Corradi, M., Sillmann, J., Van Aalst, M., Viner, D., Jones, R., Ruane, A. C., & Ranasinghe, R. (2020). The concept of risk in the IPCC Sixth Assessment Report: a summary of cross-Working Group discussions. *Intergovernmental Panel on Climate Change, Geneva, Switzerland. Pp15, September*, 15.

Ried, L., Eckerd, S., & Kaufmann, L. (2022). Social desirability bias in PSM surveys and behavioral experiments: Considerations for design development and data collection. *Journal of Purchasing and Supply Management*, *28*(1), 100743. https://doi.org/10.1016/j.pursup.2021.100743

Rizzo, A., & Anfuso, G. (2020). Coastal dynamic and evolution: Case studies from different sites around the world. *Water (Switzerland)*, *12*(10). https://doi.org/10.3390/w12102829

Roberts, R., Carpenter, N., & Klinac, P. (2020). *Auckland's exposure to coastal inundation by storm-tides and waves* (Issue Council technical report, TR2020/24).

Robin, M., Hauhouot, C., Affian, K., Anoh, P., Alla Della, A., & Pottier, P. (2004). Les risques côtiers en Côte d'Ivoire (Coastal hazards in Ivory Coast). *Bulletin de l'Association de Géographes Français*, *81*(3), 298–314. https://doi.org/10.3406/bagf.2004.2393

Roelvink, D., Swinkels, C., Hasselaar, R., & Hillen, M. (2013). Sédimentation Grand Bassam Exploration de mesures de mitigation. *White Paper on Vulnerability of Coral Reef*

Protected Coastlines in a Changing Environment, 1–49.
Rogers, S. R., Manning, I., & Livingstone, W. (2020). Comparing the spatial accuracy of digital surface models from four unoccupied aerial systems: Photogrammetry versus lidar. *Remote Sensing*, *12*(17), 1–17. https://doi.org/10.3390/rs12172806
Roos, A. (2014). *Tides and Tidal currents*. UNESCO-IHE Institute for Water Education.
Roscoe, K., Caires, S., Diermanse, F., & Groeneweg, J. (2010). Extreme offshore wave statistics in the North Sea. *Flood Recovery, Innovation and Response II*, *133*, 47–58. https://doi.org/10.2495/FRIAR100051
Rougier, J., Sparks, S., & Hill, L. J. (2011). Risk and uncertainty assessment for natural hazards. *Risk and Uncertainty Assessment for Natural Hazards*, *9781107006*, 1–574. https://doi.org/10.1017/CBO9781139047562
Ruggiero, P., Holman, R. A., & Beach, R. A. (2004). Wave run-up on a high-energy dissipative beach. *JOURNAL OF GEOPHYSICAL RESEARCH*, *109*, 1–12. https://doi.org/10.1029/2003JC002160
Ruz, M. H., Rufin-Soler, C., Héquette, A., Révillon, R., Hellequin, A. P., Deboudt, P., Herbert, V., Cohen, O., Lebreton, F., Le Goff, L., Schmitt, F. G., & Marin, D. (2020). Climate Change and Risk Perceptions in Two French Coastal Communities. *Journal of Coastal Research*, *95*(sp1), 875–879. https://doi.org/10.2112/SI95-170.1
Sadia, C. (2014). Risque climatique et réactivité des populations urbaines vulnérabilisées face à la montée des eaux de mer à Gonzagueville, Abidjan (Côte d'Ivoire). *VertigO*, *14*(1). https://doi.org/10.4000/vertigo.14743
Saimon, A. A. M. (2017). *Apport du remaniement sédimentaire dans la caractérisation de la couche mobile à l'échelle du cycle de marée du secteur littoral d'Abidjan*. Université Felix Houphouët Boigny Abidjan.
Saimon, A. A. M., Konan, K. E., & N'Ganza, K. P. A. (2019). Suivi , Observation et Disposition des Grains de Quartz par saison dynamique et par cycle de marée sur les plages du Golfe de Guinée au niveau d'Abidjan (Côte D'ivoire). *Geo-Eco-Marina*, *25*, 147–159.
Saimon, A. A. M., N'Doufou, G. H. C., Dangui, N. P., & Wognin, A. V. (2019). Auto-équilibre sédimentaire de plage : Cas du périmètre littoral de Port Bouët. *Revue Marocaine de Géomorphologie*, *3*, 64–75. http://revues.imist.ma/?journal=remageom
Samassy, R. (2019). *Mesures Maregraphiques semi-seculaire au Port d'Abidjan (Côte d'Ivoire) : Methodes, Tendances Evolutive du Niveau Marin et Vulnerabilités Côtières*. Université Felix Houphouet Boigny Abidjan.
Sanò, M., Jiménez, J. A., Medina, R., Stanica, A., Sanchez-Arcilla, A., & Trumbic, I. (2011). The role of coastal setbacks in the context of coastal erosion and climate change. *Ocean and Coastal Management*, *54*(12), 943–950. https://doi.org/10.1016/j.ocecoaman.2011.06.008
Santos, C. T., Toda, L., Orduña, J. R., Santos, F. D., & Ferrão, J. (2015). The impacts of Typhoon Haiyan in the Philippines: Implications to land use planning. *Climate, Disaster and Development Journal*, *1*(1), 57–66. https://doi.org/10.18783/cddj.v001.i01.a06
Sarica, G. M., Zhu, T., Jian, W., Lo, E. Y.-M., & Pan, T.-C. (2021). Spatio-temporal dynamics

of flood exposure in Shenzhen from present to future. *Urban Analytics and City Science*, *48*(5), 1011–1024. https://doi.org/10.1177/2399808321991540

Sawalha, I. H. (2020). A contemporary perspective on the disaster management cycle. *Foresight*, *22*(4), 469–482. https://doi.org/10.1108/FS-11-2019-0097

Schneiderbauer, S., & Ehrlich, D. (2004). Risk, hazard and people's vulnerability to Natural hazards: a review of definitions, concepts and data. *European Commission Joint Research Centre*, 01–40. https://www.researchgate.net/profile/S-Schneiderbauer/publication/268149143_Risk_Hazard_and_People's_Vulnerability_to_Natural_Hazards_a_Review_of_Definitions_Concepts_and_Data/links/55e6916308aebdc0f58bb763/Risk-Hazard-and-Peoples-Vulnerability-to-Natural

Seenath, A., Wilson, M., & Miller, K. (2016). Hydrodynamic versus GIS modelling for coastal flood vulnerability assessment: Which is better for guiding coastal management? *Ocean and Coastal Management*, *120*, 99–109. https://doi.org/10.1016/j.ocecoaman.2015.11.019

Sekovski, I., Del Río, L., & Armaroli, C. (2020). Development of a coastal vulnerability index using analytical hierarchy process and application to Ravenna province (Italy). *Ocean and Coastal Management*, *183*(September), 104982. https://doi.org/10.1016/j.ocecoaman.2019.104982

Serafin, K. A., Ruggiero, P., Barnard, P. L., & Stockdon, H. F. (2019). The influence of shelf bathymetry and beach topography on extreme total water levels : Linking large-scale changes of the wave climate to local coastal hazards. *Coastal Engineering*, *150*, 1–17. https://doi.org/https://doi.org/10.1016/j.coastaleng.2019.03.012

Serafin, K. A., Ruggiero, P., & Stockdon, H. F. (2017). The relative contribution of waves , tides , and non-tidal residuals to extreme total water levels on US West Coast sandy beaches. *Geophysical Research Letters*, *44*(4), 1839–1847. https://doi.org/10.1002/2016GL071020

Shand, R. D., Shand, T. D., Mccomb, P. J., & Johnson, D. L. (2011). Evaluation of empirical predictors of extreme run-up using field data. *20th Australian Coastal and Ocean Engineering Conference. 28 - 30 Sept 2011, September 2011*.

Shepard, C. C., Agostini, V. N., Gilmer, B., Allen, T., Stone, J., Brooks, W., & Beck, M. W. (2012). Assessing future risk: Quantifying the effects of sea level rise on storm surge risk for the southern shores of Long Island, New York. *Natural Hazards*, *60*(2), 727–745. https://doi.org/10.1007/s11069-011-0046-8

Shore Monitoring and Research. (2014). *Lagoon Survey Abidjan – Grand-Bassam, Ivory Coast : Field & Processing report.*

Siek, M. (2011). *Predicting Storm Surges: Chaos, Computational intelligenCe, Data assimilation, ensembles*. UNESCO-IHE Institute for Water Education.

Sirko, W., Kashubin, S., Ritter, M., Annkah, A., Bouchareb, Y. S. E., Dauphin, Y., Keysers, D., Neumann, M., Cisse, M., & Quinn, J. (2021). *Continental-Scale Building Detection from High Resolution Satellite Imagery*. 1–15. http://arxiv.org/abs/2107.12283

Small, C., & Nicholls, R. J. (2003). A global analysis of human settlement in coastal zones. *Journal of Coastal Research*, *19*(3), 584–599. https://doi.org/10.2307/4299200

Sogreah. (2000). *Etude sur modèle physique sédimentologique pochuur une ouverture permanente de l'emboure de la Comoé. Rapport général pour le Port Autonome d'Abidjan*.

Sowman, M., & Raemaekers, S. (2018). Socio-ecological vulnerability assessment in coastal communities in the BCLME region. *Journal of Marine Systems*, *188*(2017), 160–171. https://doi.org/10.1016/j.jmarsys.2018.01.008

Steffen, W. L. (William L. ., Hunter, J., Hughes, L., & Climate Council. (2014). *Counting the costs : climate change and coastal flooding*. https://climatecouncil.org.au

Stephens, S. A., Bell, R. G., & Lawrence, J. (2017). Applying principles of uncertainty within coastal hazard assessments to better support coastal adaptation. *Journal of Marine Science and Engineering*, *5*(3). https://doi.org/10.3390/jmse5030040

Stephenson, V., & D'Ayala, D. (2014). A new approach to flood vulnerability assessment for historic buildings in England. *Natural Hazards and Earth System Sciences*, *14*(5), 1035–1048. https://doi.org/10.5194/nhess-14-1035-2014

Stockdon, H. F., Holman, R. A., Howd, P. A., & Sallenger, A. H. (2006). Empirical parameterization of setup , swash , and runup. *Coastal Engineering*, *53*, 573–588. https://doi.org/10.1016/j.coastaleng.2005.12.005

Taherkhani, M., Vitousek, S., Barnard, P. L., Frazer, N., Anderson, T. R., & Fletcher, C. H. (2020). Sea-level rise exponentially increases coastal flood frequency. *Scientific Reports, 10*(1), 1–17. https://doi.org/10.1038/s41598-020-62188-4

Tano, R. A., Aman, A., Kouadio, K. Y., Toualy, E., Ali, K. E., & Assamoi, P. (2016). Assessment of the Ivorian Coastal Vulnerability. *Journal of Coastal Research*, *32*(6), 1495–1503. https://doi.org/10.2112/JCOASTRES-D-15-00228.1

Tano, R. A., Aman, A., Toualy, E., Kouadio, Y. K., François-xavier, B. B. D., & Addo, K. A. (2018). *Development of an Integrated Coastal Vulnerability Index for the Ivorian Coast in West Africa*. 1171–1184. https://doi.org/10.4236/jep.2018.911073

Tastet, J. P. (1985). Le littoral ivoirien: géologie, morphologie et dynamique. *Ann. Univ. Abidjan, Sér. C, 21 B,* pp.189-218.

Tastet, J. P. (1987). Effets de l'ouverture d'un canal d'accès portuaire sur l'évolution naturelle du littoral d'Abidjan (Afrique de l'Ouest). *Bulletin de Institut de Géologie Du Bassin d'Aquitaine*, *41*, pp 177-190.

Tate, E., Rahman, M. A., Emrich, C. T., & Sampson, C. C. (2021). Flood exposure and social vulnerability in the United States. *Natural Hazards*, *106*(1), 435–457. https://doi.org/10.1007/s11069-020-04470-2

Tavares, A. O., Barros, J. L., Freire, P., Santos, P. P., Perdiz, L., & Fortunato, A. B. (2021). A coastal flooding database from 1980 to 2018 for the continental Portuguese coastal zone. *Applied Geography*, *135*(102534), 1–17. https://doi.org/10.1016/j.apgeog.2021.102534

Tebaldi, C., Ranasinghe, R., Vousdoukas, M., Rasmussen, D. J., Vega-westhoff, B., Kirezci, E., Kopp, R. E., Sriver, R., & Mentaschi, L. (2021). Extreme sea levels at different global warming levels. *Nature Climate Change*, *11*, 746–751. https://doi.org/10.1038/s41558-021-01127-1

Tiemele, J. A., Abaka, B. M., & Kouadio, J. M. (2020). Statistical Simulation of Sea Level-Rise on the Port-Bouet Coast (Ivory Coast). *Case Studies Journal*, *9*(4), 26–31. https://www.casestudiesjournal.com/

Touré, B., Kouamé, K. F., Souleye, W., Collet, C., Affian, K., Ozer, A., Rudant, J.-P., & Biémi, J. (2012a). L'influence des actions anthropiques dans l'évolution historique d'un littoral sableux à forte dérive sédimentaire : la baie de Port-Bouët (Abidjan, Côte d'Ivoire). *Géomorphologie : Relief, Processus, Environnement*, *18*(3), 369–382. https://doi.org/10.4000/geomorphologie.9990

Touré, B., Kouamé, K. F., Souleye, W., Collet, C., Affian, K., Ozer, A., Rudant, J.-P., & Biémi, J. (2012b). The influence of anthropic actions in the historical coastal evolution of a sandy coast with high sediment drift: The Bay of Port-Bouet (Abidjan, Ivory Coast). *Geomorphologie: Relief, Processus, Environnement*, *18*(3), 369–384. https://doi.org/10.4000/geomorphologie.9990

Touré, M., Konan, E. K., & Yao, A. N. (2018). Suivi de la morphologie de l ' unité littoral Vridi-Port-Bouët (Abidjan , Côte d ' Ivoire) [Monitoring of the morphology of the Vridi-Port-Bouët coastal unit (Abidjan , Côte d ' Ivoire)]. *International Journal of Innovation and Scientific Research*, *39*(1), 49–65.

Tsesmelis, D. E., Oikonomou, P. D., Vasilakou, C. G., Skondras, N. A., Fassouli, V., Alexandris, S. G., Grigg, N. S., & Karavitis, C. A. (2019). Assessing structural uncertainty caused by different weighting methods on the Standardized Drought Vulnerability Index (SDVI). *Stochastic Environmental Research and Risk Assessment*, *33*(2), 515–533. https://doi.org/10.1007/s00477-019-01648-4

UNDRR. (2020). Hazard definition and classification review: Technical report. *Hazard Definition & Classification Reviewazard Definition & Classification Review*, 1–88. https://www.undrr.org/publication/hazard-definition-and-classification-review

UNFCCC. (n.d.). *Introduction to adaptation and resilience / Loss and Damage*. Retrieved March 25, 2023, from https://unfccc.int/topics/adaptation-and-resilience/the-big-picture/introduction

UNFCCC. (2018). *Considerations regarding vulnerable groups, communities and ecosystems in the context of the national adaptation plans*. United Nations Climate Change Secretariat.

UNISDR. (2009). UNISDR Terminology on Disaster Risk Reduction. In *The Routledge Handbook to the Political Economy and Governance of the Americas*. https://doi.org/10.4324/9781351138444-36

United Nations. (2017). Factsheet: People and Oceans General. *The Ocean Conference 5-9 June 2017*, 1–14.

United Nations. (2022). The Sustainable Development Goals Report 2022. *United Nations Publication Issued by the Department of Economic and Social Affairs*, 64. https://unstats.un.org/sdgs/report/2022/%0Ahttps://www.un-ilibrary.org/content/books/9789210018098%0Ahttps://www.un-ilibrary.org/content/books/9789210478878

Vafaei, N., Ribeiro, R. A., & Camarinha-Matos, L. M. (2018). Data normalisation techniques in decision making: Case study with TOPSIS method. *International Journal of Information and Decision Sciences*, *10*(1), 19–38. https://doi.org/10.1504/IJIDS.2018.090667

van Aalst, M. K., Cannon, T., & Burton, I. (2008). Community level adaptation to climate change: The potential role of participatory community risk assessment. *Global Environmental Change*, *18*(1), 165–179. https://doi.org/10.1016/j.gloenvcha.2007.06.002

Van Westen, C. J. (2013). Remote Sensing and GIS for Natural Hazards Assessment and Disaster Risk Management. In *Treatise on Geomorphology: Volume 1-14* (Vols. 1–14, Issue September). https://doi.org/10.1016/B978-0-12-374739-6.00051-8

Vandermeulen, H. (1998). The development of marine indicators for coastal zone management. *Ocean and Coastal Management*, *39*(1–2), 63–71. https://doi.org/10.1016/S0964-5691(98)00014-3

Velickov, S. (2004). Nonlinear dynamics and chaos: with applications to physics, biology, chemistry, engineering. In *Taylor & Francis Group*. A.A. Balkema Publishers. https://doi.org/10.5860/choice.32-0994

Vitousek, S., Barnard, P. L., Fletcher, C. H., Frazer, N., Erikson, L., & Storlazzi, C. D. (2017). Doubling of coastal flooding frequency within decades due to sea-level rise. *Scientific Reports*, *7*(1), 1–9. https://doi.org/10.1038/s41598-017-01362-7

Vousdoukas, M. I., Mentaschi, L., Feyen, L., & Voukouvalas, E. (2017). Earth ' s Future Extreme sea levels on the rise along Europe ' s coasts Earth ' s Future. *Earth's Future*, *5*, 1–20. https://doi.org/10.1002/eft2.192

Vousdoukas, M. I., Mentaschi, L., Voukouvalas, E., Bianchi, A., Dottori, F., & Feyen, L. (2018). Climatic and socioeconomic controls of future coastal flood risk in Europe. *Nature Climate Change*, *8*(9), 776–780. https://doi.org/10.1038/s41558-018-0260-4

Vousdoukas, M. I., Mentaschi, L., Voukouvalas, E., Verlaan, M., Jevrejeva, S., Jackson, L. P., & Feyen, L. (20018). Global probabilistic projections of extreme sea levels show intensi fi cation of coastal fl ood hazard. *Nature Communications*, *9:2360*, 1–12. https://doi.org/10.1038/s41467-018-04692-w

Wahl, T., Haigh, I. D., Nicholls, R. J., Arns, A., Dangendorf, S., Hinkel, J., & Slangen, A. B. A. (2017). Understanding extreme sea levels for broad-scale coastal impact and adaptation analysis. *Nature Communications*, *8*, 1–12. https://doi.org/10.1038/ncomms16075

Walsh, K. J. E., Mcinnes, K. L., & Mcbride, J. L. (2012). Climate change impacts on tropical cyclones and extreme sea levels in the South Paci fi c — A regional assessment. *Global and Planetary Change*, *80–81*, 149–164. https://doi.org/10.1016/j.gloplacha.2011.10.006

Ward, P. J., Marfai, M. A., Yulianto, F., Hizbaron, D. R., & Aerts, J. C. J. H. (2011). Coastal inundation and damage exposure estimation : a case study for Jakarta. *Nat Hazards*, *56*, 899–916. https://doi.org/10.1007/s11069-010-9599-1

Watson, P. J. (2022). Determining Extreme Still Water Levels for Design and Planning Purposes Incorporating Sea Level Rise : *Atmosphere*, *13*(95), 1–19. https://doi.org/10.3390/atmos13010095

Wechsler, S. P. (2007). Uncertainties associated with digital elevation models for hydrologic applications: A review. *Hydrology and Earth System Sciences*, *11*(4), 1481–1500. https://doi.org/10.5194/hess-11-1481-2007

Weisse, R., Bella, D., Menéndez, M., Méndez, F., Nicholls, R. J., Umgiesser, G., & Willems, P. (2014). Changing extreme sea levels along European coasts. *Coastal Engineering*, *87*, 4–14. https://doi.org/10.1016/j.coastaleng.2013.10.017

Williams, L. L. (2019). *Coastal Inundation (Enhanced Bathtub Model (eBTM))*. Department of Environment., Forestry and fisheries. https://doi.org/10.15493/DEFF.10000002

Williams, L. L. (2020). *Coastal Inundation (eBTM with variable roughness input)*. Department of Environment., Forestry and fisheries. https://doi.org/10.15493/DEFF.10000005

Williams, L. L., & Lück-Vogel, M. (2020). Comparative assessment of the GIS based bathtub model and an enhanced bathtub model for coastal inundation. *Journal of Coastal Conservation*, *24:23*, 1–15. https://doi.org/https://doi.org/10.1007/s11852-020-00735-x

Wisner, B. (2016). Vulnerability as Concept, Model, Metric, and Tool. In *Oxford Research Encyclopedia of Natural Hazard Science* (Issue August 2016). https://doi.org/10.1093/acrefore/9780199389407.013.25

Wong, T. E., Sheets, H., Torline, T., & Zhang, M. (2022). Evidence for Increasing Frequency of Extreme Coastal Sea Levels. *Frontiers in Climate*, *4*(796479), 1–12. https://doi.org/10.3389/fclim.2022.796479

Woodworth, P. L., Melet, A., Marcos, M., Ray, R. D., Wöppelmann, G., Sasaki, Y. N., Cirano, M., & Hibbert, A. (2019). Forcing Factors Affecting Sea Level Changes at the Coast. In *Surveys in Geophysics* (Vol. 40, Issue 6). Springer Netherlands. https://doi.org/10.1007/s10712-019-09531-1

Wöppelmann, G., & Marcos, M. (2016). Vertical land motion as a key to understanding sea level change and variability. *Rev. Geophys.*, *54*, 64–92. https://doi.org/10.1002/2015RG000502

World Bank. (2019). *West Africa's Coast: Losing Over $3.8 Billion a Year to Erosion, Flooding and Pollution*. https://www.worldbank.org/en/region/afr/publication/west-africas-coast-losing-over-38-billion-a-year-to-erosion-flooding-and-pollution

World Bank. (2020). Effects of Climate Change on Coastal Evolution. In *World Bank Technical Report May 2020*.

World Bank. (2022). *Compendium : Coastal Management Practices in West Africa - Existing and Potential Solutions to Control Coastal Erosion, Prevent Flooding and Mitigate Damage to Society*. https://openknowledge.worldbank.org/handle/10986/37351

World Bank Group. (2021). *Climate Change Knowledge Portal for Development Practitioners and Policy Makers*. https://climateknowledgeportal.worldbank.org

World Meteorological Organization. (2013). *Integrated Flood Management Tools Series: Coastal and Delta Flood Management* (Issue 17). www.wmo.int

Wozazek, S., & Krawinkel, H. (2002). Development of the Côte d'Ivoire Basin: Reading provenance, sediment dispersal, and geodynamic implications from heavy minerals. *International Journal of Earth Sciences*, *91*(5), 906–921. https://doi.org/10.1007/s00531-

001-0248-5
Wu, T. (2021). Quantifying coastal flood vulnerability for climate adaptation policy using principal component analysis. *Ecological Indicators*, *129*, 108006. https://doi.org/10.1016/j.ecolind.2021.108006
Xu, H., Hou, X., Li, D., Wang, X., Fan, C., Du, P., & Song, B. (2022). Spatial assessment of coastal flood risk due to sea level rise in China's coastal zone through the 21st century. *Frontiers in Marine Science*, *9*(August), 1–18. https://doi.org/10.3389/fmars.2022.945901
Xu, Z., Wang, J., Liang, B., Chen, Y., Xu, Z., Wang, J., Liang, B., & Chen, Y. (2017). Effects of Offshore Sand Motion on Wave Runup from Reflective Beaches by using XBeach Model Effects of Offshore Sand Motion on Wave Runup from Reflective Beaches by using XBeach Model. *Journal of Coastal Research*, *79*, 244–248. https://doi.org/10.2112/SI79-050.1
Yao, K. . (2012). *Etude de la dynamique sédimentaire du littoral occidental ivoirienentre Tabou et Sassandra: Approches mor pho-bathymétriques, sédimentologiques et exoscopiques*. Université Félix Houphouët Boigny deCocody-Abidjan.
Yao, K. S., Abe, J., Bamba, S. B., Konan, K. E., Aka, K., Recherches, C. De, & Abidjan, O. (2010). *Dynamique d ' un périmètre littoral portuaire : la côte de San- Pédro , Sud-Ouest de la Côte d ' Ivoire*. *3*, 1–12. https://doi.org/10.5150/revue-paralia.2010.002
Yao, K. S., Dangui, N. P., Gbegbe, M., & Abe, J. (2018). Caractéristiques du climat de houle au large de la côte ivoirienne entre 1985 et 2015 : impacts sur l ' évolution morpho dynamique du rivage. In Paralia CFL (Ed.), *XVèmes Journées Nationales Génie Côtier – Génie Civil : Du 29 au 31 Mai 2018* (pp. 313–320). La Rochelle. https://doi.org/10.5150/jngcgc.2018.035
Yavuz, S., & Deveci, M. (2012). İstatiksel Normalizasyon Tekniklerinin Yapay Sinir Ağın Performansına Etkisi [The effect of statistical normalization techniques on the performance of Artificial Neural Network]. *Erciyes University Journal of Faculty of Economics and Administrative Sciences*, *40*, 167–187. http://www.yarbis.yildiz.edu.tr/common/uploads/21dd335f3f/ERUJFEAS_Jun2012_167to187.pdf
Zanuttigh, B. (2011). Coastal flood protection: What perspective in a changing climate? The THESEUS approach. *Environmental Science and Policy*, *14*(7), 845–863. https://doi.org/10.1016/j.envsci.2011.03.015
Zhang, K., Whitman, D., Leatherman, S., & Robertson, W. (2005). Quantification of Beach Changes Caused by Hurricane Floyd Along Florida's Atlantic Coast Using Airborne Laser Surveys. *Journal of Coastal Research*, *21*(1), 123–134. https://doi.org/10.2112/02057.1
Zhu, X., Dai, Q., Han, D., Zhuo, L., Zhu, S., & Zhang, S. (2019). Modeling the high-resolution dynamic exposure to flooding in a city region. *Hydrol. Earth Syst. Sci.*, *23*(8), 3353–3372. https://doi.org/doi:10.5194/hess-23-3353-2019

LIST OF FIGURES

Figure 1-1: Picture showing a coastal flooding occurrence 10
Figure 1-2: The Water-level components that contribute to coastal flooding.......................... 11
Figure 1-3: Description of Neap and spring tides 12
Figure 1-4: Illustration of time series data depicting diurnal, semidiurnal, and mixed tides... 13
Figure 1-5: Storm surge inundation od the coastal land... 14
Figure 1-6; Process of ocean waves generation 15
Figure 1-7: Characteristics of the ocean wave 16
Figure 1-8: Conceptual sketch of wave runup on a beach 17
Figure 1-9: The interaction of three factors (vulnerability, exposure, and hazard) that influence risk. 24
Figure 1-10: The Risk management Spiral 27
Figure 1-11: The adaptation cycle under the UN climate change regime 28
Figure 2-1: Map of the Study Area 33
Figure 2-2: Location of the Côte d'Ivoire sedimentary basin. 35
Figure 2-3: Detailed presentation of the Côte d'Ivoire Sedimentary basin............................. 36
Figure 2-4: Topographic contour lines of the study site 37
Figure 2-5: Bathymetric map of the Port-Bouët littoral zone 37
Figure 2-6: Monthly climatology of minimum, Mean & maximum temperature and precipitation from 1991 to 2020 in the Abidjan District.. 40
Figure 2-7: Variability and Trends of mean temperature across seasonal cycle from 1991 to 2020 in the Abidjan District 41
Figure 2-8: Variability and Trends of precipitation across seasonal cycle from 1991 to 2020 in the Abidjan District 41
Figure 2-9: Water level measurements from 1983 to 2016at the Quai-Nord station of the Port of Abidjan 42
Figure 2-10: Wave rose off the coast of Port-Bouët precisely at the location 4.5 N -3.75 E for the period 1979-2014 43
Figure 2-11: Variations in coastal wave direction from Western Port-Bouët to the Eastern side of Grand-Bassam... 44

Figure 2-12: Wind Rose at the location 4.5 N; -3.75 E for the period 1979-2014. The average wind speed is 4.06 m. s^{-1} m for a main direction of 208 degrees 45
Figure 2-13: Pictures of the industrial area east of the Vridi canal (a) and the Ivorian refining company (b) located in Vridi 47
Figure 2-14: discharge of plastic and organic wastes by the sea on the beach of the Port-Bouët Bay 49
Figure 2-15: Picture showing dumping of domestic wastes and wastewater (shown by the red arrow) on the ground 50
Figure 3-1: Methodological Approach. “Extr.” stands for Extreme; “ST” for Storm Tide and the acronym “ESLs” denotes Extreme Sea Levels 56
Figure 3-2: Sea level rise projections for SSP1-2.6, SSP2-4.5 and SSP5-8.5 scenarios at the coordinate point (4° 0.000'N; 4° 0.000'W) off the coast of Port-Bouët. 58
Figure 3-3: Model domain 60
Figure 3-4: Comparison between modelled and observed water level (storm tide) for the period of December 10, 2014 to January 2, 2015 at the tide gauge station “Quai-Nord” of the Port of Abidjan 61
Figure 3-5: Map showing boundary line of runup 63
Figure 3-6: Return value plots of the GPD-POT model fitted to Storm Tide data and the associated 95% confidence intervals at Vridi, Petit-Bassam and Sogefiha. 68
Figure 3-7: Return value plot of the GPD-POT model fitted to Wave Runup data and associated 95% confidence intervals at Vridi, Petit-Bassam and Sogefiha. 69
Figure 3-8: Seasonal distribution of occurrences of extreme wave runup higher than 1-year, 10-year and 25-year return levels over the period 1981-2020 70
Figure 3-9: Inter-annual distribution of occurrences of extreme wave runup ≥ 1-year return level (a) and ≥ 10-year return level (b) over the period 1981–2020 at Sogefiha 71
Figure 3-10: Future of the present-day 100-year return level under different SLR Scenarios at Vridi, Petit-Bassam and Sogefiha. 73
Figure 3-11: Evolution of the return period for the current 100-year return level over time under the different climate change scenarios for each neighborhood in Port-Bouët Bay. 74
Figure 4-1: Flow chart showing the general research methodology 81
Figure 4-3: Digital Terrain Model (DTM) of the study area 84
Figure 4-4: Surface Roughness Distribution across the Study Area. 85

Figure 4-5: Land use map of the study area based on satellite imagery and ground-truthing. 88
Figure 4-6: Map showing the locations of recent observed coastal flooding (orange dots) overlaid with modeled current flood extent (blue band) to ensure the validity of the eBTM simulations. 90
Figure 4-7: Maps showing the total flood extent for present and future situation for different climate change conditions along the Port-Bouët Bay. 91
Figure 4-8: Number of population (a) and buildings (b) exposed to coastal flood events along the Port-Bouët Bay under different climate change scenarios for present and future periods. 93
Figure 4-9: Population and Building Exposure in Port-Bouët's Neighborhoods under Various Climate Change Scenarios for the Present and Future periods. 95
Figure 4-10: Land use exposure to coastal flooding in the Port-Bouët Bay for different climate change scenarios SSP1-2.6, SSP2-4.5 and SSP5-8.5. 97
Figure 4-11: Contribution of Housing Exposure by Neighbourhood in Port-Bouët Bay. 98
Figure 5-1: The adopted workflow of the study 107
Figure 5-2: Picture of an interview session in a precarious place of the neighbourhood of Sogefiha 115
Figure 5-3: Maps showing the spatial and temporal distribution of coastal flood hazard index in the Port-Bouët Bay 119
Figure 5-4: Maps showing the spatial and temporal distribution of coastal flood exposure index in the Port-Bouët Bay. 120
Figure 5-5: Map showing the spatial variation of coastal flood vulnerability index for the current period in the Port-Bouët Bay. 121
Figure 5-5-6: Spider diagram of vulnerability normalized indicator values for Vridi, Petit-Bassam and Sogefiha. 122
Figure 5-7: Map showing the spatial and temporal distribution of coastal flood risk index under climate change scenarios in the Port-Bouët Bay. 123
Figure 5-8: Contribution of the risk Components (Hazard; Exposure and Vulnerability) to the overall coastal flood risk in each Neighbourhood (Vridi, Petit-Bassam and Sogefiha) in Port-Bouët Bay 125
Figure 5-9: Contributions of the neighbourhoods to the overall coastal flood risk in Port-Bouët Bay 126

LIST OF TABLES

Table 1-1: Description of hazards' characteristics 21
Table 1-2: The different dimensions of Vulnerability 23
Table 3-1: representative representation beach slopes (βf) calculated from historical beach profiles 62
Table 3-2: Statistical error parameters obtained from comparison between observed and calculated sea levels. 63
Table 3-3: Present-day Extreme Sea Levels (ESLs) deduced from the Joint Probability Method 72
Table 4-1: Values of Extreme Sea Level (ESL) for different SSP scenarios used to run the eBTM model 86
Table 4-2: Estimates of total flooded area (in ha) per neighbourhood and per scenario 92
Table 5-1: Description of the selected hazard indicators and their impacts on coastal flood risk index 108
Table 5-2 Description of the selected exposure indicators and their impacts on coastal flood risk index 109
Table 5-3: Description of the selected vulnerability indicators and their impacts on coastal flood risk index 111

ANNEXES

Annex A

Table S1: Complete set of estimated current and future extreme sea level Scenarios at Vridi, petit-Bassam and Sogefiha: It presents the evolution of the of the present-days 1-, 5-, 10-, 25-, 50-, and 100-year return values of ESL under SSP1-2.6, SSP2-4.5 and SSP5-8.5 scenarios for the year 2030, 2050 and 2100. For each SSP both median (50th percentiles) and likely (17th – 83rd) ranges are provided.

Location	**Return period**	Present-day ESL (2020)	2030								
			SSP1-2.6			SSP2-4.5			SSP5-8.5		
			17th	50th	83rd	17th	50th	83rd	17th	50th	83rd
VRIDI	1	3.4	3.471	3.511	3.556	3.470	3.510	3.556	3.476	3.515	3.561
	5	3.78	3.851	3.891	3.936	3.850	3.890	3.936	3.856	3.895	3.941
	10	3.93	4.001	4.041	4.086	4.000	4.040	4.086	4.006	4.045	4.091
	25	4.12	4.191	4.231	4.276	4.190	4.230	4.276	4.196	4.235	4.281
	50	4.25	4.321	4.361	4.406	4.320	4.360	4.406	4.326	4.365	4.411
	100	4.37	4.441	4.481	4.526	4.440	4.480	4.526	4.446	4.485	4.531
PETIT-BASSAM	1	3.86	3.931	3.971	4.016	3.930	3.970	4.016	3.936	3.975	4.021
	5	4.3	4.371	4.411	4.456	4.370	4.410	4.456	4.376	4.415	4.461
	10	4.47	4.541	4.581	4.626	4.540	4.580	4.626	4.546	4.585	4.631
	25	4.68	4.751	4.791	4.836	4.750	4.790	4.836	4.756	4.795	4.841
	50	4.83	4.901	4.941	4.986	4.900	4.940	4.986	4.906	4.945	4.991
	100	4.97	5.041	5.081	5.126	5.040	5.080	5.126	5.046	5.085	5.131
SOGEFIHA	1	3.51	3.581	3.621	3.666	3.580	3.620	3.666	3.586	3.625	3.671
	5	3.9	3.971	4.011	4.056	3.970	4.010	4.056	3.976	4.015	4.061
	10	4.05	4.121	4.161	4.206	4.120	4.160	4.206	4.126	4.165	4.211
	25	4.23	4.301	4.341	4.386	4.300	4.340	4.386	4.306	4.345	4.391
	50	4.36	4.431	4.471	4.516	4.430	4.470	4.516	4.436	4.475	4.521
	100	4.48	4.551	4.591	4.636	4.550	4.590	4.636	4.556	4.595	4.641

Table S1 Continued (2/3)

Location	Return period	Present-day ESL (2020)	2050								
			SSP1-2.6			SSP2-4.5			SSP5-8.5		
			17th	50th	83rd	17th	50th	83rd	17th	50th	83rd
VRIDI	1	3.4	3.543	3.620	3.711	3.560	3.636	3.729	3.587	3.664	3.759
	5	3.78	3.923	4.000	4.091	3.940	4.016	4.109	3.967	4.044	4.139
	10	3.93	4.073	4.150	4.241	4.090	4.166	4.259	4.117	4.194	4.289
	25	4.12	4.263	4.340	4.431	4.280	4.356	4.449	4.307	4.384	4.479
	50	4.25	4.393	4.470	4.561	4.410	4.486	4.579	4.437	4.514	4.609
	100	4.37	4.513	4.590	4.681	4.530	4.606	4.699	4.557	4.634	4.729
PETIT-BASSAM	1	3.86	4.003	4.080	4.171	4.020	4.096	4.189	4.047	4.124	4.219
	5	4.3	4.443	4.520	4.611	4.460	4.536	4.629	4.487	4.564	4.659
	10	4.47	4.613	4.690	4.781	4.630	4.706	4.799	4.657	4.734	4.829
	25	4.68	4.823	4.900	4.991	4.840	4.916	5.009	4.867	4.944	5.039
	50	4.83	4.973	5.050	5.141	4.990	5.066	5.159	5.017	5.094	5.189
	100	4.97	5.113	5.190	5.281	5.130	5.206	5.299	5.157	5.234	5.329
SOGEFIHA	1	3.51	3.653	3.730	3.821	3.670	3.746	3.839	3.697	3.774	3.869
	5	3.9	4.043	4.120	4.211	4.060	4.136	4.229	4.087	4.164	4.259
	10	4.05	4.193	4.270	4.361	4.210	4.286	4.379	4.237	4.314	4.409
	25	4.23	4.373	4.450	4.541	4.390	4.466	4.559	4.417	4.494	4.589
	50	4.36	4.503	4.580	4.671	4.520	4.596	4.689	4.547	4.624	4.719
	100	4.48	4.623	4.700	4.791	4.640	4.716	4.809	4.667	4.744	4.839

Table S1 Continued (3/3)

Location	**Return period**	Present-day ESL (2020)	2100								
			SSP1-2.6			SSP2-4.5			SSP5-8.5		
			17th	50th	83rd	17th	50th	83rd	17th	50th	83rd
VRIDI	1	3.4	3.702	3.888	4.122	3.820	4.018	4.284	4.026	4.240	4.548
	5	3.78	4.082	4.268	4.502	4.200	4.398	4.664	4.406	4.620	4.928
	10	3.93	4.232	4.418	4.652	4.350	4.548	4.814	4.556	4.770	5.078
	25	4.12	4.422	4.608	4.842	4.540	4.738	5.004	4.746	4.960	5.268
	50	4.25	4.552	4.738	4.972	4.670	4.868	5.134	4.876	5.090	5.398
	100	4.37	4.672	4.858	5.092	4.790	4.988	5.254	4.996	5.210	5.518
PETIT-BASSAM	1	3.86	4.162	4.348	4.582	4.280	4.478	4.744	4.486	4.700	5.008
	5	4.3	4.602	4.788	5.022	4.720	4.918	5.184	4.926	5.140	5.448
	10	4.47	4.772	4.958	5.192	4.890	5.088	5.354	5.096	5.310	5.618
	25	4.68	4.982	5.168	5.402	5.100	5.298	5.564	5.306	5.520	5.828
	50	4.83	5.132	5.318	5.552	5.250	5.448	5.714	5.456	5.670	5.978
	100	4.97	5.272	5.458	5.692	5.390	5.588	5.854	5.596	5.810	6.118
SOGEFIHA	1	3.51	3.812	3.998	4.232	3.930	4.128	4.394	4.136	4.350	4.658
	5	3.9	4.202	4.388	4.622	4.320	4.518	4.784	4.526	4.740	5.048
	10	4.05	4.352	4.538	4.772	4.470	4.668	4.934	4.676	4.890	5.198
	25	4.23	4.532	4.718	4.952	4.650	4.848	5.114	4.856	5.070	5.378
	50	4.36	4.662	4.848	5.082	4.780	4.978	5.244	4.986	5.200	5.508
	100	4.48	4.782	4.968	5.202	4.900	5.098	5.364	5.106	5.320	5.628

Annex B

COASTAL FLOOD VULNERABILITY QUESTIONNAIRE

General Information

What is your name?
optional

___

Gender

- ◯ Male
- ◯ Female

How old are you?

- ◯ <20
- ◯ 20 - 30
- ◯ 31 - 40
- ◯ 41 - 50
- ◯ 51 - 60
- ◯ 61 and above

Neighborhood / Sector

- ◯ Sogefiha
- ◯ Petit-Bassam
- ◯ Vridi

GPS Coordinates

latitude (x.y °)

___

longitude (x.y °)

___

altitude (m)

___

accuracy (m)

___

Susceptibility Factors

What is the current condition of the building where the household is located [visual inspection by Interviewer]

- ◯ Good Condition [not Precarious]
- ◯ Poor condition [Precarious]
- ◯ Other

If other, Please Specify

___

Including yourself, how many people currently live in your household?

___

How many females are currently living in your household?

___

How many children in your household are under the age of 10?

___

What is the number of individuals in your household who are 65 years of age or older?

___

Are there any individuals in your household who have a disability?

- ◯ Yes
- ◯ No
- ◯ I do not know

If yes, How many People?

___

What are the types of disability?

- ☐ Physical disability
- ☐ Sensory disability (e.g. deaf or hard of hearing, blind or low vision)
- ☐ Intellectual or cognitive disability (e.g. autism)
- ☐ Mental health condition (e.g. depression, anxiety)
- ☐ Other

If Other, please specify

___

Are there any individuals in your household with a chronic illness or medical condition?

- ◯ Yes
- ◯ No
- ◯ I do not know

For how long has the chronically ill individual in your household been sick?

- ☐ Less than 1 year
- ☐ 1-5 years
- ☐ 6-10 years
- ☐ More than 10 years

What is the current employment status of the head of household?

- ◯ Employed (both public and private compagny)
- ◯ Self-employed
- ◯ Unemployed
- ◯ Retired
- ◯ Other

If Other, please specify

____

Does he/she have any other sources of income?

- ◯ Yes
- ◯ No

How many people in your household have a job?

____

How many dependent people are there in the household?

____

How do you assess the general income of your household?

- ◯ High [Very satisfactory]
- ◯ Medium [Satisfactory]
- ◯ Low [Not satisfactory]

Adaptive Capacity Factors

How many people can read and write in your household?

____

Do you receive flood alerts during periods of sea agitation?

- ◯ Yes
- ◯ No

If yes, by what means do you receive these alerts?

- ☐ Radio
- ☐ Newspapers
- ☐ Television
- ☐ Through email
- ☐ Phone call / SMS
- ☐ Alarm
- ☐ Door-to-door
- ☐ Car advert
- ☐ Other

If other, Please Specify

____

From whom or from which organization do you receive these alerts?

- ☐ The town hall
- ☐ The regional council / The District
- ☐ The general council
- ☐ Resident associations
- ☐ The government
- ☐ The International partners
- ☐ I do not know
- ☐ Other

If other, then specify

____

Do you receive training or awareness-raising on Coastal Risk Management?

- ◯ Yes
- ◯ No
- ◯ I do not know

If yes, What organisations are in charge of raising your awareness and training you?

____

Do you think you are sufficiently informed about the behavior to adopt in the event of flooding by the sea?

- ◯ Yes, absolutely
- ◯ No, rather not
- ◯ Not at all
- ◯ I do not know

Are you aware of evacuation sites in the event of coastal flooding?

- ◯ Yes, absolutely
- ◯ No, rather not
- ◯ Not at all
- ◯ I do not know

If yes, please explain a little

____

How far from your home is the nearest evacuation site?

- ◯ Not far [less than 0.5 km]
- ◯ Far [0.5 - 1 km]
- ◯ Very far [more than 1 km]

Does your household have any private flood protection measures in place to prevent or mitigate coastal flood damage?

- ☐ Yes, we have installed flood barriers, sandbags, or other flood protection measures
- ☐ Yes, we have elevated the basement or foundation to protect the building from flood damage
- ☐ Yes, we have waterproofed our basement or foundation
- ☐ Yes, we have taken other private flood protection measures (please specify):
- ☐ No, we do not have any private flood protection measures in place

If other, Please Specify

____

Annex C

Table S2: Hazard, Exposure, vulnerability and Risk indices calculated for current and future scenarios along the Port-Bouët Bay. These indices were obtained based on indicators that have been described in chapter 5.

		VRIDI				PETIT-BASSAM				SOGEFIHA			
		Hazard	Exposure	Vulnerability	Risk	Hazard	Exposure	Vulnerability	Risk	Hazard	Exposure	Vulnerability	Risk
2020		0.100	0.100	0.431	0.004	0.146	0.181	0.448	0.012	0.285	0.339	0.670	0.065
2030	SSP1	0.413	0.106		0.019	0.516	0.202		0.047	0.612	0.366		0.150
	SSP2	0.411	0.107		0.019	0.515	0.203		0.047	0.612	0.366		0.150
	SSP5	0.419	0.109		0.020	0.525	0.220		0.052	0.614	0.366		0.151
2050	SSP1	0.429	0.115		0.021	0.557	0.262		0.065	0.631	0.415		0.175
	SSP2	0.433	0.117		0.022	0.558	0.264		0.066	0.634	0.416		0.177
	SSP5	0.436	0.118		0.022	0.566	0.267		0.068	0.643	0.425		0.183
2100	SSP1	0.467	0.183		0.037	0.599	0.442		0.119	0.685	0.714		0.327
	SSP2	0.503	0.218		0.047	0.618	0.457		0.127	0.717	0.782		0.375
	SSP5	0.859	0.835		0.309	0.678	0.537		0.163	0.771	0.879		0.454

TABLE OF CONTENTS

LIST OF CONTENTS I

DEDICATION II

ACKNOWLEDGEMENTS III

ABSTRACT V

RÉSUMÉ VII

LIST OF ABBREVIATIONS IX

INTRODUCTION 1

UNDERSTANDING THE ELEMENTS OF COASTAL FLOOD RISK 8

1.1. INTRODUCTION 9

1.2. COASTAL FLOODING 9

1.2.1. Overview *9*

1.2.2. Drivers *11*

1.2.2.1. Tide 11

1.2.2.2. Storm Surges 13

1.2.2.3. Ocean Waves 14

1.2.2.4. Sea-level Rise 17

1.2.2.5. Coastal Morphological features 18

1.3. THE RISK CONCEPT 19

1.3.1. Hazard *20*

1.3.2. Exposure *21*

1.3.3. Vulnerability *22*

1.3.4. Risk Equation *24*

1.4. RISK MANAGEMENT AND ADAPTATION 25

1.5. CONCLUSION 29

STUDY AREA: PHYSICAL, SOCIOECONOMIC AND ENVIRONMENTAL CHARACTERISTICS 30

2.1. INTRODUCTION 31

2.2. LOCATION OF THE STUDY 31

2.3. PHYSICAL CHARACTERISTICS 33
2.3.1. Geology *33*
2.3.2. Geomorphology *36*
2.3.3. Sedimentology *37*
2.3.4. Drainage *38*
2.3.5. Climate *39*
2.3.6. Metocean Conditions *41*
2.3.6.1. Tides and sea level change 41
2.3.6.2. Wave and wind climate 42
2.3.6.3. Storm surges Conditions 45
2.3.6.4. Currents 46
2.4. SOCIOECONOMIC CHARACTERISTICS 46
2.4.1. Demography *46*
2.4.2. Economic Activities *47*
2.5. ENVIRONMENTAL CHARACTERISTICS 48
2.6. COASTAL MANAGEMENT 51
2.7. CONCLUSION 52
QUANTIFYING CHANGES IN EXTREME SEA LEVELS (ESLS) **53**
3.1. INTRODUCTION 54
3.2. DATA AND METHODOLOGY 55
3.2.1. Approach overview *55*
3.2.2. Data *56*
3.2.3. Methods *59*
3.2.3.1. Storm tide modelling 59
3.2.3.2. Wave runup calculation 61
3.2.3.3. Extreme Value Analysis (EVA) 64
3.2.3.4. Joint Probability Analysis (JPM) 65
3.2.4. ESL's scenarios design *66*
3.3. RESULTS 66
3.3.1. Extreme Storm tide and Wave Runup *66*
3.3.2. Present-day ESLs *71*
3.3.3. Future ESLs *72*
3.4. DISCUSSION 74

3.5. CONCLUSION 77

COASTAL FLOOD MAPPING AND EXPOSURE ASSESSMENT 79

4.1. INTRODUCTION 80
4.2. DATA AND METHODOLOGY 81
4.2.1. Coastal flood Modelling 82
4.2.1.1. Modelling Approach 82
4.2.1.2. Model input data 83
4.2.1.3. Model setup and validation 86
4.2.2. Exposure estimation 87
4.3. RESULTS 89
4.3.1. Coastal flood mapping 89
4.3.2. Coastal Flood Exposure 93
4.3.2.1. Exposed populations and Buildings 93
4.3.2.2. Land use in flooded areas 96
4.4. DISCUSSIONS 99
4.4.1. Insights 99
4.4.2. Limitations 100
4.5. CONCLUSIONS 102

ASSESSMENT OF COASTAL FLOOD RISK IN A CHANGING CLIMATE............ 104

5.1. INTRODUCTION 105
5.2. METHODOLOGY 106
5.2.1. Hazard Component 107
5.2.2. Exposure Component 108
5.2.3. Vulnerability Component 109
5.2.3.1. Indicators selections 109
5.2.3.2. Sample Size Calculation 113
5.2.3.3. Collection mode and Sampling method 114
5.2.3.4. Implementation of the field Campaign 114
5.2.4. Risk assessment 115
5.2.4.1. Normalization of indicator data 116
5.2.4.2. Weighting and Aggregation of Indicators 116
5.2.4.3. Aggregating risk components to risk 117

5.3. RESULTS 118
5.3.1. Hazard, Exposure and Vulnerability Levels in Port-Bouët Bay 118
5.3.1.1. Hazard Levels 118
5.3.1.2. Exposure Levels 119
5.3.1.3. Vulnerability Levels 121
5.3.2. Coastal Flood Risk Trends 123
5.3.3. Contributions to the overall coastal flood risk in Port-Bouët Bay 124
5.3.3.1. Contributions of the risk components 124
5.3.3.2. Contribution of the neighbourhoods 124
5.4. DISCUSSION 126
5.4.1. Insights 126
5.4.1. Limitations 127
5.6. CONCLUSION 131
RECOMMENDATIONS & CONCLUDING REMARKS 132
RECOMMENDATIONS 133
CONCLUDING REMARKS 136
REFERENCES 138
LIST OF FIGURES 163
LIST OF TABLES 166
ANNEXES 167
ANNEX A 168
ANNEX B 171
ANNEX C 176
TABLE OF CONTENTS 177